THE UNIVERSITY
of EDINBURGH

The importance of poly(A)-binding protein 4 (PABP4) in healthy pregnancy

Lenka Hrabálková

Thesis submitted to the University of Edinburgh for the Degree of Doctor of Philosophy

August 2016

Abstract

Healthy pregnancy requires a tightly regulated materno-fetal dialogue for processes such as embryo implantation, endometrial decidualisation (in the mouse), placentation and maternal adaptation to occur. Disruption of placental development as well as maternal adaptation can lead to fetal intrauterine growth restriction (IUGR) which increases the risk of late miscarriage/stillbirth (e.g. 53% of preterm stillbirth and 26% of term stillbirth are found to be IUGR). Furthermore, IUGR is a risk factor for neurodevelopmental conditions in childhood and for a spectrum of related adult health disorders such as cardiovascular disease and type II diabetes, often termed metabolic syndrome. Despite these pregnancy disorders being common (e.g. 1 in 200 pregnancies results in stillbirth in the UK) the molecular lesion(s) underlying their pathophysiology are poorly understood and in particular those with placental and/or maternal aetiologies most frequently remain unexplained.

Here we investigate the hypothesis that poly(A)-binding protein 4 (PABP4) is required for healthy pregnancy in mice. PABP4 is an RNA-binding protein and a member of the PABP family which are central regulators of mRNA translation and stability. Using all four permutations of wild-type and knock-out crosses, we find that maternal PABP4-deficiency results in a reduced litter size and IUGR. The number of implantations at e8.5 were not reduced in *Pabp4*$^{-/-}$ females, implying that the reduced litter size was not a consequence of decreased ovulation, fertilisation or implantation frequency. Further longitudinal analysis (at e13.5, e15.5 and e18.5) reveals that fetal death primarily occurred between e18.5 and birth, suggesting these mice may provide a unique opportunity to inform on the maternal causes of stillbirth. The onset of IUGR, which was found to be symmetrical in nature, was established by e15.5 preceding the majority of fetal death.

During pregnancy, a materno-fetal dialogue directs and responds to changes in gene expression to give rise to the placenta and adapt the maternal physiology. Defects in these processes may result in reduced growth and/or fetal death and were examined in *Pabp4*$^{-/-}$ mice to shed light on the mechanistic basis of these related phenotypes. Fetal to placental (F:P) weight ratio, whose changes can be indicative of placental

insufficiency or placental adaptation in an attempt to aid fetal growth, was found to be increased in *Pabp4*$^{-/-}$ dams at e15.5 and e18.5 due to the presence of IUGR fetuses with placentas of normal weight. Consistent with this observation, placental volume was unchanged at e18.5. Total placental weight and volume alone fails to discriminate potential differences in the individual placental zones which include the labyrinth zone, where materno-fetal gas and nutrient exchange occur; the junctional zone, which has endocrine functions including those that promote maternal adaptation; and the decidua basalis, derived from the maternal endometrium and is the site of trophoblast invasion and maternal vascular remodelling in early pregnancy. Therefore, volumetric analysis of these zones and the maternal blood spaces, which transcend the decidua basalis and junctional zone, was undertaken. This showed no change in the maternal blood spaces or the labyrinth, the latter being the zone whose size is most frequently altered in IUGR. Critically however, the size of the maternally-derived decidua basalis was increased with a concurrent decrease in the size of the junctional zone. These morphological changes may play a causative role either through directly affecting placental function and/or by the reduced junctional zone failing to promote appropriate maternal adaptation. Alternatively, they may reflect compensatory adaptations to a primary defect elsewhere in the mother.

Complementing these morphological studies, functional studies were undertaken: remodelling of maternal vasculature and the resistance index of vessels delivering blood to the fetus were assessed; as was delivery of nutrients to the fetus (measured by fetal glucose); and systemic maternal adaptations (maternal hormonal profile, circulating glucose levels and organ weights). Uterine, umbilical and decidual spiral arteries were examined, but displayed no apparent differences suggestive of normal blood supply to the fetus. However fetal blood glucose was reduced suggesting a reduced delivery of nutrients important for fetal growth. This was not due to lower circulating maternal blood glucose levels, and mRNA levels of the placental glucose transporters *Glut-1* and *Glut-3* were not reduced but upregulated, suggestive of an attempt to compensate for reduced fetal glucose. Furthermore, upregulation of at least one system A amino acid transporter mRNA, *Snat-2*, was observed. The maternal physiological state of PABP4-deficient dams showed deviations in some organ weights (e.g. spleen weight is reduced at e13.5 and e15.5) and the levels of some

circulating hormones (e.g. estradiol is deceased whereas progesterone is increased at e18.5). However, future work will be required to determine which, if any, of these changes are primary defects rather than downstream consequences and to identify which mis-regulated mRNAs/pathways within in the materno-fetal dialogue underlie the phenotype.

Taken together, my results suggest that the regulation of mRNA translation/stability by PABP4 is critical to achieving the correct pattern of gene expression within the materno-fetal dialogue to enable appropriate placentation and maternal adaptation. Furthermore, my results suggest that *Pabp4*$^{-/-}$ mice provide a unique opportunity to further understand the maternal causes of a spectrum of related pregnancy complications including IUGR, late miscarriage and stillbirth.

Layman's abstract

In the UK, approximately 1/200 babies are stillborn, making it more common than both Down's syndrome (1/1000) and Sudden Infant Death syndrome (1/2000). Stillbirth refers to a loss of pregnancy from 24 weeks till birth and often occurs without warning. Despite its frequency, relatively little is heard about this devastating condition as often parents find it hard to talk about what has happened. Surprisingly, UK stillbirth rates have only decreased by 5% (2000 to 2008). One barrier to progress in tackling stillbirth is our lack of knowledge about why it happens, with roughly 60% of cases being "unexplained" as both mother and baby (also known as a fetus) appeared healthy. Interestingly, another complication of pregnancy, intrauterine growth restriction (IUGR), is present in many of these unexplained cases and therefore IUGR is considered a "risk-factor" for stillbirth, being present in 26% of cases. IUGR refers to a condition where a baby's growth pace is slow-downed in the womb, meaning they are smaller than would normally be expected. This occurs in 3-7% of pregnancies. Importantly, IUGR is not only a risk factor for stillbirth and death within the first weeks after birth, but also for developmental problems in childhood and adult health conditions such as heart disease and diabetes.

Currently, they only way to protect growth restricted babies from the risk of stillbirth is early delivery. However this is fraught with problems as many of these babies would have survived and pre-term (early) birth is associated with its own health and developmental complications. Moreover, to prevent stillbirth of babies that aren't small, this approach would need to be applied to all pregnancies presenting social, ethical and medical problems. Therefore, it is important that we gain more knowledge of how such pregnancy complications arise, as this is the first step towards being able to better identify at risk pregnancies and to developing better clinical interventions. Where investigated, many cases of IUGR and stillbirth have been found to be associated with problems with the placenta, an organ which develops during pregnancy. Thus these studies highlight this pregnancy-specific organ, which provides oxygen and nutrients which are critical for the growing baby, as an important factor in these pregnancy complications.

Animal models are key to understanding the basis of human disease as they allow for detailed investigations which can uncover underlying problems and ascertain whether, and how, they lead to disease. Importantly in this regard, we have developed a mouse model that mirrors critical aspects of this spectrum of human pregnancy complications, in which we observe IUGR and some, but not all, fetuses die in late pregnancy. Using this model my studies have already shown that the development of the placenta is affected, resulting in a change in its structure rather than size and indicate that its ability to transfer nutrients to fetuses may also be compromised. In addition to providing oxygen and nutrients, the placenta also plays an important role in directing the numerous changes that have to happen in the female body to support pregnancy. We find that several aspects of "maternal adaptation" including changes in organ weights and hormone levels don't appear to have occurred correctly. Finally, we have found that even before pregnancy the red blood cells of the adult female mice, which carry oxygen around the body, are smaller than normal and contain less haemoglobin (the red blood cell component that carries oxygen). The extra "strain" of pregnancy can result in such "pre-existing" conditions becoming problematic. Importantly, each of these observations has the potential to explain the poor fetal growth and survival. Thus, future work will aim to identify which of them may be causative and to provide a detailed understanding of the series of events that lead to these abnormalities, with the long term aim of providing better diagnostic tools and interventions to improve pregnancy outcome.

Declaration

I certify that the thesis has been composed by me, and either that the work is my own, or, where I have been a member of a research group, that I have made a substantial contribution to the work, such contribution being clearly indicated, and that the work has not been submitted for any other degree or professional qualification.

Chapter 4 and 5

I acknowledge the assistance of Jenna Muir, an MSc student, who helped with e15.5 fetal and placental measurements and qPCR of the placental transporters and placental cell type markers at e15.5.

I also acknowledge the assistance of William Richardson, a senior lab technician, who carried out the RNA extraction of e15.5 placentas.

Doppler ultrasound measurements were taken by Adrian Thomson, an ultrasound technician.

Chapter 6

Blood plasma assays were run by the Wellcome Trust Supported Cambridge Mouse Biochemistry Laboratory.

Haematological analysis of whole blood was carried out at Easter Bush Pathology (The Royal (Dick) School of Veterinary Studies and The Roslin Institute, Edinburgh).

Lenka Hrabálková

August 2016

Acknowledgements

Firstly, I would like to thank my supervisor and mentor, Professor Nicola Gray, for giving me the opportunity to work on this PhD project and for all her dedicated support and guidance throughout the course of the PhD and during the writing of my thesis. I will always appreciate my time in the Gray lab where I have learned so much!

Thank you to my secondary supervisor, Dr Ian Adams, for his support, guidance and always giving me the opportunity to discuss results and ideas.

A special thank you goes to Dr Matt Brook, for being an endless source of knowledge, inspiration and support in the lab as well as during my thesis writing. I couldn't have asked for a better day-to-day supervisor and mentor.

Thank you to all the Gray lab members, particularly Bill Richardson for always being so kind and helpful in the lab. Big thanks to Taj, Jess and Caroline for the laughs in and out of the lab and for always being there for me.

I would like to thank my wonderful parents, Petr and Zorka, without whose encouragement and support I would not be doing a PhD in the first place, I will always be grateful!

Finally, thank you to my husband and my best friend, Michael, who has stood by me through all the ups and downs. Thank you for always seeing the best in me and not hesitating giving me a seater in the middle of the night to the library to keep me company.

Abbreviations

%tile……..Percentile

1° TGCs……Primary trophoblast giant cell

11β-HSD-2……...11 beta-hydroxysteroid dehydrogenase type 2

2° TGCs……Secondary trophoblast giant cell

AFP…….. α-fetoprotein

AGA…….Appropriate for gestational age

APA……. Alternative polyadenylation sites

BW:PW…… Birthweight:placental weight ratio

CAP……..Chorioallantoic plate

CAST……....Computer Assisted Stereology Toolbox system

CF…….Cleavage factor

CNS……..Central nervous system

CPSF…….Cleavage and polyadenylation specificity factor

CST……...Stimulating factor

C-TGC……..Maternal blood canal-associated trophoblast giant cell

CTR……..Centre for Trophoblast Research

DAZ……..Deleted in azoosperma

Dazl……...DAZ like

DB…….....Decidua basalis

Db……..Decidua basalis

DNA……..Deoxyribonucleic acid

e…….Embryonic day

ECM…… Extracellular matrix

ECP……...Ectoplacental cone

eIF…….Eukaryotic initiation factor

eIF…….Eukaryotic initiation factor

ELISA……...Enzyme-linked immunosorbent assay

ePABP……...Embryonic poly(A)-binding protein

eRF……....Embryonic release factor

ES cells……..Embronic stem cells

ExE……Extraembryonic ectoderm

F:P…….Fetal to placental weight ratio

FFA……Free fatty acids

FGR……...Fetal growth restriction

FMRP…… Fragile X mental retardation protein

FPR……...Fetal to placental weight ratio

FXS…….. Fragile X syndrome

GDM…….Gestational diabetes mellitus

GH……Growth hormone

GH-V……Growth hormone variant

GLUT……...Glucose transporter proteins

H&E……..Hematoxylin and eosin

Hb…….Haemoglobin

hCG……..Human chorionic gonadotropin

hCS……...Human chorionic somatomammotrophic hormone

HCT……..Haematocrit

HDL-C……..High density lipoprotein cholesterol

HELLP……..Hemolysis, elevated liver enzymes and low platelet count

HFD……..High fat diet

hPL……...Human placental lactogen

HTC……..Hematocrit

IBR……...Individualised birthweight ratio

ICM……...Inner cell mass

IFN-γ……Interferon gamma

IGF……....Insulin-like growth factor

IHC……...Immunohistochemistry

IUGR…….....Intrauterine growth restriction

Jz……...Junctional zone

KIR……Killer-cell immunoglobulin-like receptors

KO…….Knock-out

KOMP……. Knock-Out Mouse Project

LDL-C…….....Low density lipoprotein cholesterol

LGA……..Large for gestational age

LH…….Luteinising hormone

LP…….Late pregnant

LPL……...Lipoprotein lipase

Lz……..Labyrinth zone

M/AM…….....Mesometrial to anti-mesometrial distance

MCHC……..Mean cell haemoglobin concentration

MCV…….Mean cell volume

MEL……. Mouse erythroleukemia

MHC……Histocompatibility complex

MMP…….Matrix metalloproteinase

mPL……...Mouse placental lactogen

mPLF……Mouse proliferin

mPRP……Mouse proliferin related protein

mRNA……...Messenger RNA

NBF……..Neutral buffer formalin

NEFA……Non-esterified fatty acids

NK……Natural killer cells

NMD…….Nonsense mediated decay

NO…….Nitric oxide

NP…….Non-pregnant

Ob-R…….....Soluble leptin receptor

pA……..Poly A tail

PABP…….Poly(A)-binding protein

PALS…….Periarteriolar lymphoid sheath

PAM……. PABP-interacting motif

PAP……... Polyadenylation by poly(A)-polymerase

PAPP-A……. Pregnancy-associated plasma protein A

PCR……...Polymerase chain reaction

PE……..Pre-eclampsia

PERK…….Protein kinase RNA-like endoplasmic reticulum kinase

PIC…….Pre-initiation complex

PKR……..Protein kinase R

PL……..Placental lactogen

P-rich…….Prolin-rich region

PRL……...Prolactin

P-TGC……...Parietal trophoblast giant cell

qRT PCR……...Quantitative real-time polymerase chain reaction

RBC……..Red blood cell count

RDW…….Red cell distribution width

RI……..Resistance index

RNA……..Ribonucleic acid

RNAP……....RNA polymerase

RPF……...Renal plasma flow

RRM……..RNA-recognition motif

rRNA…….Ribosomal RNA

SA…….....Splice acceptor site

SD…….Standard deviation

SEM……..Standard error of the mean

sFlt…….....Soluble Flt

SGA……..Small for gestational age

SpA……...Spiral artery

SpA-TGC….....Spiral artery-associated trophoblast giant cell

SpT……Spongiotrophoblast cell

S-TGC……...Sinusoidal trophoblast giant cell

SynT……..Synciotiotrophoblast cell

TE…….Trophectoderm

TG…….....Triglycerides

TGC……..Trophoblast giant cell

TIMP……Tissue inhibitor of metalloproteinase

tPABP……...Testis poly(A)-binding protein

tRNA……Transfer RNA

uNK…….....Uterine natural killer cells

UNR…….. Upstream of n-Ras

UTR……..Untranslated region

VEGF…… Vascular endothelial growth factor

VP…….....Vaginal plug

WB……White blood cells

WBC…….White blood cell count

WHO……..…World Health organisation

WPMZ……..White pulp marginal zone

WT……Wild-type

WTSI……Wellcome Trust Sanger Institute

WVM……Vanishing White Matter

Contents

List of Figures

List of Tables

Chapter 1 - Literature review

1.1 Introduction

Although international definitions vary, in the UK late miscarriage is defined as a pregnancy loss between 12-24 weeks of pregnancy, with stillbirth occurring after 24 weeks (Smith and Fretts, 2007). In the UK, around 5/1000 babies are stillborn each year (Downe et al., 2012). Comparatively, for every 1,000 babies born, only 1 will have Down's syndrome (Down's syndrome association) and stillbirth is 10 times more common than Sudden Infant Death Syndrome (Information and Statistics Division NHS Scotland. Scottish perinatal and infant mortality report 2000. Edinburgh: ISD Scotland Publications, 2001). Despite this, UK stillbirth rates have decreased by only 5% in the period from 2000 to 2008 meaning there is an urgent unmet clinical need for research into the underlying causes of mid-late fetal mortality.

One of the risk factors for late miscarriage and stillbirth is intra-uterine growth restriction (IUGR) (Gardosi et al., 2013). The American College of Obstetricians and Gynaecologists define IUGR as a condition where the fetus is below the tenth percentile of its genetic growth potential with respect to gestational age (Gynecologists., 2001). IUGR may complicate 7-10% of all pregnancies (Demicheva and Crispi, 2014) and is of importance not only because it may lead to mortality, but also morbidities. For instance, *in utero* cardiac dysfunction can persist postnatally and may lead neurodevelopmental problems in childhood and a higher cardiovascular risk later in life (Demicheva and Crispi, 2014). Other long term consequences of IUGR include an increased risk of developing metabolic syndrome, obesity, insulin resistance and well as type II diabetes in adulthood (reviewed by (Salam et al., 2014).

Whilst the aetiology of IUGR, late miscarriage and stillbirth is attributable to multiple factors including fetal chromosomal abnormalities (10%) and haemorrhage (15%), in 59% of cases fetal deaths remain unexplained (Flenady et al., 2011) although 23% of these cases display IUGR. Where investigated, poorly-defined causes such as

uteroplacental insufficiency are often cited, but the actual molecular lesion(s) underlying these, in particular those with a maternal origin remain unknown.

Despite differences to humans, mice provide a powerful model for studying human pregnancy as many of the key features of pregnancy are maintained. In humans and mice, the yolk sac plays a role in feto-maternal exchange in early pregnancy with the placenta taking over in later pregnancy (reviewed by (Cox et al., 2009). In contrast to humans, the yolk sac is integrated into the chorioallantoic placenta in mice becoming an intraplacental yolk sac (IPYS) which remains functional throughout pregnancy. In both species the placenta is haemochorial, meaning that fetal tissue is directly in contact with maternal blood, and discoid in shape where chorionic villi are arranged in a circular plate. Furthermore, maternal blood from the uterine arteries enter the placenta from large diameter spiral arteries located in the maternal decidua which are invaded only superficially in mouse in comparison to the human where in addition to the decidua they are also remodelled in the myometrium. In both human and mouse the umbilical vessels connect the fetal capillaries of the placental exchange region with the fetal body circulation (Georgiades et al., 2002a). From an experimental point of view mice offer a number of other advantages including an ability to manipulate its genome, short reproductive cycle and accelerated lifespan. However, the short reproductive cycle means that the mouse embryo is born almost immediately after all the organs develop in contrast to the human embryo which continues to stay in the uterus for a few more months at the end of organogenesis so that organs continue to grow and eventually develop into their proper sizes for birth (Xue et al., 2013).

Observations in humans and studies in model organisms including mice, have highlighted the critical role that the placenta plays in the development and growth of the fetus. Disruption of placental development and/or function can lead to placental insufficiency, fetal growth restriction and fetal mortality (Rossant and Cross, 2001) . Successful placental development, which begins as early as embryonic day (e) 3.5 in the mouse, is complex and requires accurate embryo implantation, endometrial decidualisation (transdifferentiation of endometrial fibroblasts into decidual cells) and remodelling of maternal arteries. As a result, placentation is dependent upon a tightly regulated dialogue between the fetus and the mother (materno-fetal dialogue). The

placenta, in turn, also drives many of the required changes in maternal physiology (i.e. maternal adaptation). This complex materno-fetal dialogue is important for healthy pregnancy and requires exquisite regulation of gene expression. Gene expression can be controlled at many levels including transcription (Coulon et al., 2013), mRNA processing and export (Hocine et al., 2010), mRNA translation and/or mRNA stability (Burgess and Gray, 2010; Dever and Green, 2012; Fatscher et al., 2015; Moore and Proudfoot, 2009; Orphanides and Reinberg, 2002; Roux and Topisirovic, 2012)). However, although recent studies in other systems have drawn attention to the importance of translational control (Schwanhäusser et al., 2011), little is known regarding the contribution of regulated mRNA translation and/or stability to materno-fetal dialogue (Rossant and Cross, 2001). Interestingly in this regard, we have found that deletion of a member of the poly(A)-binding protein family (PABP), which are regulators of mRNA translation and stability, results in maternal genotype-dependent mid-late gestational mortality and IUGR.

1.2 Eukaryotic gene expression

For cells to carry out their function and respond to environmental changes appropriately, genes must be decoded into proteins in the correct spatiotemporal manner. A balance between the protein's production and degradation determines the quantity of a specific protein in a cell, at any given time. In eukaryotes the key processes for protein production, are transcription and RNA processing followed by translation. Many of these steps involve RNA-binding proteins, of which the poly(A)-binding proteins (PABPs) are an important family.

1.2.1 mRNA transcription and processing

The conversion of the genetic information, encoded by deoxyribonucleic acid (DNA), into proteins starts in the nucleus with creation of pre-messenger ribonucleic acids (pre-mRNAs), which when processed, form the template for protein synthesis. RNA polymerase II (RNAPII) transcribes all protein-coding mRNAs and most non-coding RNAs (e.g. miRNAs) in a three step process; initiation, elongation and termination. During initiation, RNAPII, associated with transcription factors, binds to the promoter region of genes which is normally near their 5' end (reviewed by (Sims et al., 2004). The activity of promoters is controlled by the binding of regulatory factors but can also be regulated by sequences located at distant sites such as enhancers (Erokhin et al., 2015). The DNA is melted to expose the DNA template strand allowing it to be read in 3' to 5' direction, creating an RNA with complementary nucleotides in which thymine is replaced by uracil (reviewed by (Sims et al., 2004). Many mRNA processing steps occur post-transcriptionally, with the first being addition of a methylated guanine to the 5' end of the emerging RNA strand. This confers stability, by protecting it from 5' to 3' exonucleases, enzymes which processively remove the 5' terminal nucleotides causing degradation (Hocine et al., 2010). Poly(A)-dependent termination couples transcription to 3' end polyadenylation, through cleavage of the nascent pre-mRNA and addition of a poly(A)tail of approximately 100-200 adenine bases. Cleavage requires a number of factors including cleavage and polyadenylation specificity factor (CPSF) which also plays a role in polyadenylation by poly(A)-polymerase (PAP). Polyadenylation is initially distributive but becomes progressive when the nascent poly(A) tail is bound by nuclear PABP (PABPN1, PABP2, PABII). PABPN1 enhances the affinity of PAP for poly(A) and also interacts with CPSF. The molecular ruler model for PABPN1 function proposes that loss of CPSF-PABPN1 interactions as the poly(A) tail is extended, disrupts CPSF-PAP-PABPN1 complexes resulting in loss of progressive adenylation and therefore PAP, thereby determining poly(A) tail length (Eckmann et al., 2011). It is worth noting that about 50% of human mRNAs are thought to have alternative polyadenylation sites (APA), with PABPN1 playing a role in polyadenylation selection (Hollerer 2014, pp. 16). Most eukaryotic mRNAs also contain non-coding regions, referred to as introns, which can be

interspersed between the exons in the pre-mRNA, and are removed by splicing to form "mature" mRNAs (Ghildiyal and Zamore, 2009; Hocine et al., 2010). Removal of introns and polyadenylation are both critical for mRNA export to the cytoplasm, with PABPN1 appearing to be an active driver of this process since both its targeting by viral proteins (Chen et al., 1998; Qiu and Krug, 1994) or siRNA knock-down block export (Apponi et al., 2010; Calado et al., 2000). Cytoplasmic PABPs (PABPCs, called PABPs hereafter) also shuttle to through the nucleus, although they are predominantly cytoplasmic in normally growing cells (Gorgoni and Gray, 2004; Mangus et al., 2003). However, nuclear functions for PABPs remains to be described but knock-down experiments suggest that, in contrast to PABPN1, they are not required for mRNA export (Burgess et al., 2011). Indeed export of PABPs appears mRNA-dependent, suggesting they exit bound to poly(A) tails, however, bulk exchange of PABPN1 by PABPs is thought to occur as mRNAs emerge into the cytoplasm (reviewed by (Muller-McNicoll and Neugebauer, 2013). Here, PABPs mediate the critical role of the poly(A) tail in mRNA translation and stability, mainly by promoting the closed-loop mRNA conformation, which enhances ribosome subunit recruitment and inhibits access of 3' to 5' exonucleases.

1.2.2 Overview of mRNA Translation

Mature mRNAs contain a 5'cap, a 3'poly(A) tail and an open reading frame flanked by 5' and 3' untranslated regions and can be specifically localised, stored, degraded and/or translated to produce proteins (Jackson et al., 2010) following their export into the cytoplasm. Translation is mediated by large ribonucleoprotein machines called ribosomes, that consist of a 40S small subunit and 60S large subunit in eukaryotes, and which together with tRNAs and numerous translation factors decode the nucleotide triplets within the open reading frame (also called coding sequence) to the correct sequence of amino acids, thereby synthesizing polypeptides. Similarly to transcription, translation is divided into three phases: initiation, elongation and termination. Initiation, where the translation machinery is assembled on mRNAs, is widely

considered to be the main rate limiting regulatory step in translation, and will be discussed in more detail below. Following initiation, elongation ensues and results in the decoding of the nascent peptide. Termination occurs, when a stop codon (UAA, UAG or UGA) is encountered and the nascent peptide is released (Dever and Green, 2012). In contrast to initiation, elongation and termination are broadly similar in prokaryotes and eukaryotes (reviewed by (Kozak, 1999).

1.2.3 Translation initiation

Initiation, requires a complex array of eukaryotic initiation factors (eIFs) and can be sub-divided into two initial mRNA-independent and seven mRNA-dependent stages: 1. Assembly of a ternary complex between the initiator tRNA, and eIF2 bound by GTP 2. Recruitment of the ternary complex to the small ribosomal subunit and associated factors (i.e. eIF1, eIF1A, eIF3, eIF5) to form a 43S pre-initiation complex (PIC). 3. Binding of eukaryotic initiation factor 4F (eIF4F), composed of eIF4E, eIF4G and eIF4A, to the 5' cap (reviewed by (Jackson et al., 2010). eIF4E is the cap binding factor but its affinity for the cap is enhanced in an RNA-dependent manner by eIF4G. 4. Removal of secondary structure from the 5'UTR to allow PIC binding, a process in which the ATP-dependent RNA helicase action of eIF4A is promoted by an additional factor, eIF4B. 5. Recruitment of the PIC at or near the cap, a process facilitated in part by the interaction between mRNA-bound eIF4G and eIF3 on the small ribosomal subunit. 6. The PIC then moves or "scans" along the 5'UTR until it reaches a suitable start codon, normally but not always an AUG. 7. Start site recognition involving base pairing between the Met-tRNAi and the AUG in the peptidyl-tRNA (P) site of the small ribosomal subunit and 8. eIF5-dependent hydrolysis of eIF2-GTP to eIF2-GDP and release of eIF2-GDP and several other eIFs. eIF2-GDP must be recycled to eIF2-GTP by eIF2B for subsequent rounds of initiation. 9. Lastly, large (60S) subunit joining occurs, catalyzed by eIF5B, in a GTP-dependent manner, to produce an 80S initiation complex containing Met-tRNAi base-paired to AUG in the P site, which is competent to begin elongation (Pestova, 2007) (Figure 1.1.).

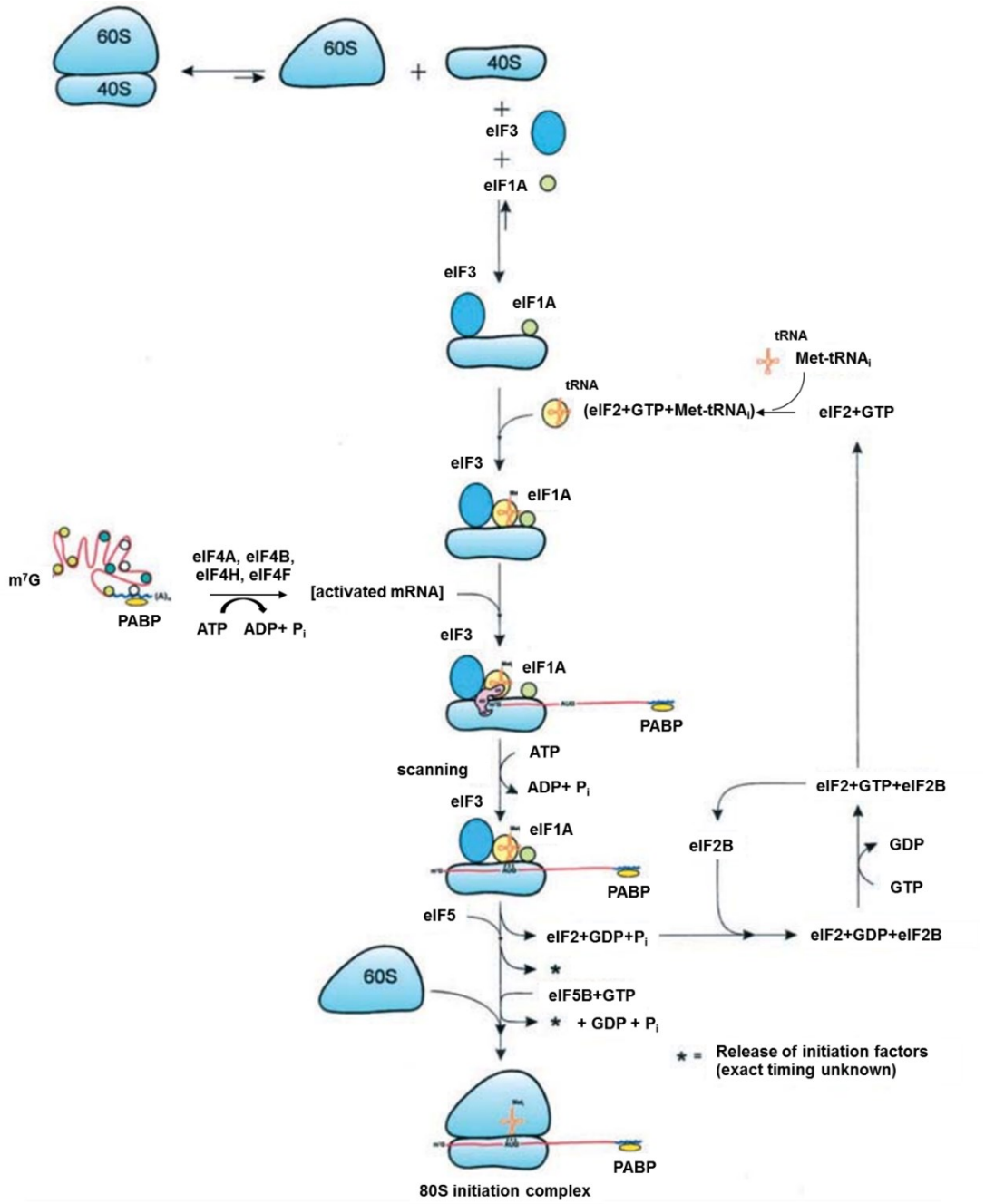

Figure 1.1. The initiation pathway in eukaryotes. (From (Merrick, 2003))

Surprisingly, since these events occur on the 5'UTR, the 3'poly(A) tail is also pivotal for efficient translation, through the action of PABPs which are a key component in the complex that forms the closed-loop conformation (reviewed by (Gallie, 1991).

1.2.4 mRNA decay

The extent to which an mRNA is utilised to make protein is not only affected by its rate of translation but also by its stability, which varies by orders of magnitude between mRNAs (reviewed by (Guhaniyogi and Brewer, 2001). The main and rate limiting step in mRNA decay is removal of the poly(A) tail (reviewed by (Brook and Gray, 2012). Poly(A) tails are initially trimmed by the PAN2-PAN3 complex until reaching a length of approximately 110 nucleotides at which point they undergo more rapid degradation by the ccr4-Not complex. Upon removal of the poly(A) tail, mRNAs are rapidly degraded either by dcp1/dcp2 driven decapping and 5' to 3' degradation by Xrn1 exonuclease or in a 3'-5' direction by the exosome (reviewed by (Fatscher et al., 2015)). Not all mRNAs are degraded in this manner, for instance, those containing premature stop-codons are degraded in a deadenylation independent manner by nonsense-mediated decay pathway (reviewed by (Brook and Gray, 2012).

1.2.5 Dysregulated mRNA translation or stability are associated with disease.

mRNA translation and stability are both highly regulated processes which are important in almost every aspect of biology . For instance, global translation may be down-regulated in response to cell stress, or up-regulated in response to growth factors and hormones (Ivanov and Anderson, 2013), enabling cells to respond to environment cues. Such global changes are often mediated through signalling cascades that result in the phosphorylation of eIF2 or 4E-BP (e.g. mTOR). eIF2 phosphorylation by kinases including protein kinase RNA-like endoplasmic reticulum kinase (PERK) and protein kinase R (PKR) blocks eIF2-GDP to eIF2-GTP exchange, by eIF2B, limiting the amount of active eIF2 available for initiation. 4E-BP is phosphorylated by mTOR, and dependent on its phospho-status interacts with eIF4E to sequesters it, preventing eIF4F formation (reviewed by (Musa et al., 2016). To achieve the necessary reprogramming of gene expression, global control is often accompanied by mRNA-

specific translational and/or stability control of individual or small subset of mRNAs e.g. encoding proteins required to adapt to a specific cell stress (reviewed by (Spriggs et al., 2010). However, mRNA-specific regulation often occurs in the absence of global changes in protein synthesis, contributing to a wide variety of biological processes and normally involves regulatory elements located within the untranslated regions which frequently provide binding sites for trans-acting proteins/protein complexes (reviewed by (Besse and Ephrussi, 2008). One of the best characterised examples of mRNA specific regulation is in iron homeostasis (reviewed by (Wilkie et al., 2005) where, dependent on intracellular iron concentrations, iron regulatory protein binds to 5'UTRs of target mRNAs (e.g. iron storage protein, ferritin) to repress their translation and the 3'UTR of other target mRNAs to enhance their stability (e.g. transferrin receptor which imports iron).

Similarly intricate networks have been delineated using the power of *Drosophila* genetics to reveal how morphogen gradients are created by a combination of mRNA specific translation and decay (e.g. of Oskar, Bicoid, Nanos, Hunchback) during development to establish body patterning (reviewed by (Gurdon and Bourillot, 2001; Lipshitz, 2009). Localised translation underlies multiple aspects of neuronal biology, including dendrite branching and plasticity and is crucial for processes such as learning and memory (reviewed by (Gray et al., 2015; Holt and Schuman, 2013). Finally, much attention has been focused in recent years on microRNAs (miRs) that bind to the 3'UTR of specific mRNAs to repress their translation and/or induce their decay (reviewed by (Janas and Novina, 2012).

Not surprisingly, aberrant control of mRNA translation and stability are associated with a wide range of diseases (reviewed by (Hollams et al., 2002). For example, dysregulated translation is linked to altered proliferation, survival, and angiogenesis and is thus omnipresent in human cancers (reviewed by (Bhat et al., 2015). Whilst cancer can be associated with specific translation factors, ribosomes, or upstream signalling pathways, one of the best described examples is eIF4E whose oncogenic potential was first described in cell lines (Lazaris-Karatzas et al., 1990) (Rinker-Schaeffer et al., 1993) and later in mice (Ruggero et al., 2004). eIF4E overexpression is commonly associated with malignant progression of a number of human cancers

such as breast, colon, bladder, lung, prostate, head and neck cancers as well as leukaemias, lymphomas and melanomas (De Benedetti and Graff, 2004) and drives cellular transformation, tumorigenesis, and metastatic progression in experimental models (reviewed by (Graff et al., 2008). Consequently it is an adverse prognosis marker in some of these cancers (Khosravi et al., 2015) but is also an emerging anticancer drug target (Lu et al., 2016). Similarly other components are causative in a wide variety of genetic conditions such as leukoencephalopathy with Vanishing White Matter (VWM) as a result of inherited mutations affecting eIF2B subunits, genetic syndromes including the Wallcott-Ralinson syndrome, a rare autosomal recessive disorder characterised by permanent neonatal or early infancy insulin-dependent diabetes in which eIF2AK3 is mutated (Delepine et al., 2000) and in numerous ribosomopathies where the biosynthesis of ribosomes is affected (reviewed by (Armistead and Triggs-Raine, 2014).

Disease can also be caused by dysregulation of specific mRNAs by mutations in regulatory elements like in hyperferritinamemia cataract syndrome where the iron responsive elements (IREs) that finely regulate ferritin mRNA translation in response to iron availability are mutated (Roetto et al., 2002). Other example include dysregulation of mRNA stability whereby altered mRNA stability, for example of human β-globin mRNA leads to thalassemia, an inherited blood disorder in which an abnormal form of haemoglobin is made (reviewed by (Peixeiro et al., 2011). Mutations can also be in the regulatory trans-acting factors such as fragile X mental retardation protein (FMRP) which both represses translation and regulates mRNA stability. Absence of FRMP disrupts this regulation and leads to fragile X syndrome (FXS), a cause of intellectual disability and common cause of autism (reviewed by (Richter et al., 2015).

1.2.6 Translation and mRNA stability in reproductive biology

Due to periods of transcriptional quiescence, germ cells and early embryos have provided many examples of mRNA-specific regulation as changes in the patterns of protein synthesis can only be achieved by the activation, repression or destruction of pre-existing mRNAs. The best characterised mechanism of regulating mRNAs in germ cells is by dynamic changes in poly(A) tail length where increase in the poly(A) tail generally leads to translational activity, whilst shortening correlates with translational inactivation (reviewed by (Brook et al., 2009; McGrew et al., 1989; Vassalli et al., 1989). For example, oocyte mRNAs contain 3′UTR elements that target them for rapid poly(A) tail shortening following export into the cytoplasm so that they remain translationally silent until they are required. Once required their poly(A) tail length is increased in a process known as cytoplasmic polyadenylation (reviewed by (Brook et al., 2009). However, not all germ cell mRNAs must undergo changes in poly(A) tail length for their activation, as exemplified by the DNA-replication histone mRNAs, the only eukaryotic mRNAs to lack a poly(A) tail (Allard et al., 2005). Germ cells also encode germ-cell specific translation factors, such as the spermatogonial proliferation factor Eif2s3y in males (Yamauchi et al., 2016).

Whilst the factors (e.g. RNA-binding protein, kinases) known to regulate mRNA specific translation/stability in germ cells are present in humans, suggesting that regulatory mechanisms are conserved, this has rarely been experimentally examined. However, it is clear that cytoplasmic polyadenylation, for instance, occurs during human oocyte maturation and injection of reporter mRNAs containing human 3'UTRs recapitulates their adenylation in other species (i.e. Xenopus) (Prasad et al., 2008). Because of the paucity of studies, the contribution of dysregulated mRNA translation and stability to human reproduction is only just starting to emerge. For example, disruption of the mammalian target of rapamycin complex 1 (mTORC1) pathway, which phosphorylates 4E-BP to regulate eIF4F complex assembly and promotes rRNA and tRNA transcription thereby regulating processes such as protein synthesis and cellular growth and proliferation (Bhat et al., 2015; Roux and Topisirovic, 2012), leads to fertility problems as well as cancer in the female reproductive tract. Specifically,

the disruption of Tsc1, a direct inhibitor of mTORC1, results in oviductal hyperplasia and implantation failure (Daikoku et al., 2013) as well a reduction in oocyte quality and primordial follicle number and subsequent premature ovarian failure (Tanaka et al., 2012).

One of the best characterised examples involving an RNA-binding protein emerged from the identification of deletions of the Deleted in AZoospermia (DAZ) genes on the Y-chromosome in 10-15% of men with non-obstructive oligo or azoospermia, which describes men with little or no sperm (Reijo et al., 1995). These observations strongly supported DAZ as a candidate infertility gene, with studies of the two autosomal family members, DAZ-Like (DAZL) and BOULE, in animal models establishing the critical role of this family in gametogenesis. For instance, Dazl, is essential for meiosis and PGC migration and proliferation in both male and female mice (Lin and Page, 2005; Ruggiu et al., 1997) and primordial germ cell migration and survival in *X. laevis* (Houston and King, 2000). In mice it has also been shown to also function in the maintenance of pluripotency and epigenetic programming of primordial germ cells (Haston et al., 2009). The absence of DAZ in model organisms has hampered its direct study but transgenic DAZ expression can rescue the Dazl phenotype in mice, providing support for a shared molecular function and DAZ deletions being causative of failed spermatogenesis in men. Molecular biology studies have further established that all family members are mRNA-specific activators of translation: they activate the translation of key germ cell mRNAs by binding to their 3'UTR and recruiting of PABPs, via direct protein-protein interactions, independent of the poly(A) tail (Collier et al., 2005).

1.2.7 mRNA translation and stability in pregnancy

In contrast to germ cells and early embryogenesis little is known regarding the contribution of regulated mRNA translation and/or stability to pregnancy in any species (Rossant and Cross, 2001). However, a handful of examples exist. For instance in mice, the knockout of *Zfp36L1*, a gene which encodes zinc finger protein 36-like 1

(Zfp36L1) accelerated mRNA degradation, and resulted in *in utero* death by e11, most likely due to aberrant or failed chorioallantoic fusion (Stumpo et al., 2004).

Furthermore, Yung et al were the first to provide evidence in 2008 of endoplasmic reticulum stress and subsequent protein synthesis attenuation in the placenta may have an important role in the pathophysiology of IUGR (Yung et al., 2008). Specifically, they showed that there is an increase in phosphorylated eIF2α and a reduction in AKT signalling in human IUGR placentas. This is further exacerbated in IUGR placentas from pregnancies affected by preeclampsia. *In vitro* experiments in two trophoblast-like cell lines, JEG-3 and JAR cells, showed that the reduced AKT signalling resulted in reduced 4E-BP phosphorylation, it's binding to eIF4E and inhibited cap dependent translation. The reduction in AKT signalling also resulted in reduced GSK-3 phosphorylation promoting its activity. Active GSK-3 binds the epsilon subunit of eIF2B preventing it from its role in regenerating eIF2.GTP from eIF2.GDP, which is crucial for translation initiation.

The work herein shows that loss of function of a member of the poly(A)-binding protein family, PABP4, results in mid-late gestational mortality and IUGR.

1.3 Metazoan poly(A)-binding proteins (PABPs)

PABPs are conserved throughout eukaryotes, with the number of PABPs being linked to organism complexity. For instance, *Drosophila* has only one PABP gene (pABP), whilst vertebrates encode three PABPs; PABP1 [PABPC1], PABP4 [PABPC4, iPABP] and embryonic PABP [ePABP/ePAB, PABP1L), and mammals two additional members, testis-specific PABP [tPABP] and PABP5 [PABPC5]. These share a common domain organization made up of four N-terminal non-identical RNA-recognition motifs (RRMs) and, with the exception of PABP5, a C-terminal region composed of a proline-rich linker region and a globular PABC domain (Fig.5) (Blanco et al., 2001; Kühn and Wahle, 2004). This is distinct from PABPN1 and ePABP2 which have a glutamic acid-rich N-terminus (E-rich), a single RNA recognition motif

(RRM) and an arginine-rich (R-rich) domain at the C-terminus. However, like PABPN1, PABPs interact with the poly(A) tail via their RNA-recognition motifs (RRMs). RRMs 1-2 are mainly responsible for high affinity poly(A)-binding (Eliseeva et al., 2013) but the specificity of RRMs 3-4 is less clear, although they can interact with AU-rich sequences (Eliseeva et al., 2013). The proline-rich region is the least conserved domain but mediates ordered binding to poly(A) through its ability to self-associate (Kühn and Pieler, 1996; Melo et al., 2003). Finally, the PABC domain appears to be the predominant protein-protein interaction domain (Albrecht and Lengauer, 2004; Kozlov et al., 2001), although the RRM regions also bind a series of important protein partners (see Figure 1.2).

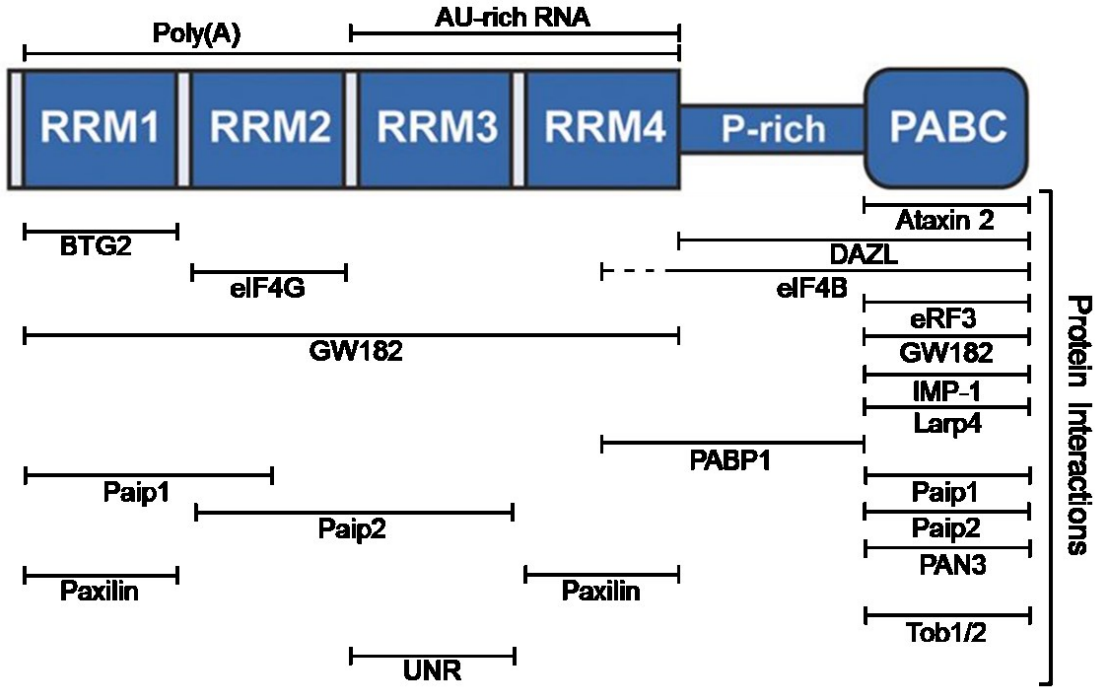

Figure 1.2 PABP1 domain-specific RNA and protein interactions.

The domain organisation of PABP1 is depicted identifying the regions of PABP1 which interact with RNA and protein partners. RRMs 1 and 2 mediate the majority of poly(A)-binding, but the RNA-binding specificity of RRMs 3 and 4 remains unclear, although affinity towards AU-rich sequences has been shown. RRM sections also bind several protein partners; B-cell translocation gene (BTG)-2, deleted in azoospermia-like (DAZL), eukaryotic initiation factor (eIF)-4B, eIF4G, glycine-tryptophan protein (GW)182, PABP-interacting protein (Paip)-1, Paip2, Paxillin and upstream of n-Ras (UNR). Many PABP1 protein partners which bind the PABC domain contain a PABP-interacting motif (PAM)-2 e.g. ataxin-2, eukaryotic release factor (eRF)-3, GW182, La-related protein (Larp)-4, Paip1, Paip2, poly(A) nuclease (Pan)3 and transducer of Erb (Tob)-1/2. NB: Although only DAZL is depicted, all DAZ family members interact with the C-terminal region. Solid line; currently defined minimal binding sites. Dashed line; eIF4B binding is not clearly defined, but requires the C-terminus. Adapted from (Burgess and Gray, 2010).

PABP1, is the prototypical family member, and is by far the best studied family member and has been ascribed multiple roles in mRNA translation, stability and localization, although there is currently no evidence for a direct role in the latter (reviewed by (Derry et al., 2006; Gorgoni and Gray, 2004; Mangus et al., 2003). The

best studied role of PABP1 is in promoting translation initiation when bound to the poly(A) tail, with the presence of the cap and poly(A) tail having synergistic effects on translation in many systems (Svitkin and Sonenberg, 2004). The magnitude of the effect of the poly(A) tail appears dependent on poly(A) tail length, the nature of the mRNA and the system in which it is being studied. PABP depletion and add back experiments *in vitro* showed that PABP was important for the effect of the poly(A) tail on translation (Svitkin and Sonenberg, 2004), whilst tethering PABP to non-adenylated mRNAs in *X. laevis* oocytes, showed that PABP could substitute for the poly(A) tail and that the function of the poly(A) tail is to provide a scaffold for PABP-binding (Gray et al., 2000). The efficiency of longer poly(A) tails being explained by their ability to accommodate more molecules of PABP and/or compete for limiting PABP more effectively. Sucrose gradient analysis using defined inhibitors of initiation to block initiation intermediates in mammalian cell free extracts showed that PABP could enhance the binding of the small ribosomal subunit (Kahvejian et al., 2005). This was consistent with reports that PABPs from several species interacted with one or more factors that acted at, or prior to, small subunit joining. In mammals these were eIF4G, eIF4B, and PABP-interacting protein 1 (PAIP1), a protein with homology to the middle and C-terminal domains of eIF4G (Derry et al., 2006; Gorgoni and Gray, 2004; Mangus et al., 2003). The interaction of PABP1 with eIF4G has been widely studied providing much support for a functionally important interaction (Gorgoni and Gray, 2004). Moreover, atomic force microscopy studies using purified yeast PAB-1, eIF4G and eIF4E showed that these three proteins were sufficient to result in the 'closed loop formation' of the mRNA, observable as diamond ring like structures (Wells et al., 1998) (Figure 1.3). These observations explained the synergy of the cap and poly(A) tail in promoting initiation and it was suggested that it would result in increased affinity of eIF4E for the cap and PABP for the poly(A) tail (Goss and Kleiman, 2013). As cap-binding is considered rate limiting, this provides a molecular explanation for the observed increase in small ribosomal subunit joining (Kahvejian et al., 2005). However, whilst this model has become dogma, some data controvert the importance of the PABP-4G interaction (reviewed by (Mangus et al., 2003), and it remains to be demonstrated that PABP actually enhances eIF4G binding to mRNA, although it is clear RNA-binding by eIF4G is required for its stabilization of eIF4E-

cap binding (Yanagiya et al., 2009). The effects of Paip1 are less well studied, although its absence reduces the effect of the poly(A) tail on translation, and it has been suggested to help stabilize the eIF4E-eIF4G-PABP end-to-end complex (Derry et al., 2006). Direct effects of the reported interaction between eIF4B and PABP on translation remain to be shown (Kahvejian et al., 2001). Moreover, it is clear that the effects of PABP are pleiotropic as the sucrose gradient analysis also showed an effect on 60S joining (Kahvejian et al., 2005), an observation that as of yet, has no firm mechanistic basis in metazoans. PABP1 has also been shown to inhibit deadenylation, the first step in mRNA turnover, as PABP depletion in cell-free extracts negates the stabilizing effect of the poly(A) tail (Brook and Gray, 2012). Although, less well understood than its role in translation, this has been explained by a simple steric model in which PABP binding to poly(A) physically occludes the entry of deadenylases, a model which is supported by the detection of deadenylation intermediates corresponding to the sequential loss of PABP footprints (Brook and Gray, 2012). The formation of the closed-loop model "clamping" eIF4E on the cap and PABP on the poly(A) tail, forming a further barrier to deadenylation-dependent decay, providing one possible explanation for the complex links between mRNA translation and stability. However, the situation is more complex as the PABC domain of PABP1 binds to and stimulates the activity of the PAN2/PAN3 complex and can recruit the Ccr4-Not complex via intermediate proteins such as TOB (Brook and Gray, 2012). These apparently opposing functions in regulating deadenylation remain to be understood. PABPs also have less well understood roles in regulating mRNA specific translation and stability (Burgess and Gray, 2010). These include their functions in promoting the translation of mRNAs undergoing cytoplasmic polyadenylation and in the poly(A) tail independent activation of mRNAs by Dazl, where it is recruited to form an alternative closed loop complex comprising of Dazl bound to the 3'UTR, PABP, eIF4G and eIF4E-bound to the 5'end (Collier et al., 2005). PABP1 can also autoregulate its own translation as part of a repressive complex with IMP-1 and Unr when all available poly(A) tail sites are occupied (Burgess and Gray, 2010). Similarly, PABP participates in a number of different complexes to regulate the decay of specific mRNAs. Well characterized examples include α-globin mRNA where its stabilises the binding of an RNA-binding protein complex to the 3'UTR occluding an

endonucleolytic cleavage site and *c-fos* mRNA where its interaction with a complex of proteins including Paip1, Unr and AUF1 bound to a site within the open reading frame prevent deadenylation of the mRNA prior to its translation. PABPs also have complex but not fully delineated roles in the control of mRNAs containing AU-rich elements (AREs) which can be stabilised, destabilized or repressed by binding of a variety of ARE-binding proteins (ARE-BPs, AUBPs) (Burgess and Gray, 2010). AUBPs can alter PABP-poly(A)-binding and its interaction with deadenylases to either favour or disfavour deadenylation. Moreover, PABPs can antagonise interactions of ARE-BPs with deadenylases and, as mentioned earlier, can bind AREs directly (Burgess and Gray, 2010).

PABP1 also participates in miRNA-mediated regulation for example via its interaction with the miRNA-containing RISC complex which enhances translational repression and deadenylation (Goss and Kleiman, 2013). Lastly, it is involved in mRNA surveillance pathways where it discriminates between mRNAs with and without premature stop codons, the former then being subject to nonsense mediated decay (NMD) (Brook and Gray, 2012). Thus, based mainly on studies of PABP1, PABPs are considered to be central regulators of mRNA translation and stability (reviewed by (Mangus et al., 2003). Many of the functions of PABP1 appear to be conserved in ePABP, with ePABP being best studied in Xenopus and mouse (Friend et al., 2012; Guzeloglu-Kayisli et al., 2012; Voeltz et al., 2001; Wilkie et al., 2005). Little information is available for tPABP with a single study providing data that both supported and contradicted a conserved function in translation (Kimura et al., 2009), however, as tPABP arose from a retrotransposition of PABP1 and is almost identical in sequence, it seems likely that their functions will be conserved. In contrast, the absence of the C-terminal region in PABP5 and its relatively poor conservation in the RRMs regions may it unlikely that it shares many of the molecular functions of PABP1. (PABP4 is discussed in section 1.3.3).

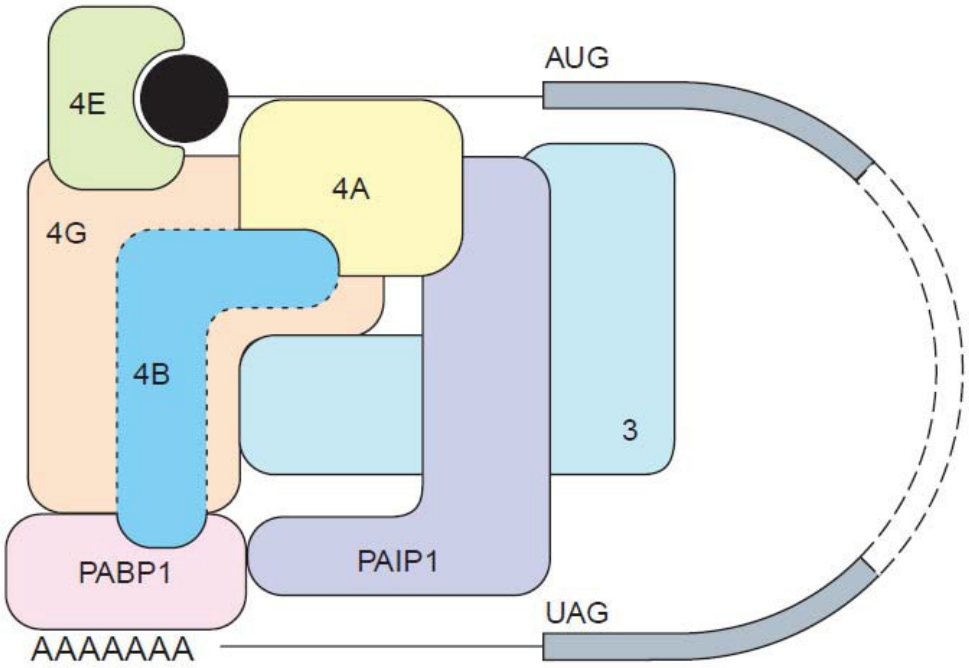

Figure 1.3 Simplified "closed-loop" model showing how PABP stimulates translation initiation by bringing together the 5' and 3'UTRs.

Interaction of PABP1 with eIF4G, which also binds the cap-binding protein eIF4E, brings the ends of the mRNA into functional proximity. Additional interactions of PABP1 with Paip1, and perhaps eIF4B (shown with a dotted outline), further stabilise this closed loop conformation, which is proposed to enhance PABP, eIF4G and eIF4E-binding, increasing the recruitment of ribosomal subunits and promoting translation (Burgess et al., 2011; Burgess and Gray, 2010; Brook et al., 2009). The formation of this 'closed-loop' conformation also protects mRNAs from deadenylation and decay. From (Brook et al, 2009)

1.3.1 Expression patterns of vertebrate PABPs

Expression patterns can be informative with respect to putative functional consequences resulting from gene deletion. However, to date very little information on the tissue and cellular expression of different PABPs is available. Northern blotting has shown that both PABP1 and PABP4 mRNAs are expressed in a wide variety of mouse tissues (Yang et al., 1995), consistent with analysis of PABP1 protein and

PABP4 mRNA in adult tissues and developmental stages in *X. laevi*s which suggest that both are widely expressed (Gorgoni et al., 2011; Wilkie et al., 2005). However, the expression pattern of PABP1 and PABP4 proteins between and within tissues remains largely unexplored. The most detailed analysis of PABP mRNA expression in mammals is in mouse and human testis, where PABP1 is found in spermatocytes and round spermatids (Feral et al., 2001). The absence of PABP1 mRNA in the spermatogonial stem cells shows that the widely held assumption that PABP1 is ubiquitous based on its lethality of PAB-1 deleted S. cerevisiae (Sachs et al., 1987) is not proven. Testis is also the site of expression of the mammalian specific tPABP with its mRNA being present in late pachytene spermatids and haploid round spermatids in mouse, and only round spermatids in humans (Kleene et al., 1994). tPABP protein distribution mirrors that of its mRNA in mouse testis (Kimura et al., 2009) with immunofluorescence suggesting that it is enriched in the chromatoid bodies of round spermatids (Kimura et al., 2009) which are RNA-protein rich granules. Proteomic analysis of these granules showed they also contain PABP1 (Meikar et al., 2014).

ePABP was first identified in *X. laevis* where it is considered to be specific to pre-neurula embryonic stages and oocytes (Voeltz et al., 2001), indeed it is considered the predominant PABP in late oocytes and early embryos, where PABP1 is scarce. ePABP mRNA can, however, also be detected at low levels in *X. laevis* and mouse testis suggesting it may be restricted to the gonads within adults (Seli et al., 2005; Wilkie et al., 2005), although in humans ePABP mRNA can be detected at very low levels in a wide range of tissues (Guzeloglu-Kayisli et al., 2012; Voeltz et al., 2001; Wilkie et al., 2005). Lastly, RT-PCR analysis of a limited number of tissues in humans suggests that PABP5 mRNA may be most highly expressed in brain and ovary (Blanco et al., 2001), although technical issues prevent strong conclusions being drawn. (PABP4 is discussed in section 1.3.3).

1.3.2 Vertebrate PABP phenotypes

Disruption of PABP (pABP) function in *Drosophila* is associated with embryonic lethality, defective oogenesis, spermatogenesis and body patterning and neuromuscular defects dependent on the allele, although many of these phenotypes have not been described in detail (Blagden et al., 2009; Blanco et al., 2001; Singh et al., 2011; Vazquez-Pianzola et al., 2011), and it is not clear to what extent protein synthesis is disrupted. *C. elegans* has two PABPs, and knock-down of either results in mild defects such as flaccid body morphology with PAB-1, but not PAB-2 knockdown also resulting in male and female infertility (Maciejowski et al., 2005; Simmer et al., 2003; Smith et al., 2014). However, the absence of clear homologs of the mammalian PABP family in these species limits the extent to which these phenotypes inform upon the potential functions of specific mammalian PABPs. In contrast, *X laevis* encodes PABP1, ePABP and PABP4 homologs each of which have been knocked-down using morpholino approaches (Gorgoni et al., 2011). Injection of morpholinos against PABP1 or ePABP into both blastomeres at the two cell stage, revealed that both were essential for embryogenesis resulting in loss of anterior and posterior structures, developmental delay, curvature of the body axis, movement defects and death with 100% penetrance, although ePABP embryos reached a maximum of stage 35, in contrast to the earlier lethality (stage 30-31) of PABP1 (Gorgoni et al., 2011). Sequestration of PABPs in fully grown *X. laevis* oocytes, by overexpression of Paip2, blocked oocyte maturation thereby underlining the importance of PABP function in germ cells at times when many mRNAs are regulated by changes in their poly(A) tail length (Friend et al., 2012). Oocyte maturation could be rescued by exogenous ePABP suggesting an important role for ePABP in this process, consistent with it being the predominant PABP present during oocyte maturation (Friend et al., 2012). This result does not preclude PABP1 also contributing to this process. Analysis of oocyte mRNAs showed that key meiotic mRNAs such as c-mos and cyclin B1 showed defects in their poly(A) tail status which prohibited their translational activation (Friend et al., 2012).

To date, only the biological function of germ cell specific PABPs have been explored in mammals and, consistent with analysis in *X. laevis*, female ePABP knock-out mice

were infertile (Guzeloglu-Kayisli et al., 2012). These females have normal oestrus but present with a significantly elevated number of secondary follicles with their oocytes failing to mature *in vivo* or *in vitro,* consistent with blocks in oogenesis and folliculogenesis. The underlying mechanism was shown, at least in part, to be due to a lack of cytoplasmic polyadenylation (Guzeloglu-Kayisli et al., 2012). In contrast, neither loss of ePABP nor tPABP affects murine spermatogenesis (Kashiwabara et al., 2016; Ozturk et al., 2014).

1.3.3 Poly(A)-binding protein 4 (PABP4)

PABP4, (also referred to as inducible PABP (iPABP) or PABPC4) was identified as one of the most upregulated mRNAs upon activation of human T cells (Yang et al., 1995). T cells are part of the adaptive immune system which are antigen activated, resulting in the production of lymphokines that act by paracrine mechanisms to regulate immune response. As regulation of mRNA stability is a widely documented means of controlling mRNAs associated with immune function, it was speculated to have a role in regulating the stability of labile mRNAs in T cells. Consistent with this idea, PABP4 is a diffusely cytoplasmic protein in cultured cells (Yang et al., 1995), is capable of binding to AU-rich sequences in vitro with a higher affinity than PABP1 (Ranson et al., 1973) and is capable of interacting with Tob (Okochi et al., 2005), a protein which recruits deadenylases (Hosoda et al., 2011). Addition of Tob to cell-free extracts, programmed with IL-2 mRNA, showed that it could inhibit the modest (2-fold) enhancement of IL-2 translation by recombinant PABP4 (Okochi et al., 2005). Inhibition of IL-2 translation is vital to induce T cell anergy and Tob acts as an anti-proliferative protein and maintains T cell anergy/quiescence (Hua and Thompson, 2001) suggesting that the Tob-PABP4 interaction may be important in the translational repression of IL-2 mRNA in anergic T cells (Okochi et al., 2005).

Consistent with the modest effect of mammalian PABP4 on IL-2 translation in cell-free systems (Okochi et al., 2005), knock-down of PABP4 in HeLa cells, either alone

or in combination with PABP1, did not significantly impact 35-S methionine incorporation, suggesting it may not significantly contribute to overall cellular translation rates (Burgess et al., 2011). However, these observations may reflect the poor poly(A)-dependence of rabbit reticulocyte cell-free translation extracts (Okochi et al., 2005) and the respective levels of PABP1 and PABP4 in HeLa cells (Burgess et al., 2011) as PABP4 is polysome associated in mammalian cell lines (Burgess and Gray, 2012). Alternatively, a more mRNA specific role in translation would be consistent with all these findings and its preference for AU-rich RNA sequences (Sladic et al., 2004). However, PABP4 may make a more significant contribution to overall protein synthesis rates in some biological contexts, as knock-down in *X. laevis* embryos results in a loss of polysomes (Gorgoni et al., 2011), indicative of a substantial protein synthesis defect. Studies in *X. laevis* also established that PABP4 has the ability to stimulate translation as efficiently as PABP1 when tethered (Gorgoni et al., 2011) and interact with PABP1 partners with roles in translation initiation (eIF4G, Paip1), as well as those implicated in regulating PABP1 function (Paip2), and in mRNA surveillance (eRF3) (Cosson et al., 2002; Gorgoni et al., 2011).

Experiments in cell lines suggest that mammalian PABP4 may contribute to changes in gene expression during specific viral infections and/or cell stresses, as like PABP1, it becomes relocated to either stress granules or the nucleus (Burgess et al., 2011). Stress granules are foci within the cytoplasm that act as sites of mRNA storage (Kedersha et al., 2013), and nuclear relocalisation makes PABP4 unavailable to interact with the mRNA translation or stability machinery. However, PABP4 is not required for stress granule formation or mRNA export and exits the nucleus bound to mRNAs (Burgess and Gray, 2012; Burgess et al., 2011). Thus, these changes in PABP4 localisation are likely driven by mRNA redistribution, as bulk mRNA accumulates with PABP4 in the nucleus or stress granules during specific infections/stresses (Burgess and Gray, 2012; Burgess et al., 2011), although it is possible that partitioning PABP4 to different locations may result in different outcomes in terms of mRNA fate.

Recent investigations of PABP4 in mammalian lines has also identified a potential role in erythroid maturation based on a model in which lymphoma-derived murine cells, mouse erythroleukemia (MEL), are treated with dimethylsulfoxide (Kini et al., 2014). The final stages of erythroid maturation are dependent on mRNA translation/stability control, due to the lack of a nucleus, and interestingly, shRNA-mediated depletion of PABP4 blocked MEL cell differentiation, as measured by criteria such as haemoglobin content. Microarray analysis showed altered levels of a relatively small subset of mRNAs including those with AU-rich elements (AREs), suggesting that PABP4 normally prevents their mRNA decay (Kini et al., 2014). However, the underlying mechanism requires further clarification.

The only whole organism study of PABP4 is in *X. laevis* (Gorgoni et al., 2011). Morpholino knock-down experiments showed it is essential for normal vertebrate development, with lethality by stage 51 (Gorgoni et al., 2011). In contrast to PABP1 and ePABP morphants, PABP4 morphants displayed a range of anterior defects (i.e. abnormal intestinal coiling, malformation of the head and eye, cephalic and ventral oedema), rather than both anterior and posterior defects (Gorgoni et al., 2011). Importantly, cross-rescue experiments revealed that expression of PABP4 was unable to completely rescue the early embryonic lethality associated with PABP1 knock-down (Gorgoni et al., 2011) showing that despite their functional similarities, their molecular functions must be at least partly distinct.

According to the human protein atlas PABP4 is expressed in a wide array of tissues including the ovary, endometrium, placenta, pancreas, and brain. Here we extend our knowledge of PABP4 function in whole organisms by examining its role in mouse, defining an unexpected role in pregnancy.

1.4 Physiology of normal pregnancy

Pregnancy is a fascinating and unique physiological state during which the female body undergoes profound anatomical and physiological changes in almost every organ system. These adaptations begin soon after conception, evolve throughout pregnancy and almost completely revert back to the non-pregnant state either near the end of pregnancy or after parturition. The ultimate purpose of these alterations is to accommodate the needs of the feto-maternal unit. A fully comprehensive review of all the changes that occur is beyond the scope of this thesis but the following brief review will cover some of the key adaptations, as understanding changes in normal pregnancy is key to understanding pregnancy complications, particularly those with a maternal origin.

1.4.1 Metabolic adaptations in pregnancy

Pregnancy has been described as a situation of genetic conflict between the fetus and mother, where a fetus first needs to modulate the maternal immune response to its alloantigens in order to prevent is rejection and a balance between fetal nutrient demands with maternal resource allocation has to be achieved (Burton and Fowden, 2012; Haig, 1993). Maternal glucose and lipid metabolism changes dramatically during pregnancy to ensure that the developing and growing fetus has a continuous and sufficient supply of nutrients during intermittent maternal food intake, particularly in late pregnancy when fetal energy demands peak due to exponential fetal growth.

1.4.2 Glucose metabolism

Maternal physiology during pregnancy is primarily influenced by placental and pituitary hormones. These regulate glucose and lipid metabolism to ensure that the

fetus has an ample supply of fuel and nutrients at all times but most importantly in late pregnancy, when fetal growth and nutrient demand is at its maximum (Butte, 2000; Homko et al., 1999). The maternal response is characterized by a switch from carbohydrate to fat utilization that is facilitated by both insulin resistance and increased plasma concentrations of lipolytic hormones (Butte, 2000). These adaptations result in large fluctuations of glucose and insulin between the fed and the fasted state (such as an overnight fast) which is characterised by "accelerated starvation" during which glucose is stored for the fetus and alternative fuels, such as plasma ketone, free fatty acids and glycerol, are maintained for the mother (Butte, 2000; Homko et al., 1999).

In early- to mid-gestation the so called "first-phase insulin secretion", which occurs in response to a meal, is enhanced as a result of increased stimulation of β cells in the pancreas (insulin producing cells within the islets of Langerhans). Overall there is a 60% increase in insulin secretion but insulin sensitivity remains unaltered promoting maternal fat storage due to the lipogenic properties of insulin (Kersten, 2001). In the second half of gestation maternal metabolism is modified by the emergence of insulin resistance whereby insulin sensitivity becomes 45-70% lower than in non-pregnant women, primarily in skeletal muscle, the principal site of whole-body glucose uptake (Freemark, 2006; Newbern and Freemark, 2011). In order to overcome the insulin resistance, and to prevent gestational diabetes mellitus developing, there is a compensatory increase in pancreatic β cell number in conjunction with a lower threshold for glucose-stimulated insulin secretion (Brelje et al., 1994; Parsons et al., 1992). As a result, in the fed state maternal nutrients are utilised for the production of fat (adipogenesis), glycogen (glycogenesis) and energy storage. Conversely, in the fasted state the mother utilises free fatty acids for energy and spares glucose, amino acids, essential fatty acids, and ketones for placental growth and nutrient transport (reviewed by (Newbern and Freemark, 2011).

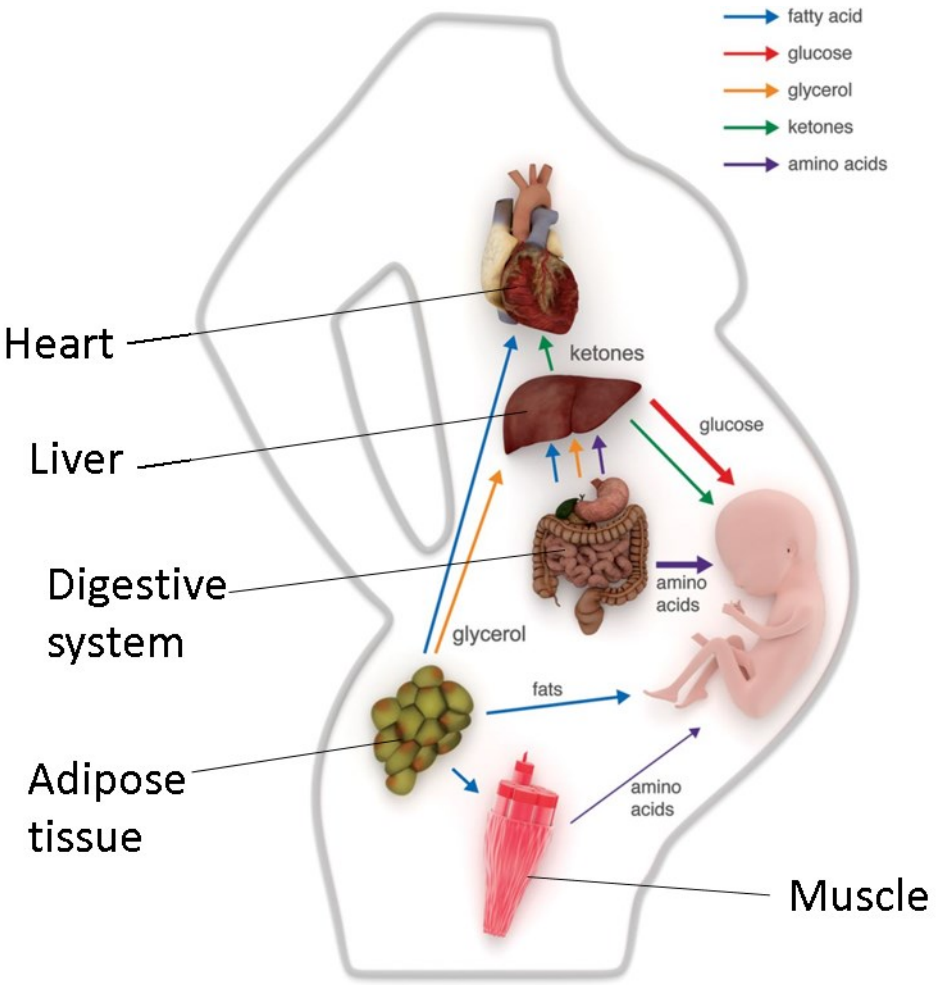

Figure 1.4 Metabolic changes during late pregnancy.

Late pregnancy is marked by maternal catabolism that serves to support the dramatic anabolic growth of the fetus. The liver uses glycerol and (less so) amino acids to make glucose for the fetus and consumes fats, generating in the process ketones that are usable by the brain, muscle, and fetus. Adipose tissue releases fatty acids for consumption by both the liver and muscle. The fetus uses amino acids, fats, and roughly half of incoming glucose for anabolic growth, while largely relying on the other half of glucose for energetic needs. (From (Liu and Arany, 2014)).

1.4.3 Lipid metabolism

Maternal adaptive changes also occur in lipid metabolism including accumulation of maternal fat depots in early pregnancy and hyperlipidaemia, elevated lipids in the blood, in late pregnancy (Alvarez et al., 1996; Lopez-Luna et al., 1991; Montelongo et al., 1992). The increased levels of lipids in early pregnancy are not only important for fat storage, to be used as an alternative energy source to glucose later in pregnancy, but are also important for fetal growth and development. Maternal plasma concentrations of triglycerides (TG) and non-esterified fatty acids (NEFA) have been shown to correlate with fetal lipid concentrations and fetal growth more so than maternal plasma glucose (Kitajima et al., 2001; Nolan et al., 1995; Schaefer-Graf et al., 2008). Furthermore, intrauterine growth restriction has been associated with impaired placental transfer of lipophilic compounds, including not only fatty acids but also lipophilic vitamins like retinol and γ - and α-tocopherol (Gauster et al., 2007) which prevent the oxidative deterioration of lipids (lipid peroxidation) (Kamal-Eldin and Appelqvist, 1996; Rozanowska et al., 2005). The accumulation of fat in early pregnancy is not only the result of increased insulin in the setting of normal insulin sensitivity, but also due to an increase in adipose tissue lipoprotein lipase (LPL) activity which results in the uptake of NEFA and glycerol by tissues (Herrera et al., 1988). The decrease in insulin sensitivity in late pregnancy combined with increased levels of placental hormones (e.g. growth hormone and placental lactogen II (Fielder and Talamantes, 1987)) with lipolytic effects such as increasing lipolysis, decreasing LPL activity and increasing TG utilization causes fat stores to decline (Ramos and Herrera, 1995).

These changes in maternal metabolism are brought about by hormones produced by the placenta and maternal pituitary gland including oestrogen, progesterone, cortisol (in humans), corticosterone (in mice) and, in particular, the Prolactin (PRL)/growth hormone (GH)/placental lactogen (PL) family. PRL and GH are secreted by the pituitary and share the same ancestral gene (reviewed by (Rawn and Cross, 2008), and have been duplicated to take on different functions in the placenta. In mice *GH* gene is single copy whereas in humans, 4 *GH* genes are expressed exclusively in the

placenta and one distinct gene in the pituitary (Rawn and Cross, 2008). The *Prl* gene on the other hand is single copy in humans whereas mice contain 23 *Prl* gene copies, each having a unique spatial and temporal expression pattern and are therefore used as markers for different subtypes of trophoblast cells which constitute much of the placenta (Rawn and Cross, 2008; Simmons et al., 2008).

1.4.4 Adipokines - with a focus on leptin and adiponectin

It wasn't until 1994 that white adipose tissue was firmly established as an endocrine organ that, in addition to its role as a reservoir for storing calories, releases a variety of bioactive peptides called adipokines (also termed adipocytokines) (reviewed by (Kershaw and Flier, 2004). Furthermore, it expresses several receptors that respond to circulating hormones and allow it to communicate with distant organs, including the central nervous system (CNS). As a result, adipose tissue has a role in a number of biological processes including energy metabolism, neuroendocrine function and immune function (Kershaw and Flier, 2004). Two adipokines which are associated with insulin resistance are leptin and adiponectin (Fasshauer and Paschke, 2003; Weyer et al., 2001). Adiponectin has insulin sensitizing, anti-inflammatory and antiatherogenic properties (Lihn et al., 2005). Maternal adiponectin serum levels have an inverse relationship with birth weight (Ategbo et al., 2006; Jansson et al., 2008; Lowe et al., 2010). Fetal adiponectin, on the other hand, is positively correlated with birthweight and increased fat stores in early life (Qiao et al., 2012; Sivan et al., 2003).

Leptin signals to receptors of the cytokine receptor class I superfamily that are found in both the CNS and periphery (Bjorbaek and Kahn, 2004).. Leptin is known to reduce appetite and increases energy expenditure signalling via the hypothalamus (Campfield et al., 1995; Vaisse et al., 1996) but also has direct metabolic effects on several tissues primarily stimulating glucose utilization and lipolysis (Barzilai et al., 1997; Bryson et al., 1999; Kamohara et al., 1997). In normal pregnancy, adiponectin levels decline in mid- to late-gestation resulting in an increased leptin to adiponectin ratio (Catalano et al., 2006; Jansson et al., 2008; Masuzaki et al., 1997). Interestingly, a disruption in this

ratio has been associated with pre-eclampsia (Atamer et al., 2005; Aydin et al., 2008; Hendler et al., 2005; Herse et al., 2009; Lu et al., 2006; Nakatsukasa et al., 2008; Naruse et al., 2005; Ouyang et al., 2009; Ozkan et al., 2005; Sharma et al., 2007) and gestational diabetes (Ategbo et al., 2006; Kautzky-Willer et al., 2001). Leptin also serves as a mitogen for endothelial cells (Bouloumie et al., 1998), haematopoietic cells (Gainsford et al., 1996), lung epithelial cells (Tsuchiya et al., 1999) and pancreatic β-cells (Islam et al., 1997), therefore it may also have a mitogenic role in the placenta, in addition to stimulating growth of tissues in the developing fetus. Leptin is important in early pregnancy as it is required at the time of preimplantation/implantation and subsequent placental formation (Malik et al., 2001). Interestingly, in humans leptin has been found to be secreted by the placenta (Masuzaki et al., 1997), and its maternal plasma concentrations increase during pregnancy (Hartmann et al., 1997). The gene for placental leptin has a placenta- specific upstream enhancer, implying that placental leptin is differentially regulated from leptin of adipose origin (Gavrilova et al., 1997).

Furthermore, leptin concentration in umbilical serum has a strong positive correlation with neonatal fat mass (Marchini et al., 1998; Okereke et al., 2002) and higher leptin concentrations have been found in fetal plasma and placentas from women with either type I diabetes or gestational diabetes mellitus (GDM) (Gross et al., 1998; Lepercq et al., 1998). Indeed maternal circulating levels increase in rodents and humans, particularly mid-late gestation but significantly drops at around birth (reviewed by (Herrid et al., 2014). However, in contrast to humans neither the murine conceptus nor the placenta are the source of leptin, instead the placenta produces soluble leptin receptors (Ob-R) which most likely increases the peptide half-life and allow leptin to act on the placenta via a paracrine signalling system (Gavrilova et al., 1997; Malik et al., 2005). There is evidence that high levels of PRL or PLs during pregnancy may directly interfere with leptin receptor signalling in the brain, resulting in leptin resistance (Nagaishi et al., 2014). When the role of high maternal leptin was examined during pregnancy in mice it was found that maternal hyperleptinemia isolated from maternal obesity or diabetes resulted in decreased placental leptin concentrations and reduced fetal birthweight (Yamashita et al., 2001). In this study, leptin administration from day 10 of pregnancy for 7 days reduced adiposity and improved glucose tolerance in offspring of the diabetes (db/+) mouse model of spontaneous GDM.

However, the same leptin treatment of WT mothers decreased placental leptin concentration and reduced fetal birth weight. In a separate study leptin injections in C57BL/6 mice on day 17 of pregnancy decreased birth weight in both male and female offspring (Makarova et al., 2013). Furthermore, maternal hyperleptinemia has been shown to result in reduced weight gain in offspring in adulthood even on a high fat diet (HFD) (Pollock et al., 2015). Placental leptin may regulate fetal growth and placental function by regulating glucose metabolism and insulin sensitivity (Magarinos et al., 2007; Malik et al., 2005; Sagawa et al., 2002a; Sagawa et al., 2002b). Furthermore, leptin regulates multiple placental functions such as nutrient transfer (Jansson et al., 2003), trophoblast cell invasion (Schulz and Widmaier, 2004) trophoblast giant cell differentiation (Schulz et al., 2009) and protein synthesis (Perez-Perez et al., 2010).

1.4.5 Cardiac and haemodynamic adaptations

Pregnancy is characterized by an increase in blood volume (Longo, 1983), cardiac output, glomerular filtration rate and remodelling of spiral and uterine arteries. Together these changes bring about a state of high blood flow with low vascular resistance that provides the fetus with constant supply of oxygen and nutrients. The increase in blood volume leads to cardiac volume overload, which in turn results in cardiac hypertrophy that is defined as an increase in heart muscle mass with changes in cardiac geometry (reviewed by (Chung and Leinwand, 2014). Cardiac hypertrophy associated with pregnancy is physiological rather than pathological and it is reversible as early as 7-14 days post-partum in rodents (Umar et al., 2012) and up to a year in humans (Clapp and Capeless, 1997). It is characterized by an increase in chamber dimension (Eghbali et al., 2005), which can be associated with a proportional increase in wall thickness (Chung et al., 2012). Furthermore, cardiac output reaches its maximum in the second trimester that persists until term and is associated with an increase in heart rate and stroke volume (Clapp and Capeless, 1997). This pregnancy-induced cardiac adaptation is believed to be, at least in part, mediated by sex steroid

hormones. Progesterone has been shown to increase protein synthesis in cardiac muscle (Goldstein et al., 2004) whereas estradiol attenuates the development of pressure-overload hypertrophy (van Eickels et al., 2001). Abnormal cardiac adaptation to pregnancy is often present in women with pre-existing or pregnancy-induced hypertensive disorders such as pre-eclampsia (Tiralongo et al., 2015; Tomsin et al., 2012). However, it is also present in women with IUGR pregnancies, manifesting as significantly smaller left atrial diameter and a cardiac output that failed to increase (Duvekot et al., 1995).

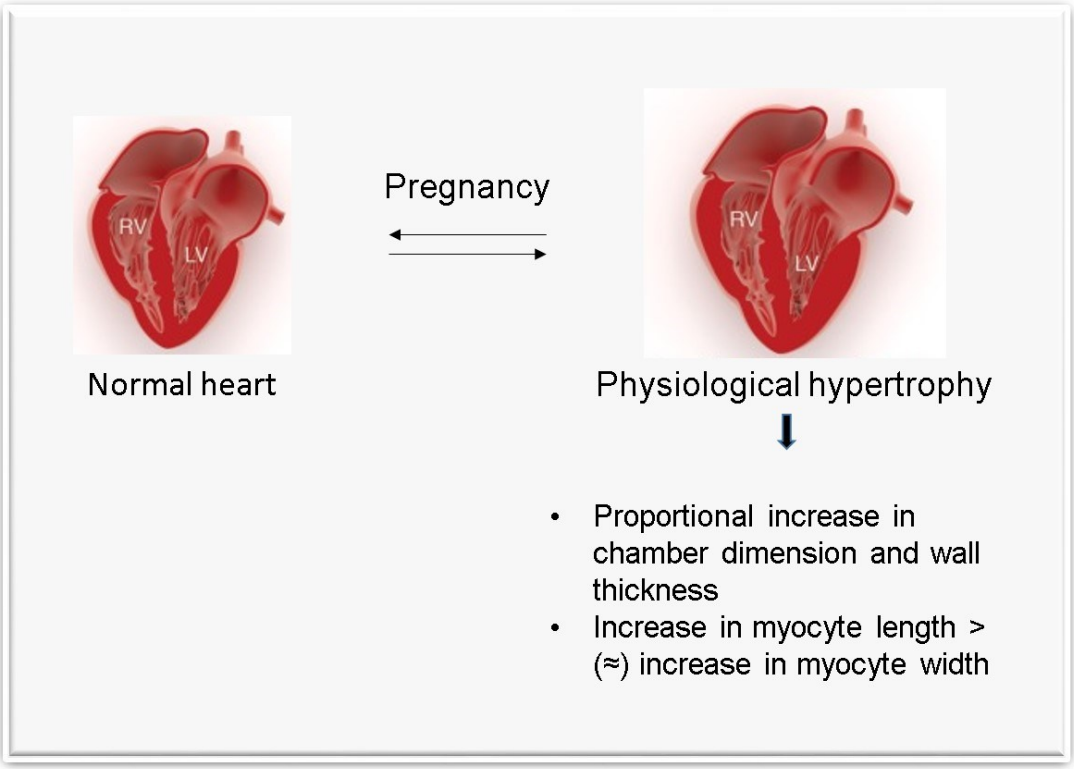

Figure 1.5 Morphometric alterations of the heart in response to pregnancy.

Pregnancy leads to physiological rather than pathological cardiac hypertrophy which is reversible post-pregnancy and is characterised by an increase in chamber dimension which can be associated with a proportional increase in wall thickness as well the increase in myocyte length and width. (Adapted from (Chung and Leinwand, 2014)).

Aberrant cardiac and haemodynamic changes in pregnancy are often associated with a defective invasion of trophoblast cells into uterine tissue, resulting in poor placentation and insufficient spiral artery and uterine artery remodelling. In a normal pregnancy, the uterine artery, radial arteries (Palmer et al., 1992) and spiral arteries of the myometrium and decidua (Pijnenborg et al., 1983) undergo structural remodelling to reduce vasoactivity (the constriction and dilation of the artery) and increase diameter/capacity (reviewed by (Cross et al., 2002; Osol and Mandala, 2009). In humans, the remodelling of uterine spiral arteries is the result of a specific trophoblast lineage called the extravillous cytotrophoblast which replaces smooth muscle cells and thus alters vascular tone (Cross et al., 1994). In mice it is the action of uterine natural killer (uNK) cell derived interferon γ (IFN-γ) that results in a similar loss of smooth muscle cells within the metrial gland region at around mid-gestation (Ashkar and Croy, 1999, 2001; Ashkar et al., 2000). Downstream of this the arterial endothelial cell layer is also lost, resulting in haemochorial blood flow through sinuses, however the mechanism by which this occurs is not well understood (Cross et al., 2002). Some of the primary evidence for the role of uNK cells in spiral artery remodelling is that is mice lacking uNK cells or components of the IFN-γ signalling pathway consistently present with abnormal spiral artery remodelling which manifests as smaller artery diameter and persistence of the smooth muscle layer (Croy et al., 2000; Guimond et al., 1997). In contrast to spiral artery remodelling, the mechanism by which the uterine artery remodels is largely unknown however, as reviewed by Mandala and Esol (Mandala and Osol, 2012) steroids such as estrogen and progesterone are believed to initiate the process (Guenther et al., 1988; Magness et al., 1993; van der Heijden et al., 2005) and as gestation progresses, fetoplacental factors, which are unknown but vascular endothelial growth factor (VEGF) and placental growth factors (PlGF) produced by myometrial and trophoblast cells, become predominant in later gestation as demonstrated in a single-horn pregnancy in mice where arterial remodelling is restricted the implanted horn (Fuller et al., 2009). Other mechanism include nitric oxide (NO), the renin-angiotensin system (reviewed by (Mandala and Osol, 2012) and relaxin (Vodstrcil et al., 2012).

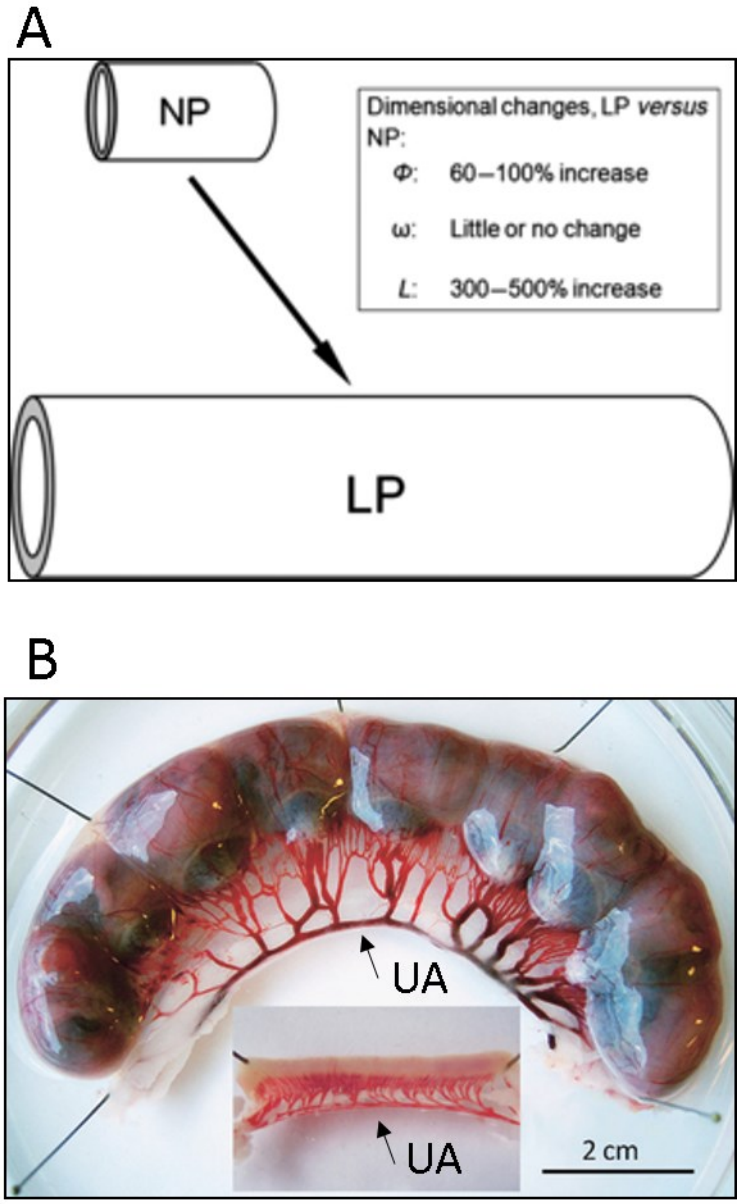

Figure 1.6 Uterine artery remodelling in rodents.

A) A scaled drawing showing the approximate extent of uterine artery widening and lengthening, with no change in wall thickness in the rat which accompanies pregnancy. **B)** Photograph showing late pregnant uterine horn and extent of vascular remodelling in comparison to an age-matched non-pregnant uterus and associated vasculature; the uterine artery (UA) and connected arcuate and radial vessels (inset, bottom). Ø = dimeter; ω = wall thickness; L = axial length; LP = late pregnant; NP = age-matched non-pregnant; UA = uterine artery. (From (Mandala and Osol, 2012)).

1.4.6 Haematologic adaptations

Similarly to other body systems, the haematologic system adapts to pregnancy to accommodate the demands of the fetoplacental unit but also acts as to protect the mother in the event of haemorrhage during pregnancy and at parturition. One major change that occurs is an increase in blood volume that is the combined result of an increase in plasma volume and red blood cell (RBC) number. In women, plasma volume begins to increase by 6 weeks and expands at a steady pace until it plateaus at 30 weeks of gestation (Gordon, 2007). In comparison, RBC number increases at a slower rate beginning at about 10 weeks but, stimulated by erythropoietin, continues to increase progressively until term. As a result, maternal haematocrit (HTC) falls in early pregnancy but may rise in later pregnancy. Women with multiple pregnancies have larger increases in blood volume than those with singletons and volume expansion correlates with infant birth weight; it is unknown whether this is a cause or an effect (Gordon, 2007). The exact mechanism underlying the expansion of blood volume is unknown, but the hormonal and nitric oxide (NO) changes in pregnancy are likely candidates, as the inhibition of NO synthase in pregnant animals results in reduced plasma volume as well as increased blood pressure, implying it is also important for pregnancy-induced vasodilation (Salas et al., 1995; Zhang and Kaufman, 2000). Due to a greater increase in plasma volume relative to the increase in RBC number, early pregnancy is also characterised by a small decrease in total haemoglobin concentration, referred to as physiologic anaemia of pregnancy. Later in pregnancy, when plasma expansion plateaus and RBC continues to increase, total haemoglobin concentration rises. Interestingly, high haemoglobin concentration at first antenatal clinic presentation is associated with an increased risk of IUGR and an almost 2-fold increased risk in stillbirth (Stephansson et al., 2000). This association may be more of a reflection of an insufficient plasma volume increase which normally ensures reduced blood viscosity that not only favours blood flow in the maternal part of labyrinth of the placentas (zone of the placenta where maternal and fetal vasculature come into close proximity), thus favouring fetal growth and nourishment, but also acts as a preventative adaptation to reduce risk of thrombosis in the uteroplacental circulation. Other haematological changes include an increase in platelet aggregation and, in some

women, a decline in the platelet count in the third trimester of pregnancy (Boehlen et al., 2000), possibly due to hyperdestruction and/or haemodilution (Boehlen et al., 2000; Fay et al., 1983). Since the risk for trauma and haemorrhage in pregnancy is high, platelets become activated resulting in a hypercoaguable state relative to non-pregnancy. Interestingly, women that present with platelet activation before and during early pregnancy have a higher risk of developing pre-eclampsia and IUGR (Dundar et al., 2008; Hladunewich et al., 2007; Kanat-Pektas et al., 2014), most likely because platelet activation, amongst other potential causes, is associated with hypertension and inflammation.

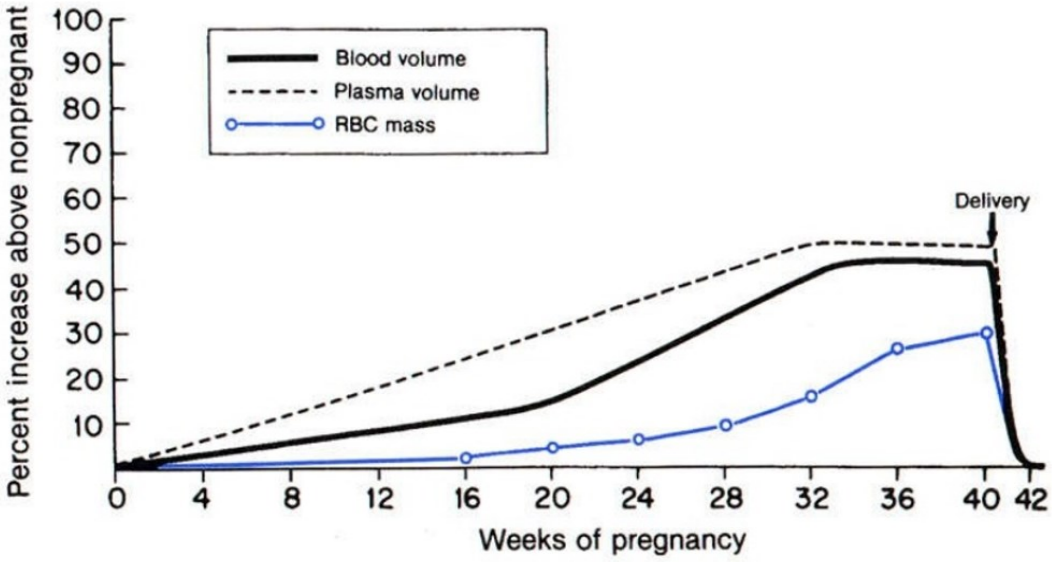

Figure 1.7 Blood and plasma volume and RBC mass changes during pregnancy.

Plasma volume progressively increases during pregnancy but tends to plateau from about 30 weeks of gestation. Blood volume follows a similar pattern with a slower rise from day 0 which further increases from approximately 20 weeks of gestation. RBC mass/number rises slowly in early pregnancy but in contrast to blood and plasma volume it continues to increase all the way to term. These changes result in a fall of the haematocrit in early pregnancy but a rise towards term. (Adapted from (Scott, 1972).

Furthermore, pregnancy is characterised by a progressive increase in the peripheral white blood cell count (WBC), primarily due to a rise in segmented (mature)

neutrophils and monocytes (Kuhnert et al., 1998; Naccasha et al., 2001; Siegel and Gleicher, 1981; Veenstra van Nieuwenhoven et al., 2002). On the other hand dendritic cells and circulating natural killer (NK) cells decrease during pregnancy (Cordeau et al., 2012; Kuhnert et al., 1998; Shin et al., 2009; Veenstra van Nieuwenhoven et al., 2002).

1.4.7 Immune adaptations

Maternal immune cells such as uterine natural killer cells, dendritic cells, macrophages and T cells are important for reproduction and mediate some key process such as fetal allograft recognition and tolerance as well as trophoblast invasion and spiral artery remodelling (reviewed by (Bulmer et al., 2010; Erlebacher, 2013; Moffett and Colucci, 2014). In the haemochorial human and mouse placenta, fetal trophoblast cells come in direct contact with maternal immune cells. This contact primarily occurs in early pregnancy in the maternal decidua but also in the labyrinth of the placenta where the syncytiotrophoblasts are bathed in maternal blood. Innate immune cells, including uterine NK (uNK) cells and macrophages, are dominant in the decidua during pregnancy in both mice and humans (Ashkar et al., 2000; Barber and Pollard, 2003; Hanna et al., 2006; Moffett and Loke, 2006). Uterine NK cells are phenotypically and functionally different from peripheral NK cells (Hanna et al., 2006; Koopman et al., 2003) and are regulated by stress signals, adhesion molecules and receptors for major histocompatibility complex (MHC) expressed by trophoblast cells, including killer-cell immunoglobulin-like receptors (KIR) and murine lectin-like Ly49 receptors (Lanier, 2008). Both KIR and Ly49 are highly polymorphic and individual NK cells express from zero to five KIRs (Kieckbusch et al., 2014). The variability of these receptors and MHC ligands in both fetus and mother enable each pregnancy to be subtly different (Parham and Moffett, 2013). Kieckbusch *et al* demonstrated in mice that uNK cells specific for MHC class I allotype are less responsive as they bind inhibitory variations of the receptors mentioned above, resulting in defective remodelling of the decidual spiral arteries and reduced fetal growth (Kieckbusch et al.,

2014). This is demonstrative of the uNK's critical role in the development and growth of the fetus by balancing the invasion of the fetal trophoblast cells, such that the invasion isn't too intrusive where the mother would be at risk of uterine rupture and death, whilst promoting the remodelling of spiral arteries for an increased blood flow to the feto-placental unit (reviewed by (Moffett et al., 2015).

Macrophages are the second most abundant leukocyte population at the materno-fetal interface (Bulmer et al., 1988) and unlike uNK cells, their population does not alter dramatically in pregnancy. However, functional studies suggest that they have a role in immunosuppression (Mizuno et al., 1994), phagocytosis of cell debris produced by during implantation (reviewed by (Abrahams et al., 2004; Mor and Abrahams, 2003) and the prevention of maternal T lymphocyte activation (Heikkinen et al., 2003).

T helper cells are the third most abundant leukocyte and are the least studied in pregnancy in comparison to uNK cells and macrophages (Bulmer et al., 2010). Similarly to macrophages, their numbers do not change with gestation however, their importance is highlighted by the fact that their absence in pregnancy is associated with increased levels of fetal death and reduced placental growth (Athanassakis et al., 1987; Chaouat et al., 1988). A balance between T helpers type 1 (Th1) and type 2 (Th2) is key for fetal survival (reviewed by (Athanassakis and Vassiliadis, 2002; Sykes et al., 2012). Th1 and Th2 differentiate from T helper 0 (Th0) cells and whilst Th1 produces an array of inflammatory cytokines, Th2 produces more cytokines considered to be anti-inflammatory and associated with a strong antibody response (Sykes et al., 2012) therefore a bias towards Th2 in pregnancy is present (Saito et al., 1999), particularly at the maternal-fetal interface where trophoblast also contribute to the shift in Th1:Th2 ratio (Chaouat et al., 1988). However, the complex nature of the immune adaptation is highlighted by the fact that despite a Th2 predominance being favourable in pregnancy, Th1 cytokines are important in early pregnancy and during labour (Saito et al., 1999).

Also important in pregnancy are regulatory T (Treg) cells (reviewed by (La Rocca et al., 2014) which are involved in the regulation of peripheral self-tolerance and immune homeostasis (Sakaguchi, 2004, 2005; Wing and Sakaguchi, 2010) and constitute 5-

50% of the peripheral CD4+ T cell compartment in mice and humans. In pregnancy, there is a peripheral increase of CD25+ T cells (Aluvihare et al., 2004) with seminal fluid being one of the main drivers of this adaptation (Robertson et al., 2009). There are several lines of evidence indicative of their role in promoting the survival of the allogeneic fetus by mediating maternal tolerance specifically in early pregnancy (Aluvihare et al., 2004; Jin et al., 2009; Shima et al., 2010; Winger and Reed, 2011; Zenclussen et al., 2005).

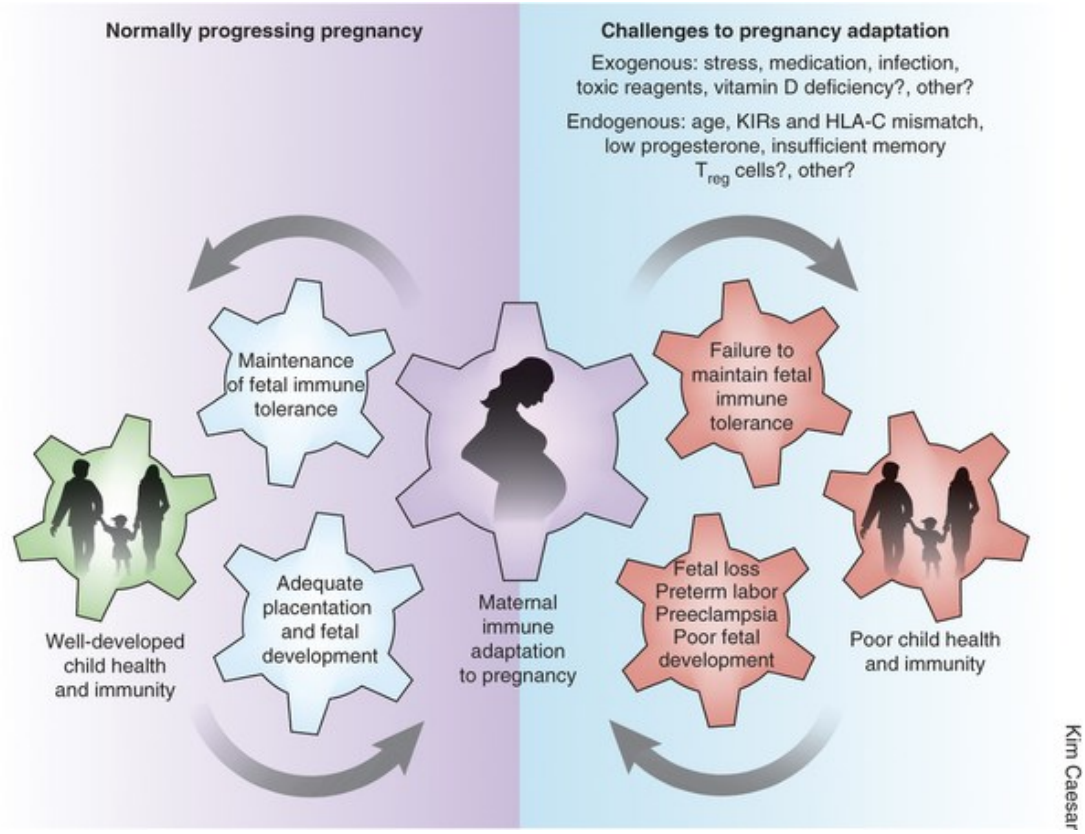

Figure 1.8 Normal and compromised maternal immune adaptations to pregnancy.

In normally progressing pregnancies, maternal adaptation to pregnancy occurs, resulting in the maintenance of fetal immune tolerance (left). In turn, proper placentation and fetal development is supported. This successful adaptation is reflected by a well-developed immune system and a healthy child postnatally. Adverse effects of maternal immune adaptation to pregnancy may result from or be aggravated by exogenous or endogenous challenges (right). Endogenous challenges may include a KIR and HLA-C mismatch (Chazara et al., 2011) (Hiby et al., 2008), low amounts of maternal progesterone

(Hartwig et al., 2013) , advanced maternal age, which can be associated with low amounts of progesterone (Arck et al., 2008) or 'inflamm-aging' (Cannizzo et al., 2011) (the low-grade, chronic, systemic inflammatory state that characterizes the aging process), possibly insufficient memory T_{reg} cells and yet-to-be-identified factors. Exogenous challenges may include stress perception (Glaser and Kiecolt-Glaser, 2005) (Karimi and Arck, 2010) , infections (Van Kerkhove et al., 2011) , medication such as acetaminophen (Thiele et al., 2013) and possibly vitamin D deficiency (Brannon, 2012). These challenges may result in a failure to maintain fetal immune tolerance and lead to pregnancy complications such as fetal loss, preterm labor, preeclampsia and poor fetal development. These complications may adversely affect the child's health and compromise their immunity later in life. (From (Arck et al., 2008).

1.4.8 Adaptations in other organs

1.4.8.1.1 Kidney

Other organs undergo adaptation to pregnancy as well (summarised in Table 1.1). The kidney has a number of essential physiological roles such as the excretion of specific metabolic waste products (urea, creatinine and uric acid), regulation of water and solute excretion. Additionally, secreting hormones (renin, prostaglandins and bradykinin) it also plays a role in the regulation of systemic and renal haemodynamics, red blood cell production (Adamson, 1996) and bone metabolism (Fukagawa et al., 2006). Throughout the course of pregnancy, the kidney increases in size and weight as a result of the dilatation of the collecting system including the renal pelvis (funnel for urine flowing to the ureter) and the ureter (duct for urine passing from kidney to bladder) (Gordon, 2007). Global haemodynamic changes including vasodilation, high arterial flow and low resistance, as described previously, are primarily the effects of the hormone relaxin, released by the ovarian corpus luteum, which also induces increased renal plasma flow (RPF) and glomerular filtration rate (GFR) (reviewed by (Jeyabalan and Conrad, 2007). Kidney problems in pregnancy such as hypertension, renal insufficiency and nephrotic range proteinuria increase the risk of poor pregnancy outcome (Imbasciati and Ponticelli, 1991). For example, women with chronic renal disease are predisposed to IUGR and preeclampsia. Interestingly, there is also

suggestion that anti-angiogenic proteins released by the placenta, such as soluble Flt-1 (sFlt-1), may play a role in the development of proteinuria and hypertension in preeclampsia (reviewed by (Karumanchi et al., 2005).

1.4.8.1.2 Spleen

The spleen is a the body's largest lymphatic organ and has a number of important roles including the production of antibodies, storing platelets, recycling iron, filtering blood of foreign material and old/damaged red blood cells and platelets, and finally inducing adaptive immune responses (reviewed by (Mebius and Kraal, 2005). The spleen is organised into different functional regions including white pulp, red pulp and the marginal zone. White pulp, is involved in responding to blood-borne antigens, is the splenic lymphoid region containing T-cell zones, also known as periarteriolar lymphoid sheath (PALS), and B-cell zones. The red pulp is where blood filtration takes place and is composed of sinusoids and connective tissue known as the splenic cords of Billroth. Splenic adaptations to pregnancy include an increase in size, associated with the expansion of red pulp, and a significant accumulation of mRNAs associated with the erythroid lineage (Bustamante et al., 2008). Additionally, it can also act as a secondary site of erythropoiesis during stress (Mattsson et al., 1984) (Welniak et al., 2001) including pregnancy (Fowler and Nash, 1968) (de Rijk et al., 2002; Mattsson et al., 1984). In the mouse, spleen size peaks at day e13.5 but returns to a non-pregnant size by e18.5. The splenic adaptations are believed to be mediated by the actions of PRL and PRL-like proteins produced by the placenta, both of which regulate haematopoiesis (Abkowitz et al., 2002; Jepson and Lowenstein, 1964; Zhou et al., 2002).

1.4.8.1.3 Liver

The liver, the largest solid organ in the body, has a wide range of essential functions including glycolytic and urea metabolism, blood detoxification and modulating cholesterol levels, while supporting the digestion by processing the nutrients absorbed from the small intestine and secreting bile to aid in the digestion of lipids. Moreover, the liver is the primary site of haematopoiesis in the fetus with the bone marrow gradually replacing this role by the time of birth (reviewed by (Golden-Mason and O'Farrelly, 2002). In adulthood, this haematopoietic potential is retained and can be activated stress situations such as severe bone-marrow dysfunction (Golden-Mason and O'Farrelly, 2002). The liver contains an array of cells including cholangiocytes, endothelial cell, stellate cells and Kupffer cells but is primarily composed of hepatocytes (approx. 80%). The liver of the mouse adapts to the demands of pregnancy by increasing in size as a result of hepatocyte hyperplasia and hypertrophy (Dai et al., 2011; Milona et al., 2010). The increase in size is evident by e13, peaks at e18 and returns to a pre-pregnancy weight by day 10 postpartum (Dai et al., 2011). The enhanced liver metabolism is essential to accommodate the increase demand for energy from the developing fetus and the detoxification of fetal metabolites. Liver adaptations are most likely driven by mechanisms similar to those previously described, including changes in insulin, insulin growth factor (IGF), GH, PLs and sex steroids (Augustine et al., 2008; Celton-Morizur et al., 2009; El Khattabi et al., 2006; Yamamoto et al., 2006). The potential pathological consequences of gestational metabolic stress on the liver are highlighted by pregnancy-specific liver diseases including intrahepatic cholestatis of pregnancy, haemolysis, elevated liver enzymes and low platelet count (HELLP) syndrome, and acute fatty liver of pregnancy (Hay, 2008).

1.4.8.1.4 Pancreas

The pancreas is both an endocrine and exocrine organ that releases enzymes, such as trypsin, amylase and lipase, to help break down foods to mobilise nutrients, and also regulates the levels of circulating glucose by releasing insulin and glucagon. Insulin is produced by pancreatic β-cells in response to a rise in blood glucose, resulting in the uptake of glucose by tissues. Glucagon is secreted by α-cells in response to decreases blood glucose and leads to glycogenolysis, the breakdown of glycogen to glucose, primarily in the liver. As discussed previously , insulin resistance manifests in late pregnancy and is compensated by a higher rate of insulin biosynthesis resulting from a combination of increased β-cell proliferation and, primarily, increased β-cell sensitivity/hyperfunctionality in response to glucose (reviewed by (Bernard-Kargar and Ktorza, 2001; Ernst et al., 2011; Sorenson and Brelje, 1997). In rodents, β-cell hyperfunctionality is observed between days e11 and e19 of gestation and returns to normal by parturition. These adaptations are brought about by PLs, PRL, and the sex steroids; oestrogen and progesterone (Brelje et al., 1993). Numerous studies indicate that failed β-cell adaptation during pregnancy can lead to gestational diabetes mellitus (GDM), which increases the risk for fetal mortality or morbidity by increasing a risk of large-for-gestational-age (LGA) babies (reviewed by (Devlieger et al., 2008).

Organ	Physical changes in pregnancy	Examples of functional changes in pregnancy
Kidney	Increase in weight and size (increased vascular volume, glomerular size, dilated and elongated pelvises and ureters)	Increased renal blood flow and glomerular filtration rate Increase in secretion of renin, erythropoietin and active vitamin D
Spleen	Increase in weight and size (primarily increase in red pulp)	Increase in blood filtration rate Possible secondary site of erythropoiesis
Liver	Increase in weight and size (hepatocyte hyperplasia and hypertrophy) (in mice but not human)	Enhanced metabolism Possible secondary site of erythropoiesis
Pancreas	Increase in weight and size (increased β-cell proliferation)	β-cell hyperfunctionality/ increase in sensitivity

Table 1.1 Summary of some of the physical and functional changes of organs in pregnancy.

1.4.9 The placenta

The placenta is a transient organ that is unique to pregnancy and is vitally important for the survival, development and growth of mammalian embryos. It is the first organ to form during mammalian development and problems in its formation and/or function underlie many pregnancy complications (reviewed by (Rossant and Cross, 2001). It

acts as the main interface between mother and fetus and is where their circulations come into close proximity, allowing efficient nutrient and gas exchange as well as removal of fetal metabolic waste, all of which are essential for fetal growth and development. Furthermore, it acts an important source of pregnancy-associated hormones and growth factors, and is involved in immune protection of the fetus. Aberrant placental development and/or dysfunction, as a result of genetic or environmental insult, is believed to be a central factor in a high proportion of mid-late pregnancy complications such as abruption, pre-eclampsia and unexplained stillbirth (Smith and Fretts, 2007). Low birthweight/intrauterine growth restriction, without any obvious environmental or fetal causes, is often attributed to placental insufficiency.

1.4.10 Placenta development

In order to uncover the mechanisms that underlie impaired placental function it is essential to understand its structure and some of the key milestones in its development. Although the gross architecture of the human and mouse placenta differ slightly, their overall structures and molecular mechanisms behind placental development are considered to be similar (Rossant and Cross, 2001; Watson and Cross, 2005). When mature, both human and mouse placenta are composed of three major functional layers; 1. the outer maternal layer, decidua basalis (Db), which consists of uterine decidual cells, and maternal blood vasculature that supplies, as well as takes away, blood from the embryo; 2. an intermediate layer called the junctional zone (Jz) (also called spongiotrophoblast layer) which has a largely endocrine function; 3. an inner layer closest to the chorionic plate, the labyrinth zone (Lz), where the maternal and fetal circulations are brought into close proximity to allow for haemotrophic exchange. The labyrinth, analogous to the villus in humans, is involved in the transport of gases, nutrients and waste products between the maternal and fetal circulations throughout the majority of pregnancy (Cox et al., 2009).

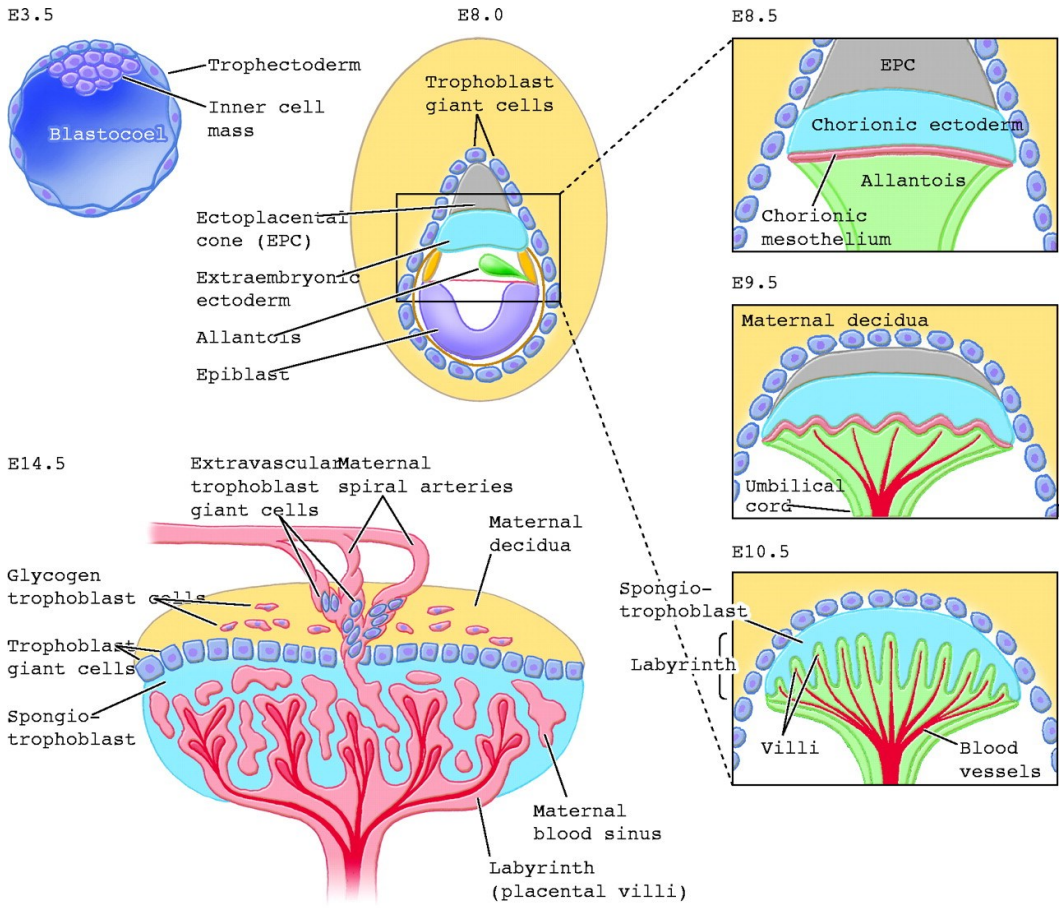

Figure 1.9 Placental development in the mouse.

After formation of the blastocyst, where extraembryonic lineage formation begins, chorioallantoic attachment occurs at e8.5, followed by branching morphogenesis of the labyrinth to form dense villi, within which nutrients are exchanged (e8.5–10.5). The mature placenta (e14.5) consists of three layers: the labyrinth, the spongiotrophoblast, and the maternal decidua. (From (Watson and Cross, 2005)).

The placenta develops (Figure 1.9, Figure 1.10) from the trophectoderm layer that is set aside from the inner cell mass in the blastocyst at embryonic day (e) 3.5. In parallel with implantation, the mural trophectoderm (TE) (i.e. trophectoderm not touching the inner cell mass) differentiates into trophoblast giant cells (TGCs) to become the first terminally differentiated cell type to form during development. These TGCs are vital for successful embryo implantation and promoting maternal adaptations to pregnancy (Hu and Cross, 2010). This is followed by the differentiation of the polar trophectoderm into extra-embryonic ectoderm which develops into trophoblast cells of the chorion layer and subsequently the labyrinth, and the ectoplacental cone, the

precursor of junctional zone which, when mature, contains spongiotrophoblast cells, glycogen trophoblast cells and trophoblast giant cells which line its border with the decidua (Simmons et al., 2007).

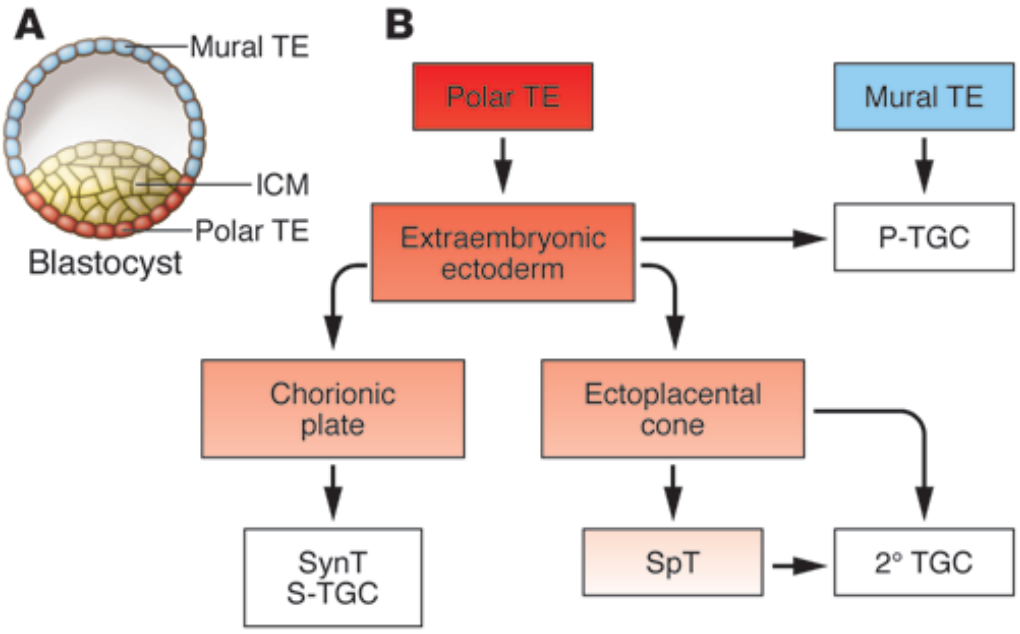

Figure 1.10 Lineage segregation within the mouse blastocyst and early placenta.

A) At day e3.5, the blastocyst comprises an outer trophectoderm (TE) destined to populate the placenta and an inner cell mass (ICM) destined to form the embryo. TE cells not in direct contact with the ICM form the mural TE, whereas those adjacent to the ICM form the polar TE. The polar TE gives rise to the extraembryonic ectoderm. **B)** Following implantation, mural TEs initiate the first wave of trophoblast giant cells (TGC) differentiation to form primary TGCs (1° TGCs), which contribute directly to the parietal TGC (P-TGC) population. Cells within the polar TE continue to proliferate and populate the ExE. Some secondary TGCs (2° TGCs) arise directly from the extraembryonic ectoderm. Along with 1° TGCs, they compose the parietal TGC (P-TGC) population that lines the implantation site. Cells within the extraembryonic ectoderm then differentiate to form the chorionic plate and the ectoplacental cone (EPC). The chorionic plate is responsible for populating the mouse labyrinth with multinucleated syncytiotrophoblasts (SynTs) and a subset of 2° TGCs called sinusoidal TGCs (S-TGCs). Together, these cells are responsible for the transport functions of the placenta. Cells within the ectoplacental cone can either differentiate into a population of lineage-committed progenitors known as spongiotrophoblasts (SpTs), which then differentiate into 2° TGCs, or they can directly differentiate into various 2° TGCs subtypes. From (Maltepe et al., 2010).

Glycogen trophoblast cells differentiate within the spongiotrophoblast layer of the junctional zone and after e12.5 they begin to interstitially invade the decidua (Adamson et al., 2002). The extraembryonic mesoderm, also known as the allantois, gives rise to the vascular portion of the placenta. At e8.5 the allantois fuses with the chorion (the cellular, outermost extraembryonic membrane) in a process called chorioallantoic attachment. The chorion begins to fold in order to create spaces called villi into which fetal blood vessels grow from the allantois (Cross et al., 2006). During this time, the chorionic trophoblast cells begin to differentiate into the two labyrinth cells types – the syncytiotrophoblast cells which surround the fetal endothelium of the capillaries and the sinusoidal trophoblast giant cells which line the maternal blood sinuses. These trophoblasts, together with the fetal vasculature, mark the third milestone of placental development where they generate extensively branched villi of the labyrinth, starting after e8.5, that continue to grow and become larger and increasingly branched up until birth (Cross et al., 2006). If this process fails and the labyrinth is not appropriately vascularised (i.e. suitable patterning, branching and dilation) it impairs placental perfusion, which can result in poor oxygen and nutrient diffusion (Pardi et al., 2002; Watson and Cross, 2005). Following chorioallantoic attachment branching of morphogenesis of the labyrinth occurs so that from e10 the placenta is capable of hemotrophic exchange where blood-borne materials can be exchanged between maternal and fetal blood. Maximum hemotrophic exchange doesn't occur until 14.5 when the placenta is fully mature (reviewed by (Watson and Cross, 2005) (Figure 1.9)

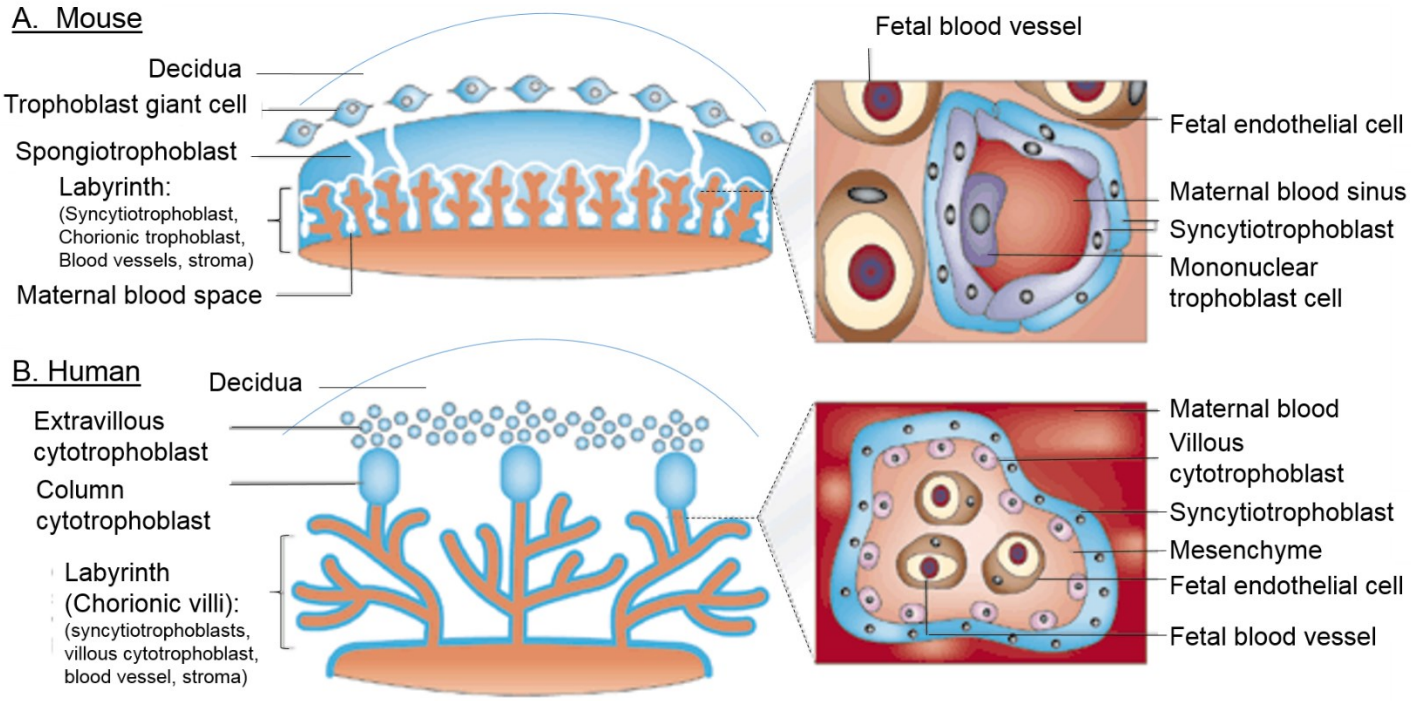

Figure 1.11 Comparison of human and mouse gross placental structure. (Adapted from (Rossant and Cross, 2001).

1.4.11 Placenta functions

The placenta is not only the main interface between the mother and the fetus, responsible to nutrient transport, but is also an endocrine organ capable of controlling maternal physiological adaptations to pregnancy. Moreover, evidence is emerging that the placenta actively responds to nutritional and metabolic signals from both mother and fetus is able to respond to these different cues by altering its structure and function thereby regulating fetal growth (reviewed by (Diaz et al., 2014).

1.4.11.1.1 Nutrient and gas transport

Fetal growth is largely dependent on the supply of nutrients and gases (oxygen and carbon dioxide) across the placenta (reviewed by (Lager and Powell, 2012). Gas transfer is primarily determined by blood flow whereas transport of nutrients can be passive or active. Factors that influence placental transport include uteroplacental and umbilical blood flows, size of the labyrinth, maternal and placental metabolism, and activity/expression of specific transporter proteins in the placental barrier; the syncytiotrophoblast layer (Lager and Powell, 2012).

1.4.11.1.2 Glucose

Glucose, the primary energy source for the fetus, is transported by facilitated diffusion and dependent on a number of factors (reviewed by (Baumann et al., 2002) such as glucose supply (determined by maternal blood glucose concentration and blood flow) and the maternal-fetal glucose concentration gradient, placental glucose metabolism (dependent on supply of other energy generating substrates such as oxygen), and placental glucose transporter density in the syncytiotrophoblasts of the labyrinth.

Glucose transporter proteins (GLUTs) are responsible for the facilitated carrier-mediated diffusion, in particular GLUT-1 (*Slc2a1*) and GLUT-3 (*Slc2a1).*

1.4.11.1.3 Amino acids

Amino acid transport is mediated by active transporters which are either accumulative transporters; increasing intracellular amino acid concentrations by mediating uptake against their concentration gradient, or exchangers; exchange amino acids between the intracellular and extracellular compartments (Lager and Powell, 2012). Amino acid transporters are sub-divided into systems (system A, system L and systemβ) depending on which type of amino acids they transport and whether they are sodium-dependent. System A is sodium-dependent and transports small non-essential neutral amino acids such as glycine, serine and alanine. Importantly, it increases the intracellular concentration of these amino acids, which are exchanged by system L for extracellular essential amino acids, which cannot be made by the body (Lager and Powell, 2012). The three isoforms of system A include SNAT1 (*Slc38A1*), SNAT2 (*Slc38a2*) and SNAT4 (*Slc38a4*). System L includes LAT1 (*Slc7a5*) or LAT2 (*Slc7a8*) (reviewed by (Verrey, 2003). System β transports taurine, not strictly an amino acid, but which the fetus is unable to synthesize, against its concentration gradient energized by co-transport with sodium and chloride (Lager and Powell, 2012).

1.4.12 Endocrine functions

The placenta has important endocrine functions that ensure the maintenance of pregnancy and reprogram maternal physiology in order for the fetus to thrive. Placental endocrine functions in humans and mice are associated with primarily with the junctional zone but also the decidua, and although they differ to some extent, both species synthesise overlapping sets of pregnancy-specific hormones that bring about very similar effects (reviewed by (Malassine et al., 2003) (Figure 1.12). The primary

difference is that in mouse, the placenta takes over stimulating the corpus luteum to produce hormones for the maintenance of pregnancy, substituting for PRL produced by the maternal pituitary, whereas in humans the placenta itself takes over in the production of hormones (Strauss et al., 1996). The placental hormones responsible for this regulation are mouse PL I (mPLI) and mouse PL II (mPLII). Both these hormones are PRL-like hormones and bind to the prolactin receptor (PRLr), which is found not only in the ovary but also in a range of maternal tissues. Therefore, the PLs display a wide range of activities in addition to the continuous production of progesterone by the corpus luteum. PLs also promote fetal growth directly (Talamantes et al., 1980) and indirectly by inducing many maternal adaptations such as the changes in maternal glucose metabolism (Handwerger and Freemark, 2000) and mobilization of glucose from maternal liver glycogen by promoting hepatic gluconeogenesis (Ogren and Talamantes, 1988). mPLI and mPLII are both produced by trophoblast giant cells in the junctional zone, with mPLI peaking on day e10, declining after day e11 and remaining low. Following the peak of mPLI, mPLII increases rapidly by e14 and remains high for the remainder of gestation (Talamantes et al., 1980). Furthermore, the mouse placenta also produces two non-classical members of the same family; proliferin (mPLF) and proliferin-related protein (mPRP) which are also expressed by trophoblast giant cells. Both can modulate angiogenesis and have been implicated in the appropriate vascularization of the implantation site in early pregnancy by stimulating growth of maternal blood vessels in the decidua toward the implantation site (Jackson et al., 1994).

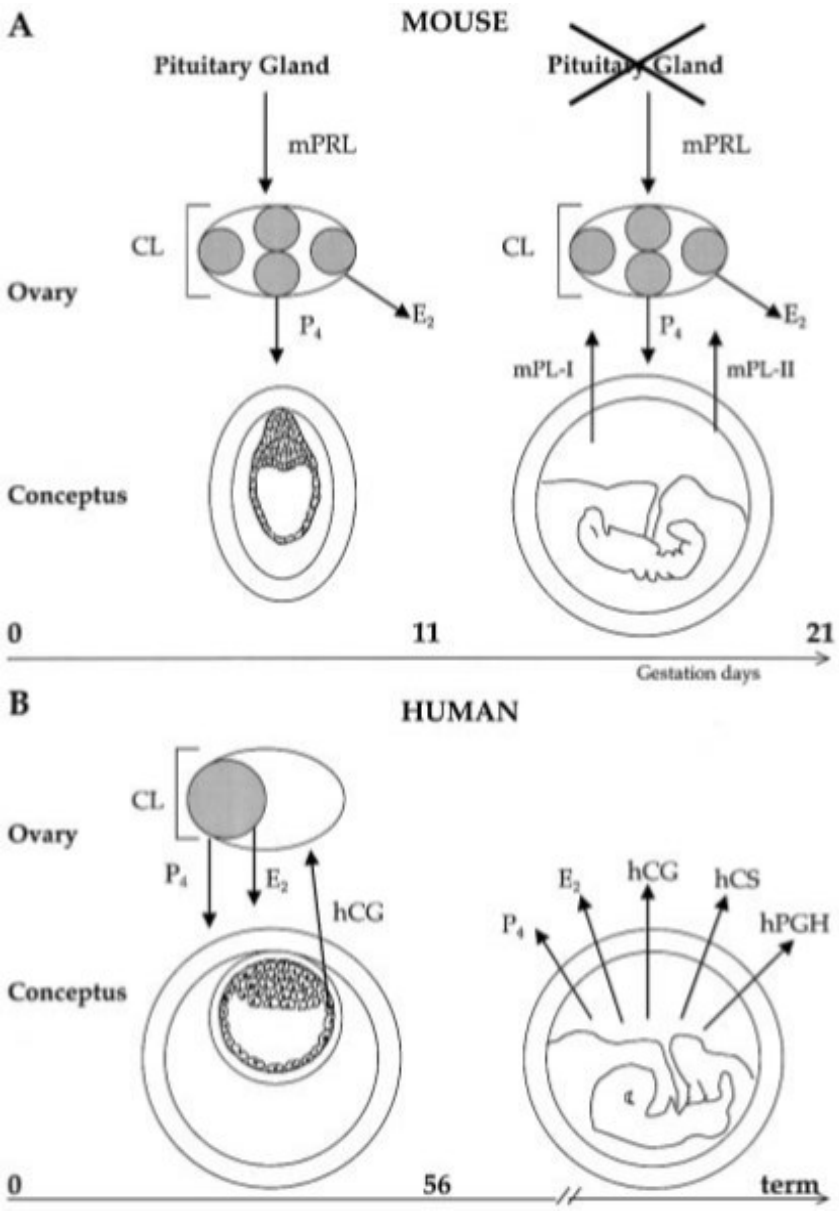

Figure 1.12 Endocrine comparison of mouse and human placenta.

Comparative endocrine functions of the murine and human placenta. (A) In mice, the corpus luteum is the primary source of progesterone (P4) and estradiol (E2) production required for the maintenance of pregnancy as well as maternal adaptations to pregnancy. Initially, mouse pituitary prolactin (mPRL) secreted by the pituitary stimulates the endocrine function of the ovary but in later gestation this is taken over approx. on day 11 by mouse placental lactogen I (mPLI) and mouse placental lactogen II (mPLII) produced by the trophoblast giant cells (TGCs) in the junctional zone of the placenta.(B) In humans, the maintenance of the pregnancy is also initially maintained by the corpus luteum stimulated by hCG. In later pregnancy, the syncytiotrophoblast layer of the placenta takes over P4 and E2 production and also

produces human chorionic somatomammotrophic hormone (hCS) and human placental growth hormone (hPGH). (From (Malassine et al., 2003).

Humans also produce PL (hPL), also known as human chorionic somatomammotrophic hormone (hCS), which similarly to mPL lactogen has been shown to regulate maternal metabolism and fetal growth (Chellakooty et al, 2004 pp. 384; Mirlesse et al, 1993 pp. 439; Koutsaki et al, 2011 pp. 31; Handwerger and Freemark et al, 2000 pp. 343). The PLs regulate fetal growth in concert with maternally- and placental-derived insulin-like growth factors (IGF-I and IGF-II) and their cell surface receptors (IGF-IR and IGF-IIR) (Constancia et al., 2002; Forbes et al., 2008). This has been demonstrated in placental-specific IGF-II knockout mice (P0), which lack the placental-specific IGF-II promoter, resulting in reduced placental weight and IUGR (Constancia et al., 2002) and in human studies where low circulating IGF-I levels or mutations cause severe IUGR (Gibson et al., 2001). Specifically, these growth hormones ensure placental blood flow and nutrients to the fetus by controlling placental cell turnover, proliferation, survival and differentiation as demonstrated *in vitro* (Forbes et al., 2008) .

In humans, the placenta produces human chorionic gonadotropin (hCG) which acts as a luteinising hormone (LH) -superagonist to maintain the corpus luteum, for the production of progesterone, which is taken over approximately after 8 weeks of gestation by the syncytiotrophoblast cells in the labyrinth of the placenta. hCG is also involved in the differentiation of cytotrophoblasts into syncytiotrophoblasts (Shi et al., 1993; Yang et al., 2003) further ensuring progesterone production.

A second major difference between the mouse and human placenta is that the human placenta in the second half of gestation produces high amounts of steroids (Albrecht and Pepe, 1990; Pepe and Albrecht, 1995). Both progesterone and oestrogen are produced by syncytiotrophoblasts, where progesterone is synthesized from maternal lipoprotein cholesterol and oestrogen is synthesized from the conversion of androgens by syncytiotrophoblastic cytochrome p450 aromatase (reviewed by (Malassine et al., 2003). Furthermore, differences in the expression of 11 beta-hydroxysteroid

dehydrogenase type 2 (11β-HSD-2) are present, as it is expressed throughout gestation in human but switched off in mid-gestation the mouse (Brown et al., 1996). 11β-HSD-2 inactivates corticosterone (cortisol in humans) by conversion into inert forms (cortisone, 11-dehydrocorticosterone) which is believed to protect the fetus from maternal glucocorticoids. In humans, low levels or absence of 11β-HSD-2 is associated with IUGR (Dave-Sharma et al., 1998; McTernan et al., 2001), but this effect is strain dependent in mouse as 11β-HSD-2 null mice can exhibit normal (Kotelevtsev et al., 1999) or reduced birthweight (Holmes et al., 2006).

1.4.13 Pregnancy complication: IUGR and stillbirth

Intrauterine growth restriction, present in 7-10% of pregnancies (Demicheva and Crispi, 2014), is defined as the failure of the fetus to reach its genetic growth potential and, next to prematurity, is the second leading cause of perinatal death (Chiswick, 1985; Gardosi et al., 1998). A review of perinatal mortality records highlights that up to 53% of preterm stillbirths and 26% of term stillbirths are growth restricted (Gardosi et al., 1998). Currently, no treatment is available for growth restriction *in utero*, with the only option to prevent *in utero* death being pre-term delivery, which may also compromise the fetus if it is very premature. Furthermore, IUGR is associated an increased risk of neurodevelopmental problems in childhood as well as with a number of adult-onset morbidities such as obesity, hypertension, cardiovascular disease and type 2 diabetes, in both human epidemiologic studies and in animal models (reviewed by (Salam et al., 2014). IUGR also present signs of cardiac dysfunction *in utero* that persist postnatally and may condition a higher cardiovascular risk later in life (Demicheva and Crispi, 2014). IUGR is associated numerous causative factors which can either individually or synergistically impact fetal growth. Generally, the causes of IUGR are classified as maternal, placental and/or fetal although in at least 40% of IUGR cases the underlying cause is unknown (reviewed by (Wollmann, 1998). Maternal causes include nutritional deficiencies, poor maternal weight gain as well as conditions such hypertensive disorders, chronic renal disease, severe anaemia, uterine

malformations and diabetes mellitus (Wollmann, 1998). Aberrant maternal uterine artery remodelling and subsequent decreased uteroplacental blood flow accounts for a high number of IUGR cases (Lyall et al., 2013). IUGR generally develops either in early gestation, often referred to as early-onset IUGR, or late in gestation referred to as late-onset IUGR. Early-onset IUGR is often associated inappropriate spiral artery remodelling and is therefore often considered to be a vascular disorder as in the case of preeclampsia (Muresan et al., 2016). Late-onset IUGR in humans is most often cause by fetal hypoxemia/hypoxia secondary of placental insufficiency (Muresan et al., 2016).

Interestingly, epidemiological studies demonstrated that women born growth-restricted have an increased risk of having an IUGR baby (Skjaerven et al., 1997). Furthermore, a previous IUGR baby increases the risk of IUGR reoccurrence in a subsequent pregnancy (Skjaerven et al., 1988). Feto-placental causes include chromosomal and or structural anomalies in the fetus and/or the placenta, intrauterine infections and multiple pregnancies (Wollmann, 1998). Placental insufficiency is recognized as the leading cause of IUGR and refers to the inability of a placenta to provide sufficient oxygen and/or nutrients to the fetus; it results from numerous factors such as inappropriate placental development, insufficient maternal uterine artery remodelling and/or fetal spiral artery remodelling and reduced nutrient transport. When diagnosing IUGR it is important to be able to distinguish between fetuses which are constitutionally small and not at an increased risk of an adverse outcome versus those which are pathologically small and at risk of mortality or morbidity. In order for this distinction to be made, a classification of birthweights using population-based sex-adjusted centiles is often used and is sub-divided as birth weights which are very small for gestational age (<3rd percentile), small for gestational age (<10th percentile), appropriate for gestational age (10th to 90th percentile) and large for gestational age (>90th percentile). Recently, individualized birthweight ratios (IBRs), which take into consideration maternal variables such as parity, ethnicity, weight and height are being utilised to generate customised birthweight centiles and improve the accuracy of diagnosis and prediction of outcome (Clausson et al., 2001; de Jong et al., 1998; Gardosi et al., 1995). However, there is divide in opinions over the use of IBRs in

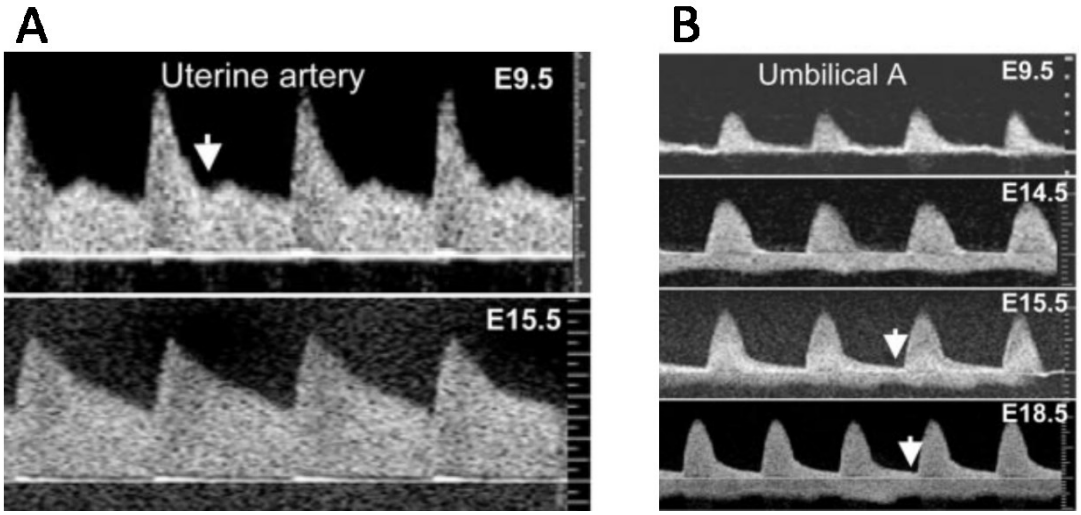

Figure 1.13 Changes in Doppler flow velocity waveforms of the uterine artery and umbilical artery in mouse during gestation.

A) At e9.5 Doppler flow velocity waveforms show a prominent notch (arrow) which is absent at e15.5 following remodelling. If inappropriate remodelling occurs waveforms in late gestation resemble those of early gestation. B) Normal umbilical velocity waveforms during gestation showing the increase of end diastolic velocity from e15.5 (arrow). (Adapted from (Mu and Adamson, 2006).

accurately defining IUGR (Alexander et al., 1996; Brenner et al., 1976; Gardosi et al., 1995; Hadlock et al., 1991; Resnik, 2007; Zhang et al., 2011). IUGR is also classed as either symmetric or asymmetric. Asymmetric IUGR is characterised by a reduction in fetal abdominal circumference, which results from the reduction in liver volume due to glycogen depletion in an attempt to compensate for the limited nutrient supply. However, the head circumference remains relatively normal. It is believed to often manifest in the second half of gestation and is commonly associated with uteroplacental insufficiency whereby 'elevations in placental blood flow resistance increase right cardiac afterload and promote diversion of the cardiac output toward the left ventricle owing to the parallel arrangement of the fetal circulation and the presence of central shunts. Blood and nutrient supply to the upper part of the body thus increase and result in relative head sparing' (Gordon, 2007). Symmetric IUGR is where body and head growth are affected to the same degree resulting in a uniformly small fetus. This type of IUGR is most often associated with congenital anomalies of fetal origin such as aneuploidy syndromes and infection and is believed to more commonly

manifest in early pregnancy. It is important to note that the IUGR type can change over the course of pregnancy depending on the underlying cause and duration of the insult.

IUGR is a major risk factor for stillbirth; a devastating outcome of pregnancy which in the UK occurs in about one in 200 pregnancies (Smith and Fretts, 2007). Other risk factors in women include placental dysfunction (being the most common cause of IUGR), nulliparity, advanced age and obesity (Smith and Fretts, 2007). Many cases of stillbirths however, occur in women with none of the above risk factors and often remain unexplained, particularly after 28 weeks of gestation, irrespective of whether the fetus was classifies as SGA or AGA (Figure 1.14). This is partly due to a lack of uniform protocols globally for assessment and classification of stillbirths as well as a low rate of autopsies (Smith and Fretts, 2007). There is a limited number of test that can be done in humans to assess the risk of stillbirth such as measurement the measurement of a some placental proteins including pregnancy-associated plasma protein A (PAPP-A) (Dugoff et al., 2004; Smith et al., 2002) and α-fetoprotein (AFP) in maternal blood (Waller et al., 1993). Additionally, the hemodynamic properties of the uterine and placental arteries, essential for providing an adequate blood supply to the feto-placental unit, can be assessed using Doppler ultrasound (Lees et al., 2001). However, these techniques are rarely used in pregnancies which are considered at low risk of complications and therefore fail to prevent stillbirths in such cases. Further research is needed particularly into the pathophysiology of stillbirth as well as developing new, reliable and easy predictive and preventative tests.

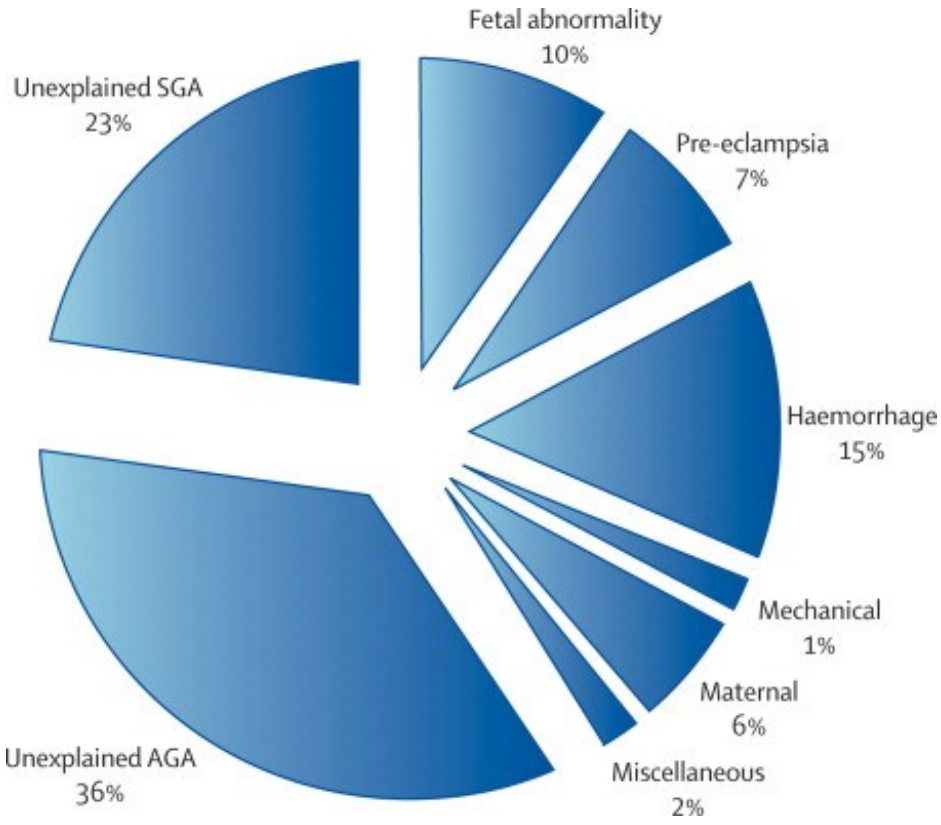

Figure 1.14 Causes of stillbirth with modified version of Wigglesworth classification for all singleton births in Scotland, 1992–2001.

Data from 2635 antepartum stillbirths, from a total of 563 719 births (rate 4·7 per 1000). Over the same period, there were 320 intrapartum stillbirths in 561 084 singletons alive at the onset of labour. 75% of these stillbirths were anoxic, 17% were classified as caused by congenital abnormality, and the remaining 8% had diverse other causes. SGA=small for gestational age (smallest decile of birthweight for sex and week of gestation). AGA=appropriate for gestational age (rest of population). From (Smith and Fretts, 2007).

1.5 Work leading up to PhD project

Prior to the start of my PhD, preliminary characterization of the phenotype of *Pabp4*$^{-/-}$ and *Pabp4*$^{+/-}$ mice was undertaken. Interestingly, this revealed a role for maternally expressed PABP4 in fetal viability and growth during mid to late pregnancy; forming the basis for my PhD studies. Specifically, *Pabp4*$^{-/-}$ crosses led to a severe reduction in litter size (Figure 1.16.A). Analysis of uteri of pregnant *Pabp4*$^{-/-}$ females 1-2 days prior to birth revealed multiple resorbing embryos (Figure 1.16.B). The resorptions were not specifically positioned within the uterus and were heterogeneous in size, suggesting that death occurred at different developmental stages. Importantly, ~50% of resorbing embryos were similar in size to viable embryos and possessed placentas, suggesting mid-late intrauterine mortality (Figure 1.16.B). Within these litters, a significant number of surviving pups appeared growth restricted (Figure 1.16.C). Interestingly, these phenotypes were also present, but less prominent, in *Pabp4*$^{+/-}$ intercrosses, signifying that complete absence of PABP4 function is not required for phenotype development (i.e. haploinsufficiency). A histopathological survey showed an absence of gross histological abnormalities in other tissues that normally express PABP4 (Figure 1.15) which, taken together with the haploinsufficiency, increases the likelihood that similar phenotypes occur in the human population.

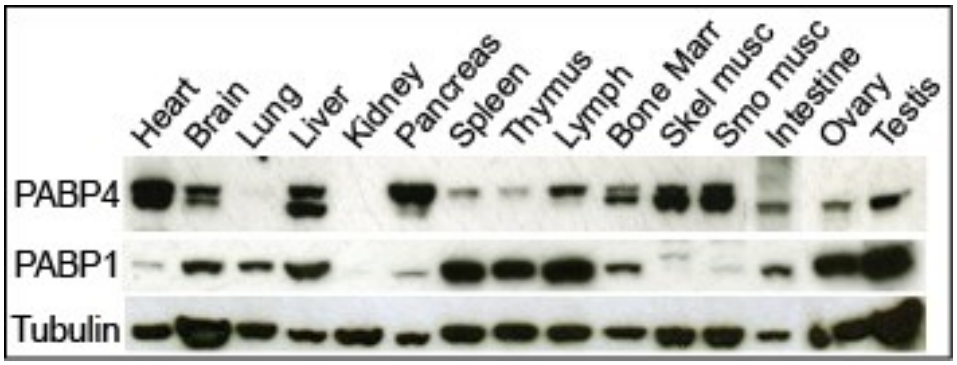

Figure 1.15. A western blot showing PABP4 and PABP1 in a range of mouse tissues (courtesy of Hannah Burgess).

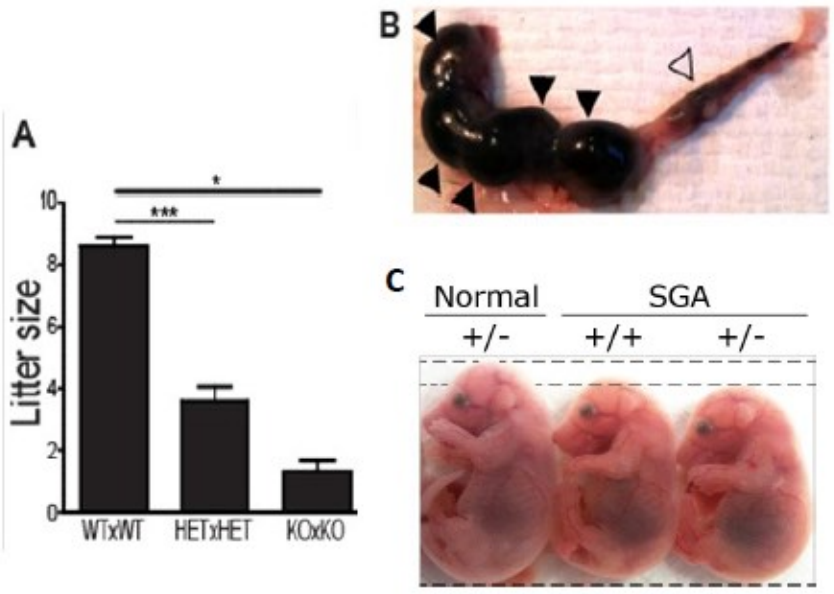

Figure 1.16. PABP4 haploinsufficiency and deficiency results in reduced litter size at birth and small fetuses (courtesy of Matt Brook).

A) Litter sizes from timed matings are significantly reduced in *Pabp4*$^{+/-}$ x *Pabp4*$^{+/-}$ (HetxHet) (n=14) and *Pabp4*$^{-/-}$ x *Pabp4*$^{-/-}$ (KOxKO) (n=7) crosses in comparison to Pabp$^{+/+}$ (WT) control crosses (n=6) at e18.5. Statistical significance was assessed by Students t-test and significance was accepted at $p<0.05$. B) e18.5 uterus containing both mid- (▽) and late-stage (▲) resorptions. No viable embryos were present. C) Example of observed small for gestational age (SGA) fetuses of different genotype at e18.5 suggesting SGA is independent of fetal genotype.

Surprisingly, genotype analysis of *Pabp4*$^{+/-}$ intercrosses at e18.5 revealed that *Pabp4*$^{-/-}$ pups were present at approximately Mendelian ratios (Figure 1.17. A) and that additional crosses between *Pabp4*$^{-/-}$ males and *Pabp4*$^{+/+}$ females resulted in a normal mean litter size (Figure 1.17. B). In contrast, *Pabp4*$^{+/+}$ male x *Pabp4*$^{-/-}$ female crosses resulted in a reduced mean litter size (Figure 1.18), indicating that maternal PABP4 deficiency results in the reduction of litter size.

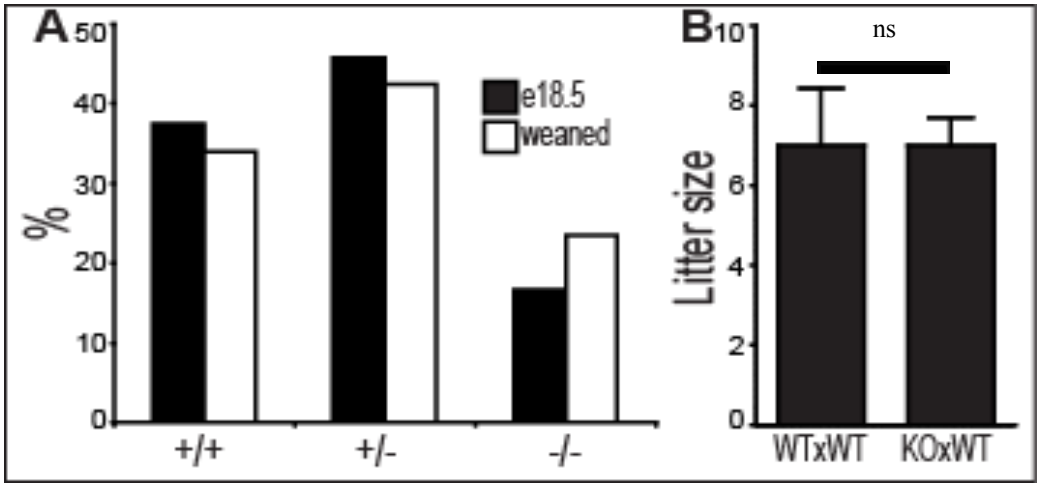

Figure 1.17. Mendelian ratios are observed at e18.5 and PABP4 KO males show normal sized litter at e18.5 (courtesy of Matt Brook).

A) Mendelian ratios are observed for litters at weaning and in viable e18.5 embryos (n=11). B) *Pabp4*$^{-/-}$ (KO) males show normal-sized litters at e18.5. Comparison of mean litter sizes based on litters from *Pabp4*$^{+/+}$ (WTxWT) crosses (n=6) and KOxWT crosses (n=7) at e18.5 (Labels correspond to ♂x♀). Statistical significance was assessed by two-tailed Mann Whitney test and significance was accepted at $p<0.05$.

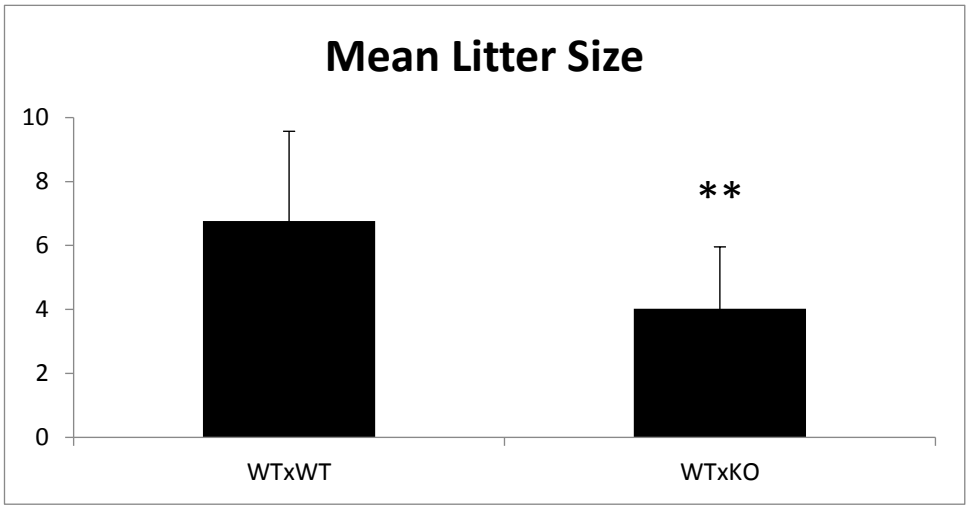

Figure 1.18. Maternal PABP4 deficiency results in a reduced litter size (courtesy of Matt Brook).

Comparison of mean litter sizes from *Pabp4*$^{+/+}$ WTxWT crosses (n=7) and WTx*Pabp4*$^{-/-}$(KO) crosses (n=11) housed as pairs for 30 weeks at birth (Labels correspond to ♂x♀). Statistical significance was assessed by two-tailed Mann Whitney test and significance was accepted at $p<0.05$. $p=0.0028$

Overall, these data indicate that maternal PABP4 deficiency may provide a novel tool for studying defects in the maternal environment, which can lead to pregnancy problems including late miscarriage, IUGR and stillbirth.

Thus, the aim of my PhD is to characterise the phenotype of PABP4-deficient mice to establish the timing, nature and physiological and/or cellular basis of the primary defect. This will shed light on the biological roles of PABP4 in mammals and, in so doing, will contribute to the knowledge of how regulated mRNA translation and stability contribute to the feto-maternal dialogue.

1.6 Hypothesis

PABP4 acts as a "master regulator" of the expression of factors required for coordinated development and/or function of the materno-fetal interface, by regulating mRNA translation and stability.

This hypothesis is addressed in the next four results chapters.

Chapter 2 - Materials and Methods

2.1 Buffers and solutions

6 x DNA loading buffer

-0.03% bromophenol blue

-0.03% xylene cyanol FF

-30% glycerol

-60 mM EDTA

-10 mM Tris-HCl (pH 7.6)

TAE agarose gel running buffer

-90 mM Tris-HCl (pH 8.3)

-90 mM acetic acid

-2 mM EDTA

NuPAGE Transfer buffer (pH 7.4)

-25 mM Tris-base

-200 mM glycine

-20% methanol

PBS (Phosphate buffered saline) (pH 7.4)

-137 mM NaCl

-6.5 mM Na_2HPO_4

-2.7 mM KCl

-1.5 mM KH_2PO_4

PBS-T (PBS-Tween-20) (pH 7.4)

-PBS (pH 7.4)

-0.1% Tween-20

Phospho-Radio-Immunoprecipitation Assay (RIPA) buffer (pH 7.4)

-50 mM Tris-base

-150 mM NaCl

-1 mM EDTA

-1% NP40

-0.2% SDS

-10 mM sodium pyrophosphate

-25 mM β-glycerophosphate

-0.5% sodium deoxycholate

-100 mM sodium orthovanadate

-5 mM sodium fluoride

-1 mM DTT

-1 complete protease inhibitor cocktail tablet (Roche)

-10 nM Calyculin A

Protein purification lysis buffer (on ice)

-20 mM Tris-HCl (pH 8)

-150 mM NaCl

-10 mM Imidazole

-1 complete protease inhibitor cocktail tablet, EDTA free (Roche)

-1 x BugBuster solution (Novagen)

-1 mM DTT

-25 units/ml benzonase

-1000 units/ml lysozyme

4 x Sample Loading Buffer

-20% Glycerol

-200 mM 2-mercaptoethanol

-4% SDS

-0.2% Bromophenol blue

-100 mM Tris-HCl (pH 6.8)

Sodium dodecyl sulphate polyacrylamide gel electrophoresis (SDS-PAGE) running buffer (pH 8.8)

-25 mM Tris-base

-250 mM Glycine

-0.1% SDS

20 x SSC (Sodium Chloride / Sodium Citrate buffer) (pH 7.0)

-3 M NaCl

-0.3 M $Na_3C_6H_5O_7.2H_2O$

TBS (Tris-buffered saline) (pH 7.4)

-10 mM Tris-base

-137 mM NaCl

TBS-T

-TBS

-0.1% Tween-20

2.2 Mouse work

2.2.1 PABP4 Knock-out mouse strategy

The vector and ES cell(s) used to generate the mice for this project were generated by the trans-NIH Knock-Out Mouse Project (KOMP) and obtained from the KOMP Repository (www.komp.org). NIH grants to Velocigene at Regeneron Inc (U01HG004085) and the CSD Consortium (U01HG004080) funded the generation of gene-targeted ES cells for 8500 genes in the KOMP Program and archived and distributed by the KOMP Repository at UC Davis and CHORI (U42RR024244). (For more information or to obtain KOMP products go to www.komp.org or email service@komp.org.)

Knock-out first conditional ready PABP4 (MGI:2385206) mice used were created by the Sanger Centre (Hinxton, Cambridgeshire, UK) but were missing a loxP site and were therefore not conditional. These mice were named NTP4 (knock-out) and were maintained on a C57BL/6N background.

The PABP4 KO strategy is outlined in detail at the start of Chapter 3.

2.2.2 Mouse husbandry and welfare

Animals were maintained in the Biomedical Research Facility at Little France, University of Edinburgh on a 12 hour light/dark regime, with humidity maintained at 55% and temperature between 20 and 25°C as specified in the Animal Act, 1986 (Scientific Procedures). Food and water were available *ad libitum.* All animals were fed commercial pelleted mouse feed. All procedures were undertaken according to the UK Home Office regulations. Animals were culled by inhalation of rising concentration of carbon dioxide (Schedule 1 method). Timed matings were carried out under my direction by facility staff.

2.2.3 Timed matings

To investigate timing of the phenotype and underlying defects timed matings with individual pairs were set up using virgin females between 8-12 weeks and male studs between 8 weeks up to 6 months. The following crosses were used, *Pabp4*$^{+/+}$ x *Pabp4*$^{-/-}$ (KO cross) and *Pabp4*$^{+/+}$ x *Pabp4*$^{+/+}$ (wild-type control cross), male genotype is listed first. Females were examined for post-copulatory vaginal plugs with the morning of discovery being designated as 0.5 days post-coitum (0.5dpc). Following the discovery of a plug, females were separated from the male. Following Schedule 1, pregnant dams were placed in a supine position to allow for collection of blood (see Blood collection and blood glucose measurements) and the removal of the intact uterus through the abdomen.

2.2.4 Maternal organ and feto-placental unit collection and measurements

For the collection of e8.5 and e10.5 and e13.5 materno-fetal units, the entire uterus was placed into fix (see Fixation, embedding and sectioning). Once fixed, individual implantation sites were dissected out and trimmed from excess inter-implantation uterine muscular wall (Figure 2.5). Where appropriate maternal body weight was determined after removal of the uterus.

Uteri from later gestation time-points (e15.5 and e18.5) were removed from the abdomen with embryos and placentas dissected out prior to measurement and were subsequently fixed. This was done by cutting the muscle layer of the uterus followed by tearing of the yolk sac with tweezers to obtain the embryo and placenta. The allantois was cut to free the placenta from the embryo. The embryo crown-rump length was measured using a digital calliper (World Precision Instruments, Ltd.) before being weighed and placed into fix. Placental diameter was also measured using a digital calliper, weight was also recorded. Placentas were either fixed whole immediately in 4% NBF (see Fixation, embedding and sectioning) or hemisected using a double-edged razor blade with one half snap frozen and the other half fixed in 4% NBF. For all time-

points maternal organs (brain, heart, thyroid gland, liver, kidney, adrenal gland,pancreas and spleen) were dissected out, spot blotted, weighed and fixed.

2.2.5 Fetal and Head and abdominal measurements

Following fixation, head and abdominal measurements were taken using digital callipers (World Precision Instruments, Ltd.) (*Figure 2.1*). Head and abdomen circumference were calculated from these measurements using the following Ellipse formula:

$$= \pi * \sqrt{(2 * ((\frac{1}{2}\ long\ axis)^2 + (\frac{1}{2}\ short\ axis)^2)}$$

The head:abdominal ratio was calculated from this to determine whether growth restriction is symmetrical or assymetrical.

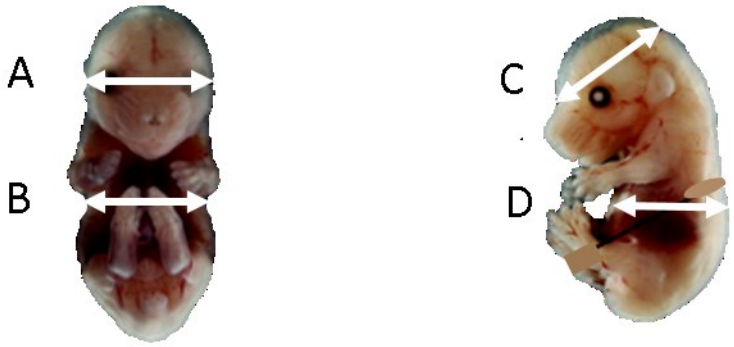

Figure 2.1 Fetal head and abdomen measurements.

Head measurements; A – short axis, C – long axis. Abdominal measurements; B – long axis, D – short axis. The callipers are placed flush against the fetus and in the same position each time to limit variability.

2.2.6 Blood collection and blood glucose measurements

Following Schedule 1, non-pregnant and pregnant dams were placed in a supine position, the abdomen was immediately cut open and blood was collected from the abdominal aorta. Prior to being transferred to Lithium Heparin 1.3ml microtubes (Sarstedt, Germany) blood glucose levels were determine using maltose free Accu-chek strips and an Accu-chek glucose meter (Aviva, Roche). For haematological analysis, whole blood in the Lithium Heparin tubes was placed on ice and transported to Easter Bush Pathology (Edinburgh) where it was analysed using an automated flow cytometer-based haematological analyser. For plasma analysis, blood samples were centrifuged at 1000 x g for 5 mins in a refrigerated centrifuge at 4 °C. Plasma (the resulting supernatant), was immediately transferred into a clean polypropylene tube using a pipette. Samples were stored at -20°C prior to analysis, transferred on wet ice and immediately analysed on arrival at the the Wellcome Trust Supported Cambridge Mouse Biochemistry Laboratory (Table 2.1).

Fetal blood glucose was obtained using the same strips and glucose meter as maternal blood following decapitation, once weight and crown-rump measurements were taken.

Assay	Reagents/Assay Type	additional info
HDL	Randox colourimetric assay - converted into Siemens assay format	Siemens Dimension RXL analyser
Insulin	electrochemical luminescence immunoassay - MesoScale Discovery	MesoScale Discovery (MSD) Mouse Metabolic assay
Leptin	electrochemical luminescence immunoassay - MesoScale Discovery	MesoScale Discovery (MSD) Mouse Metabolic assay
Estradiol	competitive time resolved fluorescence immunoassay (DELFIA) - Perkin Elmer	Perkin Elmer DELFIA kit (human)
Progesterone	competitive time resolved fluorescence immunoassay (DELFIA) - Perkin Elmer	Perkin Elmer DELFIA kit (human)
NEFA	Roche Free Fatty Acids - half micro test kit	Modified for use in microtitre plates
Corticosterone	competitive enzyme immunoassay (EIA)	Immuno diagnostics systems (IDS) kit
IGF-I	ELISA immunoassay	Immuno diagnostics systems (IDS) kit

Table 2.1 Details of assays used for blood plasma analysis carried out by the Wellcome Trust Supported Cambridge Mouse Biochemistry Laboratory.

2.2.7 Stereology

The Computer Assisted Stereology Toolbox (CAST) 2.0 system (Olympus, Ballerup, Denmark) was used to for stereological analysis of the placenta and has been described elsewhere (Coan et al., 2004) but is briefly outlined below.

2.2.7.1 Absolute Placental Volume

A 32-point grid was superimposed on placenta sections using a 1.25x objective lens allowing to view a complete placenta section. Points of the 32-point grid which fell on the placenta section were counted and the Cavalieri principle was applied to determine a volume estimate (Gundersen and Osterby, 1981):

$$V_{(obj)} = t \times \Sigma a = t \times a_{(p)} \times \Sigma P$$

$V_{(obj)}$ is the estimated placental volume, t is the total thickness of the placenta (total number of sections multiplied by section thickness), $a_{(p)}$ is the area associated with each point, and ΣP is the sum of points on sections (Coan et al., 2004).

Shrinkage due to the process of fixation and embedding was taken into account by measuring the diameter of randomly selected maternal erythrocytes and comparing this value to that of a fresh maternal erythrocyte and used to calculate a shrinkage factor and placental volume was corrected accordingly (Coan et al., 2004).

2.2.7.2 Volume of Placental zones

A so called 'meander' sampling function of the CAST software was used to view random fields with the placenta section using a 10x objective lens and point counting was done for points which fell on each placental zone. Volume of each zone was then estimated using the following equation:

$$V_{v(struct,ref)} = P_{(struct)} / P_{(total)}$$

where $V_{v(struct)}$ is the volume fraction of a component (e.g., labyrinth zone) within a reference space (e.g., placenta), $P_{(struct)}$ is the number of points falling on the component, and $P_{(total)}$ is the total number of points falling on the reference space (including the component) (Coan et al., 2004). Finally the volume densities for each zone were multiplied by total placental volume to convert to absolute quantities (Coan et al., 2004).

2.2.8 Ultrasound Doppler imaging

Vevo 770 High-Resolution In Vivo Micro-Imaging System (FUJIFILM, VisualSonics, Toronto, Canada; equipped with four different transducers with central frequencies ranging from 20- 40 MHz) was used to collect ultrasound data from non-pregnant or pregnant females at e17.5 of gestation. Females were anesthetized using isoflurane (2%), laid in a supine position and paws taped to limb leads on the platform to monitor heart and respiration rates whilst ventilated with 100% oxygen and isoflurane anesthesia (*Figure 2.2*). Body temperature was monitored using a rectal thermometer and maintained between 36-38°C using a heating pad and a lamp. The abdomen of the mouse was shaved and remaining hairs were removed using a chemical hair remover. Remnants of the chemical hair remover were washed away using water and gauze. As the procedure was terminal lubricant was not applied to the eyes which is normally used to prevent damage of the corneas as a result of dehydration. Pre-warmed

ultrasound gel was applied to the shaved abdomen and used as an acoustic coupling medium. The platform on which the mouse is laid out in a supine position is tilted to displace the abdominal organs in the cranial direction helping to reveal the uterine artery in the pelvis. The uterine was located ventral to the bladder, by the uterocervical junction (*Figure 2.3*). Furthermore, ultrasound waveforms were obtained for umbilical arteries of at least three fetuses in each litter, maternal carotid artery and common carotid artery. Ultrasound measurements were taken in collaboration with an experienced ultrasound technician, Adrian Thomson. All waveform were analysed offline using VevoStrain™ Analysis software.

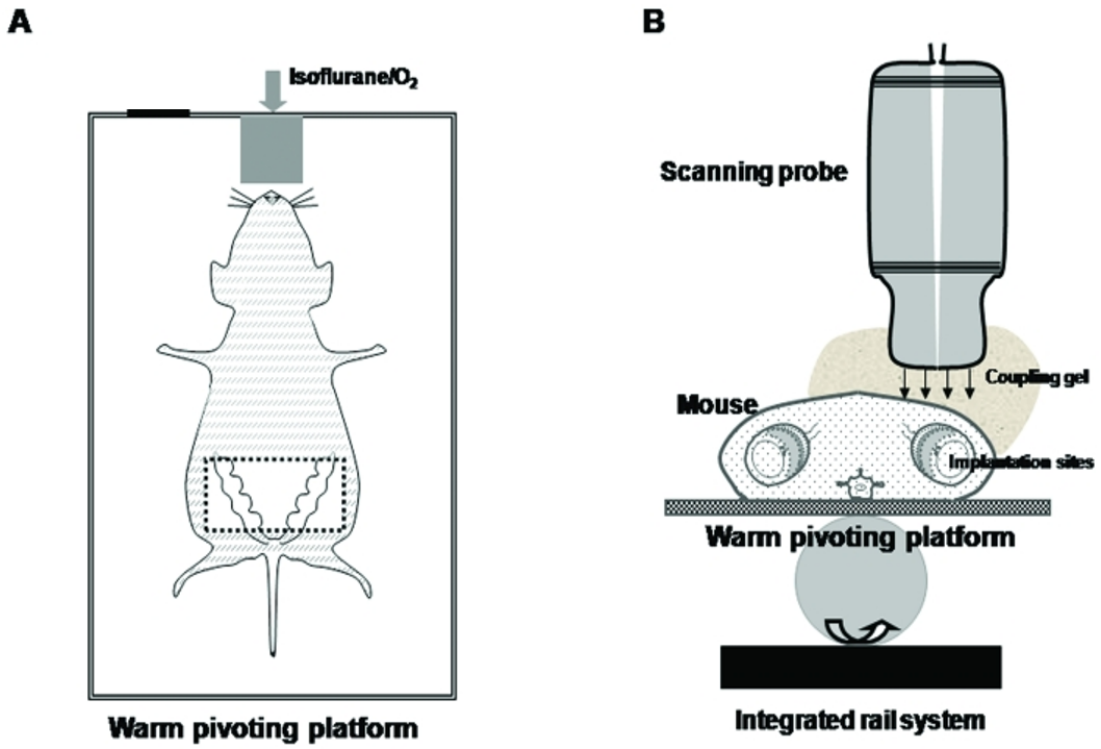

Figure 2.2. Ultrasound imaging of females.

Positioning and ultrasound imaging of an anesthetized, dorsally recumbent pregnant mouse (A) as an aerial view and (B) in transverse cross-section. All hair was removed from the ventral abdomen after the mouse was anesthetized with approximately 2.0% (1.5% to 2.5%) isoflurane. The mouse then was placed on the platform and held in position with surgical tape. A thick layer of warm water-based coupling gel was applied over the skin of the area to be imaged. A 30-MHz transducer probe was applied

to the skin to collect images. The transabdomenal area (boxed region in A) is used for detection of the pregnant uterus. All waveforms are saved for later offline analysis. Maternal heart and respiration rates were monitored by using an automated system and body temperature was maintained as 36 to 37 °C by the warmed platform, which is supported by an integrated rail system. Figures are not to scale. Adapted from (Zhang and Croy, 2009).

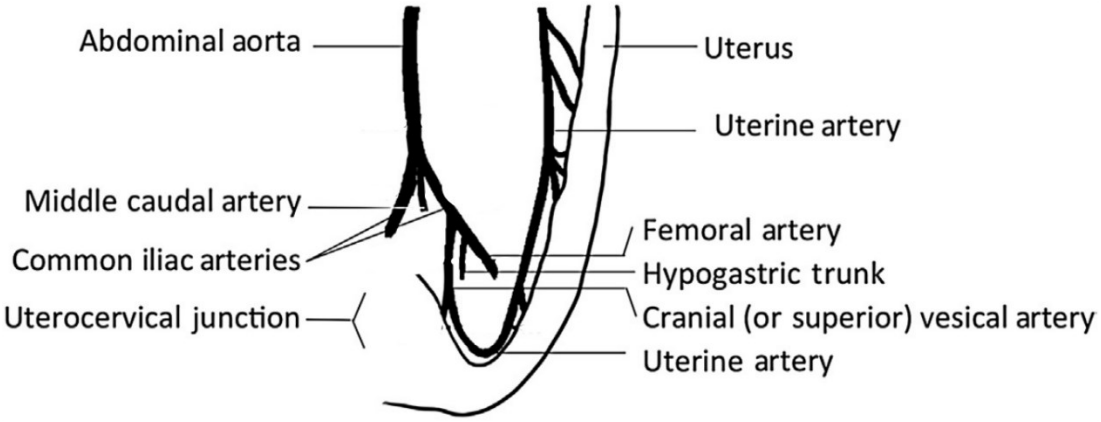

Figure 2.3. Diagram showing the uterine artery and other arteries close to the iliac bifurnication and uteroplacental junction. Adapted from (Qu, 2014).

2.2.9 Calculation of resistance index (RI)

Waveforms obtained from ultrasound were saved during scanning and were later analysed offline using ImageJ software peak systolic and end diastolic velocities were measured (Figure 2.4.) and RI index was calculated using the following equation:

RI = (Peak systolic velocity- End diastolic velocity)/Peak systolic velocity

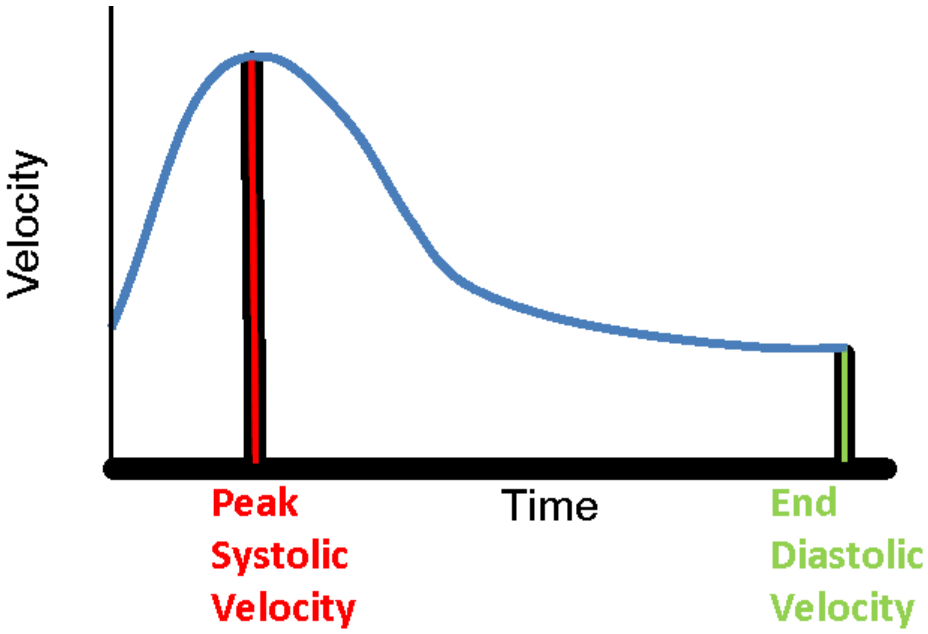

Figure 2.4. A diagram showing where measurements of peak systolic velocity and end diastolic velocity on a waveform, obtained by ultrasound, were taken.

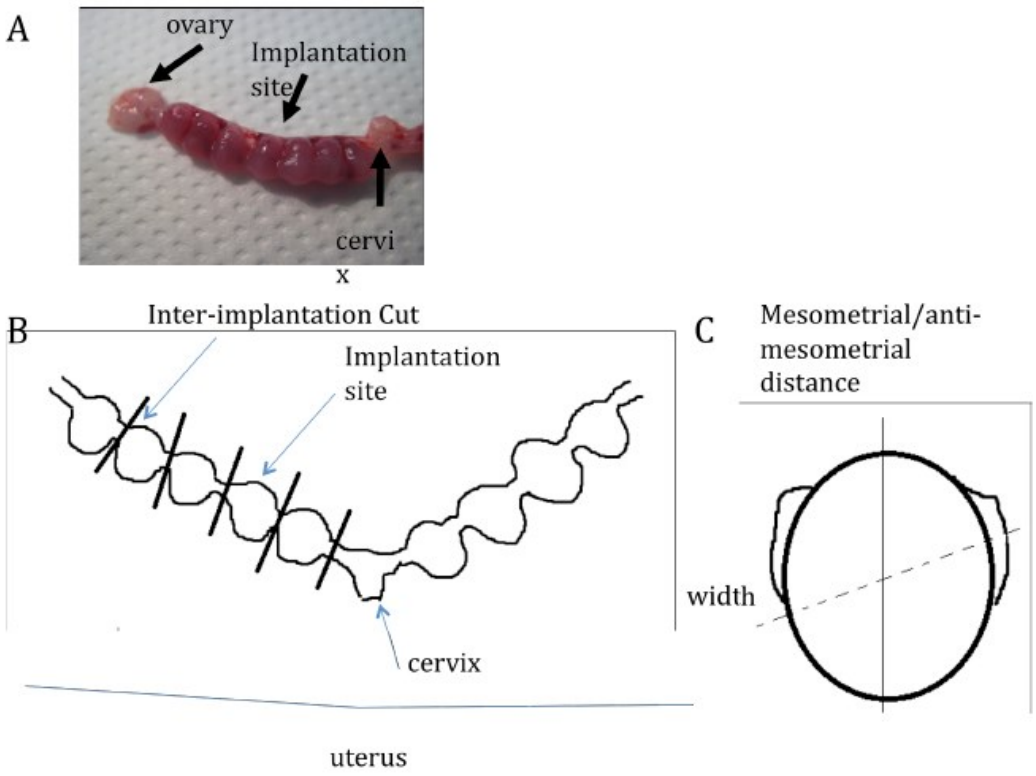

Figure 2.5 Collection of e8.5 Implantation sites.

A) Photograph depicting an ovary, a uterine horn containing embryos, and the cervix. B) An illustration to show where the inter-implantation cuts were made. C) The mesometrial to anti-mesometrial distance and width of each implantation site was measured using a digital calliper.

2.2.10 Genotyping

Genotyping was initially done by extracting genomic DNA followed by a PCR but was switched to being outsourced to Transnetyx® (Cordova, TN). Both techniques are outlined below.

Ear clips from pups were used to extract genomic DNA (gDNA). 25 µl of TE/Tween + 10 µl of Proteinase K was added to each ear clip in a PCR tube to submerge. Samples were digested to liberate genomic DNA on a 55/95 programme (55° C for 2 hours, 95°C for 5 mins, room temp. 10 mins), vortexed and centrifuged at 14000 rpm. 30 µl of the resulting supernatant was diluted in 270 µl of water and used for PCR to genotype. For each animal, 3 primer sets were used including a negative control where the primers were replaced by dH_2O.

A PCR reaction in a total volume of 25 µl was set up as follows:

dH_2O 7.5 µl

MyTaq HS Mix (Bioline) (components include MyTaq buffer, dNTPs, $MgCl_2$, enhancers and stabilizers) 12.5 µl (containing 0.1 µl of 100 mM of each forward and reverse primer) (Table 1)

DNA 5 µl

PCR reactions were run on a Dyad PCR machine (Bio-Rad) on the following programme:

95 ° C	3 min	
95 ° C	5 sec	28 cycles
60 ° C	5 sec	
72 ° C	20 sec	
72 ° C	2 min	

Products were then run on a 2.5% TAE/agarose gel with a 100bp ladder (NEB) with the Wild-type generating a single band of 632bp, the KO two bands (230bp and 550bp) and Hets 3 bands (230bp, 550bp, 632bp).

				Band size (bp)
Knock-out	Name	686F	CASR1	230
	Sequence	5'TGG GTT TGG TTT TCC TCC TG	3' TCG TGG TAT CGT TAT GCG CC	
Wild-type	Name	686F	686R	632
	Sequence	5'TGG GTT TGG TTT TCC TCC TG	3'CAG ACC ACC TCA CAG CAC TC	
Heterozygous	Name	LacF-60	LacR1-60	550
	Sequence	5' TCT AGA GGA TCC CGT CGT TT	TGC ACC ACA GAT GAA ACG CCG	

Table 2.2.Primer sets used for genotyping of mice.

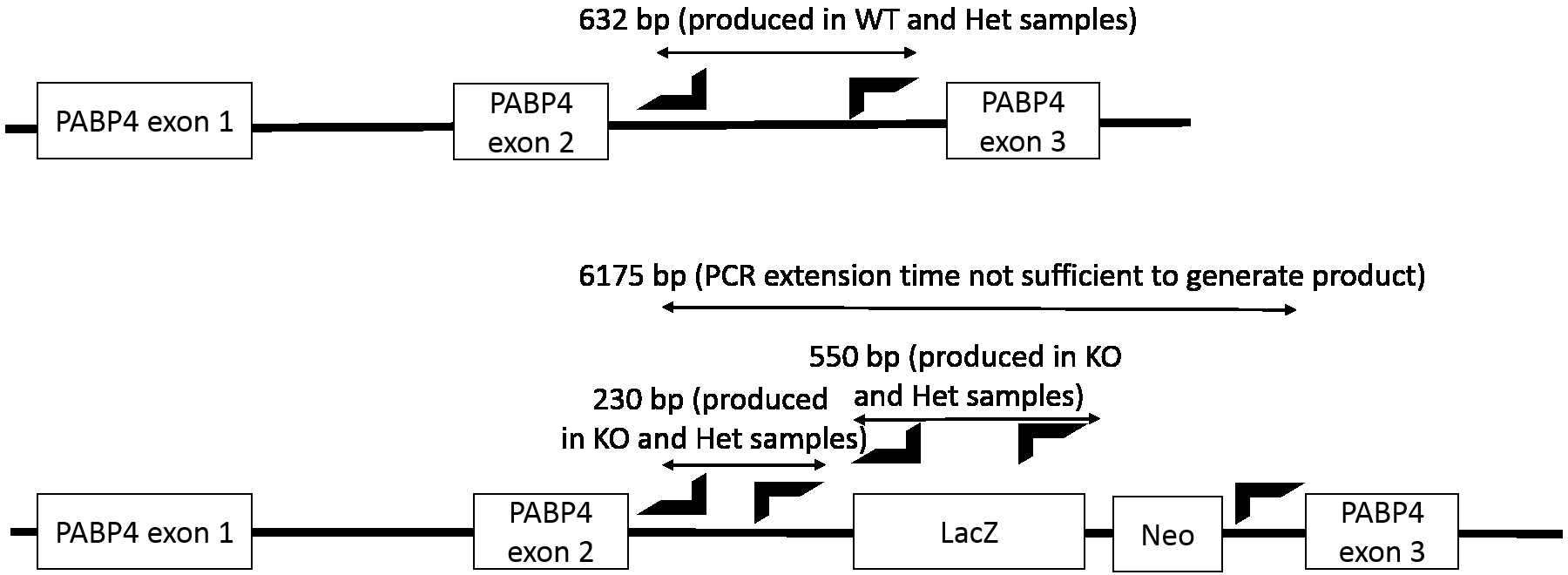

Figure 2.6 Representative position of primers used for genotyping of NTP4 mice.

2.2.11 Gel Electrophoresis

Agarose (2-3% w/v) was dissolved in TAE by heating in a microwave until boiling. After cooling down, Gel-Red (Biotium) was added to a final concentration of 1/10 000 and 6x DNA loading buffer was added to samples before loading. 100bp or 1kb DNA bench-top ladder (Promega) was loaded in addition to samples for determining DNA band sizes. Gels were run in TAE agarose gel running buffer at 25-100 volts and subsequently visualised using a trans-illuminator (Geneflash).

2.2.12 Transnetyx®

Mouse genotypes from ear clips were determined using Transnetyx services (Cordova, Tennessee, USA) which use an automated genotyping system using real time PCR with primers and specific labelled probes designed for each gene (Table 2.3) which identify the presence or absence of the desired genetic region. Briefly tissue samples were lysed using Proteinase K and DNA was isolated using the proprietary microbead-based method by Transnetyx. The DNA was then tested in duplicate using a specific quantitative PCR assay with results normalized to a single-copy housekeeping gene.

Name	Pabpc4-1 WT
Forward primer	CCCAAGGGCTGGTGTTACAAG
Reverse primer	CCAGCCCAGGGTTTTATTTTGTTTT
Labelled Probe	TTGCCACCACAGTCTGC
Name	LacZ
Forward primer	CGATCGTAATCACCCGAGTGT
Reverse primer	CCGTGGCCTGACTCATTCC
Labelled Probe	CCAGCGACCAGATGAT

***Table* 2.3 Primers and specific labelled probed used in genotyping by Transnetyx.**

2.3 Histological analysis

2.3.1 Fixation, embedding and sectioning

Tissues were fixed in 4% NBF (10x the volume of the tissue). After 24 hours of fixation, tissues were washed 3x in 70% ethanol before being stored at room temperature in 70% ethanol prior to being processed. Tissues were embedded in paraffin wax by the in house histology core facility in the MRC Centre for Reproductive Health (CRH) on a Leica TP1050 processor (Leica Microsystems).
Paraffin embedded tissues were sectioned (5 μm) using a Leica RM2135 microtome. Sections were floated on a 50°C water bath and mounted on electrostatic charged glass slides and dried overnight at 50°.

2.3.2 De-waxing and re-hydration

Prior to immunohistochemistry paraffin tissue sections were dewaxed in xylene (2x 5 min washes) and then rehydrated in graded alcohols (100%, 90%, 70%, 20 sec each). Finally, sections were rinsed in tap water.

2.3.3 Immunohistochemistry

Following de-waxing and re-hydration slides were submitted to heat-induced antigen retrieval in 0.01 M citrate buffer (pH 6.0) for 40 min in a pressure cooker which provides good heat-source regulation. Heat induced-antigen retrieval improves staining by breaking down-cross linking of proteins caused by NBF fixation and revealing protein epitopes necessary for complementary antibody binding. Tissue slides were slowly cooled in tap water and transferred to 3% (v/v) H_2O_2 in dH2O for 30 min to block endogenous peroxide activity. This was followed by 2x 5min washes

in Tris Buffered Saline (TBS). If a mouse antibody was being used on mouse tissue a Mouse on Mouse (M.O.M) ImmPRESS^{TM} mouse blocking reagent was applied and incubated with tissue for an hour. To block non-specific binding the tissue was then blocked in ready to use (2.5%) normal serum from the animal species used to raise the secondary antibody (ImmPRESS™, Vector laboratories) (see Table 2.4 for detail)(BSA) for 30 min. Excess serum was blotted from sections and incubated with 1˚antibody diluted in appropriate diluent solution overnight at 4℃.

The following day slides were washed in TBS (2 x 5min) and incubated with ImmPACT™ polymer IgG reagent (Vector laboratories) raised against the species primary antibody was raised in (see Table 2.4 for detail). Slides were washed in TBS (2 x 5 min) before DAB substrate was added (1 drop/ml, ImmPACT™ DAB Substrate Kit - Vector Laboratories). Incubation periods with DAB solution vary depending on the antibody and the tissue, therefore each slide was prepared individually and colour change monitored under a light microscope for between 30 seconds to 1 minute. DAB reaction was stopped by washing slides in tap water. Slides were counterstained with haematoxylin and dehydrated, prior to mounting. Negatives controls included an isotype of the primary antibody at the same concentration. Images were captured by a Canon DS6031 camera (Canon Europe) using Provis AX70 microscope (Olympus Optical) and the Axiovision Rel. 4.8. Software.

Protein	Source	Species raised in	Dilution	Antigen retrieval	Secondary Antibody	Serum used
PABP4	Sigma	Rabbit	1/1000	Yes	Anti-Rabbit IgG ImmPRESS™ reagent	Horse
PABP1	Gray lab	Rabbit	1/3500	Yes	Anti-Rabbit IgG ImmPRESS™ reagent	Horse
Cytokeratin 7/8	NIH Develop-mental Studies Hybridoma Bank	Rat	1/270	Yes	Anti-Rat IgG ImmPRESS™ reagent (mouse adsorbed)	Horse
Smooth muscle actin	Dako	Mouse	1/200	Yes	Anti-Mouse M.O.M ImmPRESS™ reagent	Horse

Table 2.4. Details of antibodies and conditions used for Immunohistochemistry.

2.4 Nucleic acid techniques

2.4.1 RNA extraction from snap frozen tissues

Snap frozen placental samples were lysed and total RNA extracted and purified using TRI reagent (Sigma-Aldrich) by Bill Richardson (senior lab technician).

In brief, during sample preparation the snap frozen tissue samples were homogenised using a hand held mortar/pestle (Anachem) in TRI Reagent (1ml per 50-100 mg of tissue). Samples were allowed to stand for 5 min at room temperature to allow the dissociation of nucleoprotein complexes to occur. 0.2 ml of chloroform per ml of TRI Reagent was added, shaken for 15 seconds and left to stand at room temperature for 2-

15min. Samples were centrifuged at 12, 000 x g for 15 min at 2-8 °C resulting in separation of the mixture into a red organic phase (containing protein), an interphase (containing DNA), and an aqueous phase containing RNA. 0.5ml of 2-propanol per ml of TRI Reagent used was added to the aqueous phase and allowed to stand at room temperature for 5-10 min. This was followed by centrifugation at 12, 000 x g for 10 min at 2-8 °C resulting in an RNA pellet at the bottom of the tube which was air dried for 5-10 min and subsequently dissolved in 0.1 ml of RNAse-free water. Was concentration determined and how stored.

2.4.2 RNA extraction from NBF fixed tissues

RNA was extracted from formalin-fixed tissues using RecoverALL™ Total Nucleic Acid Isolation Kit (Life technologies) according to manufacturer's instructions. In brief, the lab bench, pipettes and cutting equipment was cleaned using Ambion RNase *Zap* decontamination solution (Invitrogen) before an approximately 35 mg slice of fixed placenta was ground using a pestle and mortar on dry ice. 1ml of 100% ethanol was added to the ground up placenta and centrifuged for 2 min at room temperature at 20817 x g to pellet the tissue. The ethanol was gently removed without disturbing the pellet and this was repeated once more after which as much ethanol was removed without disturbing the pellet. The pellet was then air dried for 45min at room temperature. Digestion buffer and protease was added to each sample and gently swirled for the tissue to immerse and incubated for 15min at 50°C, then 15min at 80°C. An isolation additive/ethanol mixture was added to the sample and mixed by pipetting up and down. The mixture was passed through a filter cartridge and centrifuged at 10,000 x g for 30 sec and flow through discarded. The sample was washed, centrifuged at 10,000 x g for 30 sec and flow through discarded. An additional 30 sec centrifuge was undertaken to obtain residual fluid from the filter. 60µl of DNase mix was added to the sample and incubated for 30min at room temperature. The sample was washed, centrifuged at 10,000 x g for 30 sec and flow through discarded and an additional centrifugation performed for 1min to obtain residual fluid from the filter. The filter

cartridge was then transferred to a fresh collection tube and eluted with 60µl of room temperature elution solution and allowed to sit at room temperature for 1 min. The assembly was then centrifuged for 1min at maximum speed to obtain the eluate containing RNA and stored at -20°C. The extracted RNA was quantified and standardized to a concentration of 100 ng/µL using water.

2.4.3 RNA quantification

Extracted RNA was quantified using a Nanodrop® ND-1000 spectrophotometer (Nanodrop Technologies, USA). Absorbance ratio values of 260nm/280nm were used as an indicator of the RNA purity with a ratio of approximately 2.0 accepted as sufficiently pure RNA. Absorbance ratio values of 260nm/230nm were used as a secondary measure of nucleic acid purity with samples having a lower than the expected ratio of approximately 2.0 being rejected, due to the likelihood of contaminants absorbing at 230nm.

2.4.4 cDNA synthesis

RNA samples were converted into cDNA (reverse transcription) using SuperScript® III First-Strand Synthesis System (Invitrogen) following the manufacturers' guidelines. Briefly, 1µl of random primers, 1 µl of 10mM dNTP mix, and 400ng of mRNA were made up to a total volume of 10 µl in an Eppendorf tube and incubated at 65°C for 5 min. The tube was then placed on ice and the following added: 4µl $MgCl_2$, 2µl RT buffer, 2µl 0.1 DTT, 1µl RNase inhibitor and 1µl of SuperScript III RT. Contents were gently mixed by pipetting up and down and incubated at 25°C for 10 min followed by an incubation at 50°C for 50 min. The reaction was terminated at 85°C for 5 min. Finally, 1 µl of RNase H was added prior to incubation at 37°C for 20 min.

2.5 Real-time quantitative PCR (qRT-PCR)

qRT-PCR works on the same principle as PCR, however the PCR product is measured during each cycle. TaqMan® (Life technologies) method of qRT-PCR was utilised.

In TaqMan® fluorescent light is produced through the addition of a 5' fluorescently labelled probe containing a quencher dye at the 3'-end, specific forward and reverse primers to allow for quantification of the target gene relative to a housekeeping gene. In this assay the probe anneals to the target DNA sequence in between the forward and reverse primers. During amplification the 5'-3' exonuclease *Taq* DNA polymerase cleaves the probe, releasing the reporter dye from the quencher resulting in transmission of fluorescent light when excited by the laser. The amount of fluorescent is directly proportional to the amount of DNA produced by the PCR.

The mastermix was pipetted into a 384-well MicroAmp Fast Optical reaction plate (Applied Biosystems), followed by addition of the cDNA and control samples in duplicate. The Taqman reaction was performed using the Applied Biosystems 7900HT Fast real-time PCR system (Life Technologies, Paisley, UK) as follows; 95°hot start for 3 minutes, followed by a 5 second denaturation at 95°C. 40 cycles at 60°C for 15 seconds for the primers to anneal. The final step in the dissociation stage involved the melting of the double stranded PCR (dsPCR) product at 95°C for 15s, annealing at 60°C for 15 seconds, followed by a final melting of the dsPCR products at 95°c for 15 seconds. Analysis of qRT-PCR data was carried out using the comparative $\Delta\Delta C_t$ method. The fluorescence detected from TaqMan® is represented as an amplification plot. The cycle threshold (C_t) is directly proportional to the amount of target nucleic acid and indicated the number of amplification cycles that cross the threshold. The threshold was set to distinguish relevant fluorescence/amplification signal. Each cDNA sample was run in triplicate. The expression levels of the target genes were normalised to the expression level of *Sdha* (ΔCt) which was found to be the most stable housekeeping gene in the samples in comparison to *Gapdh* and *Acth* using SLqPCR package in R This value was expressed as a change relative to the reference sample

(ΔΔCt = ΔCt sample - ΔCt reference sample). The fold change was then calculated using the equation 2-ΔΔCt.

Target gene	Catalogue number of Taqman primer
Snat-1 (*Slc38a1*)	Mm00506391_m1
Snat-2 (*Slc38a2*)	Mm00628416_m1
Snat-4 (*Slc38a4*)	Mm00459056_m1
Glut-1 (*Slc2a1*)	Mm00441480_m1
Glut-3 (*Slc2a3*)	Mm00441483_m1
Gapdh	Mm03302249_g1
Sdha	Mm01352366_m1
Acta	Mm00808218_g1

Table 2.5 Table of TaqMan® primers used.

2.6 General protein work

2.6.1 Protein extraction from tissues

Throughout protein extraction, samples and buffers were kept on ice to minimise protease activity.

Mouse organs were snap frozen upon collection on dry ice and kept at -80°C before being homogenised in phospho-RIPA buffer. The volume of phospho-RIPA buffer used was the minimum required to submerge the tissue (approx. 1ml for bigger tissues such as liver, 500µl for smaller tissues such as spleen and kidney).

Qiagen TissueLyser homogeniser (Qiagen) was then used to homogenise the tissue (25Hz, 1-2 minutes) followed by 5 minute incubation on ice. Homogenised solutions were centrifuged at 14,000 rpm for 10 minutes at 4°C to pellet debris and the supernatant collected and stored at -20°C for future applications.

2.6.2 Bradford assay

Protein concentrations were quantified using Bradford Protein Assay Reagent (Bio-Rad). 1 µl of protein sample was added to 99 µl of water and 900 µl of Bradford Reagent in a spectrophotometer microcuvette. Using a Genequant Pro spectrophotometer (GE Healthcare) the 595 nm absorbance was read and the concentration of the sample calculated using a standard curve generated with bovine serum albumin (0-20 µg).

2.6.3 Polyacrylamide gel electrophoresis (PAGE)

SDS-polyacrylamide gel electrophoresis was performed using 4-12% NuPAGE MOPS (Invitrogen) gels. Samples calculated to have the same protein concentration were mixed with the appropriate volume of 4 x sample loading buffer and heated at 75°C for 10 minutes before loading alongside pre-stained or unstained protein Benchmark ladders (Invitrogen). Pre-cast gels purchased from Invitrogen were run using NuPAGE MOPS SDS Running Buffer (50 mM MOPS, 50 mM Tris, 0.1% SDS, 1 mM EDTA; pH 7.7) (Invitrogen) at 100-150V. Gels were run until the loading dye reached the bottom of the gel.

2.7 Western Blotting

2.7.1 Transfer and staining of membrane

After SDS-polyacrylamide gel electrophoresis, the gel was immersed in NuPAGE transfer buffer for 2 minutes and then transferred onto Immobilon membrane (Thermo Fisher) (previously hydrated in 100% methanol for 5 mins and immersed in NuPAGE

transfer buffer). The gel and Immobilon-P membrane were then sandwiched between 4 sheets (2 either side) of Whatman filter paper soaked in NuPAGE Transfer Buffer. Proteins were transferred using a fixed current of 100mA per gel for 1 hour using a V20-SDB semi-dry blotter (SCIE-PLAS). Transferred protein on the Immobilon membrane was visualised by staining using Gelcode Blue (Thermo Fisher) for 10-15min accordingly to the manufacturer's instructions. Excess stain was washed off by immersing the membrane in 50% methanol before being dried and the positions of the molecular weight markers marked using a permanent marker. Following this, the membrane was rehydrated in 100% methanol.

In the following section, all manipulations were performed with the minimal volume required to submerge the gel or the membrane except washes which were performed in an abundant volume of TBS-T at room temperature on a rocking platform.

2.7.2 Blocking, antibody incubation and detection

Membranes were blocked in either 5% (w/v) skimmed milk in TBS-T or 5% (w/v) BSA in TBS-T for 1 hour at room temperature on a rocker, dependent on antibody. Primary antibodies were diluted in 5 % (w/v) skimmed milk in TBS-T or 5% (w/v) BSA in TBS-T and incubated for 1 hour at room temperature or overnight at 4°C on a rocking platform. Following primary antibody incubation, the membrane was washed 3 times for 5 minutes in TBS-T before incubation with an appropriate secondary antibody conjugated to HRP diluted in either 5% skimmed milk in TBS-T or 5% (w/v) BSA in TBS-T. The membrane was then washed 3 times in TBS-T for 10 minutes and incubated in enhanced chemiluminescence solution (ECL) (GE Healthcare) for 1min or SuperSignal west femto maximum sensitivity substrate (ultra-sensitive ECL) (Thermo Scientific) for 5 min. Finally membranes were blotted dry and exposed to ECL Hyperfilm (GE Healthcare) and developed using Exograph compact x4 X-ray processor (XoGraph Imaging Systems) or detected using Odyssey Fc Imaging system (LI-COR Biosciences).

2.8 Microscopy

2.8.1 Brightfield Microscopy

Brightfield images were taken using an Axiocam camera (Zeiss, Welwyn Garden City, UK) on an Olympus Ax70 Provis microscope with UPlanFl objectives. Image capture was performed using Axiovision software (Zeiss).

2.9 Statistical Analysis

Data are expressed as mean ± standard error of the mean (SEM). Statistical analysis was performed using GraphPad (GraphPad Software, San Diego, California, USA). The specific statistical test used are described in the legend of each figure. Statistical significance was accepted at $p < 0.05$. Data was not subjected to normality tests.

Chapter 3 – Investigation into the breeding characteristics of *Pabp4*$^{-/-}$ dams

3.1 Introduction

The *in vivo* role of PABP4 in mammals has not been previously explored. To this end, *Pabp4*-targeted, knock-out first, conditional ready mice were created on request by the Wellcome Trust Sanger Institute (WTSI) (Hinxton, Cambridgeshire, UK). To create these mice, targeted homologous recombination was performed in C57BL/6N embryonic stem (ES) cells of parental line JM8.N4 through electroporation of a *Pabp4*-targeting construct to facilitate insertional mutagenesis at the *Pabp4* locus (Figure 3.1). The resulting ES cells were injected into C57BL/6NTac mouse blastocysts to produce multiple chimeric mice which were checked for germline transmission. Chimeric mice, where the ES-derived cells containing the *Pabp4*-targeting construct contributed to the germline, where mated to create offspring that were used to breed to mice which heterozygously contained the *Pabp4*-targeted mutation. In "knock-out first" mice, gene function is ablated by the inserted cassette (as depicted in Figure 3.1), which contains a *lacZ* expression marker gene and neomycin coding sequences (used for selection), both with polyadenylation signals that result in cleavage of the nascent pre-mRNA and consequently transcriptional termination which should create a whole body functional null. Breeding these mice to mice expressing the FLP recombinase allows removal of most of targeting cassette but leaves *loxP* sites flanking a 'critical' exon, creating 'conditional-ready' mice. For PABP4 exon 3, which is present in all *Pabp4* splice variants and removal of which causes a frame shift leading to complete gene inactivation, is the critical exon. These mice can be bred against Cre recombinase expressing mice to delete exon 3 in a time- and/or cell-specific manners. The *Pabp4*-targeted mice used in this PhD project contained the "knock-out first allele" and were found to be missing a loxP site and therefore did not have the potential to become conditional-ready. The full systematic genetic nomenclature of this targeted non-conditional strain is B6N;B6NTac;B6N-*Pabpc4*$^{tm1e(KOMP)Wtsi}$ (for simplicity referred to as *Pabp4*$^{-/-}$ from now on) and unless

otherwise stated this strain was utilized in all experiments. To determine whether the genotype of the mice was *Pabp4*$^{+/+}$, *Pabp4*$^{-/-}$ or *Pabp4*$^{+/-}$, polymerase chain reaction (PCR) was used using allele-specific oligonucleotides (*Figure 3.2*. A, B and C) such that different products were observed in wild-type, knock-out and heterozygous mice. Importantly, the absence of a PABP4 protein in *Pabp4*$^{-/-}$ mice was verified by western blot (*Figure 3.2*. C).

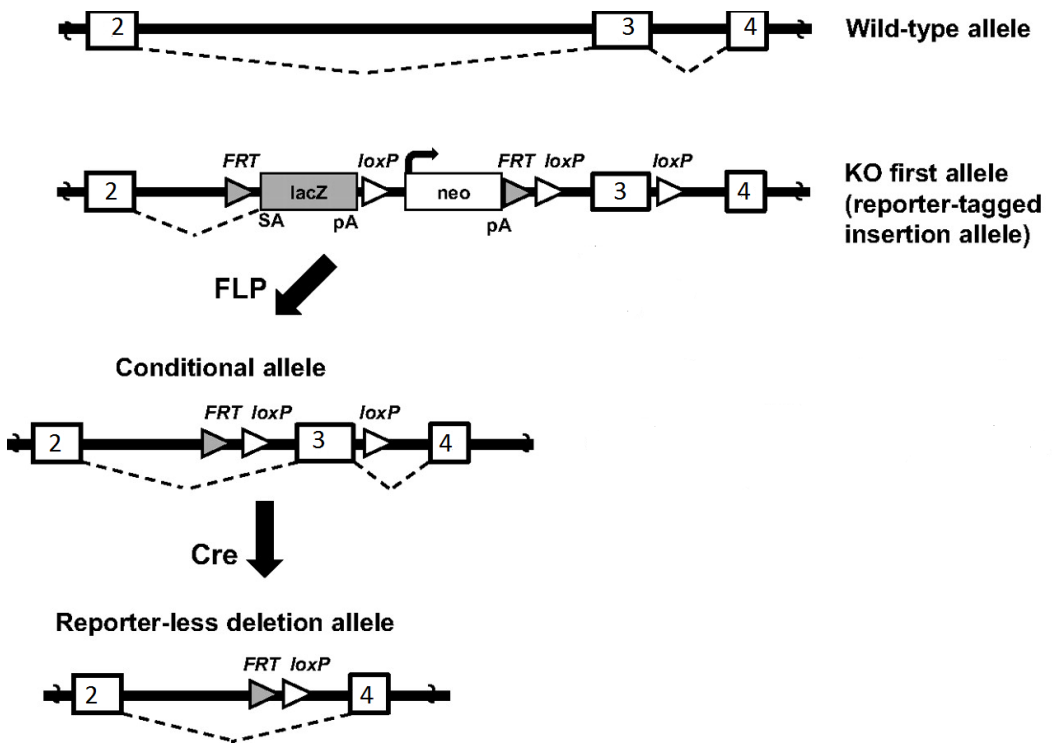

Figure 3.1 The PABP4 knock-out strategy.

In "KO first" alleles gene function is ablated by a polyadenylation signal-mediated transcriptional stop at the end of the ***lacZ*** expression marker gene that is driven off the target gene promoter. The Neo cassette used for selection also contains a polyadenylation signal. Removal of the targeting cassette by breeding to a mouse expressing FLP recombinase should leave ***loxP*** sites flanking a "critical" exon generating a conditional-ready mice. Breeding such mice to strains expressing Cre recombinase should result in deletion of the critical exon. SA, splice acceptor site; pA, poly A. Adapted from (Doetschman and Azhar, 2012).

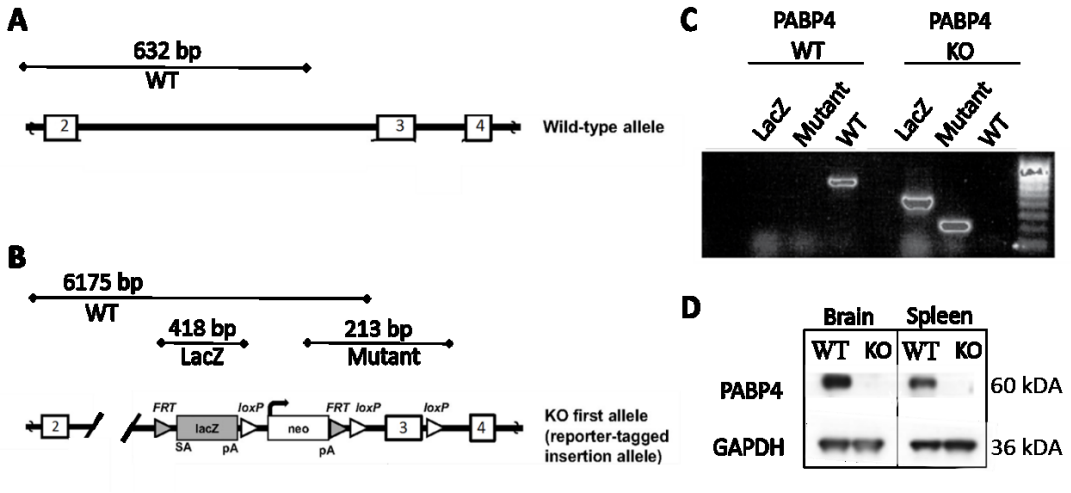

Figure 3.2. Confirmation of PABP4 knock-out.

A schematic diagram (not to scale) of the genotyping strategy of **A)** PABP4 wild-type mice and **B)** PABP4 knock-out mice. Vertical lines represent the relative positions of oligonucleotide primers used to amplify the specific alleles and visualised on an agarose gel. The expected sizes of the PCR products are indicated. **C)** PCR products representing the different genotypes visualised on a 1% agarose gel. In PABP4 KO mice, the PCR extension time is not sufficient to generate the long WT PCR product length (as a result of the cassette insertion), therefore no product is obtained. **D)** Western blot confirming that PABP4 protein is absent in indicated tissues of PABP4 knock-out mice. WT, wild-type; KO, knock-out.

3.2 Results

Prior to the start of my PhD, preliminary data from a small cohort of mice indicated that PABP4 is not absolutely essential for viability but, interestingly, maternal PABP4-deficiency led to a reduction in litter sizes at birth with observations of late *in utero* death (see section 1.5 Work leading up to PhD project), opening the possibility that *Pabp4*$^{-/-}$ females may provide a unique model of late miscarriage/stillbirth that is maternal in nature. However, the experimental data had relatively low power, the mice

utilised had a low backcross status and were not matched for age or parity. Thus, it was critical to confirm the veracity of these early observations. Unless stated otherwise, all females utilised in experiments here were aged 8-12 weeks, were backcrossed against C57BL/6N approximately 8-10 times and were virgin females and proven males. Firstly, to verify the parental genetic contribution to the phenotype and test the hypothesis that there is an absence of a male genetic contribution to the reduced litter size observed at birth, the entire spectrum of PABP4-crosses were set-up and litter size at birth monitored. These crosses served simultaneously as breeders therefore the litter sizes recorded were of females aged between 8-20 weeks and included various parity status. Importantly, no statistical difference in litter size was observed when *Pabp4*$^{+/+}$ females were mated to either *Pabp4*$^{+/+}$, *Pabp4*$^{-/-}$, or *Pabp4*$^{+/-}$ males (*Figure 3.3*.). However, all crosses involving *Pabp4*$^{-/-}$ females showed a statistically significant decrease in litter size compared to *Pabp4*$^{+/+}$ (*Figure 3.3*.). These data confirm that the phenotype is independent of paternal genotype. They also strongly suggest that reduced litter size is not driven by fetal genotype, since it is only altered in crosses between *Pabp4*$^{-/-}$ females with *Pabp4*$^{+/+}$ males but not the reciprocal cross (*Pabp4*$^{+/+}$ females with *Pabp4*$^{-/-}$ males), despite both resulting in heterozygous pups. Thus, the data support preliminary results that the reduction in litter size is dependent on maternal genotype. Furthermore, crosses of *Pabp4*$^{+/-}$ females crossed with either *Pabp4*$^{+/+}$, *Pabp4*$^{-/-}$, or *Pabp4*$^{+/-}$ males results in a normal litter size (*Figure 3.3*.) and therefore suggests that a single copy of the *Pabp4* gene does not result in haploinsufficiency replicating the WT phenotype.

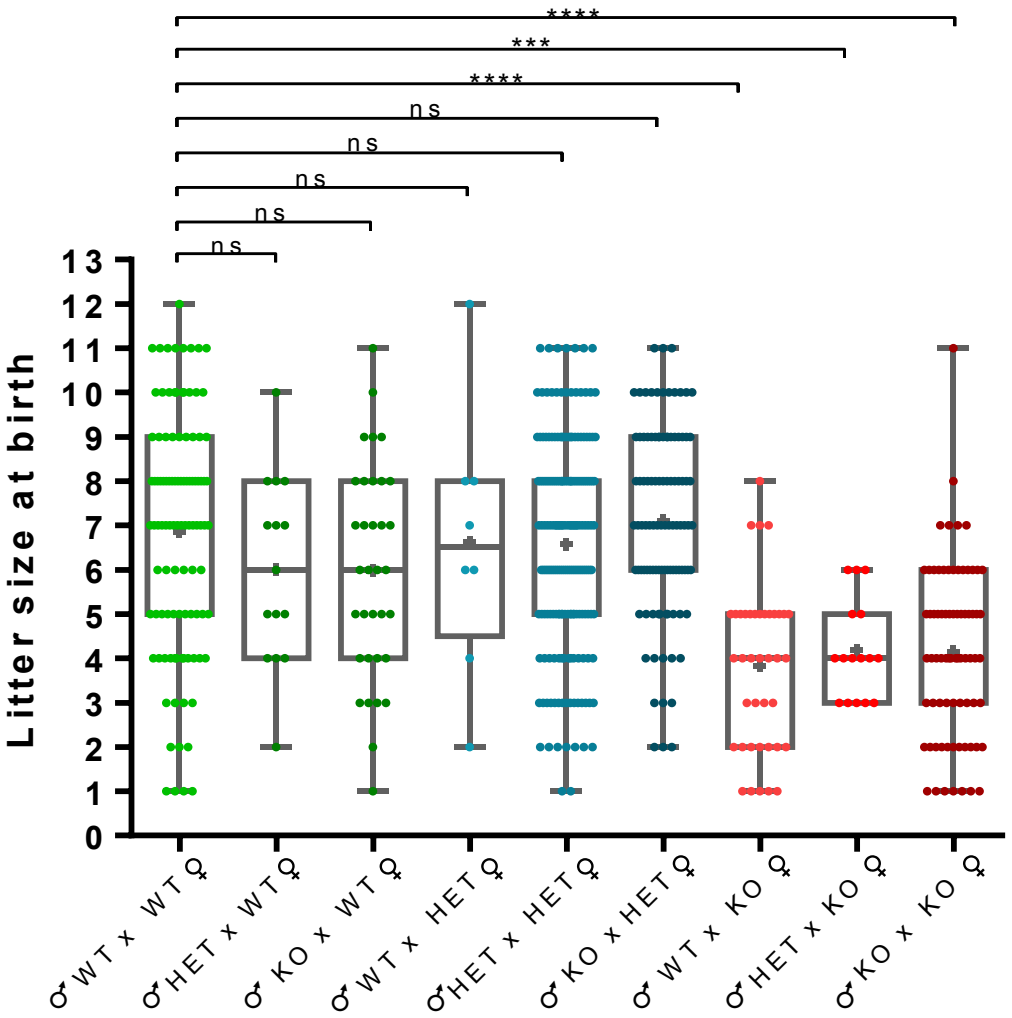

Figure 3.3. Maternal PABP4 deficiency results in reduced litter size at birth.

Litter size at birth of the entire spectrum of PABP4 crosses. Sample sizes are as follows: ♂ WT x ♀ WT (light green dot) *n* = 104; ♂ HET x ♀ WT (green dot) *n* = 15; ♂ KO x ♀ WT (dark green dot) *n* = 34; ♂ WT x ♀ HET (light blue dot) *n* = 8; ♂ HET x ♀ HET (blue dot) *n* = 190; ♂ KO x ♀ HET (dark blue dot) *n* = 103; ♂ WT x ♀ KO (light red dot) *n* = 40; ♂ HET x ♀ KO (red dot) *n* = 16; ♂ KO x ♀ KO (dark red dot) *n* = 75. Data are shown as shown as box and whisker plots with the median (long line) and mean (cross) indicated. Significance was analysed by Kruskal -Wallis test and Dunn's multiple comparison test. ns = ≥ 0.05; *** p = ≤ 0.001; **** p = ≤ 0.0001.

To further test the hypothesis that fetal genotype does not contribute to the phenotype, Mendelian ratios from *Pabp4*$^{+/-}$ inter-crosses were determined at embryonic day (e)

18.5/19.5 and at weaning. Consistent with the conclusion drawn from data in *Figure 3.3*, genotypic analysis of *Pabp4*$^{+/-}$ inter-crosses at e18.5/19.5 revealed that *Pabp4*$^{-/-}$ and *Pabp4*$^{+/-}$ fetuses were present at approximately Mendelian ratios of 25% and 50% respectively (*Figure 3.4*. A). However, at weaning, whilst *Pabp4*$^{+/-}$ fetuses remained to be present at the expected Mendelian ratio of 50%, the ratio of *Pabp4*$^{-/-}$ offspring was found to be only 19% and a chi square test this to be significantly deviant from the expected ratios (*Figure 3.4*. B). Given that *Pabp4*$^{+/-}$ inter-crosses did not produce reduced litter sizes at birth (*Figure 3.3*.) these data imply that neither fetal PABP4 deficiency nor haploinsufficiency contribute to the reduction of litter size observed at birth in *Pabp4*$^{-/-}$ females. However, whilst inter-cross litter size is normal at birth, a proportion of pups die prior to weaning (*Figure 3.4* C), which combined with the non-Mendelian ratios at weaning imply that post-birth *Pabp4*$^{-/-}$ offspring have an increased risk of death compared to *Pabp4*$^{+/-}$ and *Pabp4*$^{+/+}$ offspring.

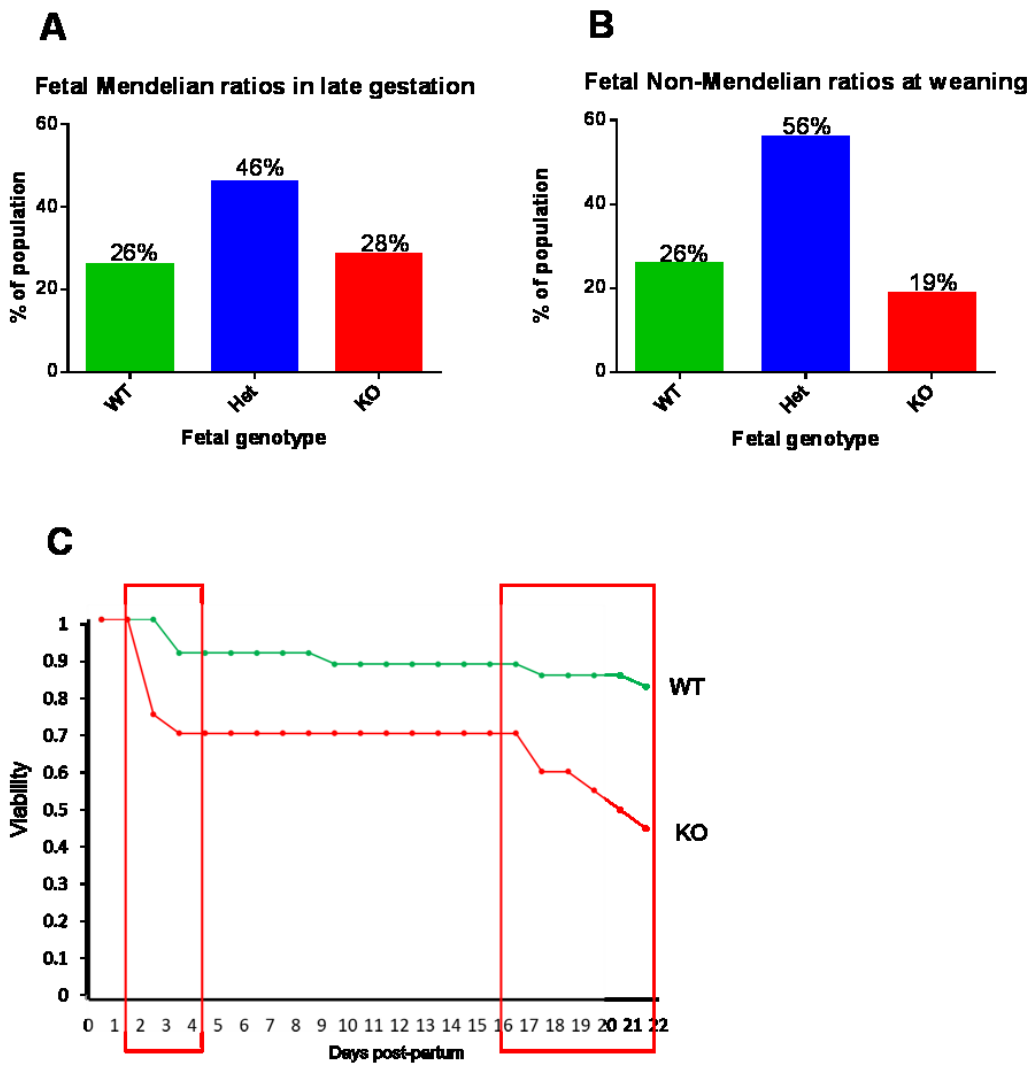

Figure 3.4. Genotypic analysis shows Mendelian ratios at e18.5-e19.5 but not at weaning.

Pabp4$^{+/-}$ females were crossed with *Pabp4*$^{+/-}$ males and progeny was either (**A**) collected and genotyped at e18.5-19.5 or (**B**) genotyped at weaning. Frequencies of fetal genotype at e18.5-e19.5 *Pabp4*$^{+/+}$ (*n* =34), *Pabp4*$^{+/-}$ (*n* =60) and *Pabp4*$^{-/-}$ (*n* =37); $\chi^2 = 0.5$; at weaning *Pabp4*$^{+/+}$ (*n* =149), *Pabp4*$^{+/-}$ (*n* =324) and *Pabp4*$^{-/-}$ (*n* =108) $\chi^2 = 13.5$. Data were analysed using the chi square test (test value = 5.99). (**C**) Post-partum loss of *Pabp4*$^{-/-}$ pups appears to bi-phasic with the first loss occurring between 2-4 days post-partum (pp) and the second loss occurring from day 17pp until weaning.

To interrogate the breeding characteristics of *Pabp4*$^{-/-}$ females in more detail and, importantly, to assess them in the context of a reproductive life span, individual pairs of *Pabp4*$^{-/-}$ females with *Pabp4* $^{+/+}$ males (from now on referred to as 'PABP4 maternal KO pairs' for simplicity) and *Pabp4* $^{+/+}$ females with *Pabp4*$^{-/-}$ males (from now on referred to as 'PABP4 paternal KO pairs' for simplicity) were set up for 30 weeks at the age of 8 weeks. Both parental crosses produced heterozygous offspring providing a suitable control for investigating the maternal nature of the phenotype believed to be independent of both paternal and fetal genotype.

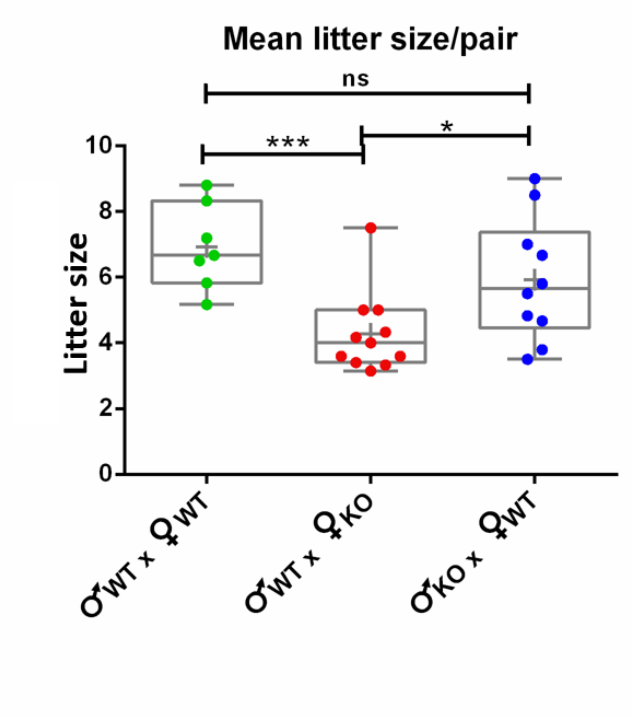

Figure 3.5. Average litter size from multiple pregnancies in PABP4 female mice is reduced.

Combined mean litter sizes at birth (+/- SD) from 30 weeks. ♂WT X ♀WT (green dots) n = 7; ♂WT X ♀KO (red dots) *n* = 11; ♂KO X ♀WT (blue dots) *n* = 10. Data are shown as shown as box and whisker plots with the median (long line) and mean (cross) indicated. Significance was analysed by Kruskal - Wallis test and Dunn's multiple comparison test.. ns = ≥ 0.05; * p = ≤ 0.05; ** p = ≤ 0.01; **** p = ≤ 0.0001.

In parallel, pairs of age matched *Pabp4*$^{+/+}$ females and *Pabp4*$^{+/+}$ males (from now referred to as 'PABP4 WT pairs' for simplicity), of the same strain, were set up as wild-type controls. Firstly, data gathered from this experiment showed that *Pabp4*$^{-/-}$ females produced significantly smaller litters based on mean number of fetuses born per litter from each pair (*Figure 3.5*.) compared to both other pairings. However, no significant difference was observed between the mean litter size of PABP4 WT pairs and PABP4 paternal KO pairs suggesting that the reduced litter sizes from the *Pabp4*$^{-/-}$ females was not due to heterozygous fetuses being haploinsufficient, providing further support for the maternality of the phenotype.

Generally, inbred females of most strains do not produce more than five litters (Green, 1991) and exhibit greatly reduced fecundity by the age of 8-10 months (Silver, 1995). It was hypothesized that *Pabp4*$^{-/-}$ females may have an exacerbated decline in fecundity in comparison to *Pabp4*$^{+/+}$ females and to this end litter sizes were interrogated in consecutive pregnancies over the 30-week period. PABP4 maternal KO pairs had reduced litter sizes in multiple but not all of their pregnancies in comparison to PABP4 WT and PABP4 paternal KO pairs (*Figure 3.6*). However, this was due to a high variability in WT and PABP4 paternal KO pair litter sizes (i.e. 3rd and 5th litters in *Figure 3.6*.) as the litter sizes of PABP4 maternal KO pairs were consistently low throughout the 30 week period. The variability of WT and PABP4 paternal KO pair litter sizes is most likely associated with the loss of fecundity of some of the *Pabp4*$^{+/+}$ females, which also explains the low number of litters by litter 6 irrespective of pair genotype. When litter size was graphed separately according to parental genotype, it was revealed that the small litter sizes of PABP4 maternal KO pairs (1st litter size mean = 5.2) further declined by ~ 3 fold by the end of the 30 week period (6th litter size

mean= 1.7) (Figure 3.7). In contrast to this, despite the high variability of litter sizes, particularly of the PABP4 WT pairs from the 2nd litter onwards, PABP4 WT females did not show a significant decrease in litter size over time (1st mean litter size of WT pair = 7 8; 1st mean litter size of reciprocal pair = 5.9 ±; 6th mean litter size of WT pair = 6.7; 6th mean litter size of reciprocal pair = 5 [*n* of 1]) (Figure 3.7). These data imply that the fecundity of *Pabp4*$^{-/-}$ females is compromised from their first litter and further declines in an exacerbated fashion with age and number of prior pregnancies.

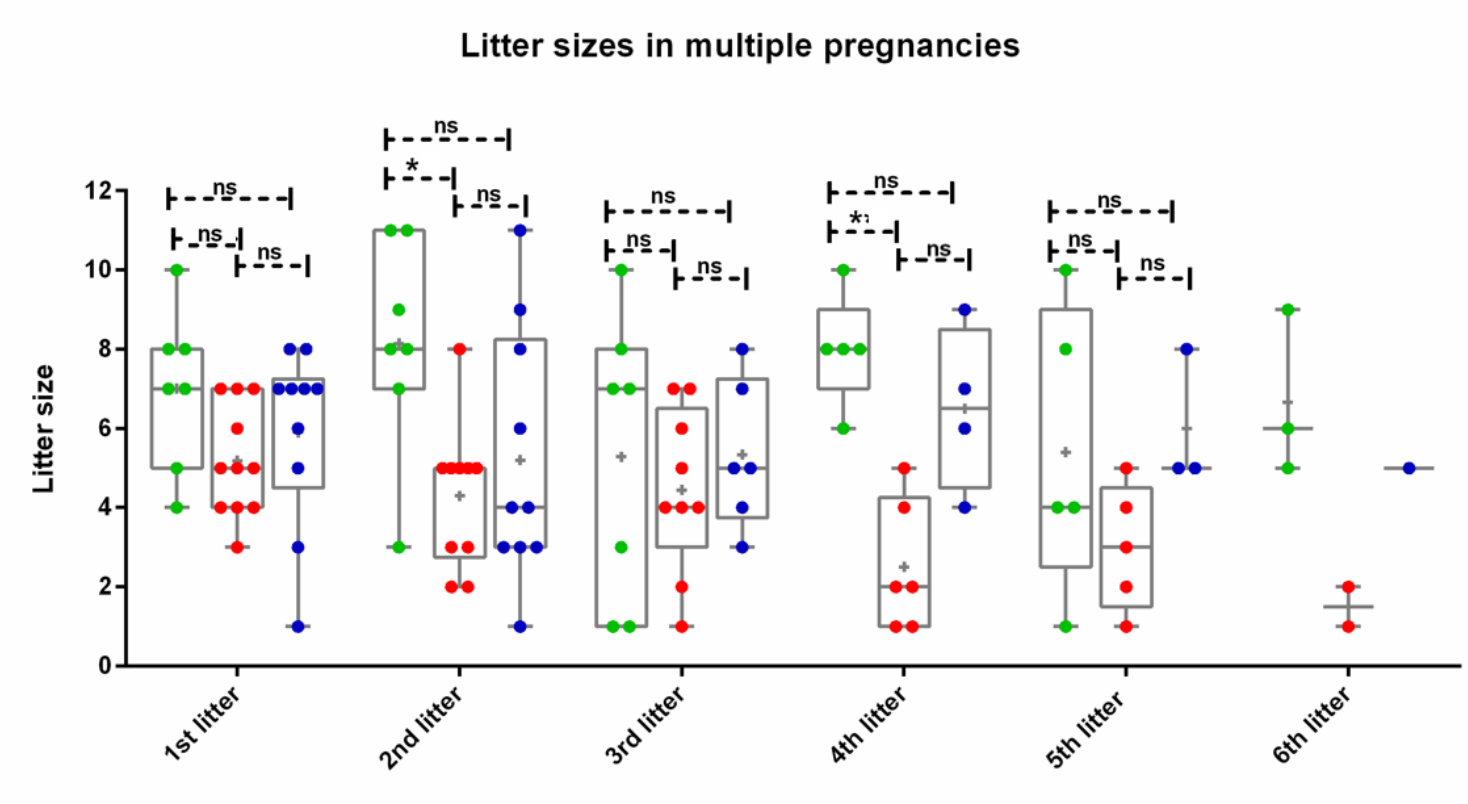

Figure 3.6. Maternal PABP4 deficiency results in reduced litter sizes in multiple pregnancies.

Mean litter size (+/- SD) in 6 consecutive litters where the same male was mated with the same female were surveyed over 30 weeks. ♂WT X ♀WT (green bars) 1st litter *n* = 7 pairs; 2nd litter *n* = 7 pairs; 3rd litter *n* = 7 pairs; 4th litter *n* = 5 pairs; 5th litter *n* = 5 pairs; 6th litter *n* = 3 pairs. ♂WT X ♀KO (red bars) 1st litter *n* = 11 pairs; 2nd litter *n* = 10 pairs; 3rd litter *n* = 9 pairs; 4th litter *n* = 6 pairs; 5th litter *n* = 5 pairs; 6th litter *n* = 2 pairs. ♂KO X ♀WT (blue bars) 1st litter *n* = 10 pairs; 2nd litter *n* = 10 pairs; 3rd litter *n* = 6 pairs; 4th litter *n* = 4 pairs; 5th litter *n* = 3 pairs; 6th litter *n* = 1 pair. Data are shown as shown as box and whisker plots with the median (long line) and mean (cross) indicated. Significance was analysed by Kruskal -Wallis test and Dunn's multiple comparison test. ns = $\geq$ 0.05; * p = $\leq$ 0.05; ** p = $\leq$ 0.01

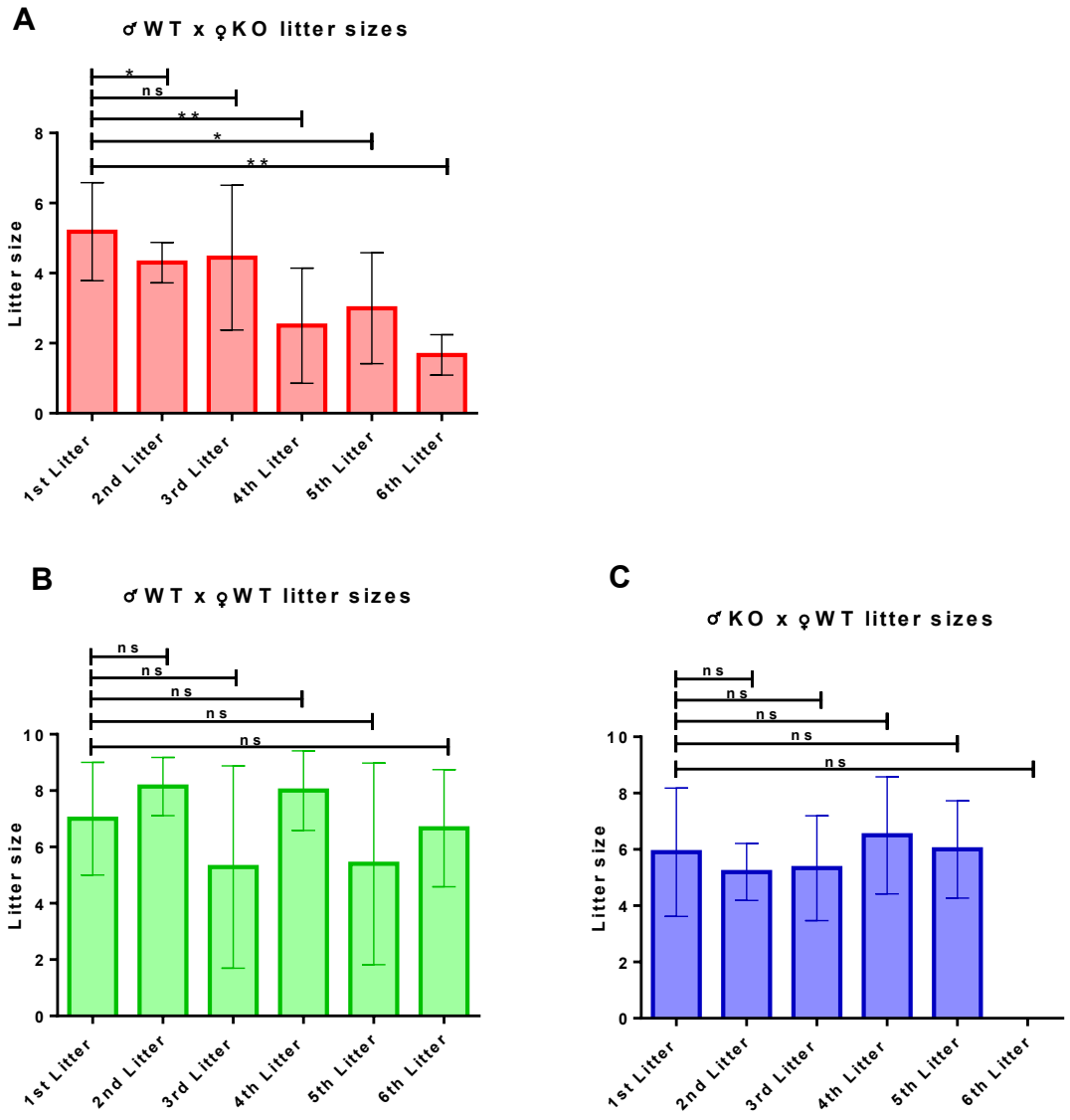

Figure 3.7. Litter size declines in consecutive pregnancies in PABP4 maternal KO pairs but not in WT or PABP4 paternal KO pairs.

Mean litter sizes (+/- SD) born in 6 consecutive litters surveyed over 30 weeks. **A)** ♂WT X ♀KO (red bars) 1st litter *n* = 11 pairs; 2nd litter *n* = 10 pairs; 3rd litter *n* = 9 pairs; 4th litter *n* = 6 pairs; 5th litter *n* = 5 pairs; 6th litter *n* = 2 pairs. **B)** ♂WT X ♀WT (green bars) 1st litter *n* = 7 pairs; 2nd litter *n* = 7 pairs; 3rd litter *n* = 3 pairs; 4th litter *n* = 5 pairs; 5th litter *n* = 5 pairs; 6th litter *n* = 3 pairs. **C)** ♂KO X ♀WT (blue bars) 1st litter *n* = 10 pairs; 2nd litter *n* = 10 pairs; 3rd litter *n* = 6 pairs; 4th litter *n* = 4 pairs; 5th litter *n* = 3 pairs; 6th litter *n* = 1 pair. Data are shown as shown as column bars with SD. Significance was analysed by two-tailed Mann Whitney test. ns = ≥ 0.05; * p = ≤ 0.05; ** p = ≤ 0.01.

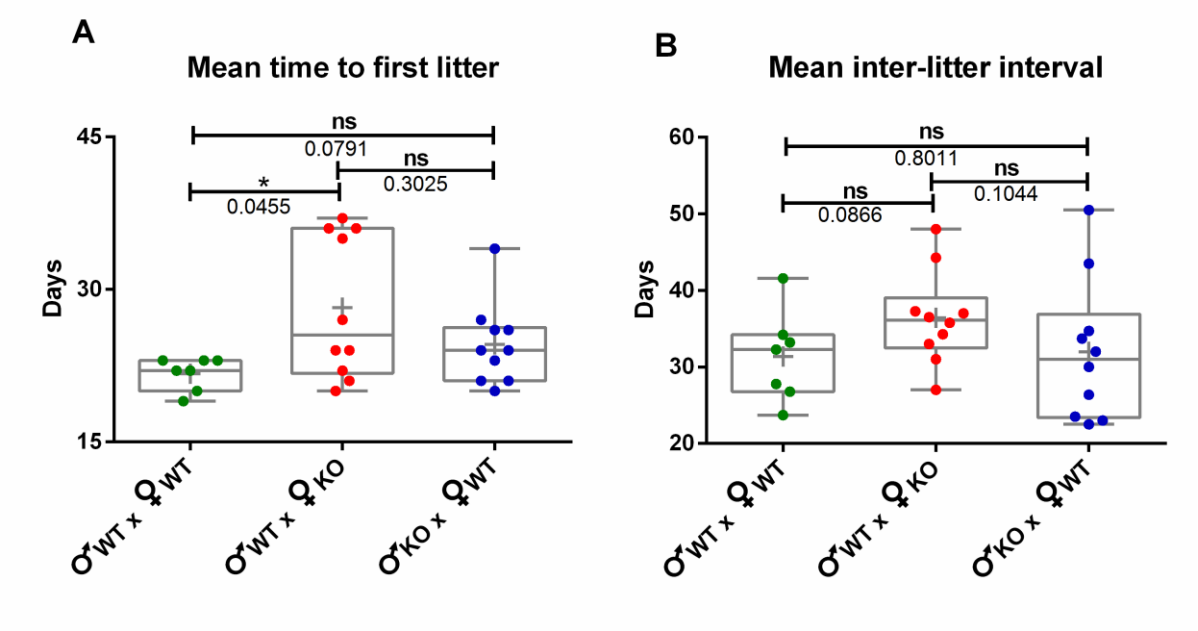

Figure 3.8. Time to first litter is increased in *Pabp4*$^{-/-}$ females but inter-litter interval is unaltered.

A) Mean time to first litter surveyed over 30 weeks. **B)** Mean inter-litter interval surveyed over 30 weeks. ♂WT X ♀WT (green dots) n = 7; ♂WT X ♀KO (red dots) n = 12; ♂KO X ♀WT (blue dots) n = 10. Data are shown as box and whisker plots with the median (long line) and mean (cross) indicated. Significance was analysed by Kruskal -Wallis test and Dunn's multiple comparison test.. ns = ≥ 0.05; * p = ≤ 0.05.

Consistent with the preliminary data implying that some litters are completely resorbed, (see section 1.5 Work leading up to PhD project), time to first litter is increased in PABP4 maternal KO pairs (*Figure 3.8*. A), although the observed increase in mean inter-litter interval does not reach statistical significance (*Figure 3.8*. B). To investigate whether the offspring of *Pabp4*$^{-/-}$ females are more likely to die post birth, the percentage offspring survival to weaning for each female was calculated but showed no statistically significant difference (*Figure 3.9*.), although a power calculation indicated that increasing the *n* number to 19 could result in statistical significance.

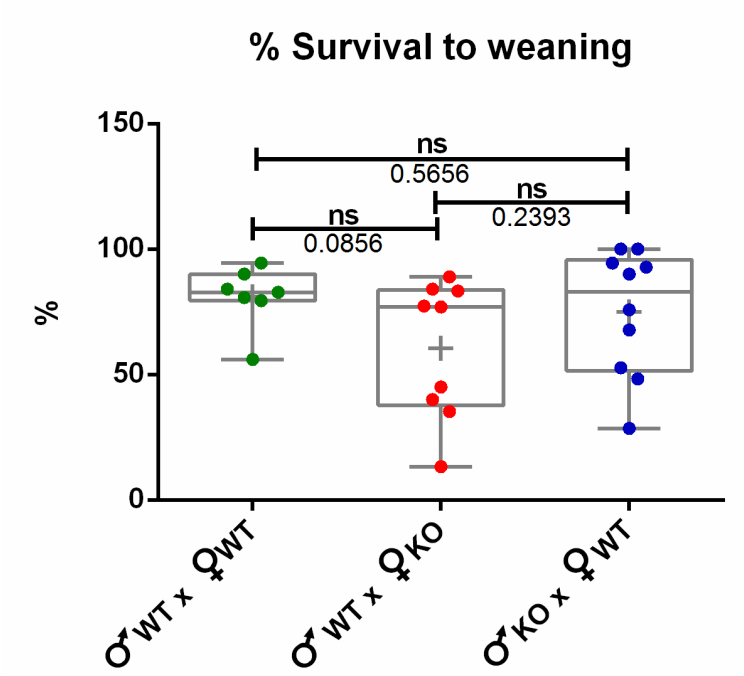

Figure 3.9. Survival to weaning is not reduced in heterozygous offspring from *Pabp4-/-* dams.

% mean survival of fetuses to weaning for each individual dam over 30 weeks. ♂WT X ♀WT (green dots) *n* = 34; ♂WT X ♀KO (red dots) *n* = 43; ♂KO X ♀WT (blue dots) *n* = 34. Data are shown as shown as box and whisker plots with the median (long line) and mean (cross) indicated. Significance was analysed by Kruskal - Wallis test and Dunn's multiple comparison test. ns = $p \geq 0.05$;

Overall from the 30 week experiment, it can be concluded that Pabp4$^{-/-}$ females have reduced fecundity which results in a reduction of litter size at birth. Interestingly, the litter size continues to decrease, proportionally more than WT, with age suggesting that loss of PABP4 results in both reduced initial fecundity and deteriorating fecundity over time. Importantly, this reduction in litter size is independent of both paternal and fetal genotype and therefore is maternal in nature.

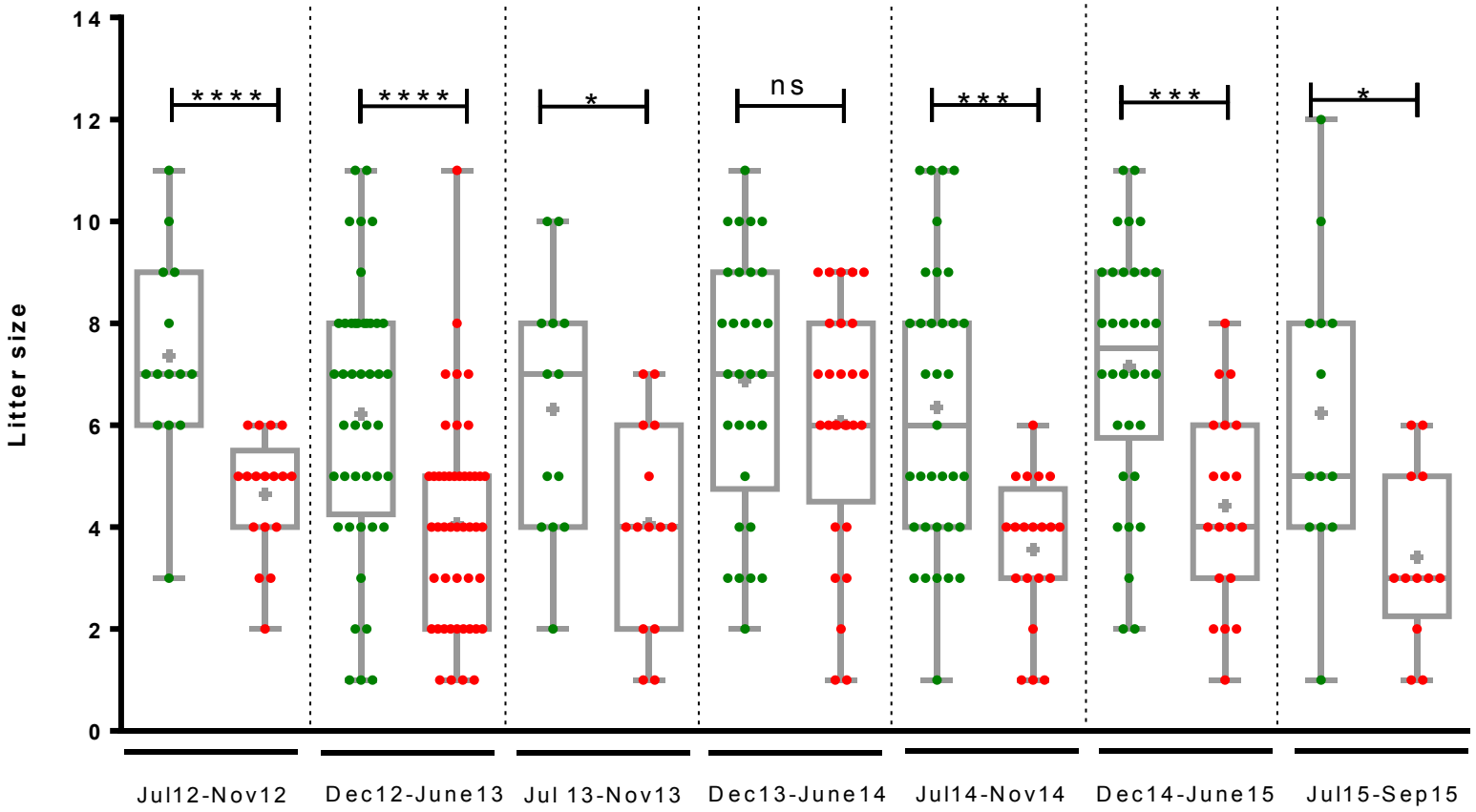

Figure 3.10. Litter size is significantly lower for *Pabp4*$^{-/-}$ dams with the exception of a period between December 2013 and June 2014.

Litter size at birth of *Pabp4* $^{+/+}$ females (WT; green dots) crossed with males of any genotype and *Pabp4* $^{-/-}$females (KO; red dots) crossed with males of any genotype. Litter size numbers are based on data collected from the colony breeding between July 2012 and September 2015 and binned into 5-6 months periods. July 2102-Nov 2012 WT n = 14, KO n = 17; December 2012-June 2013 WT n = 44, KO n = 47; July 2013- November 2013 WT n = 13, KO n = 14; December 2013- June 2014 WT n = 30, KO n = 28; July 2014- November 2014 WT n = 35, KO n = 20; December 2014- June 2015 WT n = 34, KO n = 19; July 2015- September 2015 WT n = 13, KO n = 12. Data are shown as shown as box and whisker plots with the median (long line) and mean (cross) indicated. Significance was analysed by two-tailed Mann Whitney test. . ns = > 0.05; * p = ≤ 0.05; ** p = ≤ 0.01; **** p = ≤ 0.0001.

Collated breeding data from the PABP4 colony was used to further extrapolate breeding information about *Pabp4*$^{-/-}$ females. Litter sizes at birth from *Pabp4*$^{-/-}$ and *Pabp4*$^{+/+}$ females irrespective of paternal genotype (working with the assumption that paternal genotype does not impact the phenotype, Figure 3.3.) were used to create a temporal picture of the colony's breeding over 3 years. For each year, the data collected was binned into periods of July to November and December to June. This analyses provided further support for the reduced fecundity of *Pabp4*$^{-/-}$ females, although between December 2013 and June 2014 there was no significant difference in litter size between *Pabp4*$^{-/-}$ and *Pabp4*$^{+/+}$ females. It seems unlikely that a seasonal effect would be responsible for the divergence in the phenotype, given that this effect was not observed in other years.

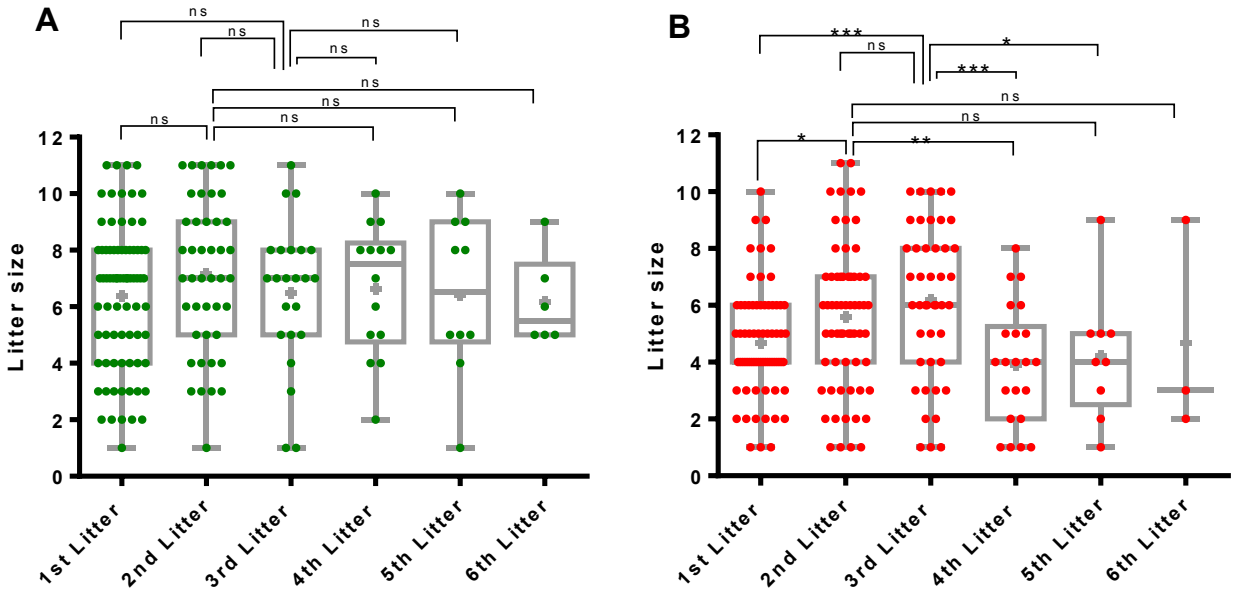

Figure 3.11. Litter size of *Pabp4*$^{-/-}$ dams is related to which ordinal litter it is.

Litter sizes of *Pabp4* $^{+/+}$ females (green dots) **A)** and *Pabp4*$^{-/-}$ females (red dots) **B)** crossed with males of any genotype in consecutive pregnancies based on data collected from the colony breeding between July 2012 and September 2015. Pabp4 $^{+/+}$females; 1st litter n = 76, 2nd litter n = 44, 3rd litter n = 23, 4th litter n = 14, 5th litter n = 10, 6th litter n = 6. *Pabp4*$^{-/-}$ females; 1st litter n = 70, 2nd litter n = 63, 3rd litter n = 44 , 4th litter n = 22, 5th litter n = 9, 6th litter n = 3. Data are shown as shown as box and whisker plots with the mean (cross) indicated. Significance was analysed by Kruskal -Wallis test and Dunn's multiple comparison test. ns = > 0.05; * p = ≤ 0.05; ** p = ≤ 0.01; *** p = ≤ 0.0005.

	Jul12-Nov12	Dec12-June13	July13-Nov13	Dec13-June14	July14-Nov14	Dec14-June15	Jul15-Sep15
Total litters born	17	44	13	33	20	19	12
1st litters	7 (41.2%)	11 (25%)	6 (46.2%)	13 (39.4%)	9 (45%)	9 (47.4%)	4 (33.3%)
1st litter size mean (±SEM)	4.4 (± 0.2)	4.1 (± 0.4)	4.8 (± 0.4014)	5.6 (± 0.5)	4.2 (± 0.4)	4.1 (± 0.4)	3.7 (± 1.1)
2nd litters	6 (35.3%)	14 (31.8%)	5 (38.5%)	9 (27.3%)	5 (25%)	7 (36.8%)	1 (8.3%)
2nd litter size mean (±SEM)	4.8 (± 0.4)	4.7 (± 0.6)	4.2 (± 1.241)	6.6 (± 0.6)	3.2 (± 0.5)	4.0 (± 0.8)	-
3rd litters	4 (23.5%)	9 (20.5%)	0 (0%)	6 (18.2%)	2 (10%)	3 (15.8%)	4 (33.3%)
3rd litter size mean (±SEM)	4.7 (± 0.9)	4.0 (± 0.7)	-	6.5 (± 1.2)	2.0 (± 1.0)	6.3 (± 1.2)	3.7 (± 1.1)
4th litters	0 (0%)	6 (13.6%)	1 (7.7%)	5 (15.2%)	1 (5%)	0 (0%)	2 (16.7%)
4th litter size mean (±SEM)	-	3.1 (± 0.7)	-	2.6 (± 0.8)		-	3.0 (± 0.0)
5th litters	0 (0%)	3 (6.8%)	1 (7.7%)	0 (0%)	2 (10%)	0 (0%)	1 (8.3%)
5th litter size mean (±SEM)	-	4.0 (± 0.5)	-	-	3.0 (± 2.0)	-	-
6th litters	0 (0%)	1 (2.3%)	0 (0%)	0 (0%)	1 (5%)	0 (0%)	0 (0%)
6th litter size mean (±SEM)	-	-	-	-	-	-	-

Table 3.1. The litter size mean is higher in 1st to 3rd litters between December 2013 and June 2014 in comparison to other time period

A number of alternative possible explanations exist, however, given that Pabp4$^{-/-}$ females showed a more severe decrease in their fecundity than WTs as they age and/or acquire multiparity (Figure 3.11. B.), it was hypothesised that during this period the breeding Pabp4$^{-/-}$ females were young with a low number of prior number of pregnancies. To investigate this, the relationship between ordinality and litter size was examined for Pabp4$^{-/-}$ and Pabp4$^{+/+}$ females (irrespective of stud male genotype). Intriguingly, the first litter in Pabp4$^{-/-}$ females tended to be smaller in size compared to second and third litters with the fourth to sixths litters being the smallest (Figure 3.11. B.). In contrast, Pabp4$^{+/+}$ females had steady litter sizes of approx. 6-7 pups throughout their reproductive life span (Figure 3.11. B). Taking this into consideration, it was hypothesized that between December 2013 and June 2014 the reduction in litter size of Pabp4$^{-/-}$ females was temporarily lost due to females having primarily their second and third litters which resulted in an increase of the litter size mean, however this was not the case (Table 3.1). Interestingly, the first 3 litters born to Pabp4$^{-/-}$ females in this period had on average a higher mean litter size ranging from 5.7 to 6.7 in comparison to an average of around 4 in the other time periods which would explain the increased litter size mean during this time-period (Table 3.1). Other explanations for this temporary change in phenotype, such as the number of breeding pairs within the room are addressed in the discussion.

The reduction and further decline in fecundity suggests that *Pabp4*$^{-/-}$ females could have problems with oogenesis/ovulation, fertilisation, implantation and/or *in utero* fetal death. Interestingly, in this regard PABP function is required for oogenesis both in invertebrates (Ciosk et al., 2004; Clouse et al., 2008; Ko et al., 2013; Ko et al., 2010; Kugler and Lasko, 2009; Lall et al., 2005; Maciejowski et al., 2005; Vazquez-Pianzola et al., 2011) and non-

mammalian vertebrates (Friend et al., 2012), and the germ cell specific ePABP is required for oogenesis in mice (Ozturk et al., 2012; Seli et al., 2005). However, a role for PABP4 in oogenesis has not been previously addressed, although PABP4 appears to be present in mammalian ovary (Figure 1.15 in section 1.5 Work leading up to PhD project). To this end, the expression of PABP4 in the adult mouse ovary was investigated (Fig. 13). *Pabp4*$^{-/-}$ ovary was analysed in parallel as a negative control in addition to an IgG negative control (C), and showed only weak immunostaining of a single large pre-antral oocyte, supporting the specificity of the antibody, and consistent with the known "stickiness" of oocytes (*Figure 3.12*. C), which can lead to "background". In the *Pabp4*$^{+/+}$ ovary, PABP4 was found to be expressed in all granulosa cells within follicles at all stages of maturation, these cells support the oocyte and are necessary for its development. It was also expressed in the progesterone secreting corpus luteum which is derived from luteinisation of the follicle following ovulation (Figure 3.12. A). Weak expression was observed in the thecal cells that surround the follicle and in the stroma. PABP4 was clearly expressed in oocytes in pre-antral follicles, and appeared to be more weakly expressed in antral follicles, however caution is required with respect to this weak antral oocytes expression, due to the background observed in oocytes from *Pabp4*$^{-/-}$ mice (*Figure 3.12* C). PABP1 expression was also investigated for a comparison to PABP4 and to detect any potentially compensatory changes in expression in the *Pabp4*$^{-/-}$ ovary. Like PABP4, PABP1 showed robust expression in the granulosa cells, but in contrast appeared to be absent in the oocytes (*Figure 3.12*. B), and it's expression pattern did not appear to change in the absence of PABP4 (*Figure 3.12*. D). It is unknown what function PABP4 may have in the ovary. Furthermore, PABP4 and PABP1 were also found to be expressed in the pituitary which releases, in addition to other hormones, gonadotropins that stimulate follicle growth and ovulation (*Figure 3.13*.). The pituitary is composed of three regions; posterior pituitary (also known as Pars nervosa), anterior pituitary (also known as pars distalis) and pars intermedia.

The anterior pituitary contains three different cell types; chromophobes, acidophils, which secrete growth hormone, and basophils which release gonadotropins, corticotrophin and thyroid stimulating hormone. Importantly, PABP4 shows robust expression in the anterior pituitary but is also detectable in the posterior pituitary and pars intermedia (*Figure 3.13*. A). PABP1 is expressed in all three regions. In the anterior pituitary which produces gonadotropins, PABP1 expression appears more uniform of that of PABP4 (*Figure 3.13*. C, D), although PABP1 expression appears less uniform in *Pabp4*$^{-/-}$ pituitary (*Figure 3.13*. E, F). Further information on the PABP4 and PABP1 expressing cell types, would require double immunohistochemical staining with specific cell markers.

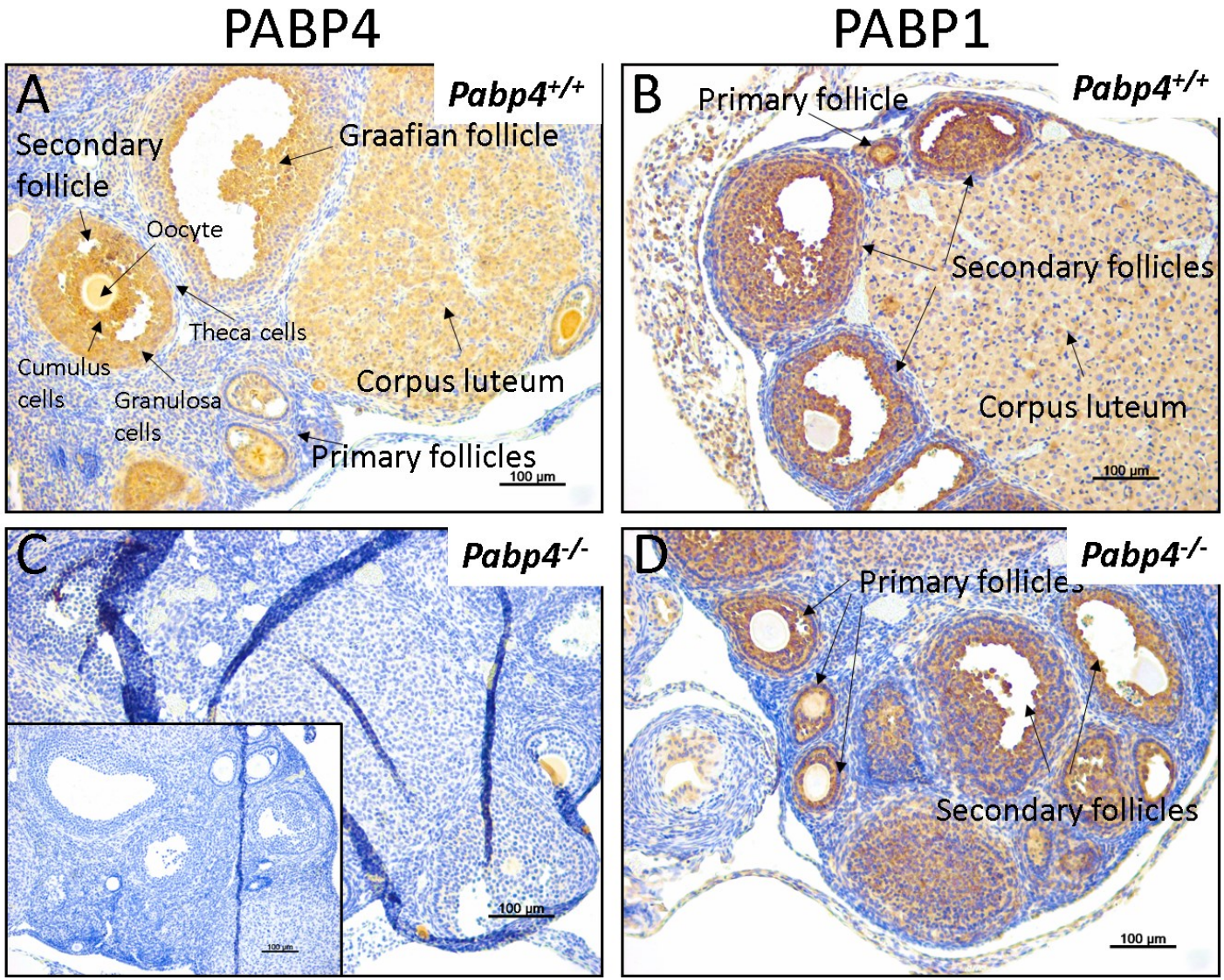
PABP4
PABP1
A
Pabp4+/+
Secondary follicle
Graafian follicle
Oocyte
Theca cells
Cumulus cells
Granulosa cells
Corpus luteum
Primary follicles
100 µm
B
Pabp4+/+
Primary follicle
Secondary follicles
Corpus luteum
100 µm
C
Pabp4-/-
100 µm
D
Pabp4-/-
Primary follicles
Secondary follicles
100 µm

Figure 3.12. Expression analysis of PABP4 and PABP1 in the adult mouse ovary.

Sections of Pabp4$^{+/+}$ and Pabp4$^{-/-}$ adult mouse ovary were stained by immunohistochemistry for PABP4 (A, C), PABP1 (B, D) or rabbit IgG control (insert in C). x10 maginifications are shown.

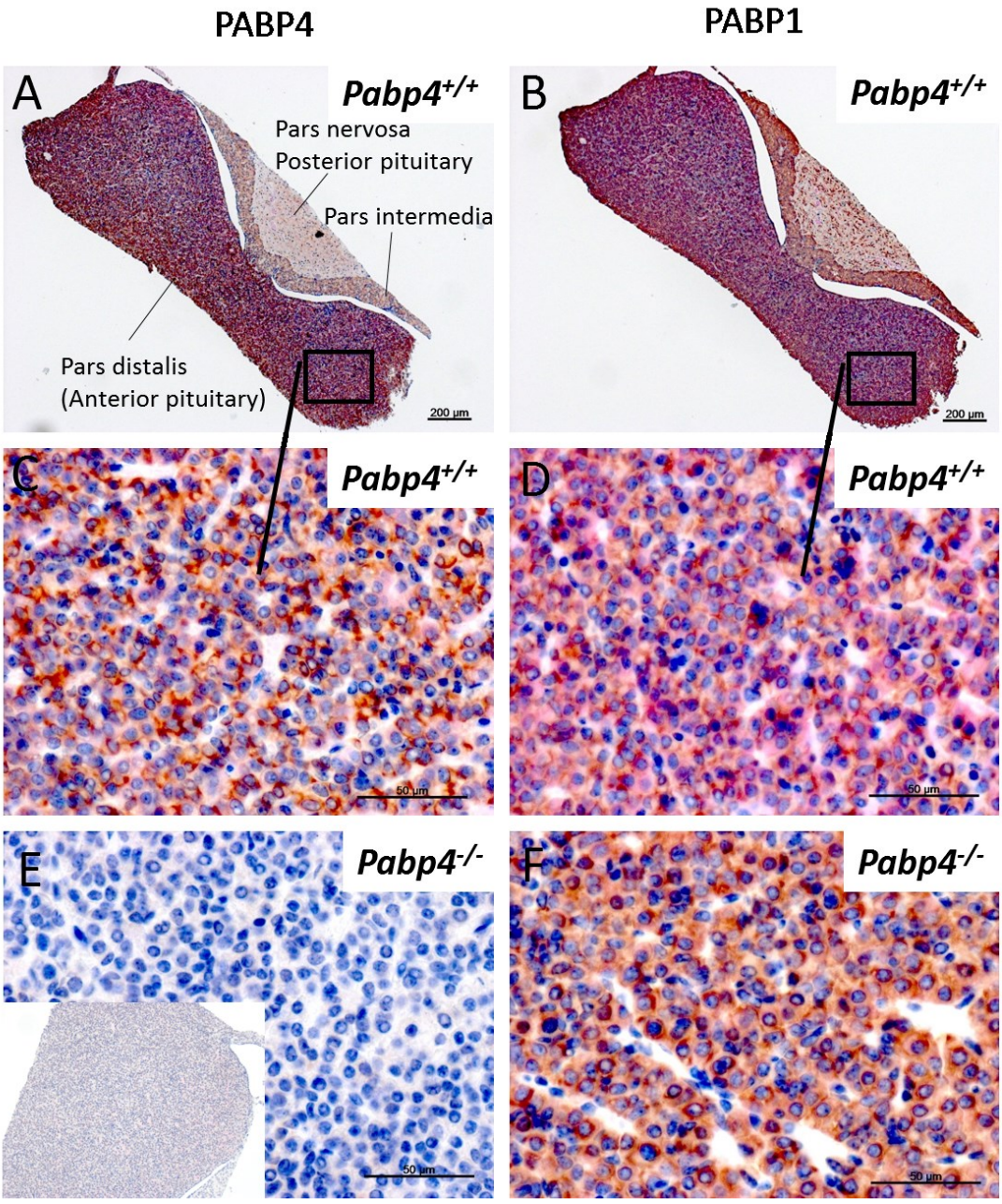

Figure 3.13. Expression analysis of PABP4 and PABP1 in the adult mouse pituitary.

Sections of Pabp4$^{+/+}$ and Pabp4$^{-/-}$ adult mouse pituitary from day e18.5 were stained by immunohistochemistry for PABP4 (**A, C, E**), PABP1 (**B, D, F**) or rabbit IgG control (insert in **E**). Images A, B x2 magnification images are shown; C, D, E, F x40 magnification images are shown.

The analysis of PABP4 expression is consistent with the defect possibly stemming from a defect in oogenesis, ovulation or implantation (e.g. poor fertilisation or oocyte quality). However, these data do not exclude *Pabp4*$^{-/-}$ females having a direct implantation (e.g. uterine) defect or failure in post-implantation pregnancy. Thus to inform upon possible causes, litter sizes were determined at a spectrum of embryonic stages including embryonic (e) days 8.5, 13.5, 15.5 and 18.5 for *Pabp4*$^{-/-}$ and *Pabp4*$^{+/+}$ females mated with *Pabp4*$^{+/+}$ males. At e8.5 no significant decrease in litter size was observed (*Figure 3.14*), strongly implying that oogenesis, ovulation, fertilisation and implantation are not majorly affected in these mice. Mean litter size was also comparable between *Pabp4*$^{-/-}$ and *Pabp4*$^{+/+}$ females at e13.5 providing further confirmation that events leading up to and including implantation did not account for the reduction in litter size, and further establishing that no significant loss of pups occurred prior to mid-gestation. In contrast to this, at e15.5 and e18.5 litter sizes showed a small but statistically significantly reduction in *Pabp4*$^{-/-}$ compared to *Pabp4*$^{+/+}$ females mated with either *Pabp4*$^{+/+}$ or *Pabp4*$^{-/-}$ males and *Pabp4*$^{-/-}$ mated with *Pabp4*$^{+/+}$ males. Consistent with this limited reduction in litter number at these stages, occasional late fetal resorptions were noted at e15.5 and e18.5. However, the most profound difference in litter size occurred after e18.5 where at birth the mean litter size of *Pabp4*$^{-/-}$ females was 4.024 (±0.3014) whereas the mean litter size of a *Pabp4*$^{+/+}$ female mated to *Pabp4*$^{+/+}$ males was 7.113 (±0.3671) or 6.345 (±0.3265) when mated to a *Pabp4*$^{-/-}$ male (*Figure 3.14*).This data directly support *Pabp4*$^{-/-}$ females having a post-implantation defect in pregnancy that leads to fetal death and becomes apparent from mid-gestation (e15.5) but mainly manifests in late pregnancy between e18.5 and birth.

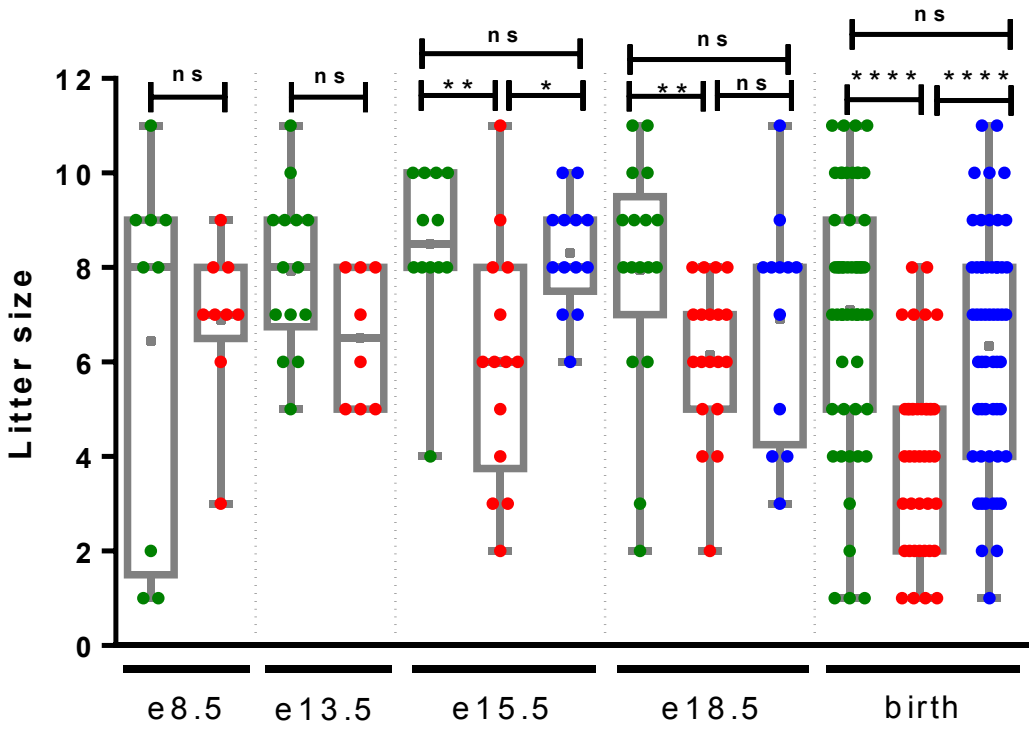

Figure 3.14. Litter size is lower in *Pabp4-/-* dams from e15.5 of gestation with biggest drop between e18.5 and birth.

Litter sizes investigated throughout gestation and at birth. **e8.5 -** ♂WT X ♀WT (green dots) *n* = 9, ♂WT X ♀KO (red dots) *n* = 9 ; **e13.5 -** ♂WT X ♀WT (green dots) *n* = 14, ♂WT X ♀KO (red dots) *n* = 8; **e15.5** ♂WT X ♀WT (green dots) *n* = 13, ♂WT X ♀KO (red dots) *n* = 14, ♂KO X ♀WT (blue dots) *n* = 13; **e18.5** - ♂WT X ♀WT (green dots) *n* = 17, ♂WT X ♀KO (red dots) *n* = 19, ♂KO X ♀WT (blue dots) *n* = 12; **at birth** = ♂WT X ♀WT (green dots) *n* = 53, ♂WT X ♀KO (red dots) *n* = 41, ♂KO X ♀WT (blue dots) *n* = 55. Data are shown as shown as box and whisker plots with the median (long line) and mean (cross) indicated. For e8.5 and e13.5 time-points significance was analysed by two-tailed Mann Whitney test and for e15.5, e18.5 and birth by Kruskal -Wallis test and Dunn's multiple comparison test. ns = > 0.05; ** p = ≤ 0.01; **** p = ≤ 0.0001.

3.3 Discussion

The role of mammalian PABP4 outside of cell lines had not been studied and to address this important gap in our knowledge an investigation of *Pabp4*$^{-/-}$ mice was undertaken. The *Pabp4*-targeted mice used contained the "knock-out first allele" where gene function is ablated by a polyadenylation signal-mediated transcriptional stop at the end of the *lacZ* expression marker gene that is driven off the target gene promoter. LacZ encodes β-galactosidase and is considered to be a convenient reporter gene as it has a simple enzymatic assay, is easily detected in situ and is cell autonomous and importantly can act as a sensitive marker of gene activity (Cohen-Tannoudji et al., 2000). Based on numerous experiments it is generally accepted that lacZ behaves as a neutral reporter gene (Forss-Petter et al., 1990; Goring et al., 1987; Klarsfeld et al., 1991) and reviewed in (Cui et al., 1994). However, interestingly when lacZ sequences are associated with regulatory sequences of ubiquitously expressed genes it can lead to a transcription-silencing effect (Cohen-Tannoudji et al., 2000). To verify that the effects we are seeing are due to the loss of PABP4 rather than the expression of lacZ experiments will need to be replicated in PABP4 KO mice with reporter-less deletion of the allele. These experiments are currently undergoing could not be initially done as the *Pabp4*-targeted mice obtained initially were missing a loxP site and therefore did not have the potential of having a reporter-less deletion allele.

The work outlined in this chapter confirm and extend upon preliminary data, establishing that PABP4 is not essential for viability or fertility in mice, but that maternal loss of PABP4 results in reduced fecundity primarily as a result of fetal lethality which occurs between e18.5 and birth. Whilst this compromise in fecundity is apparent from the first litter it further declines with increasing age and parity in an exacerbated manner in comparison to *Pabp4*$^{+/+}$ females and *Pabp4*$^{-/-}$ females take longer to produce a first litter. Whilst the genetic crosses strongly support the maternal nature of the phenotype, ideally embryo transfer experiments would be done, wherein *Pabp4*$^{+/+}$ mice transferred into a *Pabp4*$^{-/-}$ female would result in the recapitulation of the mid-late fetal death phenotype. However, embryo transfers are highly variable in terms of live births per embryos transferred, meaning that the numbers required to gain

power within this experiment are prohibitive. It would be interesting to track back the breeding history of *Pabp4*$^{-/-}$ females that had *Pabp4*$^{-/-}$ mothers to see whether their phenotype differs from *Pabp4*$^{-/-}$ females born to *Pabp4*$^{+/-}$ mothers.

Phenotypic insight into PABP4-defiency was only previously available in *X. laevi*s where PABP4 was found to be essential for development, as knock-down resulted in defects in anterior structures and lethality by stage 51 (d17 of development; final stage 66 occurs by 58 days) (Gorgoni et al., 2011). Based on the findings in *X. laevis*, the viability of *Pabp4*$^{-/-}$ mice was perhaps surprising since the additional mammalian-specific family members, tPABP and PABP5, are unlikely to compensate due to their restricted expression and lack of domain conservation, respectively. Moreover, the substantial reproductive differences between *X. laevis* and mammals mean that the phenotype observed here could not have been predicted from the prior work. This differs from ePABP where the oogenesis defects associated with loss of ePABP function in *X. laevis* (Friend et al., 2012) were recapitulated in mice (Ozturk et al., 2012; Seli et al., 2005). However, differences in ePABP phenotypes between non-mammalian and mammalian vertebrates also exist, as ePABP is not required for early development in mice (Friend et al., 2012; Ozturk et al., 2012; Seli et al., 2005), presumably due to differences in the timing of onset of zygotic transcription, when synthesis of so-called "somatic" PABPs resumes (Friend et al., 2012).

Collated breeding data from the breeding colony revealed that *Pabp4*$^{-/-}$ females temporarily diverged from the described phenotype and produced equivalent litter sizes to *Pabp4*$^{+/+}$ females. This was not correlated with age, multi-parity or likely seasonal in nature. There was a high number of *Pabp4*$^{+/-}$ males crossed with *Pabp4*$^{-/-}$ females in this time-period, however, this is unlikely to be the cause for the divergence as there is no supporting evidence that paternal *Pabp4* genotype is a determinant of litter size. In support of this conclusion, other periods with particularly high number of *Pabp4*$^{+/+}$ males crossed with *Pabp4*$^{-/-}$ females (December 2012-June 2013) did not result in an increased litter size. It has been reported that exposure to male, but not female technicians, induces a robust stress response (Sorge et al., 2014) and the mice were looked after by a male technician, however, staffing gender was constant. A factor which could potentially be the cause of the divergence is a change in the number

of breeding pairs reported by the animal facility staff, which was particularly high in this time period, meaning more male mice were present. Chemicals in male urine called 'priming pheromones' regulate the reproductive maturation and timing of ovulation in mice by inducing a series of hormonal responses by targeting production of gonadotropins or gonadotropin releasing hormone and thereby affecting ovulation rate (GnRH) (Bronson, 1971; Bronson and Maruniak, 1975). It has been shown that exposing females to male-soiled bedding results in a significant increase in both the implantation scars and litter size in mice without a reduction in bodyweight of the offspring (Zhiqin, 1992). Furthermore, exposure to a male or male urine significantly increased the number of mature follicles in voles (Jemiolo et al., 1980). If an increase in the number of males and the effect of pheromones was the cause of the transient increased litter size, it would suggest that PABP4 has a role in controlling ovulation rate. Interestingly in this respect, PABP4 was found to be expressed in the adult ovary (Figure 3.12.) and pituitary (Figure 3.13.). Thus, the hypothesis may be that the absence of PABP4 in the adult female results in a reduced ovulation rate which can be reversed by the presence of a stimulus, such as a priming hormone, which positively influences ovulation. This hypothesis is currently not supported by the presence of normal litter sizes at e8.5 and e13.5 (*Figure 3.14*), although a subtle effect on litter size may be evident at these stages (Figure 12). Whilst the data argue that rates of implantation are not significantly altered, they do not exclude the possibility that decidualisation and/or implantation are abnormal in PABP4-deficient females, with the phenotypic effects not becoming apparent till later in gestation. Attachment/implantation of the blastocyst and decidualisation are all crucial and limiting steps in placentation and the growth of the fetus and thus successful pregnancy (reviewed in (Cha et al., 2012). Deferred implantation, like in mice lacking *Pla2g4a* (a gene for Cpla2α which generates arachidonic acid for prostaglandin synthesis) for example, results in embryo crowding, conjoined placentas, retarded fetoplacental development and reduced litter size (Song et al., 2002). Abnormal endometrial stromal cells on the other hand can, for example, result in premature decidual senescence, causing preterm birth with neonatal death or abnormal placentation with shallow trophoblast invasion resulting in preeclampsia (Cha et al., 2012). This highlights the

importance of establishing if, and where, PABP4 is expressed in the endometrium and the decidua.

Although the initial preliminary data also suggested that Pabp4-/- females present with fetuses small for their gestational age (SGA), which is a known risk factor for mid-late fetal lethality or stillbirth in women, birth weight and offspring size were measured in the breeding experiments here, due to the disturbance of the breeding pairs potentially leading additional to pup death. (Breeding strategies for maintaining colonies of laboratory mice, 2007, The Jackson laboratory, Bar Harbor). However given the strong association between fetal size and stillbirth, analysis of potential IUGR is the major focus of the next chapter.

Importantly, the maternal-dependent mid-late fetal loss observed in these mice is reminiscent of stillbirth in women, an under researched area of unmet clinical need. To date, little analysis on the genetics of stillbirth has been carried out although some genome wide association studies (GWAS) are available in lifestock (Pausch et al., 2011), implicating a handful of loci. However, women whom suffer from stillbirth or late miscarriage may go onto to have healthy pregnancies but are at higher risk of subsequent stillbirth (Lamont et al., 2015), supporting a potential genetic component.

Since *Pabp4*$^{-/+}$ female mice are not haploinsufficient, loss of PABP4 function is unlikely to substantially contribute to stillbirth in human populations as a single gene disorder. However, *Pabp4*$^{-/-}$ mice are viable, fertile and lack gross morphological or behavioural abnormalities meaning that *Pabp4* mutations may act as a risk factor for stillbirth alongside other genetic or environmental factors. Moreover, identification of the pathways and mRNAs dysregulated in these mice can shed light on further pathways and gene candidates that may account for a significant proportion of stillbirths which are not attributed to factors such as fetal abnormalities.

There are relatively few animal models which report reduced litter size due to late gestational death as a result of maternal factors/genotype with the most reported underlying maternal cause being the inadequate remodelling of the maternal and/or placental vasculature resulting in low uterine and/or placental blood flow to the fetoplacental unit. Inappropriate vasculature remodelling has been reported to be

induced by for example by maternal high fat diet (Frias et al., 2011; Wallace et al., 2002) but also using genetic models which hamper the function of uterine natural killer cell (uNK) function (Kieckbusch et al., 2015), which are crucial to this process (Ashkar and Croy, 1999, 2001; Ashkar et al., 2000; Hanna et al., 2006). Furthermore, low doses of LPS to *IL10*$^{-/-}$ mice have been reported to result in increased intrauterine death believed to be associated with increased uNK cell number and cytotoxicity (Murphy et al., 2005). Reports of reduced litter size and late fetal death which do not involve the remodelling of maternal vasculature include maternal metabolic dysfunction secondary elevated maternal corticol levels which were shown to result in an increased rate of stillbirth in ovine pregnancy (Keller-Wood et al., 2014). *Pabp4*$^{-/-}$ dams may represent a unique opportunity to increase our knowledge on the underlying molecular causes of stillbirth.

Chapter 4 - Analysis of fetal intrauterine growth restriction in *Pabp4*$^{-/-}$ dams

4.1 Introduction

Intrauterine growth restriction is when a baby fails to reach its genetic growth potential due to intrinsic and/or extrinsic reasons and is the second most common cause of perinatal death (Chiswick, 1985; Gardosi et al., 1998). After excluding congenital abnormalities, more than 50% of stillbirths were found to have preceding IUGR (Gardosi et al., 2005). Furthermore IUGR is associated with morbidities in later life (Salam et al., 2014). Currently, it is impossible to predict IUGR prior to pregnancy and in early pregnancy and diagnosis poses difficulty with the detection rate in low-risk pregnancies as low as 15% (Backe and Nakling, 1993), and the majority of IUGR cases are therefore identified from birthweight of live or stillborn babies. When IUGR is detected, the only treatment is monitoring fetal well-being and the induction of delivery if well-being becomes compromised. IUGR can be classified as symmetrical or asymmetrical with symmetrical being more often early-onset and associated with by fetal intrinsic anomalies whereas extrinsic factors tend to be associated with late onset and maternal and/or placental causes (Nardozza et al., 2012). Importantly, the type of IUGR can change throughout pregnancy depending on the underlying cause and the duration of the insult. Placenta insufficiency is implicated in up to 65% of cases of stillbirth in high-income countries (Heazell et al., 2015). The fetal:placental (F:P) weight ratio and birthweight:placental (BW:PW) ratio provides an insight into placental efficiency as it informs on the grams of fetus produced per gram of placenta (Wilson and Ford, 2001). In preliminary investigations of *Pabp4*$^{-/-}$ females some fetuses were found to be putatively growth restricted. Intriguingly, initial data suggested that this may be independent of genotype as some *Pabp4*$^{+/-}$ fetuses were found to be appropriately sized whereas others appeared to be growth restricted in late gestation (Figure 4.1). The objective of this chapter was to investigate the veracity of this data, and to extend it by establishing the underlying genetics (i.e. fetal and/or

parental), the type and extent of the IUGR and whether it changes throughout gestation and by determining the F:P ratios to gain an initial insight into placental efficiency.

Figure 4.1. Preliminary data showing that some fetuses are small in comparison to litter mates. Example of observed putatively growth restricted fetuses of different genotype at e18.5 suggesting that being small is independent of fetal genotype.

4.2 Results

To address whether reduced size was a genuine phenotype of PABP4 deficiency and whether, similar to the reduction in litter size, it was maternal in nature, timed-matings of *Pabp4*$^{+/+}$ males with *Pabp4*$^{-/-}$ females and *Pabp4*$^{-/-}$ males with *Pabp4*$^{+/+}$ females were set up. The latter mating is referred to as the 'paternal KO cross'. Both matings produce *Pabp4*$^{+/-}$ foetuses but, importantly, the conceptus only grows and develops in a *Pabp4* deficient dam in one of the crosses, allowing for a comparison between maternal environments. Additionally, timed-matings of *Pabp4*$^{+/+}$ males with *Pabp4*$^{+/+}$ females were set up to determine the baseline fetal outcome in wild-type matings. If maternal PABP4 deficiency results in small fetuses in comparison to fetuses from a wild-type cross and more importantly from a paternal KO cross, they can be defined as IUGR because fetuses from these two crosses have the same genetic growth potential. Timed-mated females were checked for vaginal plugs (VP) (counted as e0.5)

and following removal of the uterus at day e18.5 of pregnancy, fetuses were weighed and crown-rump length measured, as commonly done in the clinic to establish human size for gestational age. Importantly, e18.5 *Pabp4*$^{+/-}$ fetuses from *Pabp4*$^{-/-}$ dams were found to have both significantly reduced weight (8.5%) relative to *Pabp4*$^{+/+}$and *Pabp4*$^{+/-}$ fetuses from *Pabp4*$^{+/+}$ dams, revealing that maternal PABP4 deficiency does indeed lead to IUGR (Figure 4.2.) with some fetuses more growth restricted than others (*Figure 4.3*). The crown to rump length was found to be insignificantly reduced (3%) (Figure 4.2.), however this measurement is less accurate the weights of fetuses. Interestingly, the weights of *Pabp4*$^{+/-}$ fetuses from *Pabp4*$^{+/+}$ dams showed a small but significant increase in weight compared to *Pabp4*$^{+/+}$ foetuses (Figure 4.2. A and C), although this was not replicated for crown-rump length measurements (Figure 4.2. B-C). The basis for this is unclear, but it could imply that *Pabp4*$^{+/-}$ fetuses have altered, parental dependent growth/metabolism compared to *Pabp4*$^{+/+}$ fetuses.

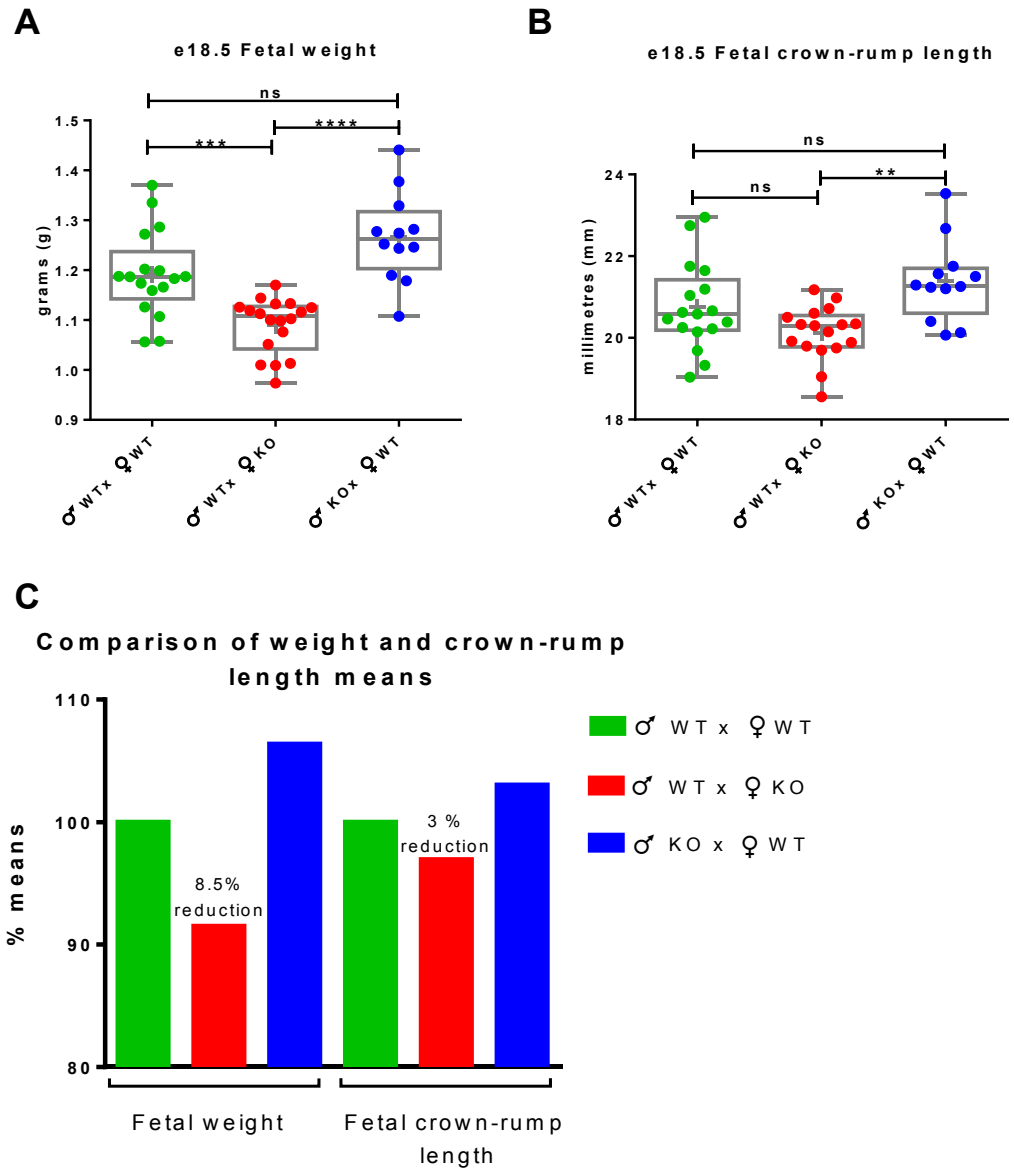

Figure 4.2. Weight and size of fetuses from *Pabp4*$^{-/-}$ dams is significantly reduced at e18.5.

Pabp4$^{+/-}$ fetuses from *Pabp4*$^{-/-}$ dams have reduced bodyweight (**A**) and (**B**) crown-rump length in comparison to both *Pabp4*$^{+/+}$ and *Pabp4*$^{+/-}$ fetuses from *Pabp4*$^{+/+}$ dams. **C)** Comparison of fetal bodyweight and crown-rump length % normalised to the ♂ WT x ♀ WT cross. Each symbol corresponds to an average per genotype within a single litter. ♂ WT x ♀ WT (green dot) n = 17; ♂ WT x ♀ KO (red dot) n = 18; ♂ KO x ♀ WT (blue dot) n = 12. Data are shown as box and whisker plots with median (long line) and mean (cross) indicated. Significance was analysed by Kruskal-Wallis test and Dunn's multiple comparison test. ns = > 0.05; * p = ≤ 0.05; ** p = ≤ 0.01; *** p = ≤ 0.001; **** p = ≤ 0.0001.

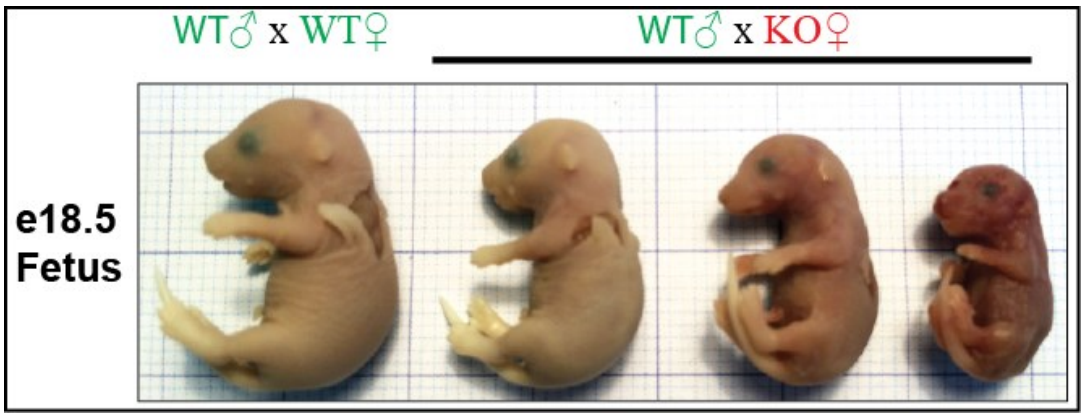

Figure 4.3. Fetuses from *Pabp4*$^{-/-}$ dams show a range of IUGR.

As maternal, dependent IUGR was present (Figure 2), placental weight and diameter were examined and found to be comparable amongst the three crosses (*Figure 4.4*.) suggesting that the IUGR was not accompanied by abnormal placental size. However an decreased F:P weight ratio was found in fetuses from *Pabp4*$^{-/-}$ dams (13.4% decrease in comparison to WT, and 5.6% compared to the paternal KO cross) (*Figure 4.4*.), revealing a disproportionality between fetal and placental size in the absence of maternal PABP4, consistent with reports that F:P ratio is commonly altered in intrauterine growth restriction (reviewed by (Hayward et al., 2016).

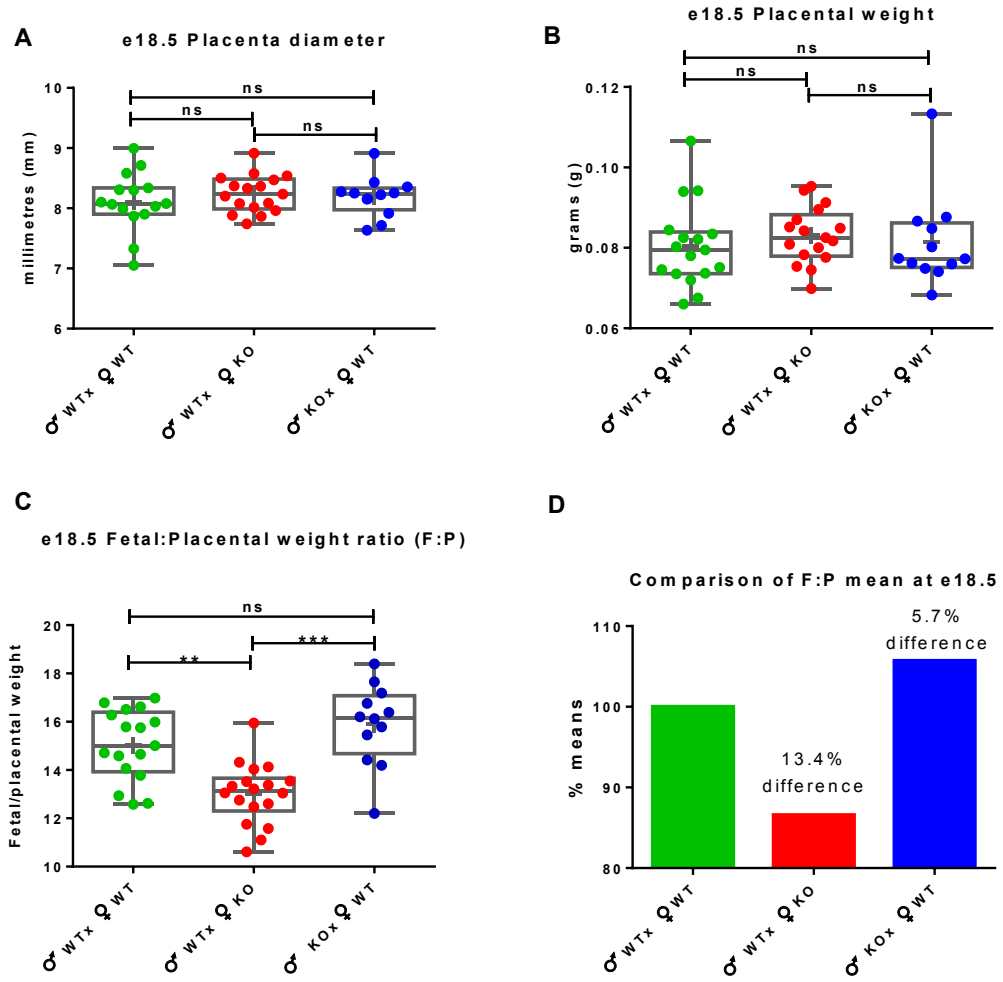

Figure 4.4. Placental diameter and weight are unaltered at e18.5 which results in an increased fetal to placental ratio in fetuses from *Pabp4*$^{-/-}$ dams.

Pabp4$^{+/-}$ placentas from *Pabp4*$^{-/-}$ dams have comparable weight (**A**) and diameter (**B**) to *Pabp4*$^{+/+}$ and *Pabp4*$^{+/-}$ placentas from *Pabp4*$^{+/+}$ dams. As a result F:P weight ratios in Pabp4$^{-/-}$ dams are reduced (**C**). Comparison of F:P % means normalised to the ♂ WT x ♀ WT cross (**D**). Each symbol corresponds to an average per genotype within a single litter. ♂ WT x ♀ WT (green dot) n = 17; ♂ WT x ♀ KO (red dot) n = 18; ♂ KO x ♀ WT (blue dot) n = 12. Data are shown as box and whisker plots with median (long line) and mean (cross) indicated. Significance was analysed by Kruskal-Wallis test and Dunn's multiple comparison test. ns = > 0.05; * p = ≤ 0.05; ** p = ≤ 0.01; *** p = ≤ 0.001; **** p = ≤ 0.0001.

To assess the IUGR phenotype further, head and abdominal circumference measurements were obtained for Pabp4$^{+/+}$ fetuses from Pabp4$^{+/+}$ dams and Pabp4$^{+/-}$ fetuses from Pabp4$^{-/-}$ dams to determine whether the IUGR observed was asymmetrical

(evidence of brain sparing) or symmetrical. Asymmetric fetuses have disproportionate growth restriction whereby the head growth is preferentially maintained resulting in a relatively normal sized head/brain and a reduced abdomen. In humans, this type of IUGR is normally observed in the second half of gestation and is most often associated with placental insufficiency and/or a lack of uterine remodelling (reviwed in (Nardozza et al., 2012)). Symmetrical IUGR is characterised by a proportional decrease of both the head and the abdomen. It generally develops in early pregnancy and is most often but not excusively associated with fetal congenital abnormalities and other causes of mainly fetal origin (Nardozza et al., 2012). $Pabp4^{+/-}$ fetuses from $Pabp4^{-/-}$ dams exhibited both reduced head and abdominal circumferences, in comparison to $Pabp4^{+/+}$ fetuses from $Pabp4^{+/+}$ dams, which resulted in normal head: abdomen ratios and therefore the IUGR was defined as symmetrical (Figure 4.5.), ruling out brain sparing in $Pabp4^{+/-}$ fetuses from $Pabp4^{-/-}$ dams. Similar measures were not understaken for reciporocal crosses as $Pabp4^{+/-}$ fetuses from $Pabp4^{+/+-}$ females do not shown growth restriction compared to $Pabp4^{+/+}$ fetuses from WT crosses. It is tempting to speculate from this observation about the etiology of the phenotype in that it suggests it may originate early in pregnancy and that oxygen and nutrient delivery to the fetus may in large be normal. Furthermore, it suggests that the pregnancy of $Pabp4^{-/-}$ dams is a model of symmetrical IUGR with maternal aetiology which is not well understood.

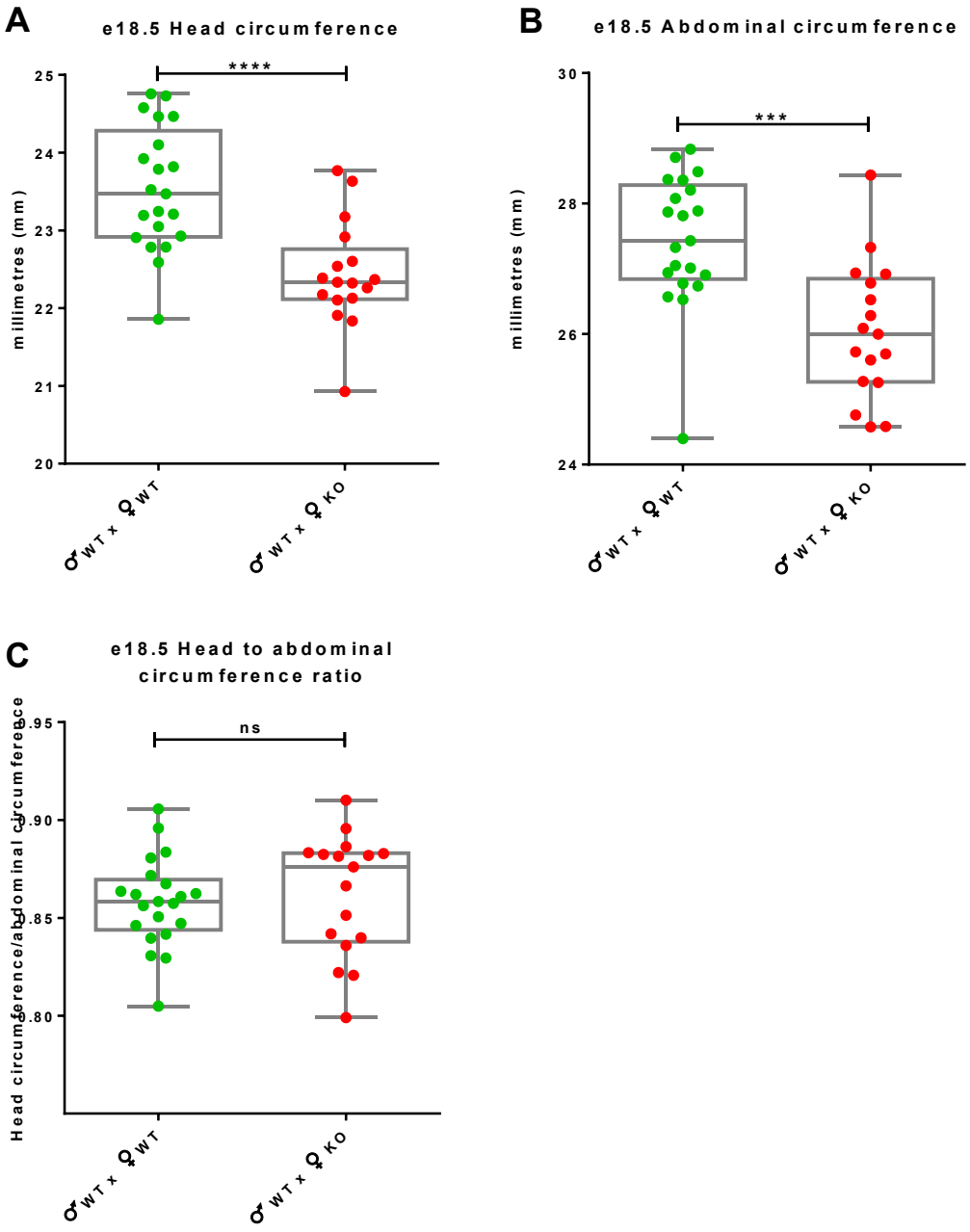

Figure 4.5. Measurements of head and abdominal circumference at e18.5 reveal symmetrical growth restriction in fetuses from PABP4 deficient dams.

A) Measurements of head circumference. **B)** Measurements of abdominal circumference. **C)** Head to abdomen circumference ratio. Each symbol corresponds to an average per genotype within a single litter. ♂ WT x ♀ WT (green dot) n = 21; ♂ WT x ♀ KO (red dot) n = 17. Data are shown as box and whisker plots with median (long line) and mean (cross) indicated. Significance was analysed by Student's t-test. ns = > 0.05; *** p = ≤ 0.001; **** p = ≤ 0.0001.

Having established that maternally dependant IUGR is present at e18.5 we then posed the question: at what stage during pregnancy does IUGR develop and does the extent and/or prevalence of restriction alter? To address this, the same crosses were set up as for the investigation of e18.5 and fetuses and placentas were weighed and measured at e15.5 and e13.5. At e15.5 *Pabp4*$^{+/-}$ fetuses from *Pabp4*$^{-/-}$ dams showed reduced weights (Figure 4.6. A, C; 11%) and crown-rump length (Figure 4.6. B, C; 3%) in comparison to both *Pabp4*$^{+/+}$ or *Pabp4*$^{+/-}$ fetuses from *Pabp4*$^{+/+}$ dams. The extent of the reduction in length was similar to that seen at e18.5, whilst weight was more reduced at e15.5 than E18.5 (compare Figure 4.2. C and Figure 4.6. C), revealing that growth was already profoundly impacted by e15.5 and is not further restricted by e18.5.

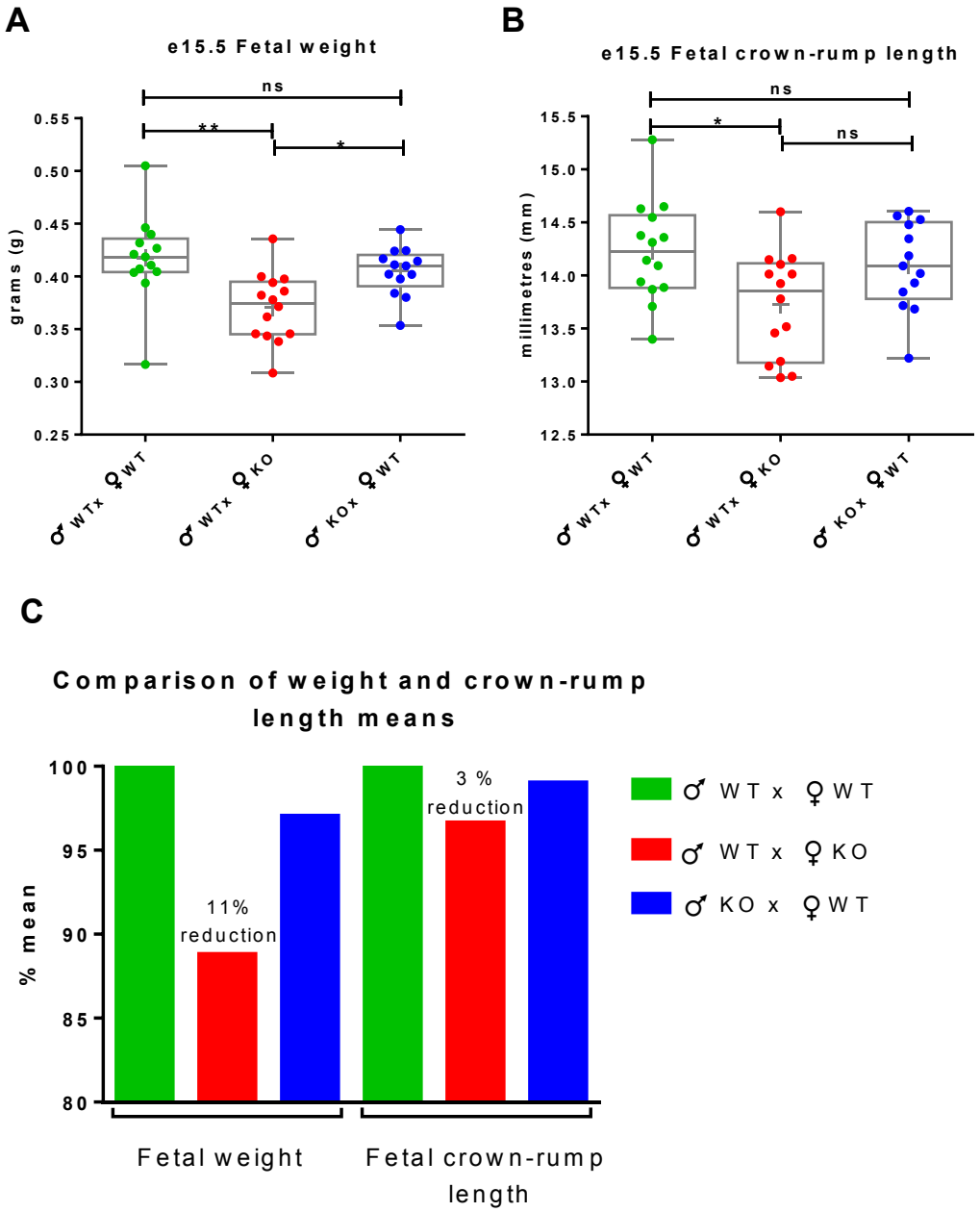

Figure 4.6. Weight and size of fetuses from PABP4 deficient dams is significantly reduced at e15.5.

Pabp4$^{+/-}$ fetuses from *Pabp4*$^{-/-}$ dams have reduced bodyweight (**A**) and (**B**) crown-rump length in comparison to both *Pabp4*$^{+/+}$ and *Pabp4*$^{+/-}$ fetuses from *Pabp4*$^{+/+}$ dams. **C)** Comparison of fetal bodyweight and crown-rump length % normalised to the ♂ WT x ♀ WT cross. Each symbol corresponds to an average per genotype within a single litter. ♂ WT x ♀ WT (green dot) n = 17; ♂ WT x ♀ KO (red dot) n = 18; ♂ KO x ♀ WT (blue dot) n = 12. Data are shown as box and whisker plots with median

(long line) and mean (cross) indicated. Significance was analysed by Kruskal-Wallis test and Dunn's multiple comparison test. ns = > 0.05; * p = ≤ 0.05; ** p = ≤ 0.01; *** p = ≤ 0.001; **** p = ≤ 0.0001.

Similarly to e18.5, placental weight and diameter were comparable amongst the three crosses and importantly the differences in F:P ratios observed at e18.5 were recapitulated at e15.5 showing an decrease of 12.0% in *Pabp4*$^{+/-}$ fetuses from *Pabp4*$^{-/-}$ dams compared to WT (*Figure 4.7.*).

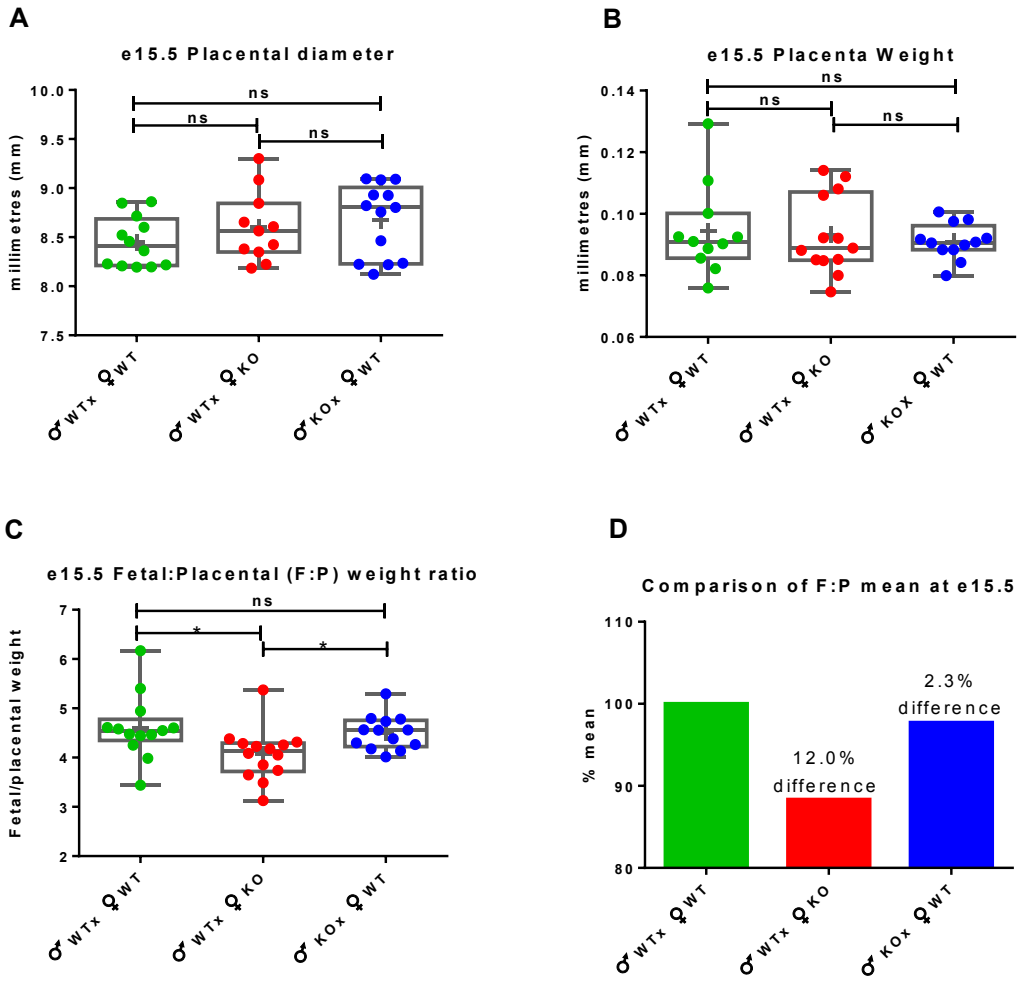

Figure 4.7. Placental diameter and weight are unaltered at e15.5 which results in an increased fetal to placental ratio in fetuses from *Pabp4*$^{-/-}$ dams.

Pabp4$^{+/-}$ placentas from *Pabp4*$^{-/-}$ dams have comparable weight (**A**) and diameter (**B**) to *Pabp4*$^{+/+}$ and *Pabp4*$^{+/-}$ placentas from *Pabp4*$^{+/+}$ dams. As a result F:P weight ratios in Pabp4$^{-/-}$ dams are reduced (**C**). Comparison of F:P % means normalised to the ♂ WT x ♀ WT cross (**D**). Each symbol corresponds to an average per genotype within a single litter. ♂ WT x ♀ WT (green dot) n = 17; ♂ WT x ♀ KO (red dot) n = 18; ♂ KO x ♀ WT (blue dot) n = 12. Data are shown as box and whisker plots with median (long line) and mean (cross) indicated. Significance was analysed by Kruskal-Wallis test and Dunn's multiple comparison test. ns = > 0.05; * p = ≤ 0.05; ** p = ≤ 0.01; *** p = ≤ 0.001; **** p = ≤ 0.0001.

To determine whether the IUGR at e15.5 was also symmetrical, head and abdominal circumference measurements were taken (*Figure 4.8*.). Compared to the *Pabp4*$^{+/+}$ fetuses from *Pabp4*$^{+/+}$ dams, *Pabp4*$^{+/-}$ fetuses from *Pabp4*$^{-/-}$ dams showed equivalent reductions in head (*Figure 4.8*. A) and body circumference (*Figure 4.8*. B) indicative of an unaltered head:abdomen ratio (*Figure 4.8*. C) representing symmetrical IUGR.

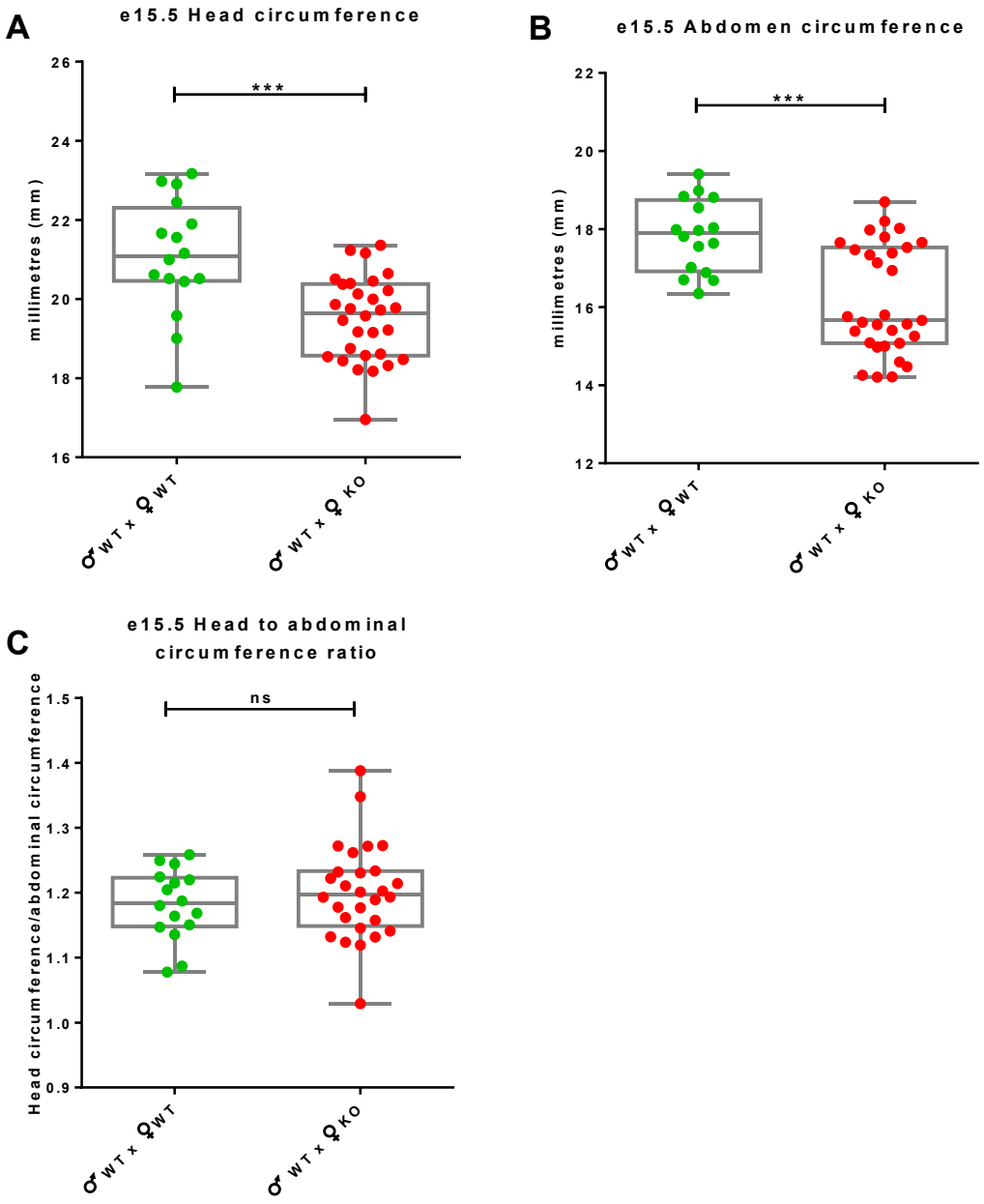

Figure 4.8. Measurements of head and abdominal circumference at e15.5 reveal symmetrical growth restriction of fetuses from *Pabp4-/-* dams.

A) Measurements of head circumference. **B)** Measurements of abdominal circumference. **C)** Head to abdomen circumference ratio. Each symbol corresponds to an average per genotype within a single litter. ♂ WT x ♀ WT (green dot) n = 16; ♂ WT x ♀ KO (red dot) n = 30. Data are shown as box and whisker plots with median (long line) and mean (cross) indicated. Significance was analysed by Student's t-test. ns = > 0.05; *** p = ≤ 0.001.

As IUGR was well established by e15.5, an earlier time-point, e13.5, was investigated to identify the onset of the phenotype. This analysis was carried out on a mixture of previously fixed and freshly collected samples, which were analysed separately (*Figure 4.9*. *Figure 4.10*.) to take into account differences that are due to fixation (see discussion). Due to lower litter numbers, fetal measurements post-fixation were plotted as individual data points as well as litter means Although plots of individual fetuses is potentially informative the data should be considered as litters given that the experimental unit is the mother and also to avoid overpowering the studies. *Pabp4*$^{+/-}$ fetuses from *Pabp4*$^{-/-}$ dams being significantly smaller in weight and size in comparison to the *Pabp4*$^{+/+}$ fetuses from *Pabp4*$^{+/+}$ dams when plotted individually (*Figure 4.9*. A-B). However, significance was not present when the data was plotted as litter means (Figure 4.9. E-F). In contrast, data collected from fetuses immediately following dissection showed no significant difference in weight or size irrespective of whether plotted as individual fetuses (*Figure 4.10*. A-B) or litter means (*Figure 4.10*. E-F, only n=3 for *Pabp4*$^{-/-}$ dams). Placenta weight and diameter were unaltered irrespective of whether they were fixed or freshly collected (*Figure 4.9*. C, G; *Figure 4.10*. C, G). As a result the F:P weight ratio was altered in the case of fixed material when considered as individual data points (*Figure 4.9*. D) but were unaltered when considered as litter means (*Figure 4.9*. H). For freshly collected data the F:P weight ratio was unaltered irrespective of whether plotted as individual data points or litter means (*Figure 4.10*. D, H). Overall, due to the low *n* numbers and the contradictive results with these two cohorts, it is difficult to draw conclusions on whether *Pabp4*$^{+/-}$ fetuses from *Pabp4*$^{-/-}$ dams have developed IUGR by e13.5.

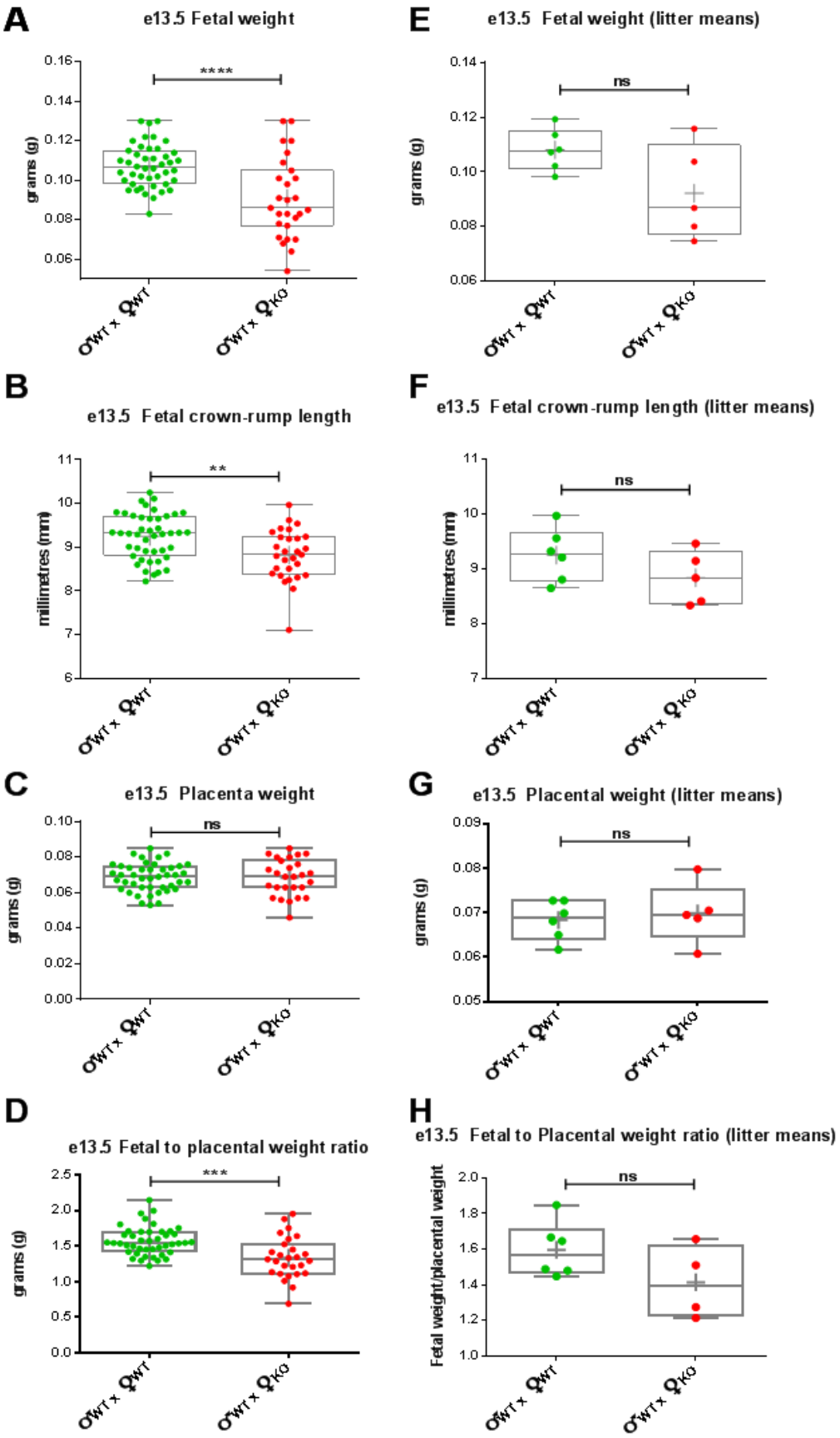
A
e13.5 Fetal weight
****
grams (g)
0.16
0.14
0.12
0.10
0.08
0.06
♂WT x ♀WT
♂WT x ♀KO
E
e13.5 Fetal weight (litter means)
ns
grams (g)
0.14
0.12
0.10
0.08
0.06
♂WT x ♀WT
♂WT x ♀KO
B
e13.5 Fetal crown-rump length
**
millimetres (mm)
11
10
9
8
7
6
♂WT x ♀WT
♂WT x ♀KO
F
e13.5 Fetal crown-rump length (litter means)
ns
millimetres (mm)
11
10
9
8
7
♂WT x ♀WT
♂WT x ♀KO
C
e13.5 Placenta weight
ns
grams (g)
0.10
0.08
0.06
0.04
0.02
0.00
♂WT x ♀WT
♂WT x ♀KO
G
e13.5 Placental weight (litter means)
ns
grams (g)
0.09
0.08
0.07
0.06
0.05
♂WT x ♀WT
♂WT x ♀KO
D
e13.5 Fetal to placental weight ratio
***
grams (g)
2.5
2.0
1.5
1.0
0.5
0.0
♂WT x ♀WT
♂WT x ♀KO
H
e13.5 Fetal to Placental weight ratio (litter means)
ns
Fetal weight/placental weight
2.0
1.8
1.6
1.4
1.2
1.0
♂WT x ♀WT
♂WT x ♀KO

Figure 4.9. Measurements post-fixation at e13.5 suggest that fetuses from *Pabp4*$^{-/-}$ dams are growth restricted presented as individual data points but not as litter means.

Fetal and placental measurements and F:P ratio at e13.5 post-fixation presented as individual data points (**A-D**) and litter means (**E-F**). *Pabp4*$^{+/-}$ fetuses from *Pabp4*$^{-/-}$ dams have reduced weights (**A**) and reduced crown-rump lengths (**C**) in comparison to *Pabp4*$^{+/+}$ and *Pabp4*$^{+/-}$ fetuses from *Pabp4*$^{+/+}$ dams when graphed as individual data points but not when compared as litter means (**E-F**). Placental weight is unaltered as individual data points (**C**) and litter means (**G**). As a result, F:P is altered for individual data points of *Pabp4*$^{+/-}$ fetuses from *Pabp4*$^{-/-}$ dams but not as litter means (H). ♂ WT x ♀ WT (green dot) n = 44 (individual fetal data points; A-D); 6 (litter means; E-H); ♂ WT x ♀ KO (red dot) n = 27 (individual data points; A-D); 5 (litter means; E-F). Data are shown as box and whisker plots with median (long line) and mean (cross) indicated. Significance was analysed by Student's t-test. ns = > 0.05; * p = ≤ 0.05; ** p = ≤ 0.01; *** p = ≤ 0.001; **** p = ≤ 0.0001.

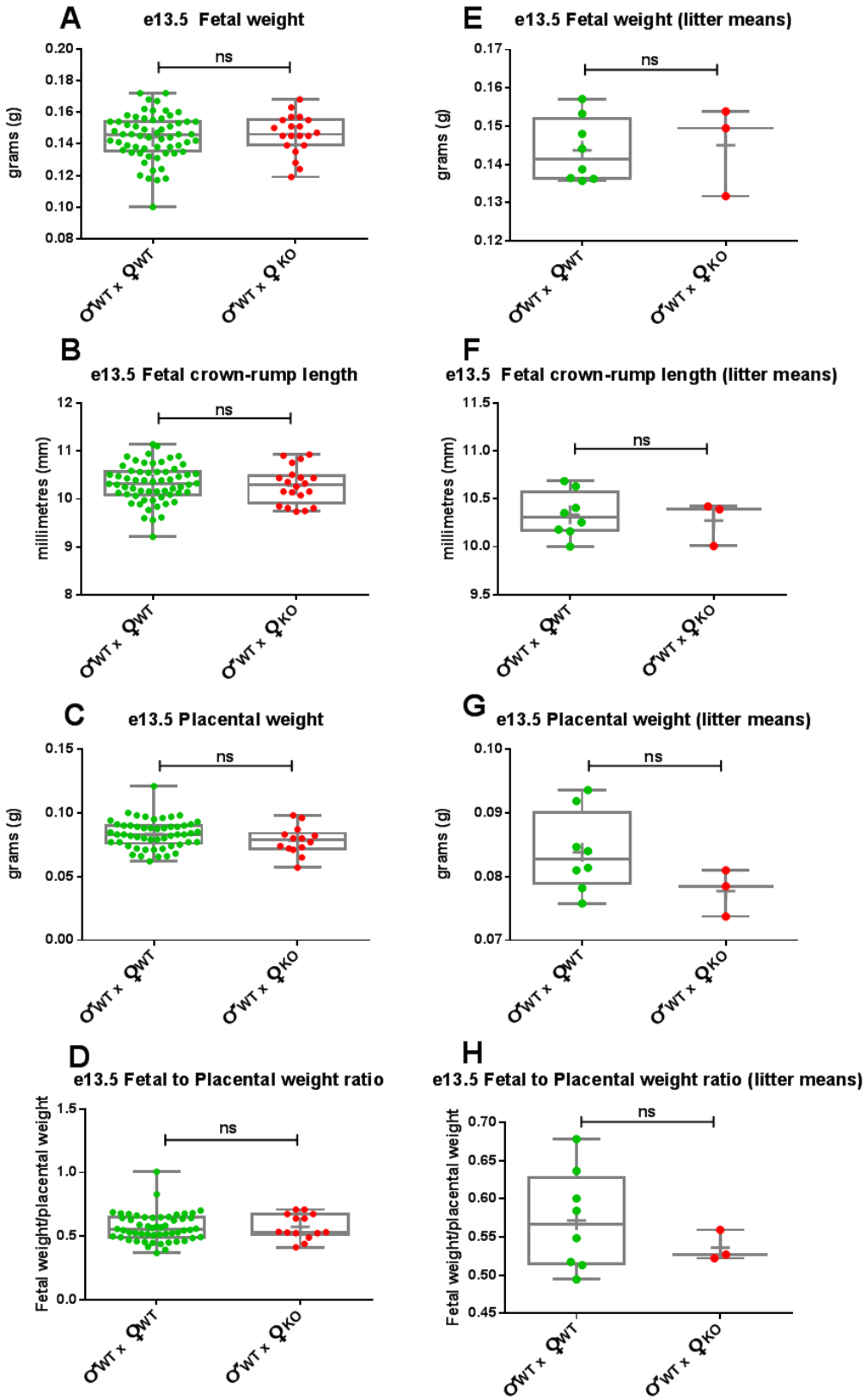
A
e13.5 Fetal weight
grams (g)
ns
0.20
0.18
0.16
0.14
0.12
0.10
0.08
♂WT x ♀WT
♂WT x ♀KO
E
e13.5 Fetal weight (litter means)
grams (g)
ns
0.17
0.16
0.15
0.14
0.13
0.12
♂WT x ♀WT
♂WT x ♀KO
B
e13.5 Fetal crown-rump length
millimetres (mm)
ns
12
11
10
9
8
♂WT x ♀WT
♂WT x ♀KO
F
e13.5 Fetal crown-rump length (litter means)
millimetres (mm)
ns
11.5
11.0
10.5
10.0
9.5
♂WT x ♀WT
♂WT x ♀KO
C
e13.5 Placental weight
grams (g)
ns
0.15
0.10
0.05
0.00
♂WT x ♀WT
♂WT x ♀KO
G
e13.5 Placental weight (litter means)
grams (g)
ns
0.10
0.09
0.08
0.07
♂WT x ♀WT
♂WT x ♀KO
D
e13.5 Fetal to Placental weight ratio
Fetal weight/placental weight
ns
1.5
1.0
0.5
0.0
♂WT x ♀WT
♂WT x ♀KO
H
e13.5 Fetal to Placental weight ratio (litter means)
Fetal weight/placental weight
ns
0.70
0.65
0.60
0.55
0.50
0.45
♂WT x ♀WT
♂WT x ♀KO

Figure 4.10. Fresh measurements at e13.5 suggest that fetuses from *Pabp4*$^{-/-}$ dams are not growth restricted.

Fetal and placental measurements and F:P ratio at e13.5 of freshly collected material presented as individual data points (**A-D**) and litter means (**E-F**). *Pabp4*$^{+/-}$ fetuses from *Pabp4*$^{-/-}$ dams have comparable bodyweight (**A, E**), crown-rump length (**B, F**), placental weight (**C, G**) and F:P weight ratio (**D, H**) as individual data points and litter means in comparison to *Pabp4*$^{+/+}$ and *Pabp4*$^{+/-}$ fetuses from *Pabp4*$^{+/+}$ dams. ♂ WT x ♀ WT (green dot) n = 53 (individual fetal data points; A-D); 6 (litter means; E-H); ♂ WT x ♀ KO (red dot) n = 20 (individual data points; A-D); 3 (litter means; E-F). Data are shown as box and whisker plots with median (long line) and mean (cross) indicated. Significance was analysed by Student's t-test. ns = > 0.05.

4.3 Discussion

The primary aim of this chapter was to establish whether, as preliminary data suggested, fetuses of *Pabp4*$^{-/-}$ dams are small for gestational age but, more importantly, to determine the extent to which they are intrauterine growth-restricted (IUGR), using fetal weight and crown-rump length measurements, and the nature of IUGR (symmetrical or asymmetrical) by obtaining anthropomorphic measurements. Further, I wished to define when in gestation the growth restriction is established and whether its severity alters over time. A final aim was to gain an insight into whether placental insufficiency is present by investigating the effect of parental genotype on placental size (diameter) and weight and thereby determining the fetal to placental weight ratio (FPR).

Pabp4$^{+/-}$ fetuses from *Pabp4*$^{-/-}$ dams have a significantly reduced bodyweight and crown-rump length at e15.5 and e18.5 in comparison to *Pabp4*$^{+/-}$ (and *Pabp4*$^{+/+}$) fetuses from WT females (*Figure 4.2* and Figure 4.6). Furthermore, at both these time-points in gestation, *Pabp4*$^{+/-}$ fetuses from *Pabp4*$^{-/-}$ dams exhibit significantly reduced abdominal and head circumferences, indicative of symmetrical IUGR (*Figure 4.5* and *Figure 4.9*). The placentas of these fetuses have equivalent diameters and weights to *Pabp4*$^{+/+}$ and *Pabp4*$^{+/-}$ fetuses from WT females resulting in a reduced F:P ratio at e18.5 (*Figure 4.3*) and e15.5 (*Figure 4.7*). Taken together, these results suggest *Pabp4*$^{-/-}$ dams provide a model of IUGR where the underlying cause is maternal. However, whilst highly suggestive, an embryo transfer experiment, as discussed in Chapter 3, would provide an additional level of proof with respect to the maternal nature. As measures of IUGR are not directly dependent on the number of pups within litters, such experiments are potentially feasible, and are ongoing (see Chapter 7).

Pabp4$^{-/-}$ female mice have the potential to be a model of a yet uncharacterised novel maternal causes of IUGR, independent of fetal and paternal genotype. In humans there remains a high number of IUGR cases with unknown aetiology, particularly in non-anomalous fetuses and in the absence of recognised maternal causes such as severe maternal medical conditions e.g. hypertension that may result in pre-eclampsia,

chronic infections (e.g. inflammatory bowel disease), maternal hypoxia (e.g. asthma, cystic fibrosis), and other diseases including diabetes, glomerulonephritis, collagen disease, and severe anaemia (reviewed by (Wollmann, 1998) (Nardozza et al., 2012). The nutritional status of the mother prior to pregnancy, pregnancy weight gain and low maternal age can also contribute to the incidence of IUGR (Wollmann, 1998). Indicators of relevant aspects of maternal health e.g. blood glucose, haematocrit and weight gain are examined in *Pabp4*$^{-/-}$ mice in later chapters.

In animal models, genetic manipulations have shown that the fetus and/or placenta are the main cause of IUGR, and only in a few cases has a maternal contribution been reported. Nonetheless these provide precedence that maternal genetics can influence pregnancy outcome. For example, a maternal contribution has been evoked for models in which loss of endothelial nitric oxide synthase (*eNos*), an enzyme which acts as a potent vasodilator via relaxation of smooth muscle cells (Moncada et al., 1991), results in aberrant uterine and spiral artery remodelling and IUGR (Kulandavelu et al., 2012; Kusinski et al., 2012). However, IUGR is present only when *eNos*$^{-/-}$ dams are carrying *eNos*$^{-/-}$ fetuses (Kulandavelu et al., 2012). Interestingly, the *eNos*$^{+/-}$ fetuses in *eNos*$^{-/-}$ dams are able to achieve normal fetal weight despite uterine arterial lumen diameter and blood flow as well as spiral artery length being compromised suggestive of a fetal/placental ability to compensate for the underlying maternal underlying defects which can lead to IUGR. However, without an embryo transfer experiment, in this case it cannot formally be concluded that the *eNos*$^{-/-}$ fetus itself is not the underlying causal factor of reduced fetal bodyweight. Nonetheless, given the importance of uterine and spiral artery remodelling in pregnancy, it is attractive to speculate that *eNos*$^{+/-}$ fetuses are capable of compensating for a maternally derived aberrant vascular remodelling to achieve a normal bodyweight. Data regarding vascular remodelling in *Pabp4*$^{-/-}$ females is presented in the next chapter.

As previously mentioned, maternal *Pla2g4a* knockout leads to a deferral of the initiation of implantation, specifically a short delay in the initial attachment reaction, which causes late development defects including retarded feto-placental development, embryo crowding, conjoined placentas and reduced litter size (Song et al., 2002). This delay is distinct from diapause in wild-type mice which can be induced by lactation or

experimentally as resumption of uterine responsiveness to the blastocyst results in a normal pregnancy outcome (Dey, 1996). A transfer of wild-type blastocysts to *Pla2g4a*$^{-/-}$ uteri results in delayed implantation frequency therefore uterine insufficiency for implantation is hypothesized to be the primary cause of the phenotype. A similar phenotype of delayed implantation and embryonic development, altered embryo spacing, conjoined placentas and embryonic death is also observed in mice lacking the gene for a lysophatidic acid (LPA) receptor LPA_3 (Ye et al., 2005). The deletion of this gene results in the down-regulation of cyclooxygenase 2 (COX2) and subsequent low levels of prostaglandins, important for implantation.

As we do not observe embryo crowding, conjoined placentas or significant numbers of resorptions by mid gestation (day12; (Song et al., 2002)), it could be hypothesized that a delay in implantation is not the underlying cause of the *Pabp4*$^{-/-}$ phenotype. However, the morphology of e8.5 implantation sites is examined in Chapter 5, and direct measures of implantations rates at e5.5 and counting the number of somites of embryos from *Pabp4*$^{-/-}$ females would more directly determine whether maternal *Pabp4*$^{-/-}$ genotype leads to any delay in implantation and/or development relative to the day of gestation. A further example in which the maternal genotype is implicated in problematic pregnancy is the knockout of metalloproteinase-9 (*Mmp9*). In this model, the loss of MMP primarily from the fetus but also partly from the mother leads to pre-eclampsia like symptoms accompanied by IUGR (Plaks et al., 2013), no pre-eclamptic symptoms have been noted in *Pabp4*$^{-/-}$ mice: Following embryo transfers of *Mmp9*$^{+/+}$ embryos into *Mmp9*$^{-/-}$ mothers, shallow invasion of the mature trophoblasts from the ectoplacental cone (ECP) into the maternal decidua was reported, as indicated by the presence of small ECPs, blood pools, and debris plugs blocking the invasion of the EPC into the mesometrial pole of the decidua (Plaks et al., 2013). Interestingly, *Mmp9*$^{+/+}$ embryos were still more likely to survive and develop more normally in a *Mmp9*$^{-/-}$ dams in comparison to the reciprocal (paternal KO) setup of *Mmp9*$^{-/-}$ embryos into a *Mmp9*$^{+/+}$ dams (Plaks et al., 2013), highlighting the importance of fetal *Mmp9*$^{-/-}$ genotype in adverse pregnancy outcome. Knockout of NFIL3 results in incomplete remodelling of spiral arteries, placental defects, fetal growth restriction but normal litter size (Boulenouar et al., 2016) 3.3 Discussion). Importantly, these effects are maternal in origin as *Nfil*$^{+/+}$ females crossed with KO produce normal sized fetuses

and placentas (Boulenouar et al., 2016). NFIL3, is a maternal transcription factor required by innate lymphoid cells (ILC) such as the uterine natural killer (uNK) cells. uNK cells increase in the uterus in early pregnancy and are important in pregnancy adaptations such as uterine spiral artery remodelling and the phenotype of this mouse closely mirrors that of natural killer (NK) cell-deficient mice (Ashkar et al., 2000; Kieckbusch et al., 2014).

At both e15.5 and e18.5 the fetuses of *Pabp4*$^{-/-}$ dams are characterised by symmetrical growth restriction (*Figure 4.5* and *Figure 4.9*), however it is unclear when this growth restriction manifests as data from e13.5 is currently inconclusive (*Figure 4.9* and *Figure 4.10*). Thus, future work will include completing a full powered data set using freshly dissected e13.5 materno-fetal units. Such measurements are normally made on freshly dissected material, as the fixation process shrinks tissue. Moreover, use of fresh material would allow direct comparisons with the datasets at e15.5 and e18.5. There are two subtypes of symmetrical IUGR; 1. congenital anomalies of fetal origin such as aneuploidy syndromes, 2. normal 'constitutionally small' fetuses with a developmental delay which are generally not associated with complications (Nardozza et al., 2012). Given that the symmetrical growth restriction phenotype described herein is maternal genotype-dependent, it suggests that it does not fall into the typical causal categories normally attributed to symmetrical IUGR, however it may be suggestive of an origin early in pregnancy. Asymmetrical IUGR on the other hand, often manifests in the second half of gestation and is most commonly associated with aberrant utero-placental insufficiency as a result of improper uterine and decidual artery remodelling that leads to reduced blood flow and elevated blood flow resistance (Nardozza et al., 2012). This could be interpreted to suggest that uterine and decidual artery remodelling is normal in *Pabp4*$^{-/-}$ dams. The use of Doppler ultrasound to establish the resistance index of the uterine artery and immunohistochemical analysis for the presence/absence of smooth muscle actin in decidual spiral arteries is used to investigate this experimentally (Chapter 5).

At both e15.5 and e18.5 *Pabp4*$^{+/-}$ fetuses from *Pabp4*$^{-/-}$ dams have reduced fetal (F) weights but their placentas (P) have comparable weights to that of WT fetuses, leading to an decreased F:P ratio with a more pronounced difference present at e18.5 (*Figure*

4.4 and *Figure 4.7*). Recently reviewed by Hayward *et al*, (Hayward et al., 2016) F:P ratio and the birthweight:placental (BW:PW) weight ratio, commonly used in humans, inform on the efficiency of the placenta as it describes the number of grams of fetus produced per gram of placenta (Wilson and Ford, 2001). Placental failure is implicated in up to 65% of cases of stillbirth in high-income countries (Heazell et al., 2015). Interestingly it is also a predictor of adverse health outcomes later in life as a low BW:PW ratio in humans increases the risk of hypertension in childhood (Hemachandra et al., 2006) with an increased risk of cardiovascular disease and stroke in adulthood (Risnes et al., 2009). Similarly to humans, in mice the F:P ratio increases as gestation progresses, but in a more dramatic manner increasing from F:P=4 at e16 to roughly F:P=11-14 at e19, reflective of the exponential fetal growth with no change in placental size but an increase in nutrient transfer rate in late gestation (Coan et al., 2008; Dilworth et al., 2011). In human problematic pregnancies BW:PW ratios are decreased in small for gestational age babies in comparison to appropriately sized for gestational age babies, with the difference being most prominent in early gestation (Imada et al., 2012; Macdonald et al., 2014; Molteni et al., 1978). In the previously mentioned mouse model of IUGR, *eNos*$^{-/-}$, F:P is reduced et e17.5 (Kulandavelu et al., 2012; Kusinski et al., 2012). Furthermore, mice lacking insulin-like growth factor 2 (*Igf2*) are growth restricted from day e12 onward and present with a reduced F:P near term, suggestive of nutrient transport not adapting appropriately in response to placenta size changes (Constancia et al., 2005). However, in placental-specific *Igf2* knockout (*Igf2-P0*) mice the fetuses have a higher F:P ratio throughout gestation, whereby placentas are small but have increased efficiency. However, their increased efficiency to compensate for size is insufficient towards the end of gestation as fetuses become growth restricted before term. These observations are indicative of both of placental adaptation and of its failure (Constancia et al., 2002). At e15.5 placental efficiency is suboptimal and by e18.5 the abnormal function becomes more pronounced. As placental insufficiency and IUGR are a significant risk factor for stillbirth (Heazell et al., 2015; Smith and Fretts, 2007) an attractive hypothesis is that the growth restriction present in *Pabp4*$^{-/-}$ dams is the cause/or contributes to the dramatic reduction in litter size between e18.5 and birth. As the nature of the placental insufficiency is unclear

from an F:P ratio, Chapter 5 focuses on placental morphology and function in pregnant *Pabp4*$^{-/-}$ females.

Chapter 5 - Placental structure and function of fetuses from *Pabp4*$^{-/-}$ dams

5.1 Introduction

Although IUGR and stillbirth are in many cases unexplained some of the known associated factors are maternal disease, fetal genetic abnormalities and/or placental insufficiency. The placenta is largely extraembryonic in origin being derived from the trophectoderm layer, which is set aside from the inner cell mass in the blastocyst at e3.5, and gives rise to the labyrinth and junctional zones. The maternal constituent of the placenta is the decidua basalis which arises from growth, proliferation and differentiation of endometrial stromal cells and an influx of immune cells during implantation. A complex bi-directional communication between the mother and fetus is key to placental development and may be aberrant in *Pabp4*$^{-/-}$ mice. Due to the maternal genotype-dependent nature of the phenotype, it is envisaged that a failure to receive or correctly respond to fetal "signals" or a disruption of maternal 'signals' to the fetus could result in aberrant placentation and subsequent placental insufficiency. One of the first important such events is the release of several cytokines from decidualised cells in response to maternal estrogen. These include leukemia inhibiting factor (LIF) which stimulates trophoblast outgrowth (Cai et al., 2000) and thus appears particularly important in triggering events required for implantation (Stewart et al., 1992). The trophoblasts of the blastocyst also secrete molecules, for example interleukin-1β (IL-1β), whose receptor is expressed on uterine epithelium and endometrial cells (Simon et al., 1994) and alters the expression of specific integrins, structurally transforming the plasma membrane of the epithelial endometrium (Simon et al., 1998).

During implantation uterine stromal cells proliferate and differentiate into enlarged secretory decidual cells which form an implantation chamber around the conceptus (Bilinski et al., 1998). Decidualisation initially occurs at the anti-mesometrial pole of the implantation site and on embryonic day 5 (e5) a wave of decidualisation occurs

around the embryo forming the primary decidual zone, followed by a second wave of decidualisation and the formation of the secondary decidual zone at e6 (Huet-Hudson et al., 1989). At e7 decidualization also takes places at the mesometrial pole which coincides with expansion of the embryo, primary trophoblast invasion and apoptosis of the anti-mesometrial decidua (Welsh and Enders, 1985). The placenta forms at the mesometrial pole where it is in direct contact with the mesometrial decidua.

Currently no information is available as to whether PABPs are expressed within implantation sites and the placenta hampering the understanding of whether mis-regulated implantation/placental development may be causative in the maternal genotype-dependent phenotype or whether they may be a consequence of a primary defect beyond the uterus. Thus this chapter investigates PABP4 expression in the non-pregnant uterus, during implantation, and in the mature placenta. Furthermore, this chapter investigates implantation site shape and weight, ectoplacental cone morphology as well as volumetric changes of the total placenta and of individual placental zones in *Pabp4*$^{-/-}$ dams. Aspects of placental function are also examined by investigating uterine and spiral artery remodelling and glucose levels in the fetal versus maternal blood.

5.2 Results

To address the current lack of information on whether PABPs are expressed within the uterus prior to pregnancy or the implantation sites following conception, expression of PABP4, and the closely related PABP1, was examined in *Pabp4*$^{+/+}$ non-pregnant uterus, e5.5 and e8.5 implantation sites by immunohistochemistry (IHC). The non-pregnant uterus is an important hormone-responsive reproductive organ whose primary role is to receive the fertilised oocyte and allow it to implant and develop successfully to term. PABP4 and PABP1 were found to be strongly expressed in the luminal epithelium and glandular epithelium with PABP1 being also strongly expressed in what is most likely stromal fibroblasts, based on morphology and location (*Figure 5.1* A, B). Neither the pattern nor levels of PABP1 expression appreciably

changed in the absence of PABP4 (*Figure 5.1* D), although conclusions with regards to levels require additional techniques, such as western blots, as IHC is not quantitative. However, because *Pabp4*$^{-/-}$ and *Pabp4*$^{+/+}$ samples were stained on the same slide, differences in staining intensity is potentially informative. Next the expression of PABP4 and PABP1 was investigated in e5.5 and e8.5 implantation sites. Interestingly, at e5.5 PABP4 was found to be largely absent in the primary decidua zone surrounding the embryo but present in non-decidualised zone in the anti-mesometrial endometrium surrounding the primary decidual zone and the mesometrial endometrium (*Figure 5.2*. A). Furthermore, it was expressed in the epithelium of endometrial glands (*Figure 5.2*. A). PABP1 showed a similar pattern of expression but was generally more widely expressed throughout the implantation site, including weaker expression in the decidualising cells surrounding the embryo (*Figure 5.2*. B.). At e8.5 PABP4 was found to be expressed in the ectoplacental cone, maternal decidua which contains large numbers of leukocytes (indicated by an asterisk), primarily uterine natural killer cells (uNK) and the embryo (*Figure 5.3*. A). Interestingly, similarly to e5.5, PABP4 appeared to be largely absent from the zones undergoing decidualisation which are outlined by a dotted line and appear as paler and larger cells (*Figure 5.3*. A). PABP1 showed a very similar pattern of expression to PABP4 at e8.5 but in contrast to e5.5 also appeared to be largely absent from zones undergoing decidualisation (*Figure 5.3*. B). These data show that a burst of expression of PABP4 occurs in the stromal cells surrounding the primary decidualised zone following conception. However its expression appears transient as it is absent in within the primary decidualised zone, suggesting it may be important for the stromal to decidual cell transition.

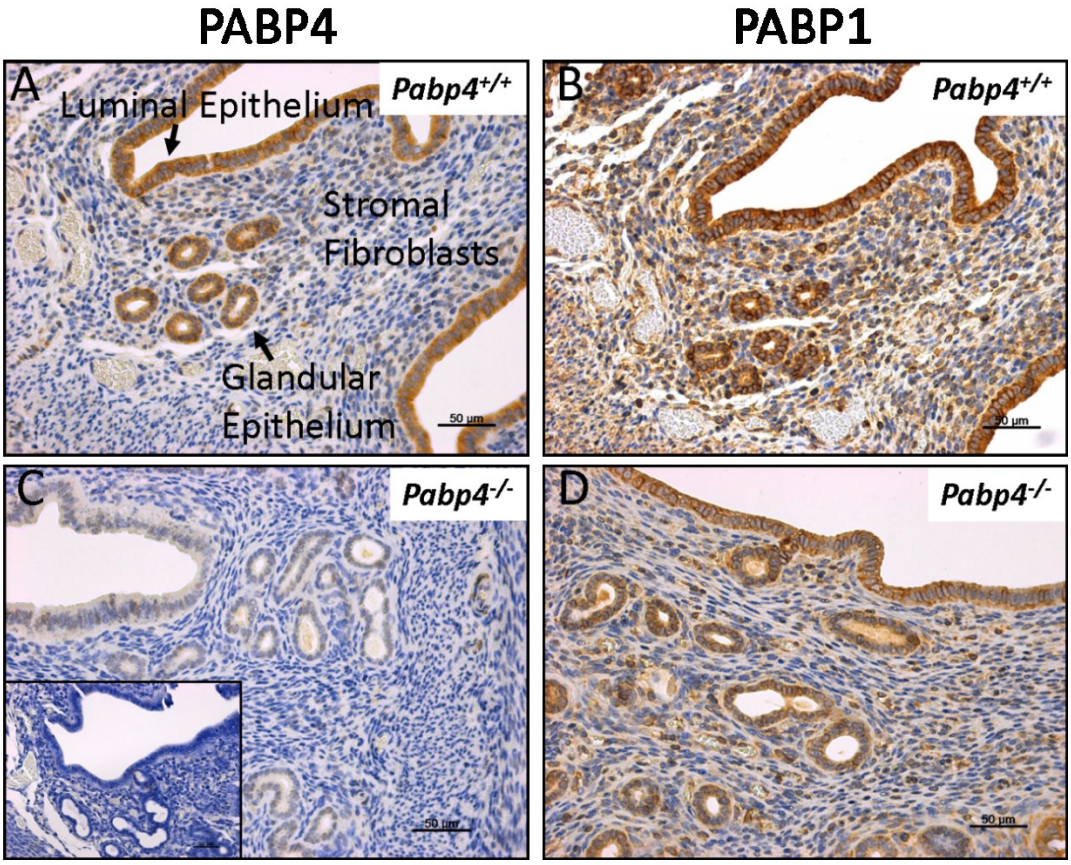

Figure 5.1. PABP4 and PABP1 expression in the non-pregnant uterus.

Immunohistochemical analysis of (**A**) PABP4 expression and (**B**) PABP1 expression in the *Pabp4*$^{+/+}$ non-pregnant uterus and analysis of (**C**) PABP4 expression and (**B**) PABP1 expression in the *Pabp4*$^{-/-}$ non-pregnant uterus. Rabbit IgG control (insert in **C**). 50 µm scale bars and x20 magnifications are shown.

The presence of PABP4 in the decidua at these stages (*Figure 5.2*, *Figure 5.3*), raises the possibility that it's loss could affect early events resulting in IUGR and fetal death later in pregnancy, despite normal number of implantations being observed at e8.5 (Figure 3.14, Chapter 3) in *Pabp4*$^{-/-}$ females. For instance, data in hand cannot rule out a delay in blastocyst attachment nor shallow invasion of trophoblasts following implantation. Thus to investigate whether implantations in *Pabp4*$^{-/-}$ females deviated from normal morphology, multiple parameters of *Pabp4*$^{+/-}$ implantation sites from *Pabp4*$^{-/-}$ and *Pabp4*$^{+/+}$ females were compared. Interestingly this revealed that all

measured parameters i.e. implantation weight, width and mesometrial to anti-mesometrial (M/AM) distance differed in *Pabp4*$^{-/-}$ females (*Figure 5.4*. A, C, E) indicating that these implantations have an altered shape (*Figure 5.4*G). However, when the measurements were considered as litter means, only the M/AM distance remained significantly increased in implantations sites from *Pabp4*$^{-/-}$ females (*Figure 5.4*. B, D, F). Whilst the apparent absence of precedents for this in the literature make it difficult to draw conclusions from this data alone, the distinct shape supports the idea that implantation may be altered e.g. due to problems such as delayed implantation, aberrant decidualisation, disparate trophoblast invasion and/or disparate degradation of the extracellular matrix (ECM).

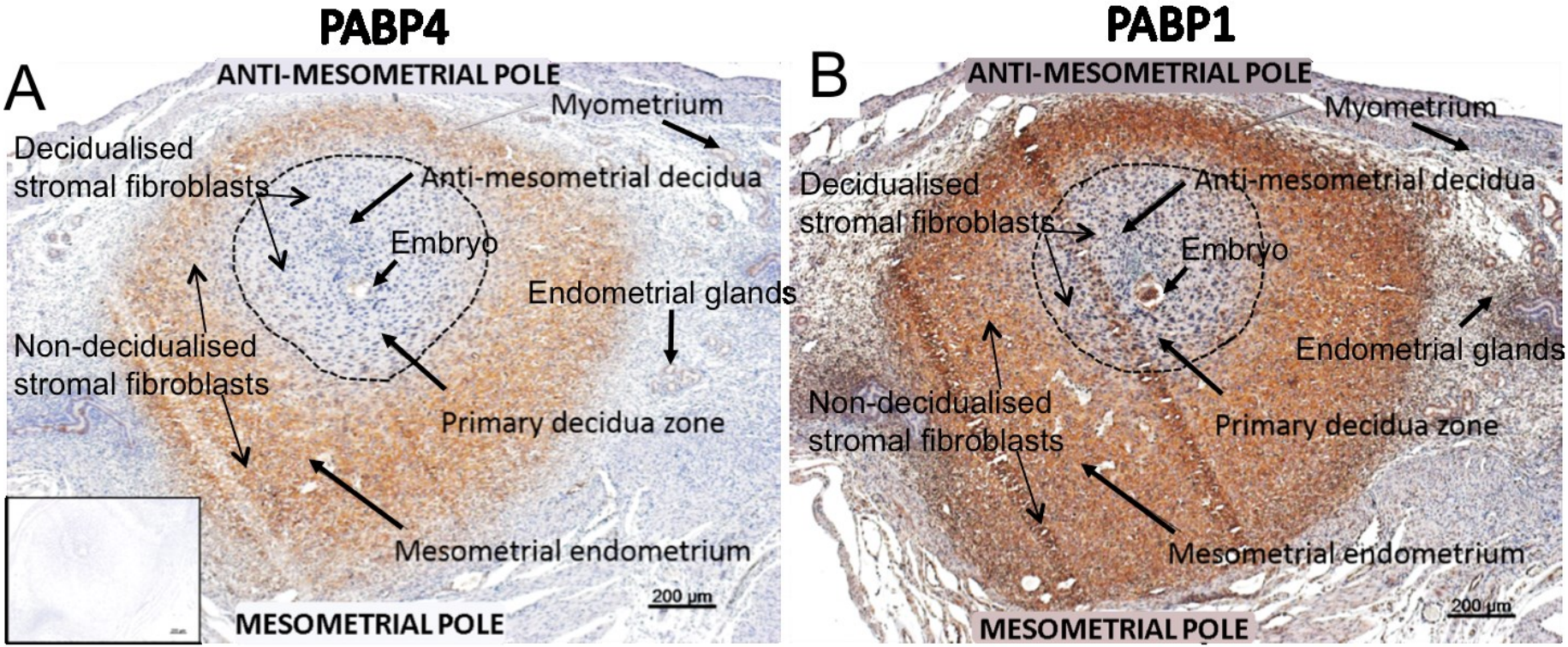

Figure 5.2. PABP1 and PABP4 expression pattern in WT e5.5 implantation sites.

Section of *Pabp4*$^{+/+}$ implantation sites at embryonic day (e) 5.5 stained by immunohistochemistry for A) PABP4 and B) PABP1. Rabbit IgG control (insert in **B**). Both are expressed in the mesometrial endometrium and both have limited expression in the primary decidua zone. x4 magnifications are shown.

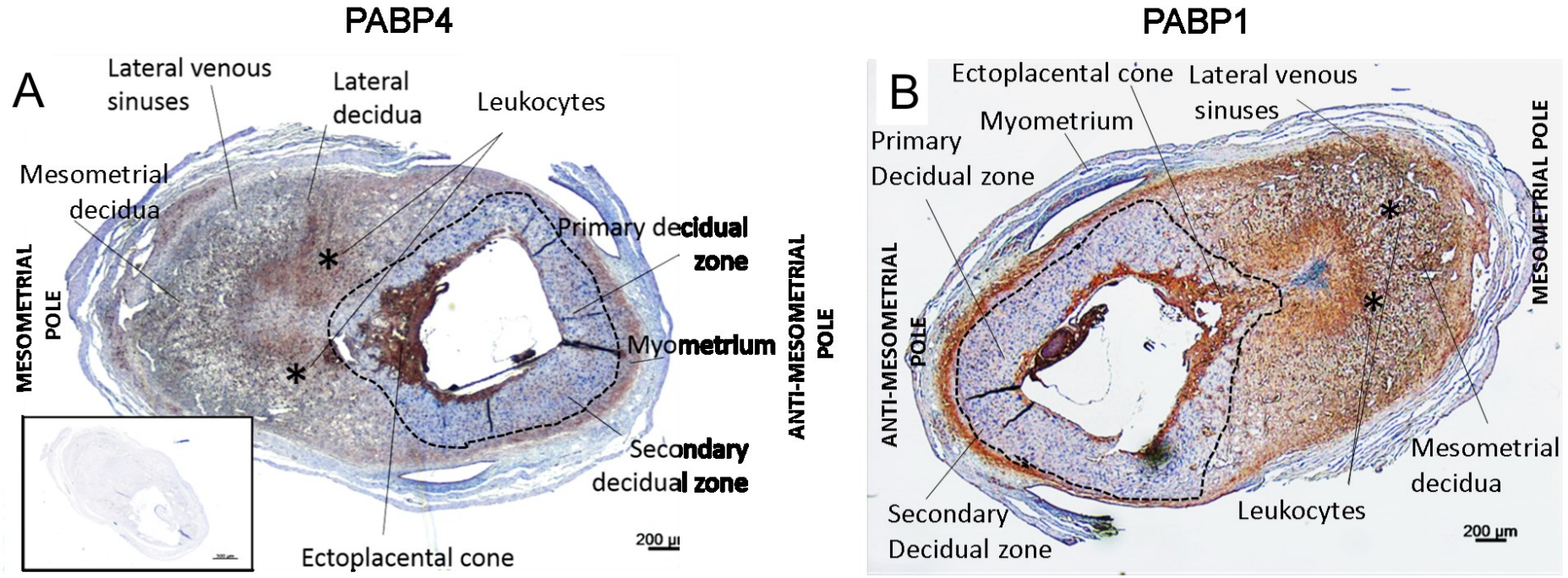

Figure 5.3. PABP1 and PABP4 expression pattern in WT e8.5 implantation sites.

Sections of *Pabp4*$^{+/+}$ implantation sites at embryonic day (e) 8.5 stained by immunohistochemistry for A) PABP4 and B) PABP1. Rabbit IgG control (insert in **B**). Dotted line outlines decidualised stromal fibroblasts in the primary and secondary decidual zone which surround the embryo. x2 magnifications are shown.

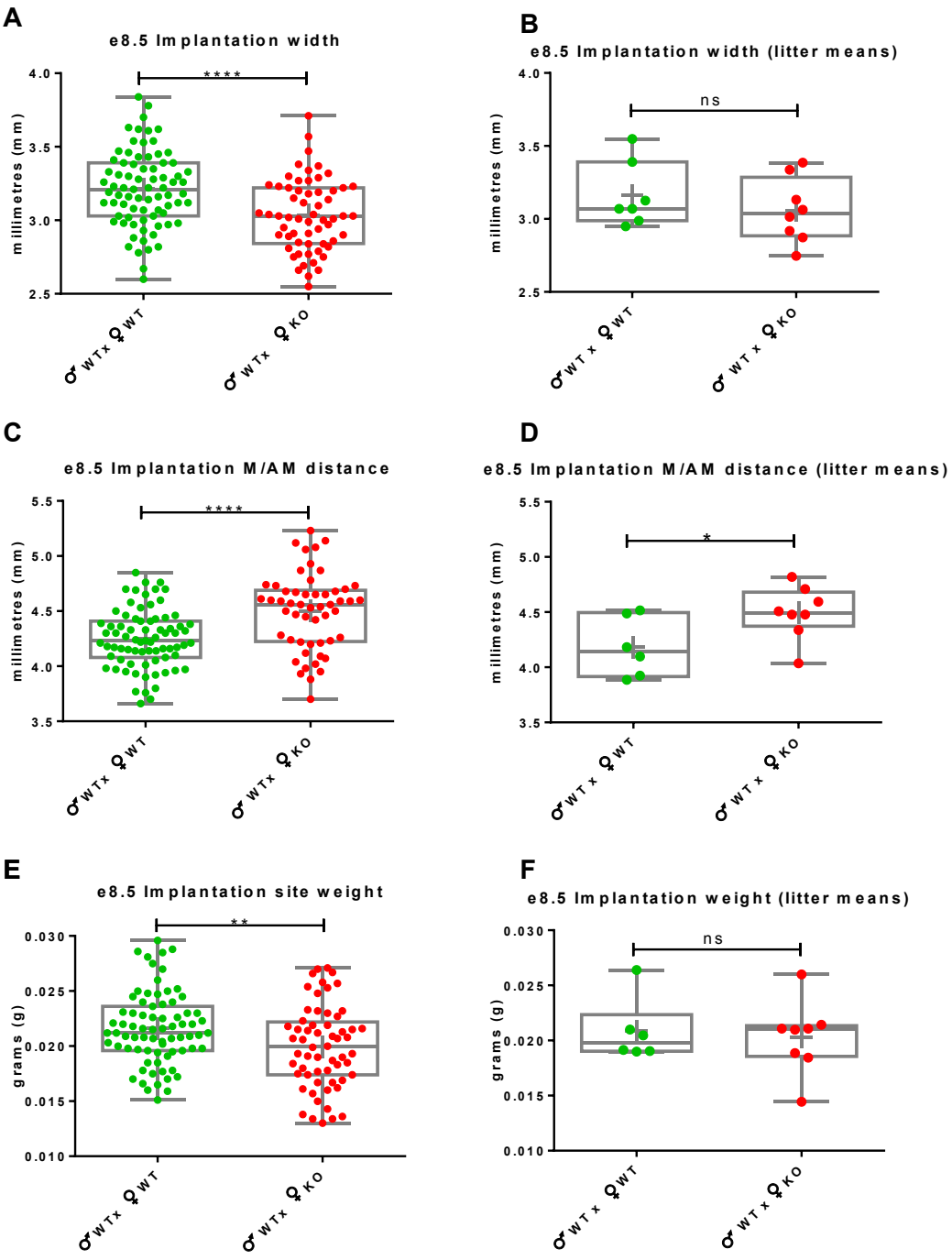
A
e8.5 Implantation width
millimetres (mm)
****
♂WT x ♀WT
♂WT x ♀KO
B
e8.5 Implantation width (litter means)
millimetres (mm)
ns
♂WT x ♀WT
♂WT x ♀KO
C
e8.5 Implantation M/AM distance
millimetres (mm)
****
♂WT x ♀WT
♂WT x ♀KO
D
e8.5 Implantation M/AM distance (litter means)
millimetres (mm)
*
♂WT x ♀WT
♂WT x ♀KO
E
e8.5 Implantation site weight
grams (g)
**
♂WT x ♀WT
♂WT x ♀KO
F
e8.5 Implantation weight (litter means)
grams (g)
ns
♂WT x ♀WT
♂WT x ♀KO
G
Mesometrial pole
WT X WT
WT X KO
Anti-mesometrial pole

Figure 5.4. Despite normal implantation numbers *Pabp4* $^{+/-}$ implantation sites from *Pabp4*$^{-/-}$ females have an altered shape and reduced weight at e8.5.

e8.5 implantation site morphometric parameters measured following 4% NBF fixation and shown as (**A, C, E**) data-points for individual implantation sites or (**B, D, F**) litter means. Morphometric parameters measured include (**A**, **B**) implantation width, (**B**) mesometrial to anti-mesometrial distance and (**C**) implantation weight. (**D**) Schematic representation of implantation sites in *Pabp4*$^{+/+}$ and *Pabp4*$^{-/-}$females. Individual implantation site data-points ♂ WT x ♀ WT (green dot) $n = 75$; ♂ WT x ♀ KO (red dot) $n = 60$. Averages per genotype within a single litter ♂ WT x ♀ WT (green dot) $n = 6$; ♂ WT x ♀ KO (red dot) $n = 7$. Data are shown as box and whisker plots with median (long line) and mean (cross) indicated. Significance was analysed by Student's t-test. ns = > 0.05; * p = ≤ 0.05; ** p = ≤ 0.01; *** p = ≤ 0.001; **** p = ≤ 0.0001.

To obtain an indication of whether trophoblast cell invasion may be impaired in the mesometrial chamber of *Pabp4*$^{-/-}$ versus *Pabp4*$^{+/+}$ females at e8.5, immunohistochemical analysis using an anti-cytokeratin 7/8 antibody was undertaken. At implantation sites cytokeratin 7/8 can be used to distinguish between maternal cells and fetal trophoblast cells and at e8.5 it reveals the ectoplacental cone (*Figure 5.5*.). Minus primary antibody controls support the specificity of this detection (data not shown). The ectoplacental cone is a derivative of the early post-implantation trophoblasts (polar trophoblasts) that continue to multiply and proliferate on the mesometrial side of the uterus, and which probably gives rise to the junctional zone of the placenta (Rossant and Cross, 2001). Cells in the ectoplacental cone act as a frontline population of cells invading the mesometrial chamber to initiate placentation (Tesser et al., 2010). No striking visual differences were apparent between the *Pabp4*$^{+/-}$ and *Pabp4*$^{+/+}$ ectoplacental cones (*Figure 5.5*) from *Pabp4*$^{-/-}$ and *Pabp4*$^{+/+}$ females respectively, although quantitative measures were not undertaken.

In summary, PABP4 expression at the time of implantation means it is feasible that the lack of maternally expressed PABP4 may result in aberrant implantation. Consistent with this idea, investigation of implantation site morphometry revealed an altered shape in *Pabp4*$^{-/-}$ females although formation of the ectoplacental cone was not notably impacted. Further quantitative measures would be necessary to determine if invasion and the thickness of the mesometrial and anti-mesometrial poles in the implantation chamber and/or size/stage of the embryo is altered as a result of an aberrant maternal response to trophoblast cues in these mice.

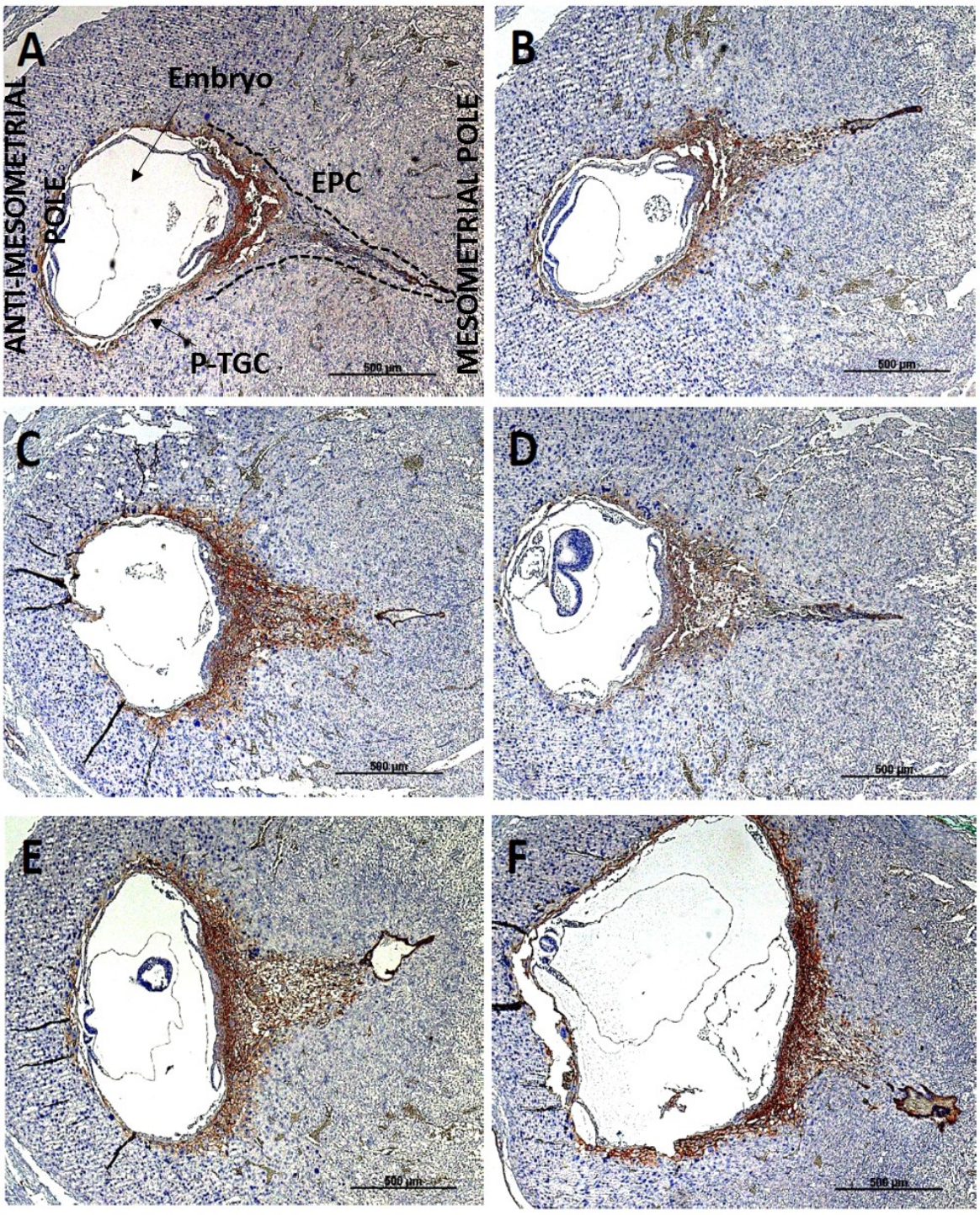

Figure 5.5. Cytokeratin7/8 expression in e8.5 implantation sites.

Sections e8.5 implantation sites immunostained for cytokeratin 7/8, which is expressed in trophoblast cells, to visualise the ectoplacental cone in implantation sites (**A, C, E**) from three different crossed of ♂*Pabp4*$^{+/+}$ x ♀*Pabp4*$^{+/+}$ and a (**B, D, F**) ♂*Pabp4*$^{-/-}$ x ♀*Pabp4*$^{-/-}$. Mesometrial pole and anti-mesometrial pole are oriented in

the same direction in all images with ectoplacental cone (EPC) and parietal trophoblast giant cells (P-TGCs) indicated (dashed lines) in (**A**). Rabbit IgG negative controls (not shown) were negative for any cytokeratin 7/8 expression.

PABP4 expression in maternal cells during implantation means that any intrinsic placental defect could have pre-placentation origins (e.g. those observed in implantations at E8.5). However, if also expressed within the maternal component of the developing/mature placenta, an intrinsic placental defect may also result from its absence at later stages of pregnancy, or a combination thereof. As described in detail in Chapter 1, the placenta is made up of several functional compartments/zones that contain different cell types namely the chorionic plate, labyrinth, junctional zone and the maternally derived decidua basalis. The decidua basalis is the outer most compartment and is the sole maternal compartment of the placenta, serving as the attachment site of the placenta to the mother, and arises from a structural and functional transformation of the endometrium in early pregnancy. It largely consists of decidual (stromal) cells and remodelled maternal vasculature which supplies oxygenated blood and nutrients to the fetus and placenta as well as removing metabolic waste from approximately e10.5. Other cell types within the decidua basalis include immune cells such as macrophages, T cells, uNK cells and fetaly derived spiral artery-associated trophoblast giant cells (SpA-TGCs) (Hu and Cross, 2010). Between the decidua basalis and the spongiotrophoblast layer sits a line of parietal trophoblast giant cells, which in early pregnancy invade the uterus by remodelling the extra-cellular matrix (Cross et al., 1994). These cells produce hormones, including prolactin-like hormones, placental lactogens and cytokines that regulate aspects of maternal physiology and paracrine factors, which regulate the feto-maternal interface (Cross et al., 1994). These cells together with spongiotrophoblast and glycogen trophoblast cells make up the junctional zone. Spongiotrophoblast cells, along with TGCs are the main endocrine cells of the placenta. As their name suggests, glycogen cells accumulate glycogen and around e16.5 these cells travel from the junctional zone to the decidua, within close vicinity of spiral arteries that supply the feto-placental unit, (Adamson et al., 2002; Georgiades et al., 2002a) and are believed to provide an energy boost in the final stage of growth prior to birth (Bouillot et al., 2006). In addition to these functions, the junctional zone has also been suggested to limit the growth of maternal blood vessels into the placenta by producing anti-angiogenic proteins such as soluble fms-like tyrosine kinase-1 (sFlt-1) and proliferin-related proteins (Adamson et al., 2002; He et al., 1999). The labyrinth zone is where hemotrophic exchange between fetal and maternal blood

occurs and is the zone of the placenta in which changes have most often been associated with IUGR (Kraus FT, 2004). It is primarily composed of two layers of multi-nucleated syncytiotrophoblast cells but also contains maternal blood canal-associated trophoblast giant cells (C-TGCs) and sinusoidal trophoblast giant cells (S-TGCs) (Hu and Cross, 2010). Finally, the chorionic plate is the result of allantois (structure from which fetal blood vessels develop and grow) and chorion (folds to form villi) fusion, called chorioallantoic attachment, at e8.5 which is the first step in labyrinth development (Rossant and Cross, 2001; Watson and Cross, 2005).

IHC was performed in mature (e18.5) *Pabp4*$^{+/+}$ placentas using PABP4 and PABP1 antibodies (Figure 5.6, Figure 5.7). Low magnification images revealed that PABP4 and PABP1 were expressed within all the functional layers (Figure 5.6 A and B). Importantly, isogenic antibody controls and the absence of PABP expression in some cell types supported the specificity of the antibodies (data not shown). Higher magnification images of the three main zones of the placenta suggested that PABP4 was most highly expressed within the junctional zone although cells lacking detectable PABP4 are also present within this layer (*Figure 5.7* A, E). It is also present in the decidua basalis, and the labyrinth zone (Figure 5.7. C, G). Within the junctional zone, PABP4 expression can be observed in parietal trophoblast giant cells and the spongiotrophoblast layer but not in glycogen trophoblast cells (*Figure 5.7* E). PABP1 showed a similar pattern of expression but was generally more widely expressed in all the different placental zones (*Figure 5.7* B, D, F, H), including the glycogen cells trophoblast cells (Figure 5.7. E). Together this data shows expression of PABP4 in the maternal, as well as fetal- derived zones of the placenta, meaning that the primary defect in *Pabp4*$^{-/-}$ mice could reside within the developing/mature placenta affecting either its structure or function.

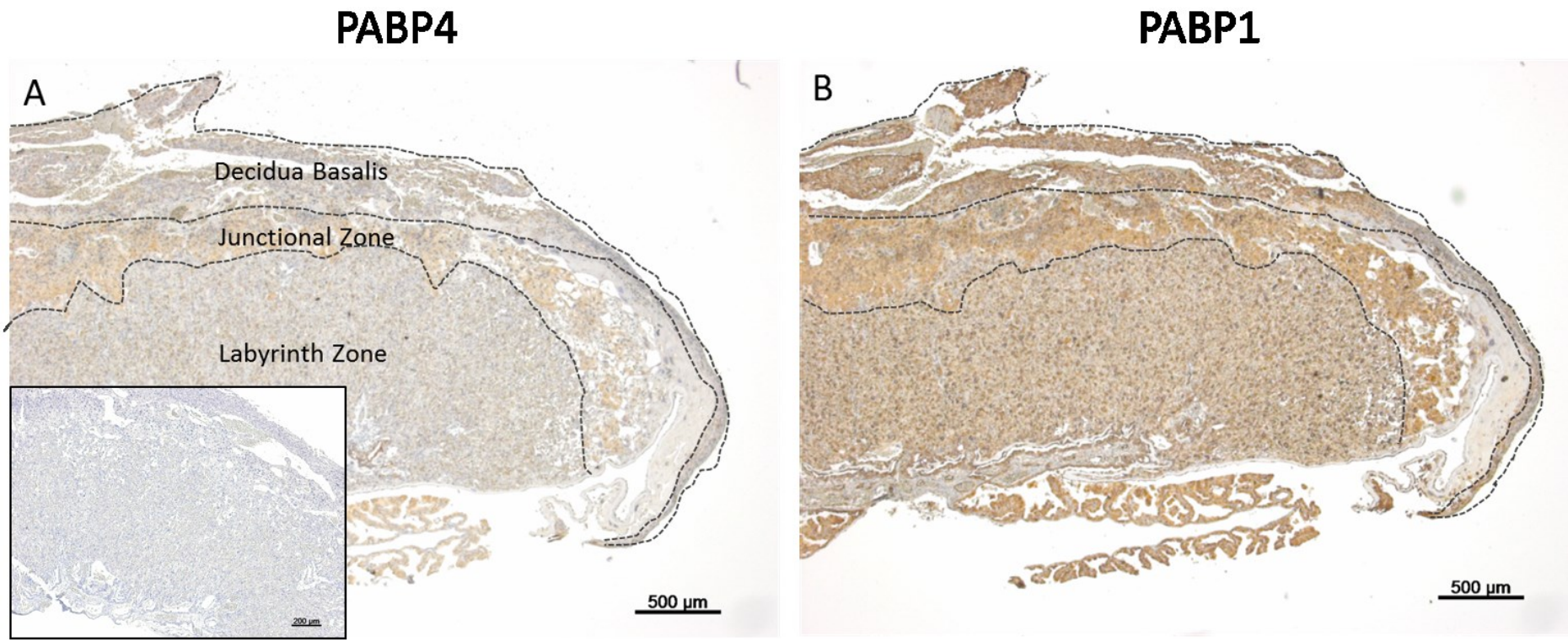

Figure 5.6. PABP4 and PABP1 expression pattern in the mature *Pabp4*$^{+/+}$ placenta.

Sections of *Pabp4*$^{+/+}$ e18.5 placenta stained by immunohistochemistry for (**A**) PABP1 and (**B**) PABP4. Dotted lines delineate the different substructures of the placenta including the decidua basalis, junctional zone labyrinth zone and the chorionic plate. Rabbit IgG control (insert in **A**). X2 magnification shown (rabbit IgG control 4X magnification is shown.

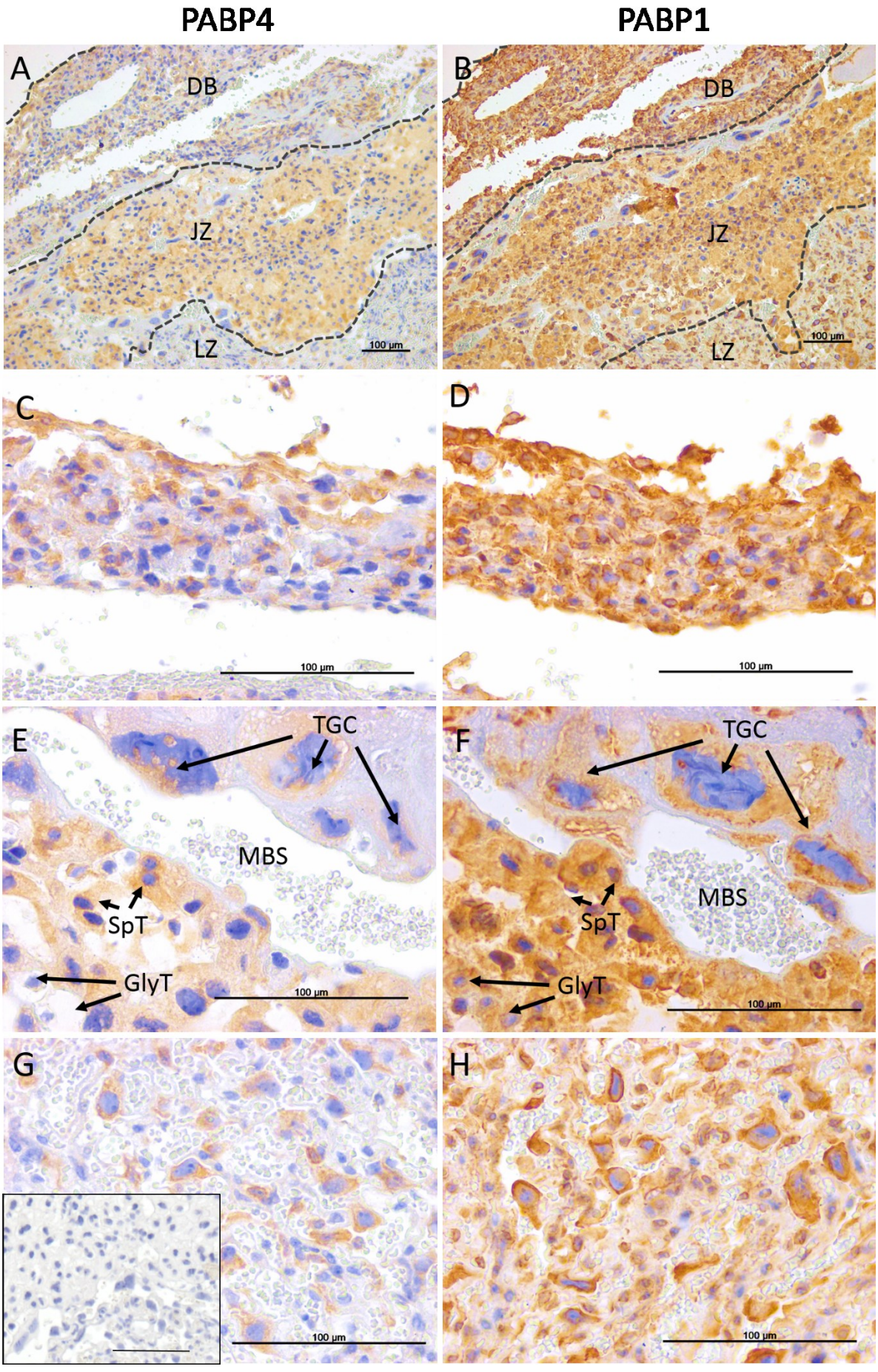
PABP4
PABP1
A
DB
JZ
LZ
100 µm
B
DB
JZ
LZ
100 µm
C
100 µm
D
100 µm
E
TGC
MBS
SpT
GlyT
100 µm
F
TGC
MBS
SpT
GlyT
100 µm
G
100 µm
H
100 µm

Figure 5.7. PABP4 and PABP1 expression in individual placental compartments of the mature *Pabp4*$^{+/+}$ placenta.

Sections of *Pabp4*$^{+/+}$ e18.5 placenta stained by immunohistochemistry for (**A, B**) PABP4 and PABP1in three main compartments of the placenta with decidua basalis (DB), junctional zone (JZ) and labyrinth zone (LZ) indicated. (**C, D**) PABP4 and PABP1 expression in the decidua basalis; (**E, F**) the junctional zone with trophoblast giant cells (TGCs), spongiotrophoblast (SpT) and glycocen trophoblast (GlyT) cells indicated and(**G, H**) the labyrinth zone. Rabbit IgG control (insert in **G**). (**A, B**) x10 magnification images, (**C, D, E, F, G, H**) x40 magnification images.

IUGR is often associated with placental insufficiency; a broad term used to describe different placental abnormalities including changes in total placenta size or that of a specific zone, placental hemodynamic changes as a result of abnormal maternal uterine artery remodelling and/or maternal decidual spiral artery remodelling and/or changes in nutrient/gas transport. Given the expression pattern of PABP4, we hypothesized that the placentas of *Pabp4*$^{-/-}$ females may present with one or more of these abnormalities, either contributing to the IUGR or as an attempt to adapt to minimise the phenotype. To explore this hypothesis, both placental morphology and function were examined. To examine placental morphology, I undertook volumetric analysis of placentas from *Pabp4*$^{-/-}$ mice in the laboratory of Prof Graham Burton at the Centre of Trophoblast Research (CTR) using stereology. Stereology is a well-established technique that can be utilised to determine three-dimensional quantities, including volumes, from two-dimensional histological sections (Coan et al., 2004). Total placental and specific compartmental volumes including that of maternal blood spaces, which transcend the junctional zone and decidua basalis, were determined for e18.5 placentas of *Pabp4*$^{-/-}$ and *Pabp4*$^{+/+}$ females crossed with *Pabp4*$^{+/+}$ males. A late (e18.5) time-point was chosen for analysis as any causal or compensatory differences in total/compartmental volumes are most likely evident by this time. From each litter, a random placenta was selected, excluding placentas of fetuses by the ovary to prevent a weight/size bias (Louton et al., 1988). Half of each selected placenta was fixed and exhaustively serial sectioned at 5 µm prior to every 20th section being stained using haematoxylin and eosin (H&E). These sections were then utilised to perform measurements using a computer assisted stereology toolbox (CAST) system as described previously (Coan et al., 2004). This revealed that the total volume of *Pabp4*$^{+/-}$ placentas from *Pabp4*$^{-/-}$ and *Pabp4*$^{+/+}$ females was equivalent (Figure 8A), consistent with the

normal placental weight and diameter (data from Chapter 4 Figure 3 is reproduced in Figure 5.8 B, C). Although the placenta achieves its maximum volume at e16.5, the relative size of its functional zones continue to change with the labyrinth expanding until term, and the junctional zone reducing in volume possibly due to decreased spongiotrophoblast proliferation and migration of glycogen cells into the maternal decidua (Coan et al., 2006). As total placental volume alone cannot inform on any differences in the volumes of individual placental zones i.e. the junctional zone, labyrinth zone and decidua basalis, additional stereological measures were taken. Importantly, the volumes of maternal blood spaces (*Figure 5.9* A) and the labyrinth zone (*Figure 5.9* B) were found to be unaltered in *Pabp4*$^{+/-}$ placentas from *Pabp4*$^{-/-}$ females in comparison to controls (*Figure 5.9* A, B). This rules out aberrant growth of maternal blood vessels into the placenta which would result in a larger volume of maternal blood spaces and a decrease in the labyrinth zone, a particularly frequent feature in IUGR that results in decreased hemotrophic exchange of nutrients (Watson and Cross, 2005), as causal in *Pabp4*$^{-/-}$ mice. Critically, the volume of the junctional zone volume was found to be significantly reduced (*Figure 5.9* C) with a corresponding increase in the volume of the decidua basalis (*Figure 5.9* D), explaining the lack of overall change in the volume of the placenta (*Figure 5.8* A). Taken together these results identify an altered placental structure as a feature of pregnancies within *Pabp4*$^{-/-}$ females (*Figure 5.9* E), in which the size of the labyrinth is maintained but reciprocal changes in the size of the junctional zone, that provides much of the endocrine function, and the maternally derived decidua are present. It is unclear if decidua volume was increased as a result of a junctional zone volume decrease or vice versa and whether these changes are a cause or an effect of the *Pabp4*$^{-/-}$ phenotype. However, given that the phenotype is dependent on maternal genotype, it is reasonable to conclude that the primary defect does not lie in the fetal-derived junctional zone but either in the decidua basalis or in another aspect of maternal physiology e.g. a reciprocal change in junctional zone size may retard its efficacy in directing maternal adaptation. It is also equally possible that a change in another aspect of maternal physiology (e.g. failure of the spleen to adapt) may be directly causative of the IUGR and the placental changes observed may be a secondary consequence/attempt to adapt to this deficiency.

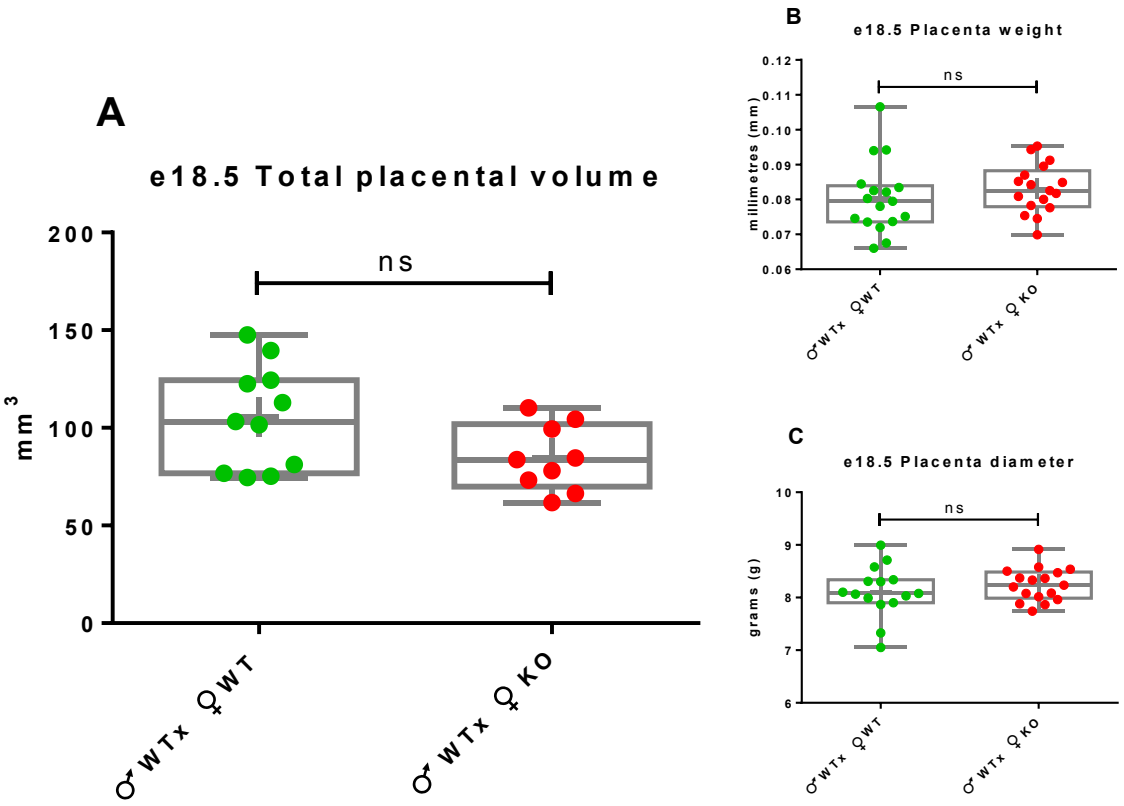

Figure 5.8. Total placental volume is unaltered in placentas from *Pabp4* $^{-/-}$ females, consistent with normal fresh placental weight and diameter.

(**A**) Total placental volume assessed by stereology in *Pabp4*$^{+/-}$ placentas from *Pabp4*$^{-/-}$ females and *Pabp4*$^{+/+}$ from Pabp4$^{+/+}$ females. (♂ WT x ♀ WT (green dot) n = 11; ♂ WT x ♀ KO (red dot) n = 9). (**B**) Weight and (**C**) diameter of freshly collected *Pabp4*$^{+/-}$ placentas from Pabp4$^{-/-}$ females and *Pabp4*$^{+/+}$ placentas from *Pabp4*$^{+/+}$ females (♂ WT x ♀ WT (green dot) n = 16; ♂ WT x ♀ KO (red dot) n = 17) – shown in previous chapter. Each data-point represents an individual placenta measurement. Data are shown as box and whisker plots with median (long line) and mean (cross) indicated. Significance was analysed by Student's t-test. ns = > 0.05.

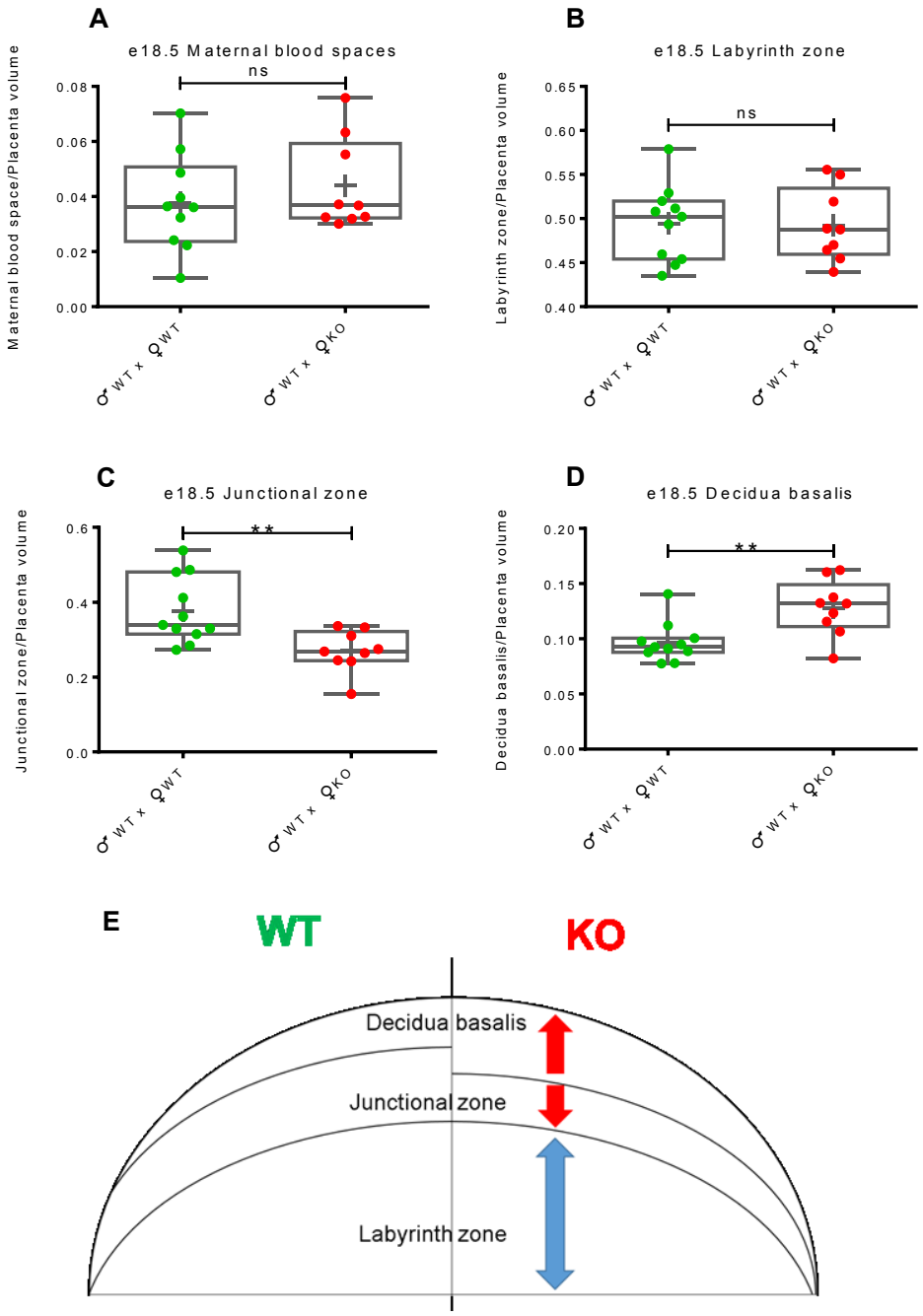

Figure 5.9. Junctional zone volume is decreased and decidua basalis volume is increased in *Pabp4*$^{+/-}$ placentas from *Pabp4* $^{+/+}$ females at e18.5.

Placental compartment volumes assessed by stereology in e18.5 placentas. *Pabp4*$^{+/-}$ placentas from *Pabp4*$^{-/-}$ dams have (**A**) normal maternal blood space and (**B**) labyrinth zone volume but (**C**) reduced junctional zone and (**D**) an increased decidua basalis volume in comparison to *Pabp4*$^{+/+}$ from *Pabp4*$^{+/+}$ females. These differences result in an altered placental sub-compartmental structure (**E**). (♂ WT x ♀ WT (green dot) n = 11; ♂ WT x ♀ KO (red dot) n = 9. Each data-point represents an individual placental measurement. Data are shown as box and whisker plots

with median (long line) and mean (cross) indicated. Significance was analysed by Student's t-test. ns = > 0.05; ** p = ≤ 0.01.

In parallel to examining effects of PABP4 deficiency on placental composition, its effects on aspects of uterine and placental function (vascular remodelling and fetal blood glucose levels), were analysed. In pregnancy the maternal cardiovascular system undergoes major adaptations in response to the developing fetus, including increased cardiac output, angiogenesis and the adaptation of existing vasculature. The remodelling of the uteroplacental vasculature from a high to low resistance and low to high flow plays a critical role in sustaining an adequate blood flow at the maternal-placental interface, thus providing the fetus with appropriate nutrients and oxygen (Small et al., 2016).

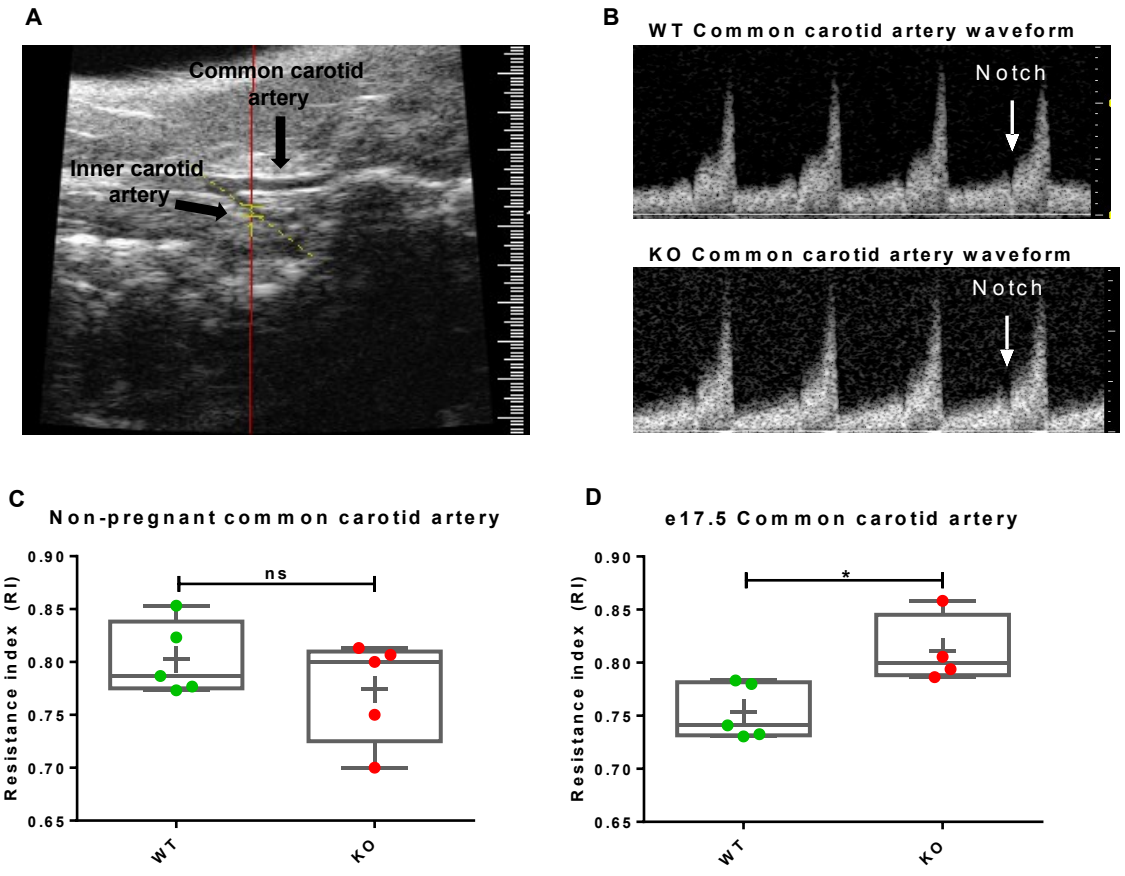

Figure 5.10. Common carotid artery resistance index is comparable in non-pregnancy between *Pabp4* $^{-/-}$ and *Pabp4* $^{+/+}$ females but is increased in *Pabp4* $^{-/-}$ females at e17.5 of gestation.

Doppler flow velocity waveforms obtained for the common carotid artery in non-pregnancy and at e17.5 of gestation for *Pabp4*$^{+/+}$ (WT; green dot) and *Pabp4*$^{-/-}$ (KO; red dot) females. (**A**) Location of common carotid artery visualised using ultrasound, common carotid artery and inner carotid artery are indicated. (**B**) Representative common carotid artery velocity waveforms of WT and KO females. Resistance index was calculated from velocity waveforms in (**C**) non-pregnant females (♀ WT (green dot) n = 5; ♀ KO (red dot) n = 5) and (**D**) in pregnant females at day e17.5 of gestation (♀ WT (green dot) n = 5; ♀ KO (red dot) n = 4). Each data-point represents an individual common carotid artery. Data are shown as box and whisker plots with median (long line) and mean (cross) indicated. Significance was analysed by Student's t-test. ns = > 0.05; *p = ≤ 0.05.

Deficiencies of the maternal uterine vasculature which become clinically evident in the last half of gestation are associated with pregnancy complications including IUGR (Todros et al., 1999). Therefore, we sought to examine the functional characteristics of uteroplacental blood flow in *Pabp4*$^{-/-}$ and *Pabp4*$^{+/+}$ females by taking Doppler measurements of the uterine artery and umbilical artery and calculating their resistance index (RI), which are commonly used in the clinic to determine placental insufficiency and the risk/presence of IUGR. The measurements of the umbilical artery reflects the vascular resistance on the fetal side whereas uterine artery measurements inform about the resistance on the maternal side but both are used in the clinic to assess the risk of IUGR.

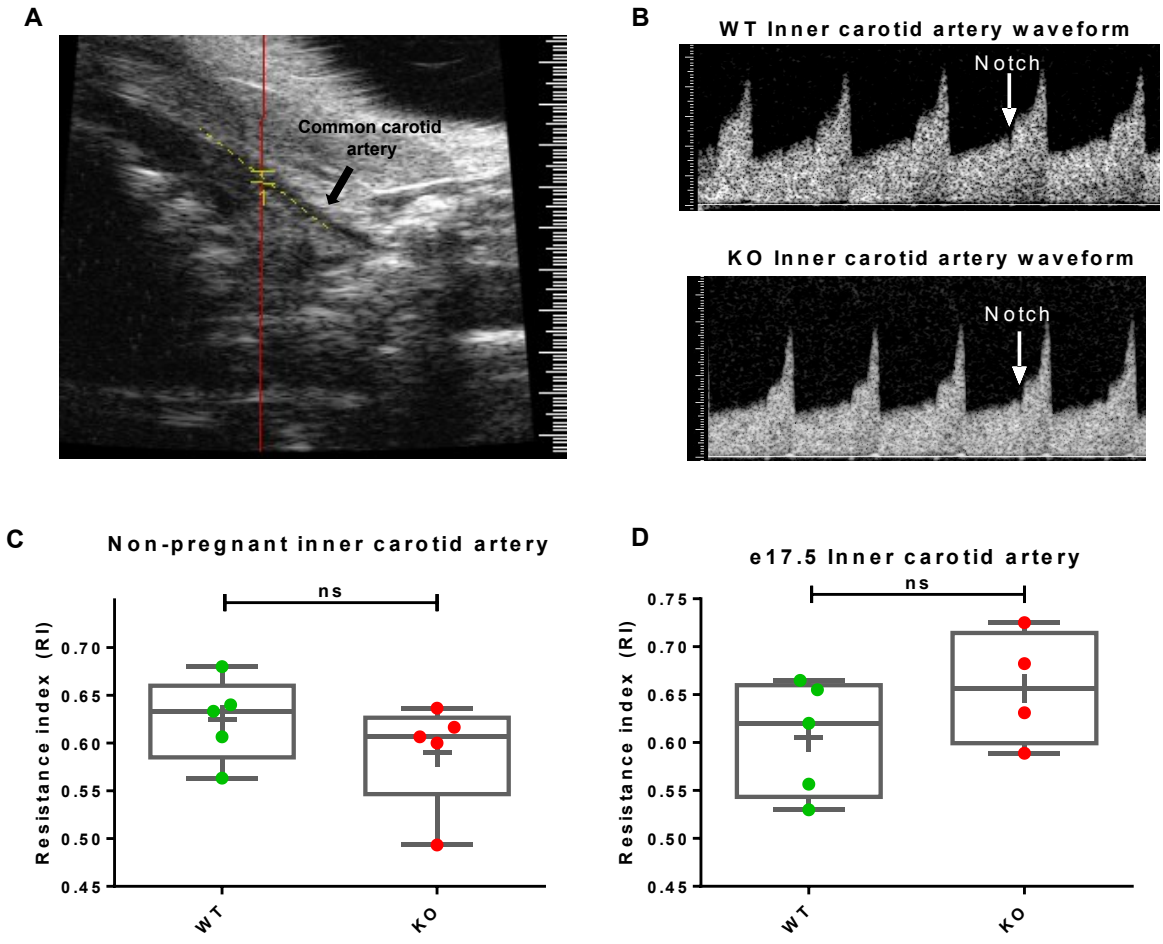

Figure 5.11. Inner carotid artery resistance index is comparable in non-pregnancy and at e17.5 between *Pabp4*$^{-/-}$ and *Pabp4*$^{+/+}$ females.

Doppler flow velocity waveforms obtained for the inner carotid artery in non-pregnancy and at e17.5 of gestation for *Pabp4*$^{+/+}$ (WT; green dot) and *Pabp4*$^{-/-}$ (KO; red dot) females. (**A**) Location of inner carotid artery visualised using ultrasound with inner carotid artery indicated. (**B**) Representative non-pregnant inner carotid artery velocity waveforms of WT and KO females. Resistance index was calculated from velocity waveforms in (**C**) non-pregnant females (♀ WT (green dot) n = 5; ♀ KO (red dot) n = 5) and (**D**) in pregnant females at day e17.5 of gestation (♀ WT (green dot) n = 5; ♀ KO (red dot) n = 4). Each data-point represents an individual inner carotid artery. Data are shown as box and whisker plots with median (long line) and mean (cross) indicated. Significance was analysed by Student's t-test. ns = > 0.05; *p = ≤ 0.05.

RI is a measure of pulsatile blood flow that reflects the resistance to blood flow caused by microvascular beds which are distal to the site of measurement and is calculated with the formula: RI = ([peak systolic velocity – end diastolic velocity] / peak systolic velocity). The

functional properties of the uterine artery can also be evaluated by examining the characteristics of the Doppler waveform, specifically whether there is 'notching'. Notching is a phenomenon where a 'notch' (indicated by white arrow in *Figure 5.10* B, *Figure 5.11*B) is present in the descending waveform in early diastole. The highest risk pregnancies present with severe notching and an abnormal resistance index. However, problems with uterine artery remodelling can present as mild notching with the absence of an abnormal resistance index, due to normal blood flow at the end of diastole, which still increases the risk of an adverse fetal outcome. Thus, it is important to evaluate both parameters.

Interestingly, arterial remodelling in pregnancy is not the same across the whole arterial tree and the carotid artery stiffens independently of other arterial beds (Visontai et al., 2002) with a decline in its elasticity towards the end of pregnancy (Karkkainen et al., 2014). This stiffening is functionally distinct from the remodelling of maternal arteries, with the notching characteristic of "normal" arteries being retained in the inner and common carotid artery in mice (Visontai et al., 2002), allowing them to serve as internal controls for the extensive changes in uterine and umbilical arteries. Therefore, Doppler measurements of the inner and common carotid artery (CCA) were also determined to assess their haemodynamic properties. Carotid artery RI was measured in non-pregnant and pregnant females, at e17.5, as opposed to e18.5, as pilot studies showed that the slightly smaller size of the fetuses at this time-point made it marginally easier to take uterine artery Doppler measurements as the uterine artery was more accessible and easier to find. The changes in remodelling at e17.5 should be reflective of those at e18.5.

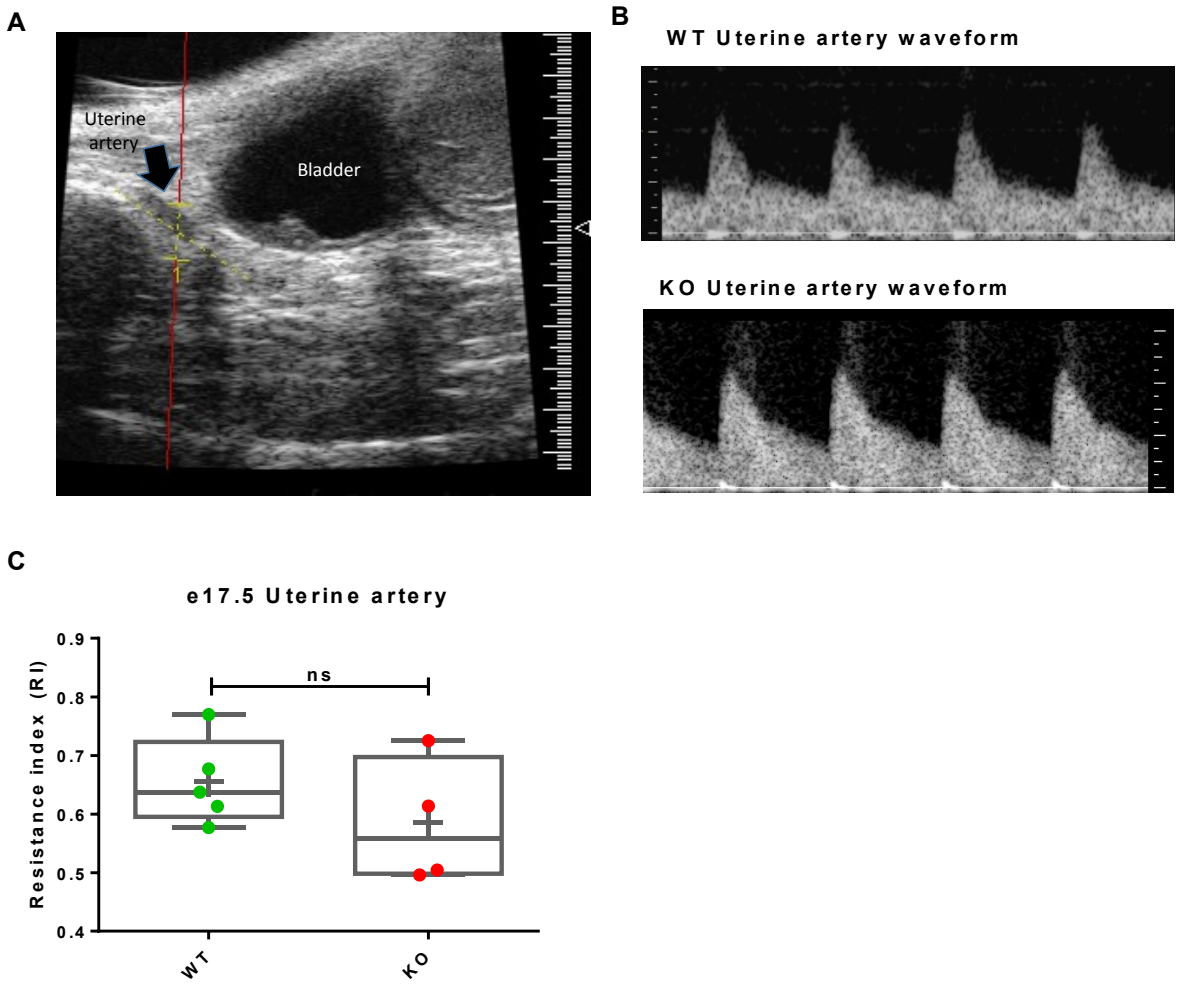

Figure 5.12. Uterine artery resistance index is comparable at e17.5 between *Pabp4*$^{-/-}$ and *Pabp4*$^{+/+}$ females.

Doppler flow velocity waveforms obtained for the uterine artery at e17.5 of gestation for *Pabp4*$^{+/+}$ (WT; green dot) and *Pabp4*$^{-/-}$ (KO; red dot) females. (**A**) Location of uterine artery visualised using ultrasound with bladder and uterine artery indicated. (**B**) Representative uterine velocity waveforms of WT and KO females. Resistance index was calculated from velocity waveforms in (**C**) in pregnant females at day e17.5 of gestation (♀ WT (green dot) n = 5; ♀ KO (red dot) n = 4). Each data-point represents an individual uterine artery. Data are shown as box and whisker plots with median (long line) and mean (cross) indicated. Significance was analysed by Student's t-test. ns = > 0.05; *p = ≤ 0.05.

This revealed that the common carotid artery RI was comparable in non-pregnant *Pabp4*$^{-/-}$ and *Pabp4*$^{+/+}$ females (*Figure 5.10*) but at e17.5 of pregnancy, despite having a similar notched waveform (Figure 5.10. B), it was significantly increased in *Pabp4*$^{-/-}$ females (*Figure 5.10*). In contrast, the RI of the inner carotid artery was the same in non-pregnant and e17.5 pregnant *Pabp4*$^{-/-}$ and *Pabp4*$^{+/+}$ females (Figure 5.11. B, C, D), with similar waveforms. It remains to be determined whether *Pabp4*$^{-/-}$ females have arterial stiffness in the CCA.

Importantly, uterine artery RI at e17.5 (Figure 5.12. B, C) was found to be unaltered between the genotypes and no notching was observed in the waveforms of uterine arteries in *Pabp4*$^{+/+}$ *or Pabp4*$^{-/-}$ dams which suggests that uterine artery remodelling preceded normally. Similarly, the umbilical arteries (*Figure 5.13* B, C) of Pabp4+/+ and Pabp4-/- mice showed equivalent RI and absence of notching indicative of the vascular resistance being normal on the fetal side. Taken together these data indicate that deficient vascular remodelling of these vessels is not the causal factor of the IUGR present in *Pabp4*$^{-/-}$ dams

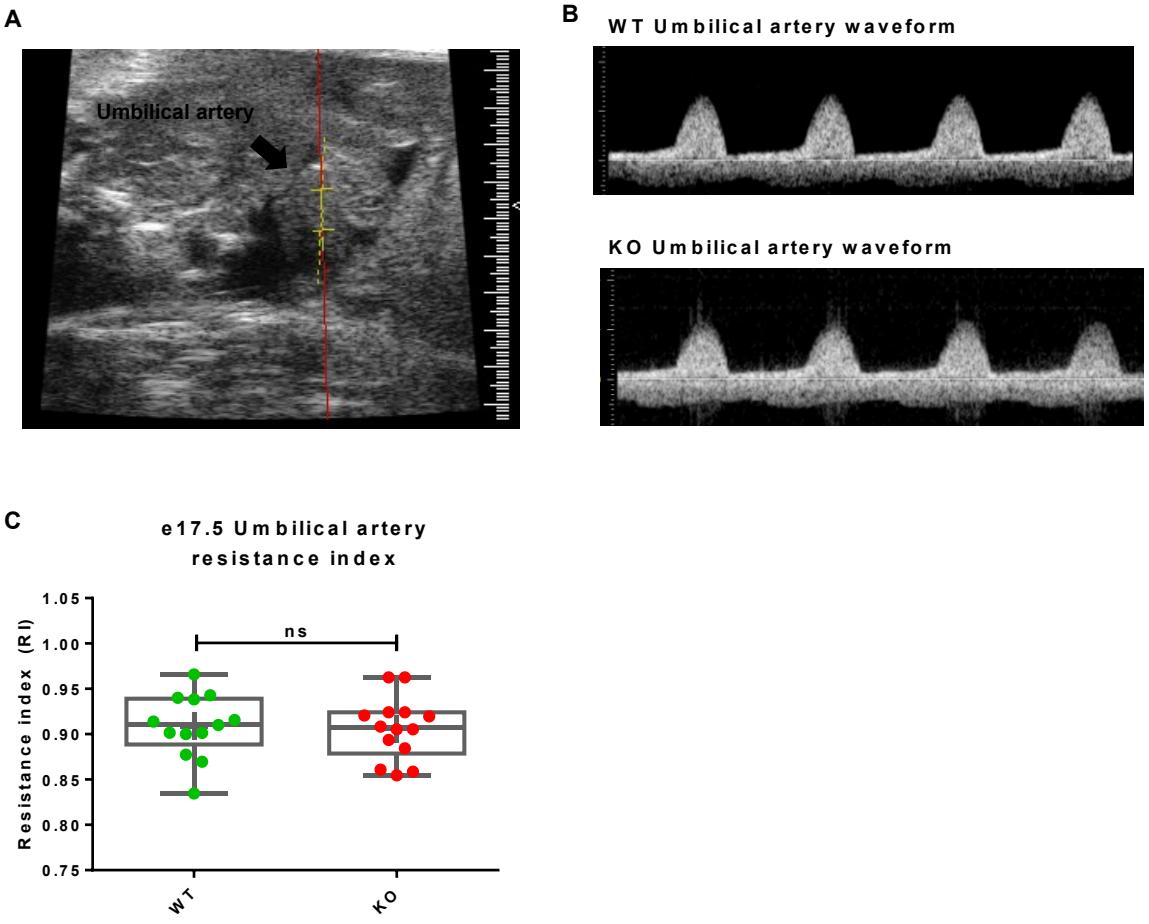

Figure 5.13 Umbilical artery resistance index is comparable in fetuses of *Pabp4*$^{-/-}$ and *Pabp4*$^{+/+}$ females.

Doppler flow velocity waveforms obtained for the umbilical artery at e17.5 of gestation for *Pabp4*$^{+/+}$ (WT; green dot) and *Pabp4*$^{-/-}$ (KO; red dot) females. (**A**) Location of uterine artery visualised using ultrasound with umbilical artery indicated. (**B**) Representative uterine velocity waveforms of WT and KO females. Resistance index was calculated from velocity waveforms in (**C**) in pregnant fetuses at day e17.5 of gestation (♀ WT (green dot) n = 13; ♀ KO (red dot) n = 14). Each data-point represents an individual umbilical artery. Data are shown as box and whisker plots with median (long line) and mean (cross) indicated. Significance was analysed by Student's t-test. ns = > 0.05; *p = ≤ 0.05.

Having gathered evidence that the uterine artery appears to be appropriately remodelled, the remodelling of spiral arteries (SpA) was investigated. SpA lie within the decidua and are remodelled between e8.5 and e12.5 (reviewed by (Zhang et al., 2011) independently of the uterine artery. This involves the action of interferon-γ derived from maternal uterine natural killer cells (Ashkar et al, 1999; Ashkar et al, 2000; Ashkar et al, 2001). Interestingly, the volume of the decidua of *Pabp4*$^{-/-}$ dams was shown to be significantly increased (*Figure 5.9*), although this may not be associated with abnormal SpA remodelling. SpA remodelling can be assessed qualitatively by the absence of smooth muscle actin (SMA) and presence of trophoblast cells, using SMA and cytokeratin 7/8 markers in IHC, respectively. SMA is normally present in endothelial cells which are replaced in the vascular media by trophoblast cells during remodelling (Adamson et al., 2002). Remodelling was assessed at day e13.5, when the maternal vasculature should be remodelled and at day e18.5 when the IUGR phenotype is well established but preceding the major onset of fetal death (*Figure 5.14*). SMA was largely absent in SpA of *Pabp4*$^{+/+}$ females at e13.5, and e18.5, as expected (Figure 5.14 A, B) and importantly was also largely absent in *Pabp4*$^{-/-}$ females (*Figure 5.14* D and E). Appropriate remodelling of the SpA was confirmed by the presence of trophoblast cells lining the arteries (*Figure 5.14* C, F) providing evidence that transition of SpA also occurs normally. Appropriate remodelling of both the uterine arteries, assessed by Doppler ultrasound, and spiral arteries, assessed by IHC, as well as the presence of normal umbilical artery haemodynamics are in line with symmetrical IUGR that is observed in *Pabp4*$^{-/-}$ females as the poor uteroplacental blood flow is generally considered to result in asymmetrical IUGR. This has been experimentally demonstrated by interventions such as uterine artery ligation and occlusion which both result in brain sparing and asymmetrical IUGR (Tanaka et al., 1994; Wigglesworth, 1974).

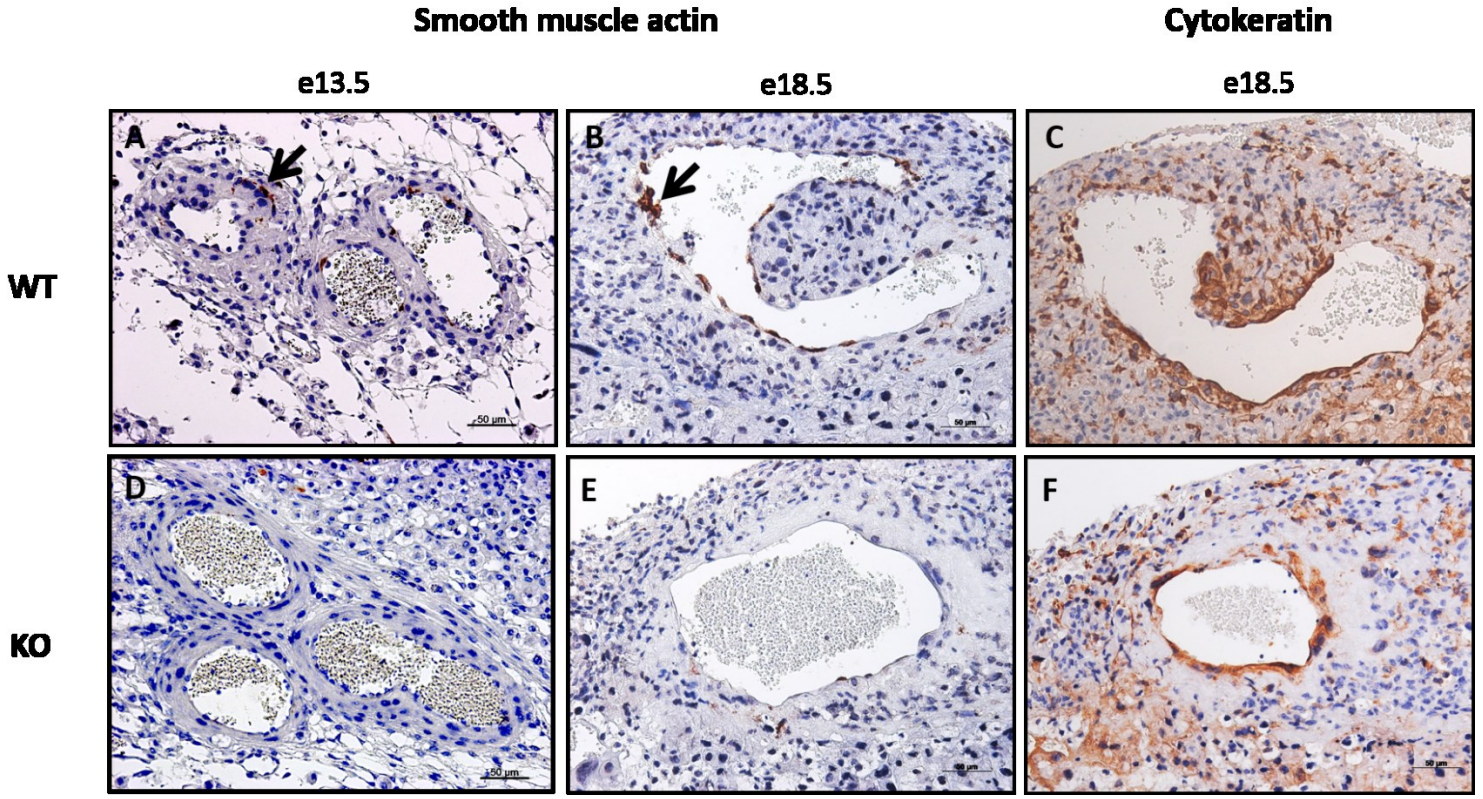

Figure 5.14. Spiral artery remodelling appears to be normal in *Pabp4*$^{-/-}$ females.

Representative images of decidua of 3 different *Pabp4*$^{-/-}$ females (D-F) and *Pabp4*$^{+/+}$ (A-C) females which were visually analysed at the midsagittal plane, a vertical plane through the midline of the decidua, following serial sectioning of 5 µm and immunostaining of one section every approximately every 30 µm, as indicated.

The previous data suggest that sufficient blood flow is delivered to and across the placenta, but does not inform on its capacity to transport nutrients across the materno-fetal interface, which are necessary for supporting growth, especially later in pregnancy where the majority of fetal growth occurs. Thus the delivery of nutrients was investigated, by measuring fetal blood glucose levels. Fetal blood glucose measurements were collected from non-fasted dams, therefore read-outs were subject to dam food-intake although the impact of this variable was minimised by collections being done at the same time of the day (around 2pm when females are resting and not feeding). The measurements revealed that at e15.5, *Pabp4*$^{+/-}$ fetuses from *Pabp4*$^{-/-}$ females have significantly lower blood glucose levels compared to those from wild-type or reciprocal crosses, the latter also producing *Pabp4*$^{+/-}$ fetuses (*Figure 5.15* A, B). Importantly, non-fasted maternal blood glucose levels were unchanged in *Pabp4*$^{-/-}$ females at e15.5 and e18.5, suggesting that maternal glucose homeostasis is normal (*Figure 5.16* A, B), and therefore that the reduced fetal glucose levels may not simply reflect less glucose reaching the placenta via the maternal circulation. Therefore, this result could be indicative of a placental nutrient transport deficiency in *Pabp4*$^{-/-}$ females, which may be reflected in, or due to, reduced glucose transporter mRNA levels. Therefore the mRNA levels of placental glucose transporters, *Glut-1* (*Slc2a1)* and *Glut-3*(*Slc2a3*), were examined at e15.5 and e18.5. No significant difference was seen in their mRNA levels at e15.5 (*Figure 5.17*), however, both were significantly upregulated in placentas from *Pabp4*$^{-/-}$ females at e18.5 (*Figure 5.18*). Taken together, these results suggest that the reduced fetal glucose is not due to decreased levels of *Glut-1*and *Glut-3* mRNAs. The upregulation of these mRNAs at e18.5 may reflect a compensatory mechanism in response to continuing low fetal glucose levels that is not sufficient to rescue levels of fetal blood glucose. Reciprocal crosses to examine glucose transporter mRNA levels remain to be completed for e18.5.

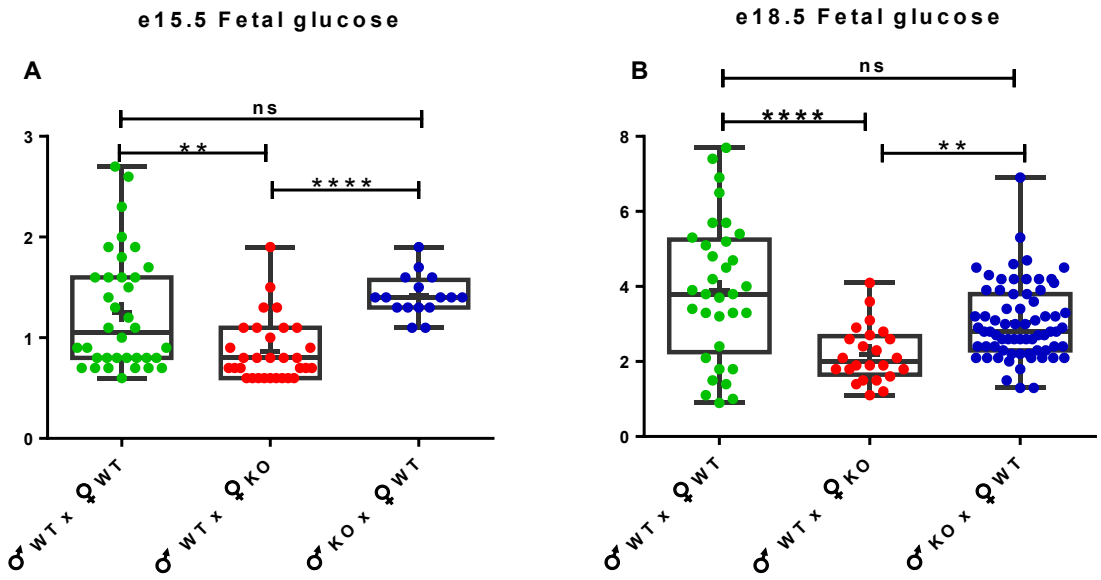

Figure 5.15. Fetal blood glucose is significantly decreased in Pabp4$^{+/-}$fetuses from *Pabp4*$^{-/-}$ females in comparison to both *Pabp4*$^{+/-}$ and *Pabp4*$^{+/+}$ fetuses from *Pabp4*$^{+/+}$ females at e15.5 and e18.5.

Non-fasted fetal blood glucose measured using a blood glucose meter at (**A**) e15.5. (♂ WT x ♀ WT (green dot) n = 36; ♂ WT x ♀ KO (red dot) n = 31; ♂ KO x ♀ WT (blue dot) n = 10) and (**B**) e18.5 of gestation (♂ WT x ♀ WT (green dot) n = 33; ♂ WT x ♀ KO (red dot) n = 24; ♂ KO x ♀ WT (blue dot) n = 69). Each symbol corresponds to an individual fetal measurement. Data are shown as box and whisker plots with median (long line) and mean (cross) indicated. Significance was analysed by Kruskal-Wallis test and Dunn's multiple comparison test.. ns = > 0.05; ** p = ≤ 0.01; *** p = ≤ 0.001; **** p = ≤ 0.0001.

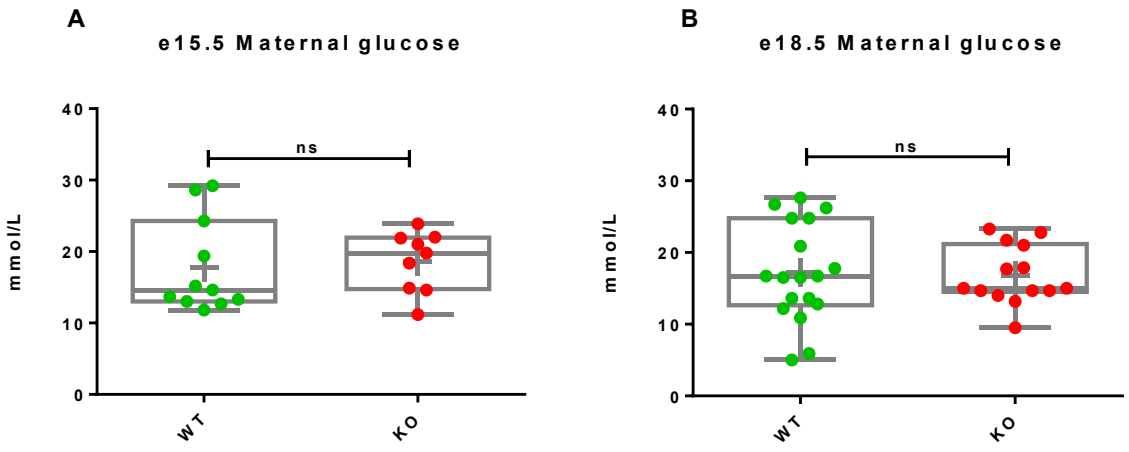

Figure 5.16. Maternal blood glucose is comparable in *Pabp4*$^{-/-}$ and *Pabp4*$^{+/+}$ females at e18.5.

Non-fasted maternal blood glucose measured using a blood glucose meter at (**A**) e15.5 (♀ WT (green dot) n = 11 ; ♀ KO (red dot) n = 9) and (**B**) e18.5 of gestation (♀ WT (green dot) n = 18; ♀ KO (red dot) n = 14). Each symbol corresponds to an individual maternal measurement. Data are shown as box and whisker plots with median (long line) and mean (cross) indicated. Significance was analysed by Student's t-test. ns = > 0.05; ** p = ≤ 0.01; *** p = ≤ 0.001; **** p = ≤ 0.0001.

Given this result, it was also of interest to examine the mRNA levels of other placental nutrient transporters. Thus the levels of three isoforms of system A placental amino acid transporters *Snat-1 (Slc38a1), Snat 2 (Slc38a2)* and *Snat-4 (Slc38a4),* were examined. These were chosen as data suggests they dysregulated in genetic and dietary models of IUGR (Constancia et al., 2002; Jansson et al., 2006; Kusinski et al., 2012; Malandro et al., 1996; Stanley, 2012). Amino acid transporter *Snat-2* mRNA levels were unaltered in *Pabp4* $^{+/-}$ placentas from *Pabp4*$^{+/+}$ and *Pabp4*$^{-/-}$ females in comparison to *Pabp4*$^{+/+}$ placentas from *Pabp4*$^{+/+}$ females at e15.5 (Figure 5.19). At e18.5 *Snat-2* mRNA levels were statistically higher in *Pabp4* $^{+/-}$ placentas from *Pabp4*$^{-/-}$ females in comparison to *Pabp4*$^{+/+}$ placentas whilst *Snat-1* and *Snat-4* remained unaltered (Figure *5.20*). Equivalent amino acid transporter mRNA levels in *Pabp4*$^{-/-}$ females in comparison to control at e15.5 with a subsequent increase in *Snat-2* mRNA levels at e18.5 may be indicative of a compensatory mechanism for abnormal amino acid levels or transport. However, reciprocal crosses to rule out a fetal genotype effect at e18.5 remain to be completed. Although the expression levels of the *Glut* and *Snat* genes was normalised to the expression of

the most stable housekeeping gene out of two ideally they should be normalised to at least two housekeeping genes as the use of only one may lead to relatively large errors.

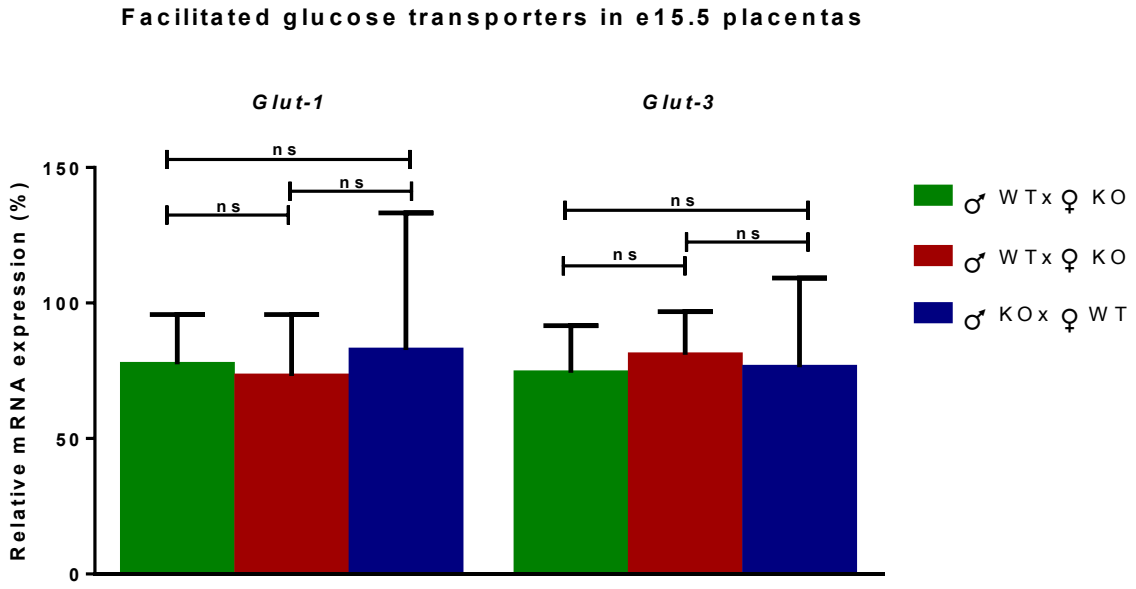

Figure 5.17 The expression of facilitated glucose transporter marker genes is unaltered in *Pabp4*$^{+/-}$ placentas, regardless of parental genotype, and in *Pabp4*$^{+/+}$ controls.

qRT-PCR for facilitated glucose transporters in e15.5 placentas. Each expression value was been normalised to the expression value of *Sdha*, the most stable housekeeping gene out of two determined using SLqPCR package in R. (♂ WT x ♀ WT (green bar) n = 6; ♂ WT x ♀ KO (red bar) n = 6; ♂ KO x ♀ WT (blue bar) n = 5). Significance was analysed by Kruskal-Wallis test and Dunn's multiple comparison test.. ns = > 0.05.

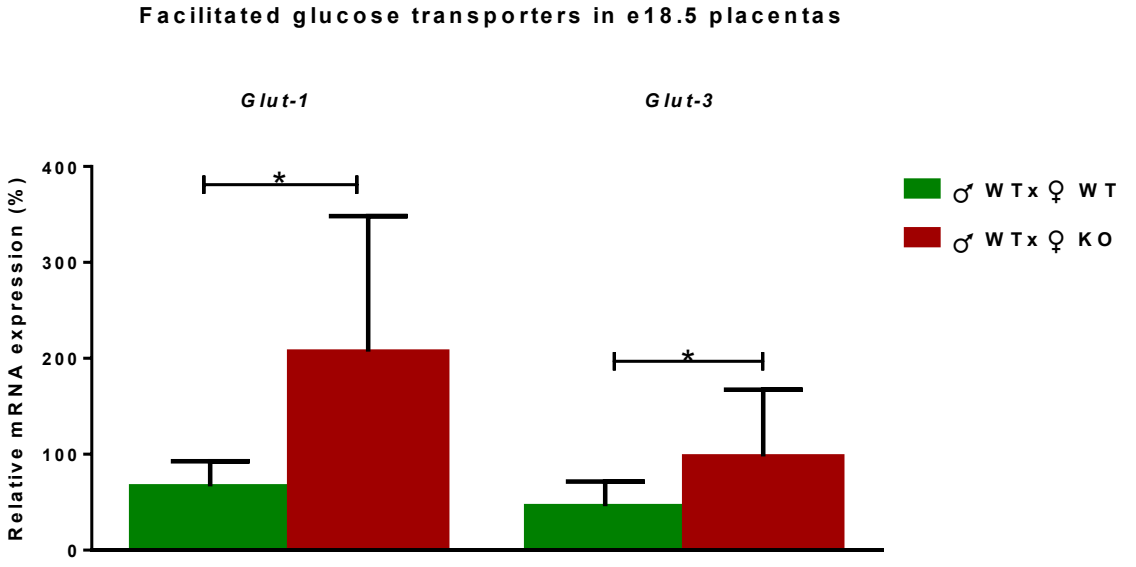

Figure 5.18 Facilitated glucose transporters, Glut-1 and Glut-3, are up-regulated in *Pabp4*$^{+/-}$ placentas from *Pabp4*$^{+/+}$ females at e18.5.

qRT-PCR for facilitated glucose transporters in e18.5 placentas. Each expression value was been normalised to the expression value of *Sdha*, the most stable housekeeping gene out of two determined using SLqPCR package in R. (♂ WT x ♀ WT (green bar) n = 11; ♂ WT x ♀ KO (red bar) n = 9). Significance was analysed by Student's t-test. * p = ≤ 0.05.

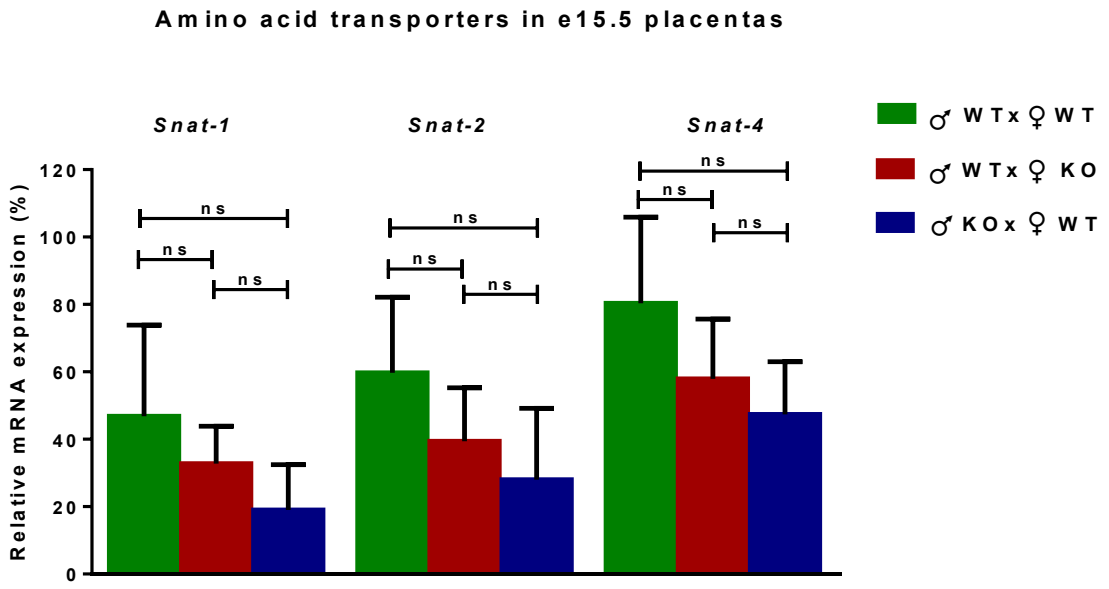

Figure 5.19 The expression of amino acid transporter reporter gene, Snat-2, is downregulated in *Pabp4*$^{+/-}$ placentas from *Pabp4*$^{+/+}$ females.

qRT-PCR for amino acid transporters in e15.5 placentas. Each expression value was been normalised to the expression value of *Sdha*, the most stable housekeeping gene out of two determined using SLqPCR package in R. (♂ WT x ♀ WT (green bar) n = 6; ♂ WT x ♀ KO (red bar) n = 6 ; ♂ KO x ♀ WT (blue bar) n = 5). Significance was analysed by Kruskal-Wallis and Dunn's multiple comparison test. ns = > 0.05; * p = ≤ 0.05.

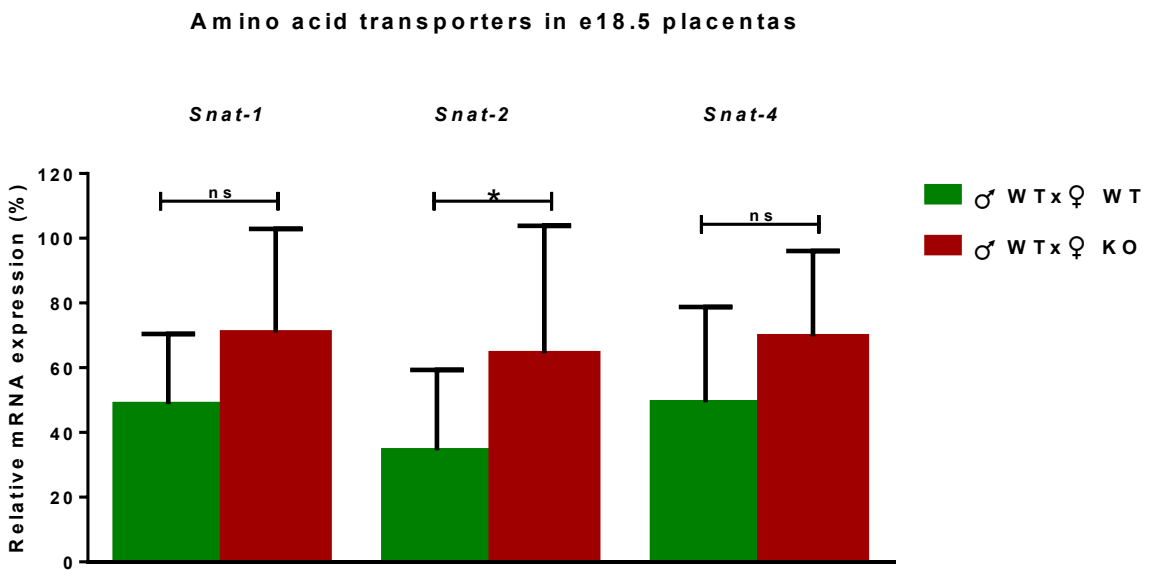

Figure 5.20 Amino acid transporter, Snat-2, is up-regulated in *Pabp4*$^{+/-}$ placentas from *Pabp4*$^{+/+}$ females at e18.5.

qRT-PCR for amino acid transporters in e18.5 placentas. Each expression value was been normalised to the expression value of *Sdha*, the most stable housekeeping gene out of two determined using SLqPCR package in R. (♂ WT x ♀ WT (green bar) n = 11; ♂ WT x ♀ KO (red bar) n = 9). Significance was analysed by Student's t-test. ns = > 0.05; * p = ≤ 0.05.

5.3 Discussion

In the previous chapter, I demonstrated that *Pabp4*$^{-/-}$ mice present with a maternal genotype-dependent reduction in the F:P ratio. One explanation for this may be placental insufficiency and therefore the aim of this chapter was to test the hypothesis that placental development at the feto-maternal interface and/or placental structure and/or function is altered in *Pabp4*$^{-/-}$ dams. PABP4 and PABP1 expression at the feto-maternal interface had not previously been investigated and it was not known which cell types, and their cognate functions, may be impacted by the deletion of *Pabp4*. Interestingly, investigation in e5.5 implantation sites revealed that PABP4 expression is present in the endometrial glandular epithelium and non-decidualised stromal fibroblasts surrounding the primary decidual zones, in which PABP4 is largely absent (*Figure 5.2* A). PABP1 showed more widespread expression including weak staining in the decidual zone (*Figure 5.2* B). It may therefore be hypothesised that PABP1 may be more important for decidualisation. However, PABP4 is absent in the stromal cells prior to conception (*Figure 5.1* A.), making it tempting to speculate that its burst of expression in the non-decidualised stromal fibroblasts surrounding the primary decidual zone may play some role in their morphologic, metabolic, and secretory changes that mark the transition to decidual cells and which allow for proper embryo implantation (Abrahamsohn and Zorn, 1993). Future expression studies at earlier stages will be needed to determine when the burst of PABP4 is initiated. Delineating the timing of onset of PABP4 expression provide some insight into the signal that induces stromal cell PABP4 expression and may inform on any potential role in decidualisation. However, PABP4 is also expressed in the endometrial uterine glands which are also important for implantation and decidualization as they secrete factors that support the early stages of pregnancy including amino acids, glucose and lipids and importantly LIF which is critical for blastocyst attachment and implantation (Filant and Spencer, 2013; Paiva et al., 2009). The importance of the glandular epithelium is shown by studies in which deletion of centromere protein B (*Cenpb*) induces abnormal uterine and glandular epithelium, resulting in age-dependent reproductive deterioration with females unable to produce more than one litter (Fowler et al., 2000).

At e8.5 PABP4 and PABP1 show very similar patterns of expression (Figure 5.3) and are primarily found in the ectoplacental cone and mesometrial decidua basalis, which is infiltrated

by a high number of macrophages and lymphocytes, primarily uNK cells.. Additionally, both PABP1 and PABP4 are expressed in non-decidualised stromal fibroblasts found outside of the secondary decidual zone at the anti-mesometrial pole (Figure 5.3 A, B). The ectoplacental cone is the result of continued proliferation of the polar extraembryonic ectoderm, is the first sign of placental development and contains precursors of the spongiotrophoblast cells and secondary TGCs (Bevilacqua, 2014). The anti-mesometrial and mesometrial endometrium are two distinct anatomical regions of the pregnant mouse uterus which exhibit differing biology and physiology. Decidualisation initially occurs at e4.5 anti-mesometrially proximal to the implanting embryo resulting in a clear distinction between the implantation sites from inter-implantation regions. Decidualisation then spreads to the mesometrial endometrium and continues to expand towards the myometrium, however, a region of non-decidualised cells is preserved throughout gestation near the myometrium, where PABP1 and PABP4 are highly expressed, in contrast to decidualised cells (Figure 5.3). At e8.5 the majority of the mesometrial decidua facing the myometrium has not yet decidualised but is highly infiltrated by $CD45^{+}$ leukocytes (Yamada, 2014). The mesometrial decidua is also the site of trophoblast invasion, maternal vascular remodelling and placental development. These raise the possibility that the knockout of *Pabp4* could directly impact the processes associated with the mesometrial endometrium such as trophoblast invasion, maternal vascular remodelling and placental development.

Multiplex detection of PABP4 and/or PABP1 with specific leukocyte markers will be needed to establish which of these are expressing one or both PABPs. However, mouse models where these leukocytes are compromised or completely absent (Croy et al., 1997) (Guimond et al., 1999; Guimond et al., 1997), would predict abnormal vascular remodelling, poor mesometrial decidual development and small placentas if their function was affected by loss of PABP4. Currently we have no evidence of any of these phenotypic characteristics since spiral arteries appear to be adequately remodelled in $Pabp4^{-/-}$ dams, as indicated by the absence of smooth muscle actin (Figure 5.14), placentas are an equivalent size to that of $Pabp4^{+/+}$ dams.

Whilst our data argue that PABP4 does not appear to be absolutely essential for decidualisation, or can be compensated for by PABP1 (see below), enabling implantation, this process may be less overtly compromised by its absence leading to downstream consequences that ultimately manifest in the observed phenotypes. Markers can be used to investigate the decidualisation process include desmin (Glasser and Julian, 1986), alkaline phosphatase (ALP) (Finn and

Hinchliffe, 1964), decidual prolactin-related protein (dPRP) (Candeloro and Zorn, 2007) and bone morphogenetic protein 2 (BMP2) (Lee et al., 2007) in *Pabp4*$^{-/-}$ mice. If appropriate, induced decidualisation can also be studied in pseudopregnant *Pabp4*$^{-/-}$ mice, for example, using blastocyst-sized Sepharose beads (Concanavalin A-coated) which in contrast to an intraluminal oil injection or scratch only induces "focal decidualisation" instead of the whole uterine horn (Bany, 2014; Yamada, 2014), more closely mirroring decidualisation triggered by a blastocyst.

As mentioned above, PABP1 may be able to compensate for the lack of PABP4 at e5.5 and e8.5 as its expression pattern appears to include most, if not all, maternal PABP4 expressing cells. To gain more insight into potential compensation, qualitative (IHC) expression of PABP1 in *Pabp4*$^{-/-}$ implantation sites would be informative, although a lack of change would not rule out compensation given their expression patterns. However, the altered shape of implantation sites from *Pabp4*$^{-/-}$ dams suggests that PABP4 may have distinct roles in early pregnancy which PABP1 is unable to fully compensate for. This is consistent with previous studies where PABP4 was unable to fully rescue the PABP1-knockdown phenotypes in *X. laevis* (Gorgoni et al., 2011). Alternatively, PABP4 and PABP1 may have identical functional roles but may differ in their expression in a given cell type with meaning PABP1 is not available to compensate, more detailed co-expression studies would inform on this. Finally, even if present and functionally equivalent, PABP1 may be unable to fully compensate if total PABP levels are critical.

It is unknown what underlies the change in the shape of implantation sites from *Pabp4*$^{-/-}$ dams. The ectoplacental cone appears to be visually grossly normal, i.e. no obvious misorientation, difference in size or anomalies such as blood pools and ECM debris between the tip of the EPC and the mesometrial decidua, as for example reported in *Mmp9*-null embryos which fail to implant properly (Plaks et al., 2013). Further investigation of the peri-implantation period is required, e.g. timing of implantation, decidualisation, trophoblast invasion depth and number of somites in embryo (to check for developmental delay), particularly considering that the M/AM distance is increased when compared both as individual data points but also when averaged per litter (*Figure 5.4*). Defects occurring during the peri-implantation period have been reported to have ripple effects with consequences later in gestation such as embryo crowding, defective decidualisation, placentation, intrauterine growth and miscarriages as reviewed by Cha et al. (Cha et al., 2012).

Our data also establish that PABP4 and PABP1 are expressed in the mature placenta (e18.5), with PABP4 present in the junctional zone with more limited expression in the decidua basalis and labyrinth zone (*Figure 5.7*). In contrast, PABP1 has a more widespread pattern of expression. At e18.5 placentas from *Pabp4*$^{-/-}$ dams have a decreased junctional zone volume and an increased decidua basalis volume with no change in labyrinth in comparison to placentas from *Pabp4*$^{+/+}$ dams (*Figure 5.9*). It is unclear whether these differences arise independently or whether one is causative of the other as suggested by the size changes appearing reciprocal. There are several models of IUGR with a reduced junctional zone which are dependent on fetal and/or placental genotype or a low maternal protein diet, however, to our knowledge no models have been reported where the decidua basalis is increased. This unusual finding may reflect that unlike other IUGR models, our phenotype is dependent on maternal genotype. The decidua basalis is the fetal-maternal interface were fetal trophoblast come into contact with maternal decidual cells and vasculature and communication between the two sides is particularly important in early gestation when the decidua is being invaded and spiral arteries are being remodelled, thus it acts as a site of maternal protection and control of trophoblast invasion. Further functions of the decidua include maternal immunomodulation, to protect against immune attack on the semi-allogeneic conceptus, and paracrine control of uterine vascular remodelling (Yamada, 2014). In later gestation the function of the decidua is not well studied and it is largely regarded as the point of attachment of the fetus and mother and the site of maternal blood entry into the labyrinth as well as a barrier. It is also the region to which the glycogen cells migrate to from the junctional zone prior to mobilisation of their glycogen stores for energy (Coan et al., 2006). As the decidua basalis, in contrast to the rest of the placenta, is maternal in origin and therefore is the only part of the placenta which is *Pabp4*$^{-/-}$ in our studies, changes in its size are intriguing. The basis for this increase, as well as its potential consequences on placental function and/or feto-maternal communication should be investigated further. For instance, expression analysis of PABPs and morphological analysis with appropriate markers at key intermediate stages of placenta development (i.e. e10.5 and e13.5) in *Pabp4*$^{+/+}$ and *Pabp4*$^{-/-}$ placentas may shed light on the origins of these differences e.g. timing of onset. Similarly, the use of markers at e18.5 could inform on the changes in cellular composition that account for the increased size and glycogen assays could shed light on whether there is a failure to mobilise glycogen stores for energy which could affect fetal growth and comparative decidua basalis size. The function of the junctional zone is better understood; it has an important endocrine role, producing hormones such as placental growth factor and placental lactogens, which effect embryonic growth both directly and indirectly by

stimulating maternal adaptation to pregnancy. In support of reduced junctional zones being implicated in impaired fetal growth, the smallest placentas of WT mouse litters have a reduced junctional zone but also decidua basalis at e16 which coincides with the fetus being significantly smaller in comparison to their litter mates (Coan et al., 2008). By e19 the junctional zone and decidua were found to be comparable to larger placentas and the fetuses were noted to catch up in their growth (Coan et al., 2008). Intriguingly Coan et al also noted that reduced junctional zones at e16 was accompanied by significant upregulation of the system A amino acid transporter system, reminiscent of our own observations that *Snat-2* is upregulated in *Pabp4*$^{-/-}$ dams at e18.5 (*Figure 5.18*). Thus it is interesting to speculate whether a smaller junctional zone negatively affects amino acids availability to the fetus due to its role in regulation maternal adaptation to pregnancy, and that upregulated amino acid transport may reflect a compensatory change? Evidence suggests that placental lactogens produced by the junctional zone interact with leptin to increase appetite and food intake which is one possible mechanism by which it may increase amino acid availability in normal pregnancy (Ladyman et al., 2010). Further histological analysis with markers can shed light on whether reductions in specific cell type populations or size account for the difference and standard molecular techniques can be used to determine whether the expression of key hormones are altered (e.g. qRT-PCR, ELISA).

It is important to remember that the junctional zone is fetal rather than maternal origin and that the maternal genotype dependence of the IUGR and mid-late fetal death means that the primary defect that drives these phenotypes does not lie in the junctional zone. Rather changes in the junctional zone are a downstream consequence of this initial defect but may still be integral to the disease mechanism. Whilst this may be true, it is important to remember that the volumetric analysis that identified this junctional zone reduction did not include a reciprocal cross. This means that *Pabp4*$^{+/+}$ and *Pabp4*$^{+/-}$ junctional zones were compared. Thus it is formally possible that fetal *Pabp4* heterozygosity leads to the reduced junctional zone, and it is therefore genetically separable from the phenotype development. In contrast a normal size junctional zone in the reciprocal cross would lend further weight to the hypothesis that the reduced junctional zone is downstream of the initial maternally derived deficit but may nonetheless be important in phenotype development e.g. via inappropriate maternal adaptation. Thus this analysis could prove powerful.

Investigations of blood flow waveforms and RI of the uterine artery using Doppler ultrasound suggest that remodelling of the uterine artery is normal in *Pabp4*$^{-/-}$ dams (*Figure 5.12*) and this is further supported by normal blood flow and RI of the umbilical cord (*Figure 5.13*) as during hypoxia the fetus directs blood supply to the brain which results in reduced flow and increased vascular resistance in the umbilical artery. Therefore, both normal uterine artery remodelling is also consistent with the symmetrical IUGR of fetuses in *Pabp4*$^{-/-}$ dams. We were unable to quantify uterine artery blood flow velocity as the small size of the uterine artery and its curvatures, together with the limitations of the greyscale Doppler, prevented us from accurately determining the direction of blood flow: this requires the angle between the ultrasound beam and the direction of blood flow to be known and as close as possible to 0° (Qu, 2014). Another limitation of using greyscale Doppler is that locating the uterine artery is more difficult and less certain. Other arteries are located in the vicinity of the uterine artery and have relatively similar Doppler waveforms and blood velocities to the uterine artery including the femoral artery, middle caudal artery, cranial vesical artery and the hypogastric trunk (Qu, 2014) In an attempt to avoid mistaking these arteries for the uterine artery a consistent anatomical location (bottom left or bottom right of the bladder, close to the utero-cervical junction) was chosen when being located. Doppler measurements of the uterine artery in non-pregnant females were not determined as the uterine artery is even smaller in non-pregnancy and we were not able to locate it. Fetal umbilical arteries on the other hand are easily located and the direction of blood flow is unambiguous. Abnormal umbilical artery Doppler is a marker of haemodynamic uteroplacental insufficiency and fetal distress and is defined by increased RI values resulting from reduced end diastolic flow which may become completely absent and eventually reverse (Maulik et al., 2010). At least three umbilical arteries of three different fetuses within each litter where assessed in each mother, providing more statistical power than for the measurements of the uterine artery. Considering that, similarly to the uterine artery, the umbilical RI index was no different in KO and WT females this is strongly indicative of normal uterine artery remodelling and adequate blood flow provided to the uteroplacental unit. Furthermore, adequate decidual spiral artery remodelling as indicated by the absence of smooth muscle actin (*Figure 5.14*).

Intriguingly, the RI of the common carotid artery is increased in pregnancy when compared to non-pregnancy (*Figure 5.10* C, D) as its elasticity declines towards the end of pregnancy (Karkkainen et al., 2014). Although initially measured as a control, an apparent genotype specific difference in this artery was noted during pregnancy. The physiological relevance of

this remains unclear since hypertension is mainly associated with stiffness in smaller vessels and we have no evidence of hypertension in *Pabp4*$^{-/-}$ mice, although tail plethysmography to examine their blood pressure would more direct inform on this point.

Interestingly, maternal non-fasted circulating glucose levels of *Pabp4*$^{-/-}$ dams are equivalent to WT females at both e15.5 and e18.5 (*Figure 5.16*), yet fetal glucose levels of fetuses from *Pabp4*$^{-/-}$ dams have significantly lower blood glucose levels in comparison to fetuses from *Pabp4*$^{+/+}$ dams (*Figure 5.15*). Suboptimal glucose and/or amino acid delivery to the fetus due to absence of maternal *Pabp4* would be predicted to retard growth e.g. dysregulated fetal glucose homeostasis due to an absent/aberrant signal from the *Pabp4*$^{-/-}$ dam to its fetuses. Whilst it is unclear whether these reduced glucose levels are causal or a consequence of an alternative lesion, *Glut-1* and *Glut-3* expression is unaltered at e15.5 (*Figure 5.17*) but upregulated at e18.5 (*Figure 5.18*), a time at which *Snat2* an amino acid transporter is also upregulated (*Figure 5.20*), suggestive of a potential compensatory change in expression. Although these results are interesting it is important to consider that the qPCR data of glucose and amino acid transporters presented in this thesis was normalised using only one reference gene. Normalisation is a critical step in the qPCR assay because it controls for variations in extraction yield, reverse-transcription yield, and efficiency of amplification and therefore enables the comparison of mRNA concentrations between samples (Bustin et al., 2009). There are a number of important criteria that a reference gene should fulfil including most importantly no change in expression levels in response to experimental factors, minimal variability in its expression between tissues and shows a similar threshold cycle with gene of interest (Kozera and Rapacz, 2013). Normalisation against a single reference gene is considered not be acceptable without confirmation of its invariant expression under the experimental conditions used (Bustin et al., 2009) and although this was confirmed to be the case for *Sdha* that was used for normalisation, it is strongly suggested that more than one stably expressed reference gene should be used to prevent misinterpretation of expression data (Chervoneva et al., 2010; Vandesompele et al., 2002). There is evidence that normalisation to a single housekeeping gene can lead to erroneous normalisation due to inherent noisy oscillations in expression levels of control genes (Vandesompele et al., 2002) and in the light of this at least three proper control genes are recommended to be used and a geometric average of these obtained to determine a suitable normalisation factor. Therefore, in the future this experiment should be ideally repeated with the suitable number of reference genes.

Additionally, it remains to be confirmed whether any transporter changes are also present at the protein level. Hormone assays (e.g. insulin) and metabolite (eg. cholesterol) analysis may be useful in further understanding the metabolic state of the mother and amino acid and glucose transport assays in vivo/ex vivo could be carried out to determine the transport capacity of the placenta (see chapter 7).

This chapter provides the first insights into the underlying changes that are present in Pabp4$^{-/-}$ mice that may lead to phenotype development. These include changes in placental morphology i.e. reduced junctional zone and increased decidua basalis. Furthermore fetal but not maternal glucose was reduced and an increase in mRNA levels for nutrient transporters that reside in the labyrinth was observed implying a possible change in placental function.

Chapter 6 - Adaptation to pregnancy in *Pabp4*$^{-/-}$ dams

6.1 Introduction

Pabp4$^{-/-}$ females, mated with a male of any genotype, give rise to IUGR fetuses which have an increased incidence of late gestational lethality between e18.5 and birth. Thus this model is useful for understanding a spectrum of closely related pregnancy disorders which encompasses IUGR and stillbirth. The placentas of fetuses from *Pabp4*$^{-/-}$ dams were found to be abnormal; having reciprocally altered volumetric proportions of two of the three main constituent layers. Specifically, the decidua basalis is increased in volume whereas the junctional zone is decreased, whilst the labyrinth remains unaltered. Whilst these changes may contribute or underlie the observed phenotypes, the placenta is largely fetal in origin but its formation and function rely on a complex feto-maternal dialogue, and its function is important for maternal pregnancy adaptation. Thus we hypothesis that defects in the materno-fetal dialogue or maternal adaptations may represent the primary defect, although their complex intertwined relationship makes it challenging to identify which phenotypic alterations, resulting from PABP4 loss, are causal as opposed to effect. Here we investigate aspects of maternal physiological adaptation to pregnancy including changes in body and organ weight, maternal haematology and hormonal and metabolic profile. In so doing we also examine these parameters in non-pregnant females allowing identification of pre-existing changes in maternal physiology which may contribute to IUGR-stillbirth. All parameters were compared to a control group of *Pabp4*$^{+/+}$ dams. To inform these investigations, the expression patterns of mammalian PABP4 and PABP1 proteins in maternal organs were addressed as such information is absent for PABP4 and only available for PABP1 in testis.

6.2 Results

The expression of PABP4 and PABP1 was examined in a number of key maternal organs including the liver, pancreas, spleen and kidney to identify organs and cell types which may be affected by loss the of PABP4 and cannot adequately adapt to pregnancy. PABP1 expression was also examined to determine organs/cells types in which PABP1 is relatively poorly expressed and which may therefore be more dependent on PABP4 function, and/or in which compensatory changes may take place. Expression was investigated in non-pregnant and pregnant e18.5 *Pabp4*$^{+/+}$ and *Pabp4*$^{-/-}$ females. All the immunohistochemical analysis consisted of at least 3 biological and two technical replicates. In addition to an IgG negative control included in each immunohistochemistry run, the specificity of the PABP4 antibody was further probed by the use of tissue from *Pabp4*$^{-/-}$ females. In all cases, *Pabp4*$^{+/+}$ and *Pabp4*$^{-/-}$ non-pregnant and pregnant tissues were run on separate slides therefore it is not possible to draw inference from any intensity differences between these states. Thus Western blotting was also done to accompany the IHC as it is more likely to reveal changes in protein levels when in the linear range. The IHC being very informative, nonetheless, with respect to determining expression patterns and any changes in expression pattern e.g. on pregnancy or PABP4 loss.

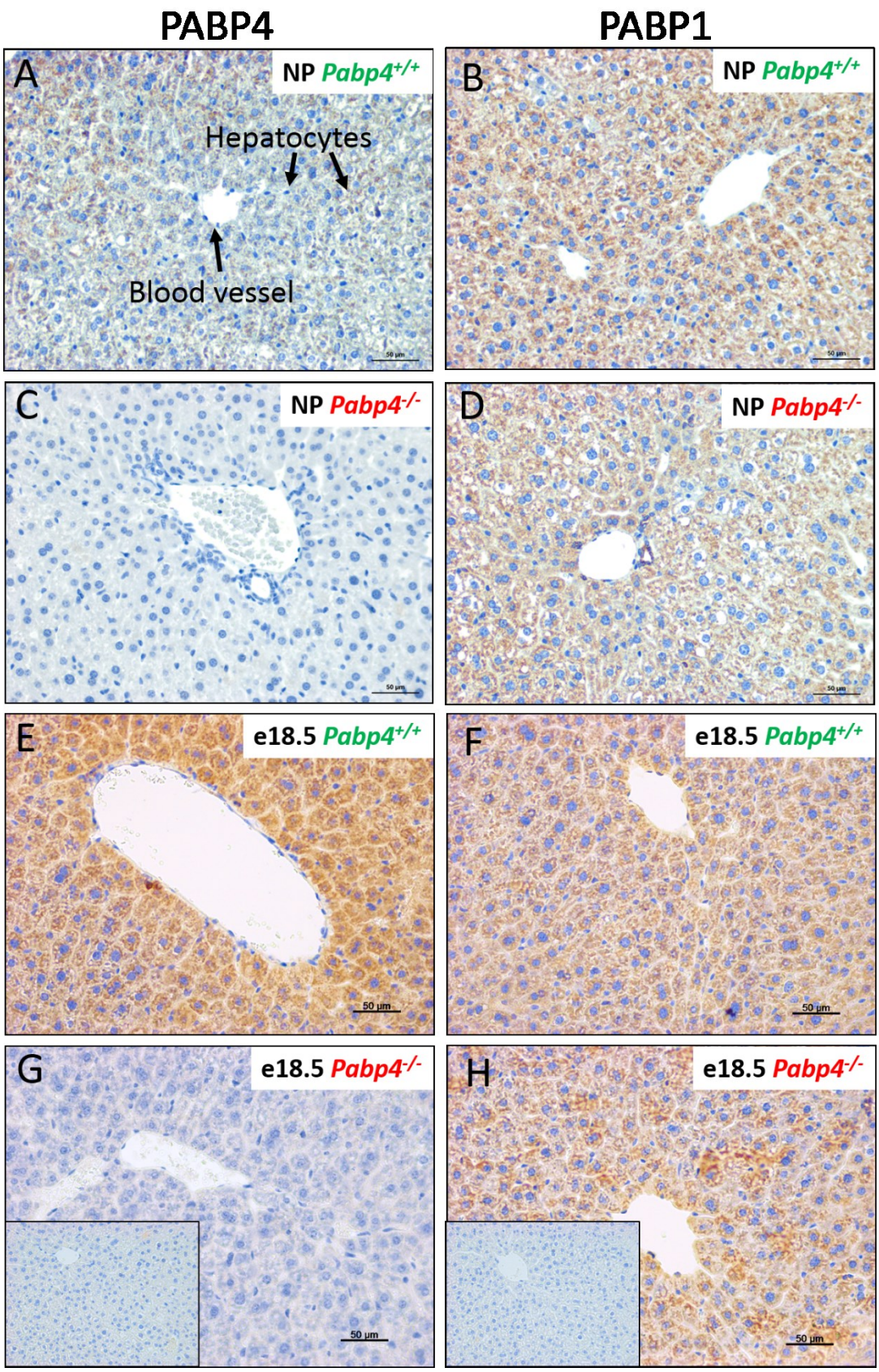
PABP4
PABP1
A
NP Pabp4+/+
Hepatocytes
Blood vessel
B
NP Pabp4+/+
C
NP Pabp4-/-
D
NP Pabp4-/-
E
e18.5 Pabp4+/+
F
e18.5 Pabp4+/+
G
e18.5 Pabp4-/-
H
e18.5 Pabp4-/-
50 µm

Figure 6.1. PABP4 and PABP1 expression in the adult non-pregnant and pregnant liver.

Immunohistochemical analysis of PABP4 and PABP1 expression in non-pregnant (**A, B**) *Pabp4*$^{+/+}$ and (**C, D**) *Pabp4*$^{-/-}$ liver and in the liver from e18.5 of gestation of (**E, F**) *Pabp4*$^{+/+}$ and (**G**, **H**) *Pabp4*$^{-/-}$ females. Rabbit IgG control (insert in **G** and **H**). NP: non-pregnant. Antibody details: PABP4 (Sigma) used at 1/1000, PABP1 (in house) used at 1/3500. x20 magnifications and 50 µm scale bars are shown.

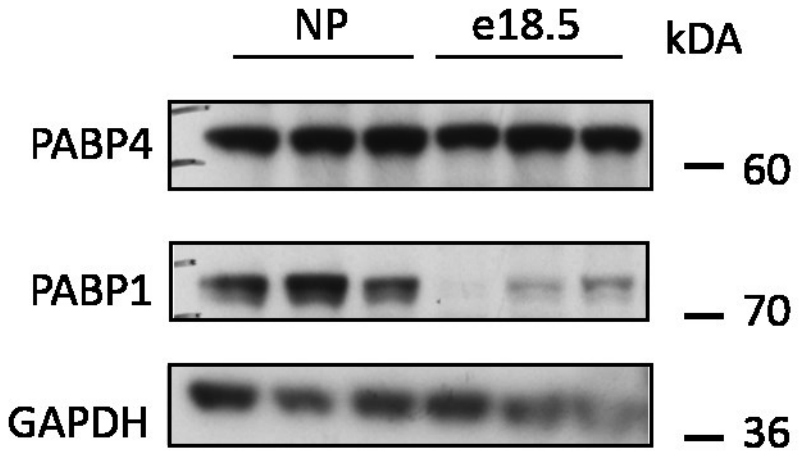

Figure 6.2. Western blot of PABP4 and PABP1 in *Pabp4*$^{+/+}$ non-pregnant and pregnant liver.

10µg of whole cell liver extract of non-pregnant and pregnant females at e18.5 gestation western blotted with anti-PABP4 (in house; 1/1000), PABP1 (in house; 1/5000) and GAPDH (Sigma; 1/10,000). NP, non-pregnant; kDA, kilo Daltons.

The liver is the largest solid organ with multiple functions including glycolytic metabolism and blood detoxification. Thus in pregnancy enhanced liver function is essential for meeting the energy demands of the fetus and for detoxification of fetal metabolites. This occurs via a combination of increased hepatocyte proliferation and cell size (Dai et al., 2011; Milona et al., 2010). Immunohistochemical analysis revealed that PABP4 was detectable in the majority of hepatocytes, the predominant cell type of the liver, in the *Pabp4*$^{+/+}$ non-pregnant liver (Figure 6.1 A), and in e18.5 pregnant liver (Figure 6.1 E). The observed pattern in non-pregnant females is consistent with data in a male mouse from another researcher in the lab using a different PABP4 antibody, although detection was stronger in that case (H. Burgess, pers. comm.). It appears likely that the non-pregnant tissue here may be under-stained as the stronger

detection noted by H. Burgess is more consistent with the multi-tissue western blot (*Figure* 1.15) and with the Western blot here (*Figure 6.2*), which shows that PABP4 protein is present at similar levels in non-pregnant and pregnant liver, although a shorter exposure may unmask differences. PABP4 was absent *Pabp4*$^{-/-}$ liver, confirming antibody specificity (*Figure 6.1* C, G). PABP1 was also found to be expressed in hepatocytes with no difference in expression pattern of between non-pregnant *Pabp4*$^{+/+}$ and *Pabp4*$^{-/-}$ liver (Figure 6.1. B, D), although western blots, indicated that PABP1 levels were diminished during pregnancy. Interestingly, at e18.5, PABP1 did show altered pattern of expression between wild-type and *Pabp4*$^{-/-}$ livers, where some hepatocytes showed more intense immunoreactivity (*Figure 6.1* F, H), suggesting potentially compensatory changes in PABP1 expression. In this regard it is interesting to note that not all hepatocytes are functionally identical and that the liver also contains hepatic oval cells, a small subpopulation of intra-hepatic stem cells induced by injury or inhibited proliferation (Fausto and Campbell, 2003; Petersen et al., 1998). Therefore the use of markers would be informative in identifying the cell types which show relatively more intense PABP1 staining.

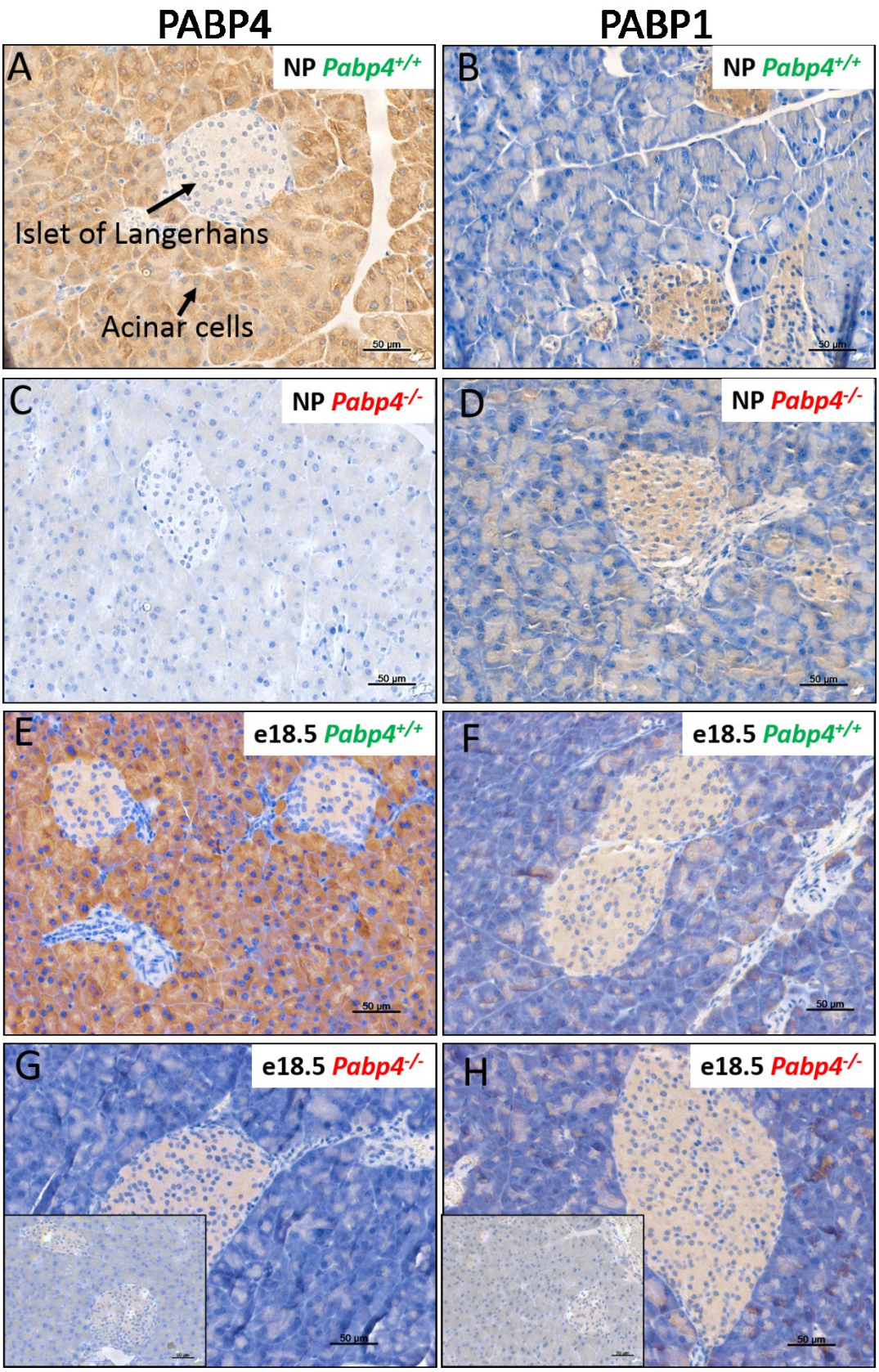
PABP4
PABP1
A
NP Pabp4+/+
Islet of Langerhans
Acinar cells
50 µm
B
NP Pabp4+/+
50 µm
C
NP Pabp4-/-
50 µm
D
NP Pabp4-/-
50 µm
E
e18.5 Pabp4+/+
50 µm
F
e18.5 Pabp4+/+
50 µm
G
e18.5 Pabp4-/-
50 µm
H
e18.5 Pabp4-/-
50 µm

Figure 6.3. PABP4 and PABP1 expression in the adult non-pregnant and pregnant pancreas.

Immunohistochemical analysis of PABP4 and PABP1 expression in non-pregnant (**A, B**) *Pabp4*$^{+/+}$ and (**C, D**) *Pabp4*$^{-/-}$ pancreas and that from e18.5 of gestation (**E, F**) *Pabp4*$^{+/+}$ and (**G**, **H**) *Pabp4*$^{-/-}$ females. Rabbit IgG control (insert in **G** and **H**). NP: non-pregnant. Antibody details: PABP4 (Sigma) used at 1/1000, PABP1 (in house) used at 1/3500. x20 magnifications and 50 μm scale bars are shown.

The pancreas is an important exocrine and endocrine organ and in pregnancy pancreatic β-cells in the islets of Langerhans become increasingly sensitive and hyperfunctional, producing more insulin to combat the insulin resistance which manifests in the second half of gestation (reviewed by (Ernst et al., 2011; Sorenson and Brelje, 1997). Failing to do so can lead to development of gestational diabetes mellitus which increases the risk of fetal mortality and morbidity (Devlieger et al., 2008). Interestingly, immunohistochemical analysis revealed that PABP4 and PABP1 show largely reciprocal expression in the endocrine and exocrine cells of the *Pabp4*$^{+/+}$ pancreas (Compare Figure 6.3. A and B). Specifically, PABP4 was found to be easily detectable in the exocrine acinar cells of the *Pabp4*$^{+/+}$ pancreas which synthesize, store and secrete digestive enzymes, and barely detectable in the islets of Langerhans. In contrast, PABP1 showed barely detectable expression in the acinar cells but stronger expression in the islets of Langerhans (Figure 6.3. A, B). This expression pattern has been independently confirmed in male mice (H. Burgess and J. Scanlon, pers. comm). No difference in the expression pattern of PABP4 was observed between the non-pregnant and e18.5 *Pabp4*$^{+/+}$ pancreas (Figure 6.3. A, E). The weak PABP4 staining in the islet of Langerhans in e18.5 *Pabp4*$^{-/-}$ pancreas (Figure 6.3. G) is also present in the negative control (Figure 6.3. insert in G), suggesting a degree of non-specific binding to this region of the pancreas. Intriguingly, the relative staining of PABP1 in the exocrine cells in *Pabp4*$^{-/-}$ females (Figure 6.3 B) suggests that it may be upregulated in the exocrine tissue in the absence of PABP4. Similar observations have been made using immunofluorescence (J. Scanlon, pers. Comm.).

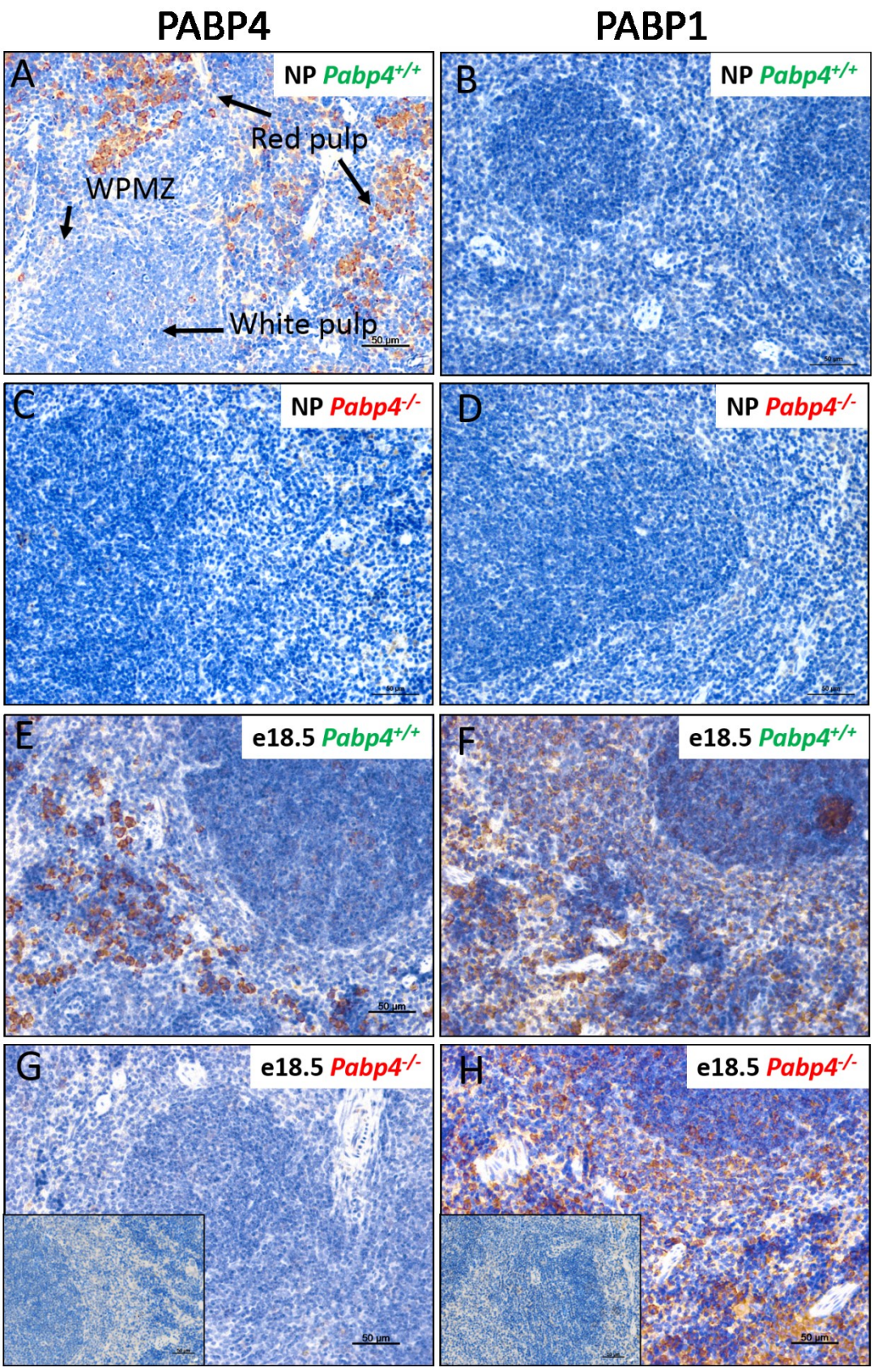
PABP4
PABP1
A
NP Pabp4+/+
Red pulp
WPMZ
White pulp
50 µm
B
NP Pabp4+/+
C
NP Pabp4-/-
D
NP Pabp4-/-
E
e18.5 Pabp4+/+
F
e18.5 Pabp4+/+
G
e18.5 Pabp4-/-
H
e18.5 Pabp4-/-

Figure 6.4. PABP4 and PABP1 expression in the adult non-pregnant and pregnant spleen.

Immunohistochemical analysis of PABP4 and PABP1 expression in non-pregnant (**A, B**) *Pabp4*$^{+/+}$ and (**C, D**) *Pabp4*$^{-/-}$ spleen and in the spleen from e18.5 of gestation of (**E, F**) *Pabp4*$^{+/+}$ and (**G**, **H**) *Pabp4*$^{-/-}$ females. Rabbit IgG control (insert in **G** and **H**). NP: non-pregnant; WPMZ: white pulp marginal zone. Antibody details: PABP4 (Sigma) used at 1/1000, PABP1 (in house) used at 1/3500. x20 magnifications and 50 µm scale bars are shown.

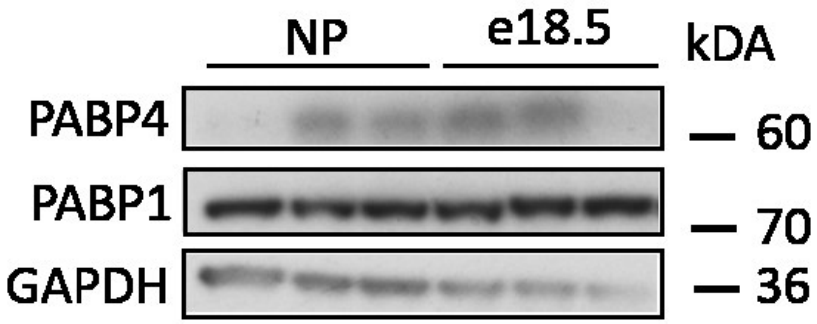

Figure 6.5. Western blot of PABP4 and PABP1 in *Pabp4*$^{+/+}$ non-pregnant and pregnant spleen.

10µg of whole cell spleen extract of non-pregnant and pregnant females at e18.5 gestation western blotted with anti-PABP4 (in house; 1/1000), PABP1 (in house; 1/5000) and GAPDH (Sigma; 1/10,000). NP – non-pregnant; kDA – kilo Daltons.

The spleen is the body's largest lymphatic organ and its functions include the production of antibodies, storing platelets, recycling iron, filtering foreign material, old/damaged red blood cells and platelets from blood and inducing adaptive immune responses (reviewed by (Mebius and Kraal, 2005). In both human and mice the spleen acts as a second site of red blood cell production in pregnancy (Fowler and Nash, 1968; Nakada et al., 2014). Immunohistochemical staining revealed that in the *Pabp4*$^{+/+}$ non-pregnant spleen, PABP4 was expressed in specific cell types within the red pulp, the region of the spleen which acts to store iron, erythrocytes and platelets and is where blood filtration and haematopoiesis takes place. The cells expressing PABP4 in the red pulp may be macrophages, based on morphology and location, but this remains to be confirmed using dual labelling with a macrophage specific marker and PABP4. More limited expression in sporadic cells is seen within the white pulp, which is involved in responding to blood-borne antigens (Figure 6.4. A). The expression pattern of PABP4 did not appear to dramatically change upon pregnancy (*Figure 6.4.* G), nor did its levels (*Figure 6.5*). However, the western blot showed a high degree of variability in PABP4 between biological

replicates (*Figure 6.5*). PABP4 was absent in the non-pregnant and pregnant *Pabp4*$^{-/-}$ spleen, as expected (*Figure 6.4.* C, G). PABP1 appeared to be absent in the non-pregnant *Pabp4*$^{+/+}$ and *Pabp4*$^{-/-}$ spleen (*Figure 6.4*. B, D), however this result is inconsistent both with the multi-tissue Western blot (*Figure 1.15*) and with the Western analysis here, which shows that PABP1 is present in equal amounts in *Pabp4*$^{+/+}$ spleen from non-pregnant and pregnant females (). Moreover, it is inconsistent with PABP1 IHC in male mice using the same antibody (H. Burgess pers. Comm.) which revealed PABP1 expression throughout the different zones including the white pulp, white pulp marginal zone and red pulp of the spleen similar to females at e18.5 of gestation (*Figure 6.4*. F, H). Thus the weight of evidence suggests that the absence of PABP1 in non-pregnant spleen is due to a technical failure, although this remains to be verified by further experimentation.

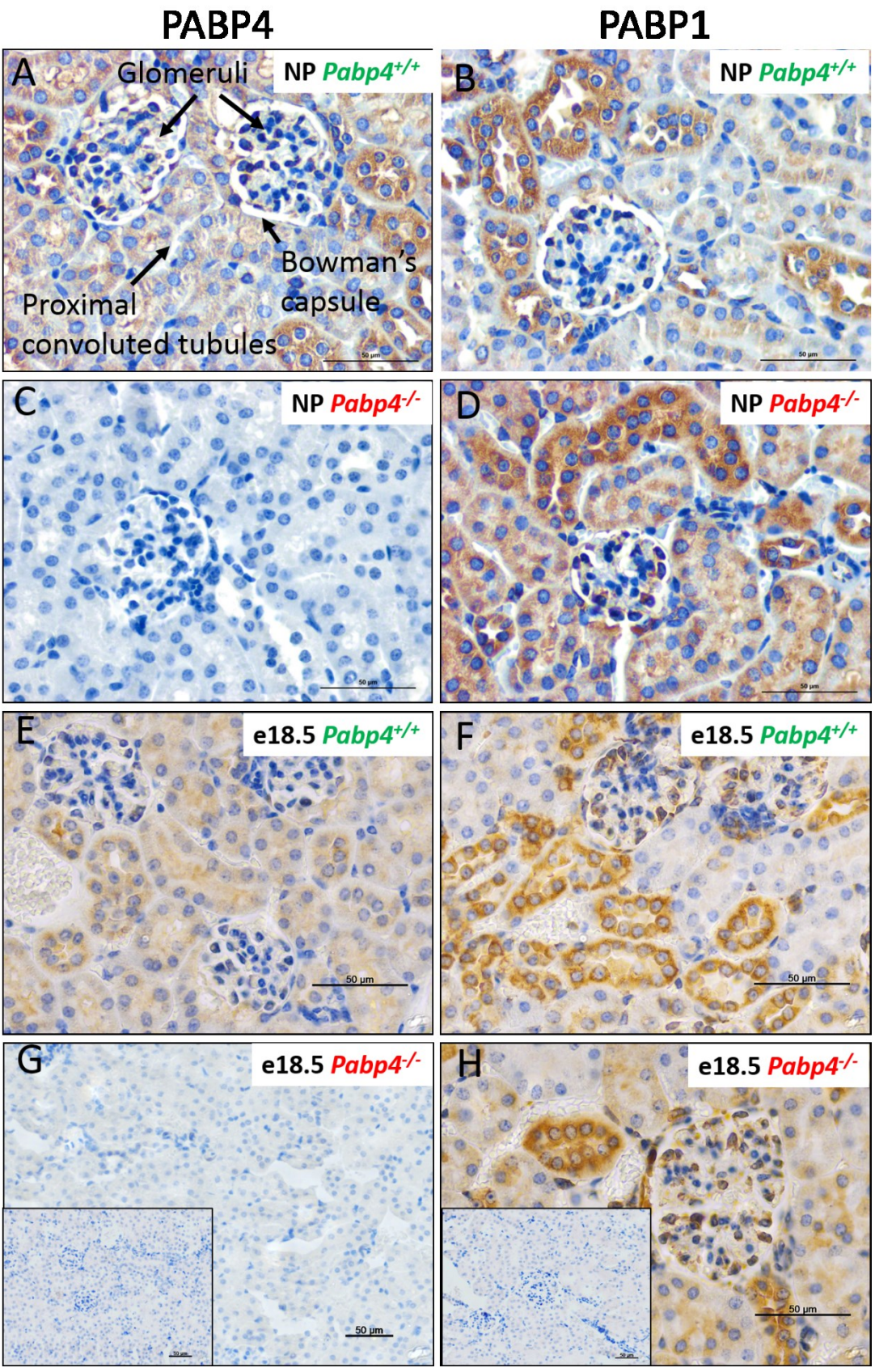
PABP4
PABP1
A
Glomeruli
NP Pabp4+/+
Bowman's capsule
Proximal convoluted tubules
B
NP Pabp4+/+
C
NP Pabp4-/-
D
NP Pabp4-/-
E
e18.5 Pabp4+/+
F
e18.5 Pabp4+/+
G
e18.5 Pabp4-/-
H
e18.5 Pabp4-/-
50 µm

Figure 6.6. PABP4 and PABP1 expression in the adult non-pregnant and pregnant kidney.

Immunohistochemical analysis of PABP4 and PABP1 expression in non-pregnant (**A, B**) *Pabp4*$^{+/+}$ and (**C, D**) *Pabp4*$^{-/-}$ kidney and in the kidney from e18.5 of gestation of (**E, F**) *Pabp4*$^{+/+}$ and (**G**, **H**) *Pabp4*$^{-/-}$ females. Rabbit IgG control (insert in **G** and **H**). NP: non-pregnant; WPMZ: white pulp marginal zone. X40 magnifications are shown Antibody details: PABP4 (Sigma) used at 1/1000, PABP1 (in house) used at 1/3500. X40 magnifications and 50 μm scale bars are shown.

The kidney is an important organ for the excretion of specific waste products, the regulation of water and solute excretion, secretion of hormones whilst also playing a role in haemodynamics, red blood cell production and bone metabolism (Adamson, 1996; Fukagawa et al., 2006). Although the initial multi-tissue panel (Figure 1.15, n=1 mouse), suggested that PABP1 and PABP4 were not expressed in kidney, subsequent western analysis on additional mice has detected their expression within kidney (M. Brook, pers comm.). In the *Pabp4*$^{+/+}$ non-pregnant kidney, PABP4 was present in glomeruli and tubules appearing more pronounced in distal compared to proximal tubules (Figure 6.6. A), although markers are required to confirm the identity of proximal versus distal tubules, PABP expressing cell types within glomeruli (e.g. glomerular epithelium or mesangium) or structures such as Bowman's capsule. This expression pattern did not appear to change upon pregnancy (Figure 6.6. E) and PABP4 expression was absent in *Pabp4*$^{-/-}$ kidneys, confirming specificity (Figure 6.6. C, G). PABP1 expression pattern was similar to that of PABP4 in both non-pregnancy and pregnancy (Figure 6.6. B,) and no changes were observed upon the KO of PABP4 (Figure 6.6. D, H).

Although further work is required to validate and complete this dataset (see discussion), it nonetheless confirms the presence of PABP4 and PABP1 in these organs and provides a first insight into their distribution in non-pregnant females and at e18.5 of pregnancy. Importantly, as each of these organs undergo changes integral to the maternal adaptation response and adaptation in one or more of these organs could be compromised in *Pabp4*$^{-/-}$ females leading or contributing to the observed phenotypes.

Maternal adaptation of the organs frequently includes changes in their weight, which tends to be normalised to body weight. Moreover, low female bodyweight prior to pregnancy and inadequate weight gain during pregnancy are associated with poor pregnancy outcome. This is often caused by low maternal circulating nutrients (Frederick et al., 2008; Mathews et al.,

2004). Thus both non-pregnant and pregnant body weight was examined to enable normalisation for organ size but also to investigate whether Pabp4$^{-/-}$ dams have reduced bodyweight prior to pregnancy or exhibit altered weight gain during pregnancy that may contribute to the observed phenotypes. To this end, the weights of non-pregnant females and mated females (presumed pregnant) at the time of detection of a copulatory plug were recorded and normalised to age. The weight of females at plugging is comparable to that of non-pregnant females, therefore, data collected for these two groups was combined, providing the necessary power. Bodyweights of the mated females were also recorded at the three collection time-points including mid- (e13.5), mid-late (e15.5) and late pregnancy (e18.5), to address weight gain. No differences were found in age to weight ratios between Pabp4$^{-/-}$ and Pabp4$^{+/+}$ females to/at the start of pregnancy (Figure 6.7), apparently ruling out low body weight prior to pregnancy as a causative factor for the poor pregnancy outcome.

A sizeable component in maternal weight gain is due to growing fetuses and their associated placentas, which will differ between *Pabp4*$^{+/+}$ and *Pabp4*$^{-/-}$ females due to IUGR and litter size, as gestation proceeds. Thus maternal body weight was measured post hysterectomy at e13.5, e15.5 and e18.5. Interestingly, at e13.5 maternal weight gain (calculated as a percentage of body weight gain) was significantly lower in *Pabp4*$^{-/-}$ dams compared to *Pabp4*$^{+/+}$ dams but at later time-points (e15.5 and e18.5) were indistinguishable (*Figure 6.8* A, B, C). As stands, the data suggest that *Pabp4*$^{-/-}$ dams initially gain less weight but appear to catch-up by mid-late pregnancy, however the *n* numbers need to be increased to confirm this finding. Such initial low weight gain followed by catch up later in pregnancy, may reflect an altered lipid metabolism in *Pabp4*$^{-/-}$ dams which could in turn have a detrimental impact on fetal growth. Lipids stores put on by the dam in early pregnancy are utilised for maternal energy output in late gestation whilst the majority of glucose intake is directed to the fetus. If this maternal adaptation is disrupted an adequate supply of glucose to enable exponential fetal growth in late gestation may not be available. In support of this, fetuses in *Pabp4*$^{-/-}$ females have reduced glucose levels at e15.5 and e18.5 (Figure 5.15, Chapter 5). However, this may be the result of aberrant glucose transport across the placenta rather than altered lipid/glucose metabolism. Levels of cholesterol and free fatty acids (FFA) and hormones associated with glucose homeostasis are measured later in this chapter.

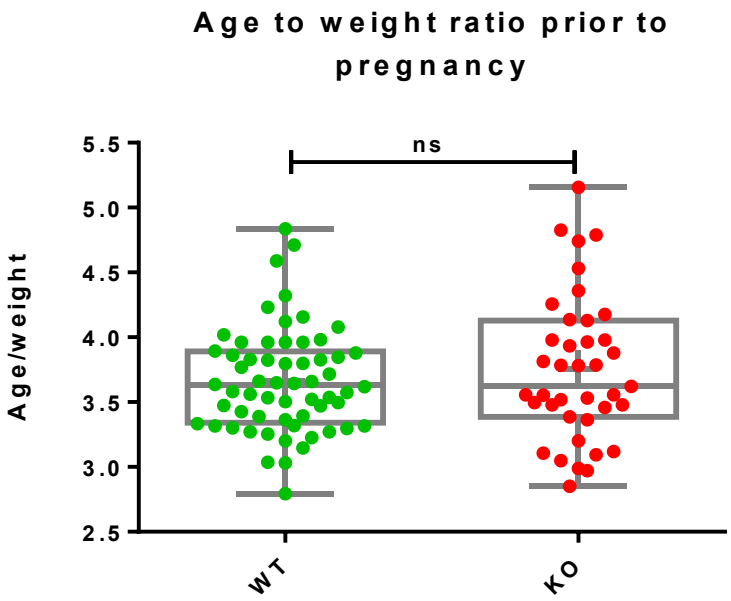

Figure 6.7. Age to body weight ratio of *Pabp4*$^{-/-}$ females is comparable to that of *Pabp4*$^{+/+}$ females prior to pregnancy.

The age of *Pabp4*$^{+/+}$ (WT, green dots; n = 60) and *Pabp4*$^{-/-}$ (KO, red dots; n = 39) females divided by weight at the time of plugging. Data are shown as shown as box and whisker plots with the median (long line) and mean (cross) indicated. Significance was analysed by student's T-test. ns p = ≥ 0.05.

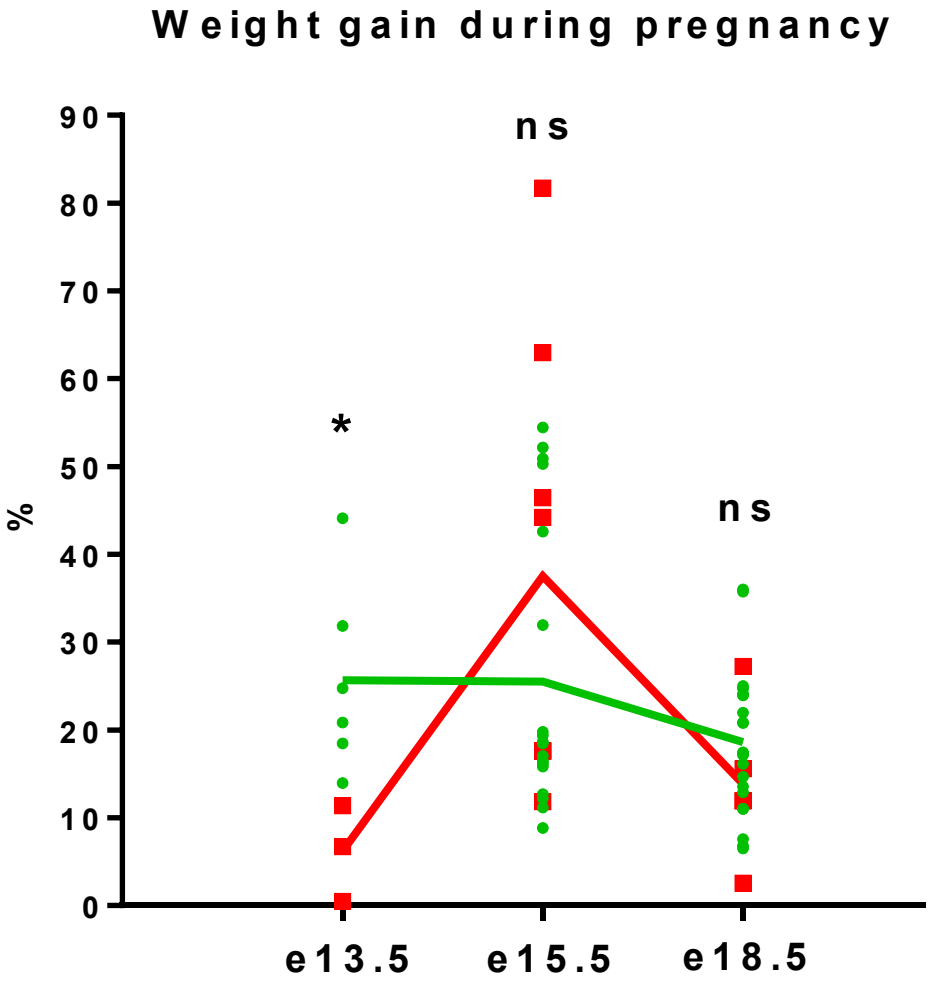

Figure 6.8. Percentage weight gain of *Pabp4*$^{-/-}$ dams may be compromised in early pregnancy.

Weight gain expressed as a percentage calculated from maternal bodyweight at the time of plugging and hysterectomised bodyweight at collection. Percentage weight gain of *Pabp4*$^{+/+}$ females (green dots): e13.5 (*n* = 6), e15.5 (*n* = 19), e18.5 (*n*=22). Percentage weight gain of *Pabp4*$^{-/-}$ females (red squares): e13.5 (*n* = 3), e15.5 (*n* = 8), e18.5 (*n*=5). Data shown as individual data points with means connected on an XY graph. Significance was analysed at each time-point by student's T-test. ns p = ≥ 0.05; * p = ≤ 0.05.

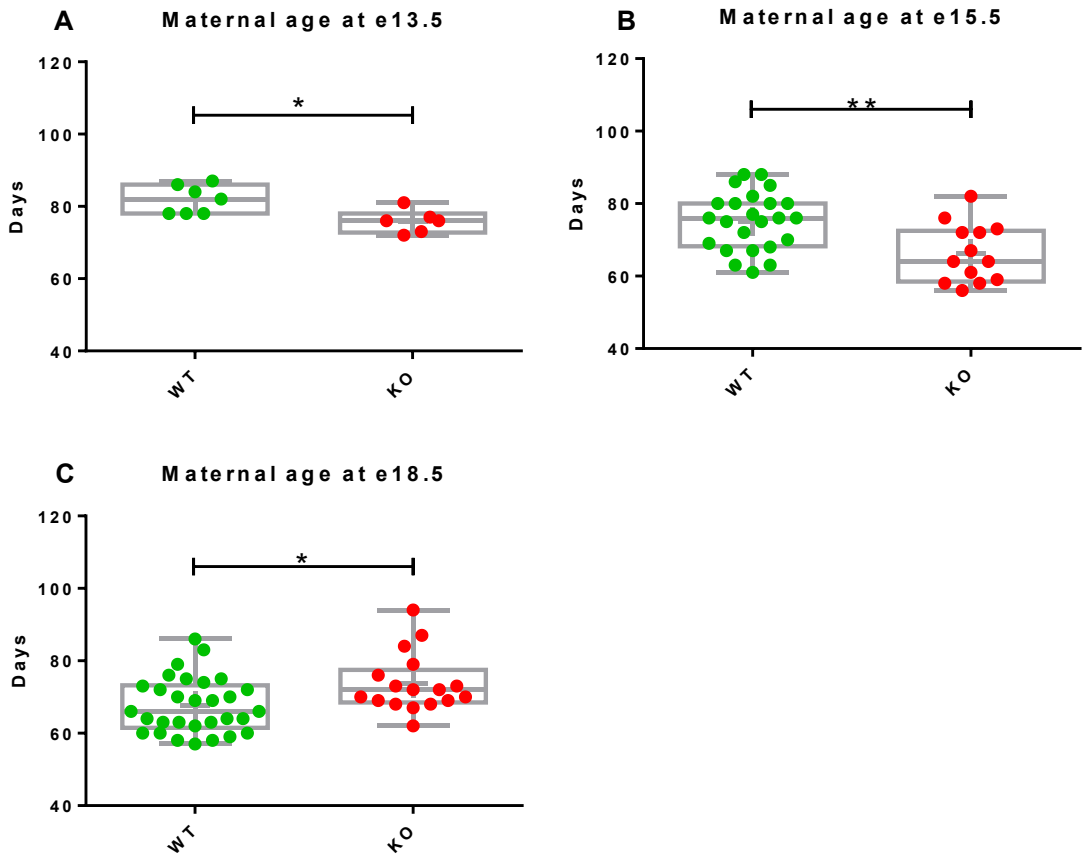

Figure 6.9. Differences in maternal age at the time of plugging of females subsequently collected at e13.5, e15.5 and e18.5.

Maternal age at the time of plugging of *Pabp4* $^{+/+}$ females (green dots) and *Pabp4* $^{-/-}$ females (red dots) subsequently collected at (**A**) e13.5 (*Pabp4* $^{+/+}$ $n = 7$; *Pabp4* $^{-/-}$ $n = 6$); (**B**) e15.5 (*Pabp4* $^{+/+}$ $n = 25$; *Pabp4* $^{-/-}$ $n = 13$) (**C**) e18.5 (*Pabp4* $^{+/+}$ $n = 30$; *Pabp4* $^{-/-}$ $n = 19$). Data are shown as shown as box and whisker plots with the median (long line) and mean (cross) indicated. Significance was analysed by student's T-test. * p = ≤ 0.05; ** p = ≤ 0.01.

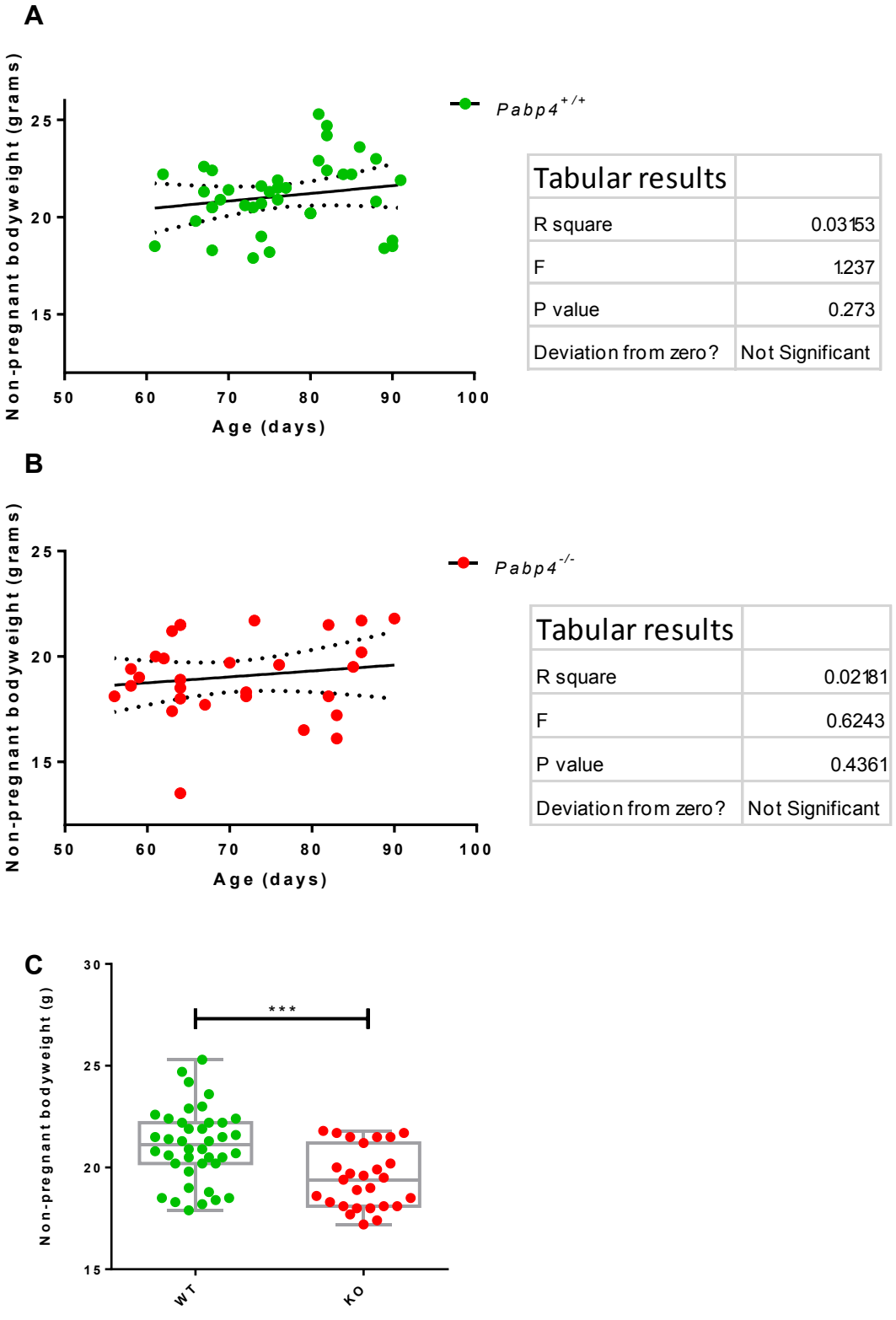

Figure 6.10. Age has no bearing on the bodyweight of *Pabp4*$^{+/+}$ and *Pabp4*$^{-/-}$ females plugged in the age window of 8-12 weeks however the KO cohort had a lower non-pregnant bodyweight.

Bodyweight versus age at the time of plugging of (**A**) *Pabp4*$^{+/+}$ females (n = 40) and (**B**) *Pabp4*$^{-/-}$ females (n = 30). Data is presented on X/Y scatterplot with mean (full line), 5 and 95% percentiles (dotted lines) indicated. The relationship between X and Y was determined by calculating R square (R^2) and a P value was calculated from an F test to determine the probability that a randomly selected point would result in an R^2 value as high as the one observed. (**C**) Non-pregnant bodyweight of *Pabp4*$^{+/+}$ females (n = 40) and *Pabp4*$^{-/-}$ females (n = 30). Data are shown as shown as box and whisker plots with the median (long line) and mean (cross) indicated. Significance was analysed by student's T-test. *** p = ≤ 0.001.

Remarkably, all maternal organ systems undergo physiological changes to adapt to pregnancy, with the expression of PABP4 in key organs leading us to hypothesise that maternal organs may not adequately adapt leading to adverse pregnancy outcome. To this end, maternal organ weights, including the liver, kidney, spleen and heart, were examined prior to and at e13.5, e15.5 and e18.5 of gestation. In collecting this data and taking into account the data from Figures Figure 6.7 and Figure 6.8, it became clear that it was important to establish whether age differences between some of the cohorts (Figure 6.9) had the potential to confound the analysis of organ size: although all females were between 8-12 weeks in age, the *Pabp4*$^{-/-}$ pregnant females collected at e15.5 were significantly younger within the given age-frame (WT age mean = 75.17 days ± 1.618; KO age mean = 66.31 ± 2.246) whereas at e18.5 they were significantly older (WT age mean = 67.67 days ± 1.395; KO age mean = 73.71 ± 1.1968) (Figure 6.9. A, B, C). This difference was mainly the result of the low number of *Pabp4*$^{-/-}$ mice by weaning, therefore *Pabp4*$^{-/-}$ mice tended to be plugged as soon as sexually mature (approx. 8 weeks) whereas *Pabp4*$^{+/+}$ mice were more readily available and random sampling inadvertently led to a skew in ages). This may be the reason why overall *Pabp4*$^{-/-}$ females had a lower bodyweight prior to pregnancy (Figure 6.10, C) as when the bodyweight of females was corrected for age no difference was found between *Pabp4*$^{+/+}$ and *Pabp4*$^{-/-}$ females (Figure 6.7) which implies that it is not a genotype dependent effect. However, if *Pabp4*$^{-/-}$ females do truly have reduced bodyweights as a failure to catch up postnatally this would imply growth restriction in utero not only due to an adverse maternal environment but also due to a pathological process in *Pabp4*$^{-/-}$ fetuses and therefore should be investigated further. A correlation coefficient, R square (R^2), was calculated for age and maternal bodyweight recorded at the time of plugging for both *Pabp4*$^{+/+}$ and *Pabp4*$^{-/-}$ females to determine whether age is indeed a confounding factor (Figure 8 focused on genotypic influence and was age corrected). Furthermore a P value was calculated from an F test to determine the probability that a randomly selected point would result in an R^2 value as high as the one observed. This

analysis revealed that age in the window of 8-12 weeks at the time of plugging does not correlate with maternal bodyweight of *Pabp4*$^{+/+}$ or *Pabp4*$^{-/-}$ females (Figure 6.10 A, B) and therefore is not a confounding factor in interpreting differences in organ weights. Using the same analysis it was found that organ weights, similarly to bodyweight, do not correlate with age. Additionally, the relationship with other potential confounding factors such as maternal bodyweight prior to pregnancy (at plugging) and at the time of collection were also analysed for each organ (for full analysis of all organs see Appendix; Figure 8.1, Figure 8.2, Figure 8.3, Figure 8.4). Resultantly, *Pabp4*$^{-/-}$ and *Pabp4*$^{+/+}$ organ weights were compared as raw organ weights but also in cases where bodyweight, at the time of plugging or at the time of collection, were found to be a confounding factor (liver, kidney, heart) were also normalised. This is demonstrated for liver and kidney; kidney weight strongly correlates with maternal weight at the time of plugging for both genotypes (Figure 6.11 A, B), whereas liver weight only strongly correlates with maternal *Pabp4*$^{-/-}$ bodyweight (Figure 6.11 C, D). It is possible that the genotype dependent confounding factors for some of the organs may be a part of the *Pabp4*$^{-/-}$ phenotype and therefore should be taken into consideration, thus where appropriate the data is provided in both formats.

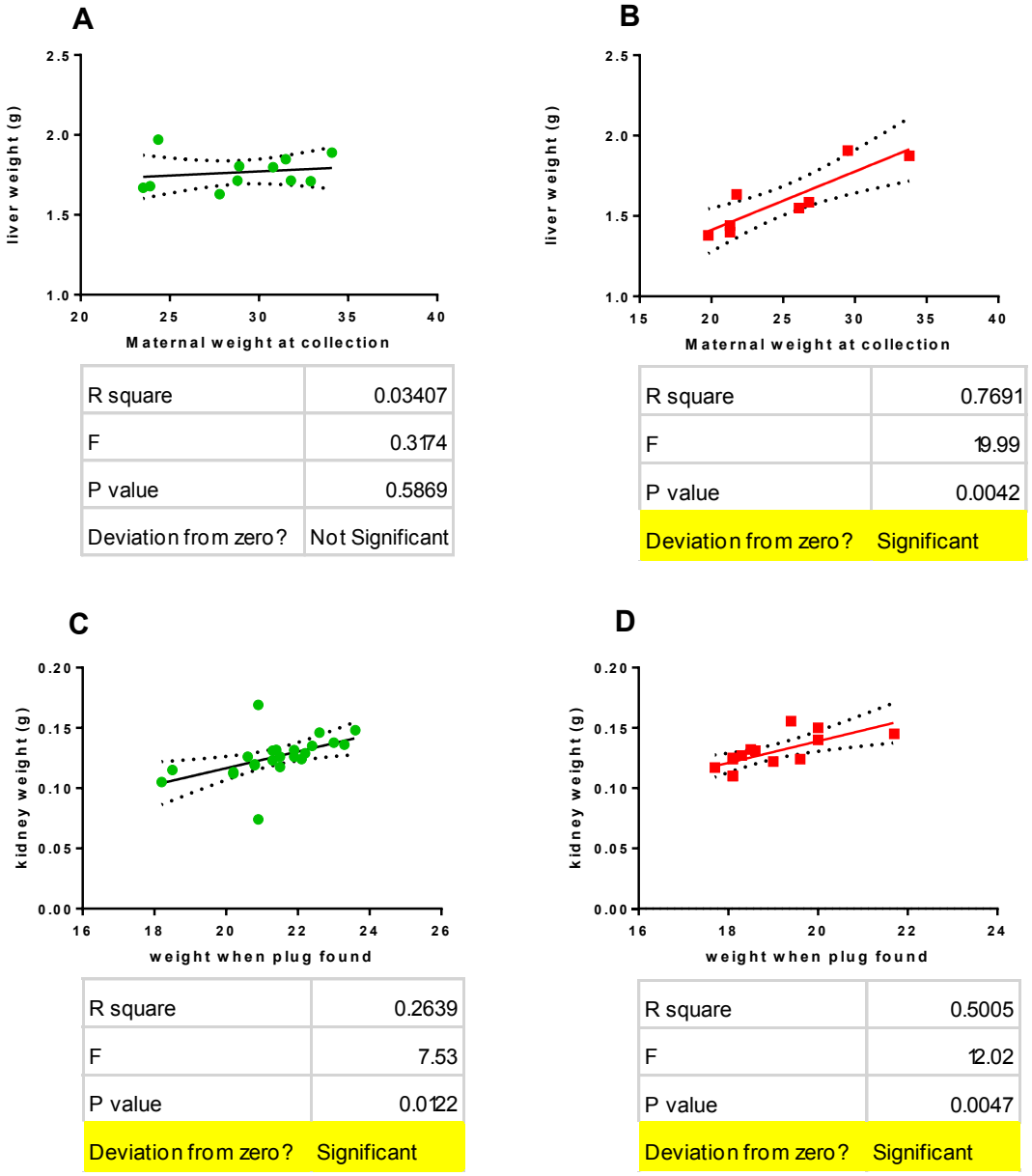

R square	0.03407
F	0.3174
P value	0.5869
Deviation from zero?	Not Significant

R square	0.7691
F	19.99
P value	0.0042
Deviation from zero?	Significant

R square	0.2639
F	7.53
P value	0.0122
Deviation from zero?	Significant

R square	0.5005
F	12.02
P value	0.0047
Deviation from zero?	Significant

Figure 6.11. Liver weight is positively correlated with maternal bodyweight at collection in *Pabp4*$^{-/-}$, but not *Pabp4*$^{+/+}$, females whereas the weight of the kidney is positively correlated with maternal bodyweight prior to pregnancy independent of genotype.

The weight of the liver collected at e15.5 plotted against the maternal hysterectomised bodyweight at e15.5 of (**A**) *Pabp4*$^{+/+}$ females (n =11) and (**B**) *Pabp4*$^{-/-}$ females (n =8). The weight of the kidney collected at e15.5 plotted against the maternal hysterectomised bodyweight when a plug was found of (**C**) *Pabp4*$^{+/+}$ females (n = 25) and (**D**) *Pabp4*$^{-/-}$ females (n =14). Data is presented on X/Y scatterplot with mean (full line) 5 and 95% percentiles (dotted lines) indicated. The relationship between X and Y was determined by calculating R square (R^2) and a P value was calculated from an F test to determine the probability that a randomly selected point would result in an R^2 value as high as the one observed.

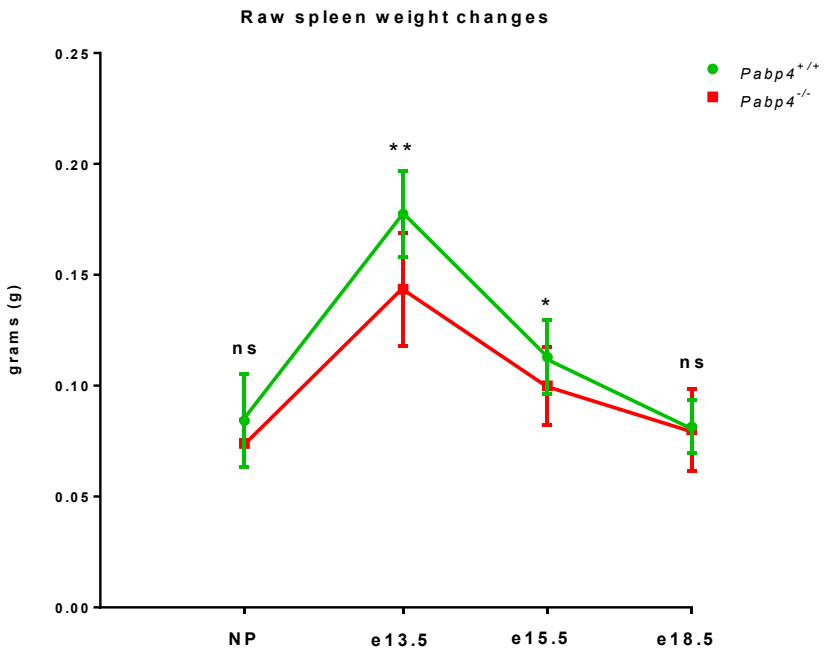

Figure 6.12. Raw spleen weight changes during pregnancy.

Raw spleen weights from non-pregnant (NP) females and females at day e13.5, e15.5 and e18.5 of gestation. Spleen weights from *Pabp4*$^{+/+}$ females (green dots): (NP n = 25; e13.5 n = 8; e15.5 n = 24; e18.5 n = 18); from *Pabp4*$^{-/-}$ females (red squares): (NP n = 12; e13.5 n = 8; e15.5 n = 15; e18.5 n = 15). Data are shown as means with standard deviation (SD) indicated as error bars. Significance was analysed at each time-point by student's T-test. ns p = ≥ 0.05; * p = ≤ 0.05; ** p = ≤ 0.01.

Raw spleen weights were found not to be correlated with maternal age or bodyweight and therefore normalisation was not required. Splenic adaptations to pregnancy include an increase in size, associated with the expansion of red pulp which becomes an important secondary site of erythropoiesis (Fowler and Nash, 1968; Mattsson et al., 1984; Nakada et al., 2014). This contributes to the increase in RBC mass that is observed during pregnancy and enables the spleen to cope with the need to filter an increased blood volume. In *Pabp4*$^{+/+}$ dams, spleen weights increased significantly between non-pregnancy and e13.5 but returned to its original weight by late gestation at e18.5 (Figure 6.12) as previously reported (Bustamante et al., 2008).

The spleen of *Pabp4*$^{-/-}$ dams followed the same trajectory but failed to reach the same increase in weight at e13.5 and e15.5 (Figure 6.12) suggesting that the red pulp does not increase in size to the same extent as in *Pabp4*$^{+/+}$ dams suggesting that splenic erythropoiesis may be negatively impacted, potentially resulting in a reduced haematocrit. Blood composition is investigated later in the chapter.

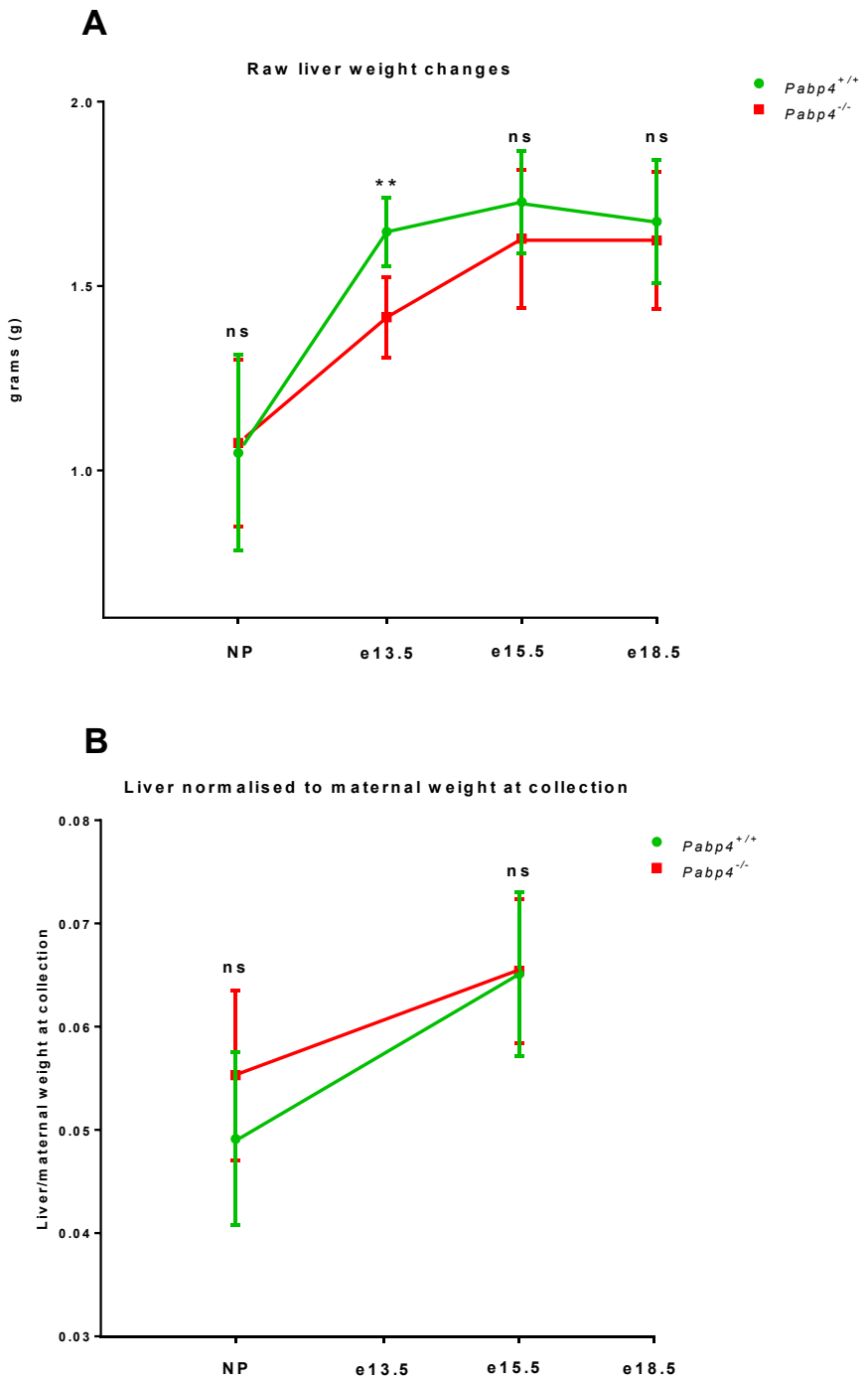

Figure 6.13. Raw and normalised liver weight changes during pregnancy.

(**A**) Raw liver weights from non-pregnant (NP) females and females at day e13.5, e15.5 and e18.5 of gestation and (**B**) liver weights normalised to maternal weight at collection from (NP) females and females at day e15.5 of gestation. Liver weights from *Pabp4*$^{+/+}$ females (green dots): (NP $n = 20$; e13.5 $n = 7$; e15.5 $n = 22$; e18.5 $n = 20$); from *Pabp4*$^{-/-}$ females (red squares): (NP $n = 13$; e13.5 $n = 6$; e15.5 $n = 14$; e18.5 $n = 18$). Data are shown as

means with standard deviation (SD) indicated as error bars. Significance was analysed at each time-point by student's T-test. ns p = ≥ 0.05; ** p = ≤ 0.01.

Due to the potentially confounding effect of body weight, analysis of organ weights hereafter are presented as raw and normalized. The liver of the mouse adapts to the demands of pregnancy by increasing in size as a result of hepatocyte hyperplasia and hypertrophy (Dai et al., 2011; Milona et al., 2010). The increase in size is evident by e13, peaks at e18 and returns to a pre-pregnancy weight by day 10 postpartum (Dai et al., 2011). Enhanced liver metabolism is essential to accommodate the increase demand for energy from the developing fetus and the detoxification of fetal metabolites. Raw liver weights of *Pabp4*$^{+/+}$ females increased in weight from a non-pregnant state to e13.5 and remained heavier beyond this time-point but did not significantly increase in later pregnancy (Figure 6.13 A). Raw liver weights of *Pabp4*$^{-/-}$ females also increased by e13.5 but not to the same extent as in *Pabp4*$^{+/+}$ females (*Pabp4*$^{+/+}$ mean = 1.65±0.03512; *Pabp4*$^{-/-}$ mean = 1.42±0.04459) suggesting that the *Pabp4*$^{-/-}$ liver may not adapt to pregnancy to the same extent as the *Pabp4*$^{+/+}$ liver (Figure 6.13 A). Beyond e13.5 there was no statistically significant difference in non-normalised liver weight between *Pabp4*$^{-/-}$ and *Pabp4*$^{+/+}$ females (Figure 6.13. A). However, following normalisation, no differences in liver weight were found between the genotypes prior to pregnancy or at e15.5 (Figure 6.13 B). Insufficient maternal bodyweight information was collected at e13.5 and e18.5 to normalise at these time-points (Figure 6.13 B). Whilst it is tempting to speculate that the *Pabp4*$^{-/-}$ liver is transiently smaller at e13.5, suggestive of a suboptimal or delayed adaptation, the absence of normalised data for this time-point make any conclusion premature.

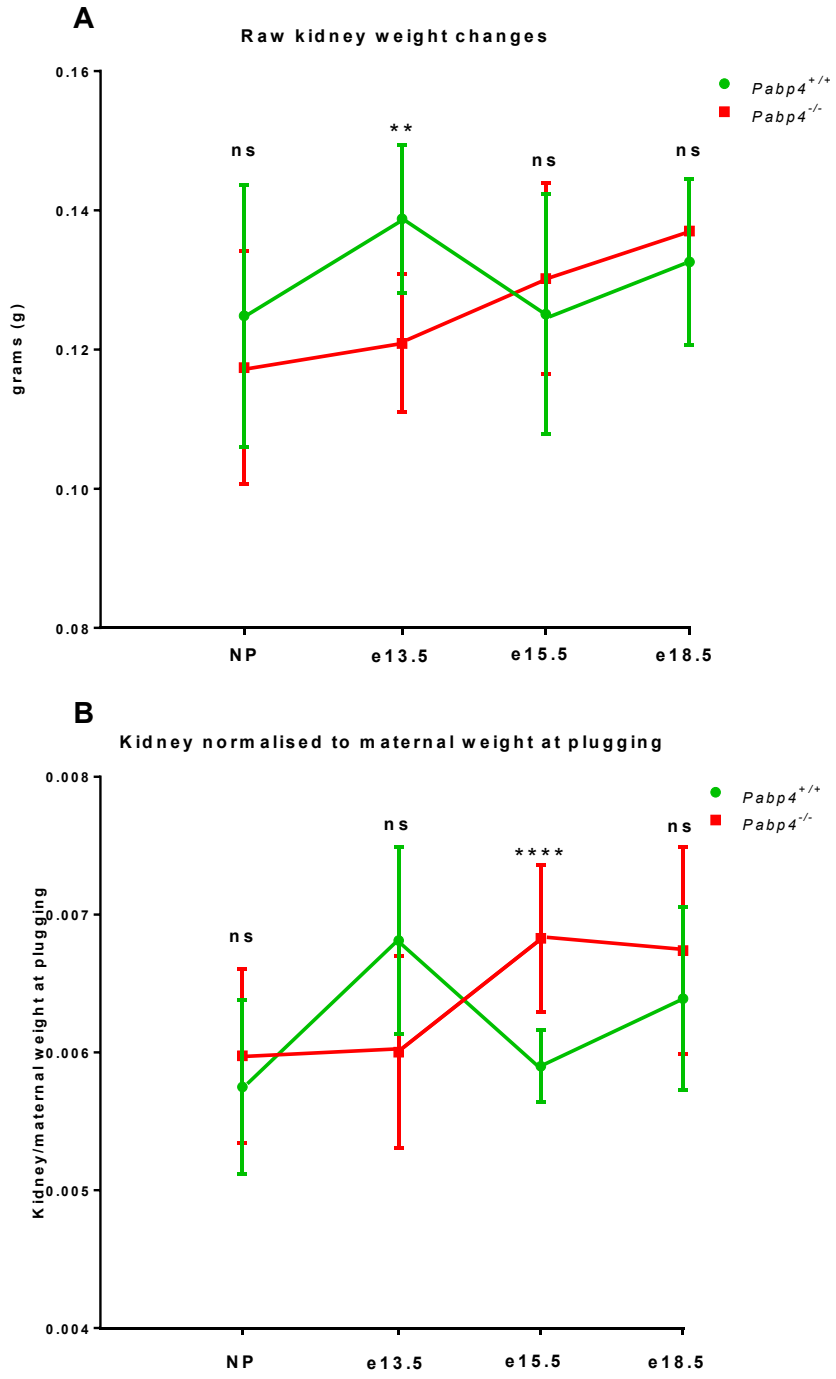

Figure 6.14. Raw and normalised kidney weight changes during pregnancy.

(**A**) Raw kidney weights and (**B**) kidney weights normalised to maternal weight at plugging a proxy for non-pregnant (NP) females and females at day e13.5, e15.5 and e18.5 of gestation. Left kidney weights from *Pabp4*$^{+/+}$ females (green dots): raw (NP $n = 26$; e13.5 $n = 8$; e15.5 $n = 25$; e18.5 $n = 20$); normalised (NP $n = 26$; e13.5 $n = 6$; e15.5 $n = 21$; e18.5 $n = 20$). Left kidney weights from *Pabp4*$^{-/-}$ females (red squares): raw (NP $n = 13$; e13.5 $n = 8$; e15.5 $n = 15$; e18.5 $n = 18$); normalised (NP $n = 11$; e13.5 $n = 3$; e15.5 $n = 14$; e18.5 $n = 11$). Data are shown as means with standard deviation (SD) indicated as error bars. Significance was analysed at each time-point by student's T-test. ns p = ≥ 0.05; ** p = ≤ 0.01; **** p = ≤ 0.0001.

In *Pabp4*$^{+/+}$ dams the kidney increased in weight from prior to pregnancy to e13.5, fell back to a lower weight at e15.5 and increased again by e18.5 (Figure 6.14 A). This pattern is disparate to that reported in literature where the kidney has been reported to progressively increase in size/weight during pregnancy as a result of the dilatation of the collecting system including the renal pelvis (funnel for urine flowing to the ureter) and the ureter (duct for urine passing from kidney to bladder). This unexpected weight trajectory of the *Pabp4*$^{+/+}$ kidney is most likely due to a small n number at the e13.5 time-point and should be increased. The weight of *Pabp4*$^{-/-}$ kidneys increased throughout gestation and was equivalent to that of *Pabp4*$^{+/+}$ kidneys apart from e13.5 when it was significantly smaller. This may be due to the e13.5 collection time-point being underpowered, resulting in an unusual peak in kidney size in *Pabp4*$^{+/+}$ mice (Figure 6.14 A). Normalised *Pabp4*$^{-/-}$ kidney weights were comparable to *Pabp4*$^{+/+}$ prior to pregnancy, at e13.5 and e18.5 but significantly greater at e15.5 (Figure 6.14 B). Thus, similarly to the liver data, the method of analysis impacts the outcome and interpretation (e.g. *Pabp4*$^{-/-}$ kidneys both with respect to the timing and whether *Pabp4*$^{-/-}$ kidneys are larger or smaller. This discrepancy may resolve with a larger dataset in which *Pabp4*$^{+/+}$ kidneys show normal weight trajectories.

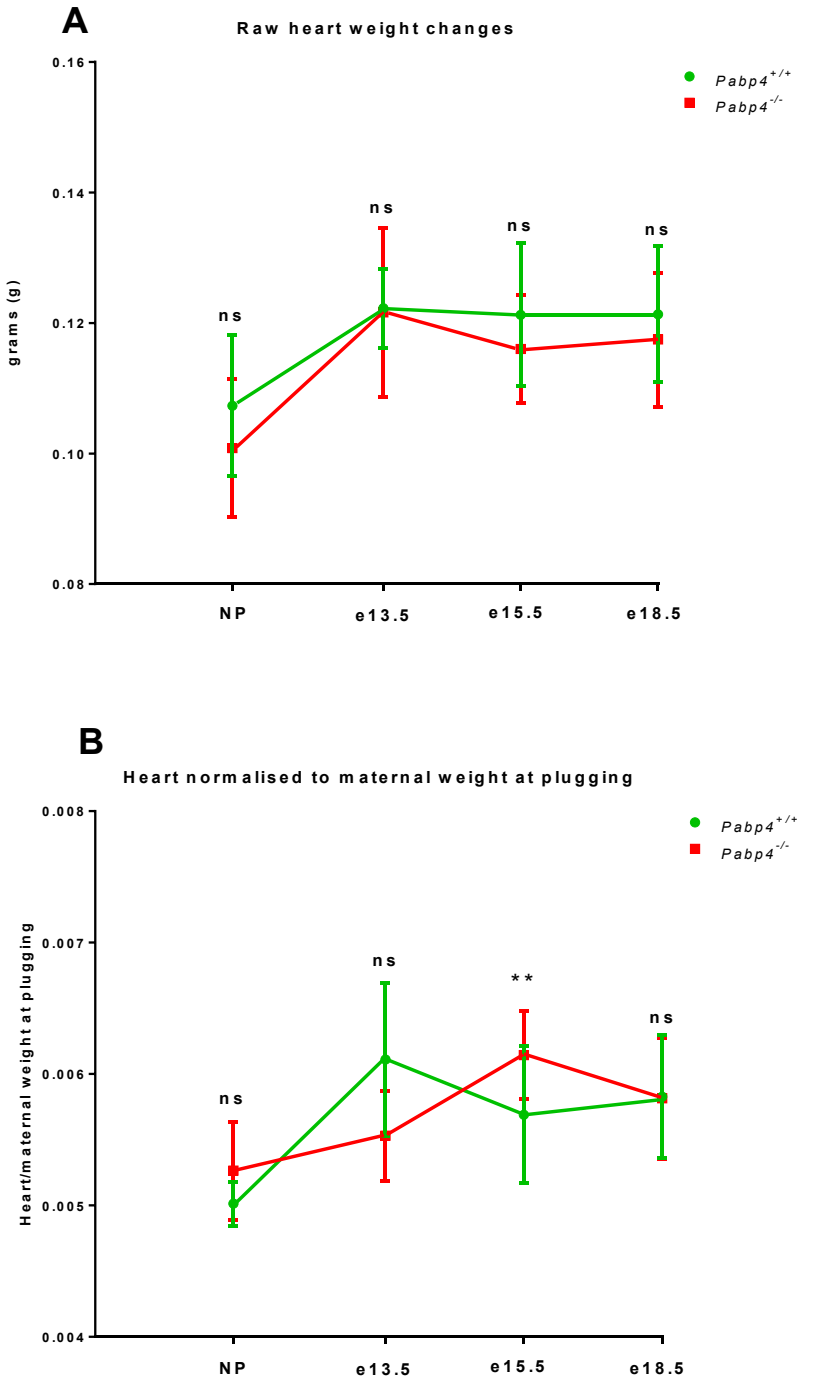

Figure 6.15. Raw and normalised heart weight changes during pregnancy.

(**A**) Raw heart weights and (**B**) heart weights normalised to maternal weight at plugging from non-pregnant (NP) females and females at day e13.5, e15.5 and e18.5 of gestation. Heart weights from *Pabp4*$^{+/+}$ females (green dots): raw (NP $n = 25$; e13.5 $n = 8$; e15.5 $n = 23$; e18.5 $n = 21$); normalised (NP $n = 17$; e13.5 $n = 6$; e15.5 $n = 23$; e18.5 $n = 29$). Heart weights from *Pabp4*$^{-/-}$ females (red squares): raw (NP $n = 13$; e13.5 $n = 8$; e15.5 $n = 15$; e18.5 $n =$

18); normalised (NP n = 11; e13.5 n = 3; e15.5 n = 14; e18.5 n = 11). Data are shown as means with standard deviation (SD) indicated as error bars. Significance was analysed at each time-point by student's T-test. ns p = ≥ 0.05; ** p = ≤ 0.01.

Similarly to the other organs, the heart also undergoes physiological changes during pregnancy, primarily due to the increase in blood volume and resultant cardiac volume (reviewed by (Chung and Leinwand, 2014). These changes result in cardiac hypertrophy whereby the heart muscle gains mass and an increase in chamber dimension which may be associated with wall thickness. The maternal raw heart weights of *Pabp4*$^{+/+}$ females increased from a non-pregnant state to e13.5 and, similarly to the liver, remained heavier beyond this point until late gestation (Figure 6.15 A) (Chung and Leinwand, 2014). These weight changes were paralleled by *Pabp4*$^{-/-}$ heart weights (Figure 6.15 A). *Pabp4*$^{+/+}$and *Pabp4*$^{-/-}$ heart weights were also equivalent following normalisation except for e15.5 when *Pabp4*$^{-/-}$ heart weights were significantly heavier (Figure 6.15 B). An increase in heart weight in *Pabp4*$^{-/-}$ dams at e15.5 may be suggestive of pathological rather than physiological hypertrophy however the disparity between the two methods of analysis, preclude conclusion in the absence of further work (see below).

	Weight changes observed			
Organ	**Raw**	**Normalised**	**Normalised to:**	**PABP4 expression in organ**
Liver	↓ at e13.5	No change (data missing for NP and e18.5)	Maternal weight at collection	YES
Kidney	↓ at e13.5	↑ at e15.5	Maternal weight at plugging	YES
Spleen	↓at e13.5 and e15.5	N/A	N/A	YES
Heart	No change	↑ at e15.5	Maternal weight at plugging	YES

Table 6.1. Summary of organ weight changes and PABP4 expression.

In summary, with the exception of spleen, the data on organ weight in *Pabp4*$^{-/-}$ dams are affected by whether they are considered as raw or normalised weights (summarised in Table

6.1). When considered as raw weights the liver, kidney and the spleen, but not the heart, are significantly reduced at e13.5 and may potentially explain the significantly reduced maternal weight gain also observed at e13.5 (Figure 6.8.). When the organ weights are normalised this weight reduction is lost and the weight for some organs is increased (kidney, heart) at e15.5 (both normalised to maternal weight at plugging) (summarised in Table 6.1). , It remains to be determined which analysis method is most appropriate and normalisation to brain weight, as often done in toxicology studies may prove useful as it is not affected by bodyweight, correlates with age and importantly does not change with pregnancy. Unfortunately, brain weights were not obtained at the time of collections and therefore this normalisation cannot be done with the current dataset. Another frequently used method that may have utility is tibia length. However, our data with spleen suggest that at least one aspect of maternal adaptation deviates from that seen in *Pabp4* $^{+/+}$ mice.

Many of the physiologic changes that occur in pregnancy are the result of an interplay between hormones, growth factors and cytokines produced by the placenta and maternal organs. Therefore the levels of several factors in maternal plasma were examined to test the hypothesis that the circulating levels of one or more of these factors may be altered in the *Pabp4*$^{-/-}$ mouse due to dysregulated production. The ovarian hormones, estradiol and progesterone, are essential for the establishment (Adams and DeMayo, 2015), maintenance (Beagley and Gockel, 2003) and initiation of parturition of pregnancy but also contribute to maternal adaptations e.g. heart (Chung and Leinwand, 2014) and haematopoietic system (Nakada et al., 2014). Chung and Leinwand (2014) grouped serum progesterone and estradiol levels of rodents from previous reports to show that serum progesterone increases in early pregnancy, peaks at e15-16 of pregnancy and significantly decreases by e18 (Chung and Leinwand, 2014). In contrast to this human serum progesterone concentration rises in a linear fashion up until term (Johansson, 1969; Tulchinsky et al., 1972) and unlike in rodents and some other species there is no dramatic drop in human progesterone prior to parturition (Tulchinsky et al., 1972). There is a lack of data regarding serum estradiol changes from non-pregnant into and throughout pregnancy in mouse, but it has been reported to peak on e18-19 and decrease 0-1 days post-partum (dpp) (Chung and Leinwand, 2014). In humans, similarly to progesterone, estradiol concentrations increase as pregnancy progresses (Levitz and Young, 1977; Lindberg et al., 1974; Tulchinsky et al., 1972). To test whether *Pabp4*$^{-/-}$ females present with a hormonal imbalance plasma estradiol and progesterone levels were quantified using ELISA at e18.5, a

time-point by which IUGR is well established and just prior to the major decrease in litter size. Interestingly, maternal plasma estradiol was significantly decreased in *Pabp4*$^{-/-}$ compared to *Pabp4*$^{+/+}$ females (Figure 6.16. A), whereas progesterone was significantly increased (Figure 6.16. B). Despite the absence of defects in implantation rates in *Pabp4*$^{-/-}$ mice, the role of these sex steroids in pregnancy maintenance means that alterations in their levels, particularly estradiol, could contribute to the development of the phenotype in the *Pabp4*$^{-/-}$ dams (see discussion).

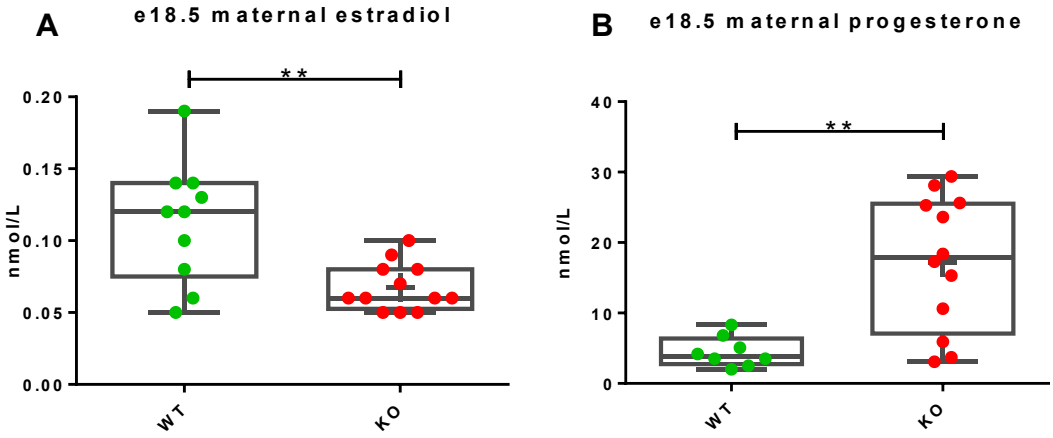

Figure 6.16. *Pabp4*$^{-/-}$ dams have an imbalance of estradiol, progesterone at e18.5.

Maternal blood plasma of *Pabp4*$^{+/+}$ (WT; green dots) and *Pabp4*$^{-/-}$ females (KO; red dots) collected at e18.5 analysed using competitive time resolved fluorescence immunoassay (TRFIA) to determine levels of (**A**) estradiol (WT $n = 10$; KO $n = 12$), (**B**) progesterone (WT $n = 8$; KO $n = 12$). Data are shown as shown as box and whisker plots with the median (long line) and mean (cross) indicated. Significance was analysed by student's T-test. ** p = ≤ 0.01.

In addition to the classic sex steroid hormones, other growth factors, hormones and metabolites in the maternal circulation are also key in fetal growth and survival. IGF-1 and IGF-2 are both important determinants of fetal growth (Baker et al., 1993; DeChiara et al., 1990; Liu et al., 1993) and placentation (Holmes et al., 1998; Qiu et al., 2005) but exert their effects by different mechanisms. IGF-1 acts by directly affecting fetal growth and diverting maternal adipose stores to the fetus in late pregnancy (Sferruzzi-Perri et al., 2006). IGF-2 on the other hand alters

placental development to favour fetal growth (Sferruzzi-Perri et al., 2006). Therefore, IGF-1 maternal plasma levels were investigated at e15.5, at which point IUGR is apparent, and at e18.5, prior to increased incidence of fetal death. However, neither of these time-points showed difference in maternal plasma levels of IGF-1 between *Pabp4*$^{-/-}$ and *Pabp4*$^{+/+}$ female (Figure 6.17 A, B), suggesting that aberrant maternal adaptation due to changed IGF-1 levels are not the cause of IUGR in *Pabp4*$^{-/-}$ females.

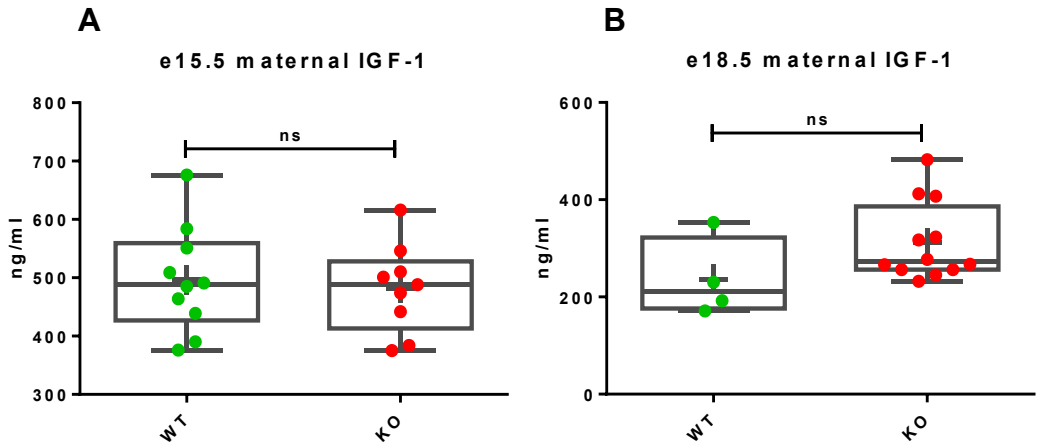

Figure 6.17.Maternal plasma IGF-1 levels are comparable in *Pabp4*$^{-/-}$ and *Pabp4*$^{+/+}$ dams at both e15.5 and e18.5.

Maternal plasma IGF-1 levels measured using ELISA immunoassay from *Pabp4*$^{+/+}$ (WT; green dots) and *Pabp4*$^{-/-}$ (KO; red dots) females collected at (**A**) e15.5 (WT $n = 10$; KO $n = 9$) and at (**B**) e18.5 (WT $n = 4$; KO females $n = 12$). Data are shown as shown as box and whisker plots with the median (long line) and mean (cross) indicated. Significance was analysed by student's T-test. ns p = ≥0.05.

As discussed, fetal growth is sensitive to the nutritional status of the mother and as a result of needing to balance the demands of the fetus with that of the mother, many changes in maternal metabolic and even behaviour (e.g. appetite) occur during pregnancy. Lipid metabolism alters in pregnancy to increase fat storage in early gestation and enhance lipid catabolism in late gestation providing an alternative maternal energy source to carbohydrates enabling the nutritional demands of the growing fetus to be met (Alvarez et al., 1996; Lopez-Luna et al., 1991; Montelongo et al., 1992). The switch from maternal carbohydrate to fat utilization, partitioning glucose for the feto-placental unit whose energy demands are particularly high in

late gestation is the result of progressive insulin resistance (Butte, 2000). Insulin levels rise to partly overcome the resistance and prevent gestation diabetes mellitus developing (Brelje et al., 1994; Parsons et al., 1992). Concurrently, there is a rise in leptin levels, an adipocytokine associated with insulin resistance and the switch in metabolism (Fasshauer and Paschke, 2003; Weyer et al., 2001). Maternal hyperleptinemia, isolated from maternal obesity or diabetes, has been shown to result in reduced fetal birthweight (Makarova et al., 2013; Yamashita et al., 2001). To investigate this, non-fasted maternal insulin and leptin plasma levels were measured at e18.5 to discern whether *Pabp4*$^{-/-}$ females have comparable levels to those of *Pabp4*$^{+/+}$ females. Maternal plasma insulin was found to be comparable between the genotypes, however, intriguingly, maternal leptin was found to be significantly increased in *Pabp4*$^{-/-}$ females (Figure 6.19 A, B). It is important to note that plasma levels do not inform on the maternal sensitivity to insulin and leptin, which would require tolerance testing. These would be useful in determining whether a disrupted response to insulin and/or leptin may be implicated in the development of the phenotype. However, the increased levels of leptin suggest that lipid metabolism may be disrupted which has the potential to be a contributing causal factor to the phenotype. In keeping with this idea, abnormal cholesterol and FFA levels have been reported for *Pabp4*$^{-/-}$ mice in the EUKOMM pipeline which are on high fat diet (http://www.mousephenotype.org/data/experiments?geneAccession=MGI:2385206&mpTermId=MP:0005376&mpTermId=MP:0005375). However, no data on mice maintained on normal diet or when pregnant is available.

It is known that low-density lipoprotein cholesterol (LDLc) and triglycerides (TGs) increase progressively in gestation (Belo et al., 2002; Serdar et al., 2003) whereas high-density cholesterol (HDLc) begins to decrease post midgestation (Belo et al., 2002). Dyslipidemia is associated with pregnancy complications such as pre-eclampsia where an increase in LDLc, TG levels and a decrease HDLc levels have been observed (Belo et al., 2002; Var et al., 2003). This increased hyperlipidemic state may lead to atherosis, atherosclerosis-like" lesions, in maternal decidual vessels and reduced placental perfusion which may result in altered placental transfer of nutrients (Catarino et al., 2008). To test whether *Pabp4*$^{-/-}$ females have altered lipid profiles, non-fasted maternal plasma HDLc and LDLc and FFA were determined but were found to be comparable in *Pabp4*$^{-/-}$ and *Pabp4*$^{+/+}$ females at e18.5 (Figure 6.18 A, B, C). The power of the *Pabp4*$^{+/+}$ female cohort for LDLc was very low and therefore additional numbers would therefore strengthen this tentative conclusion. This result is, however, in line with the

Doppler results in chapter 5, which showed normal resistance index suggesting that the maternal uterine arteries in *Pabp4*$^{-/-}$ mice were not functionally compromised.

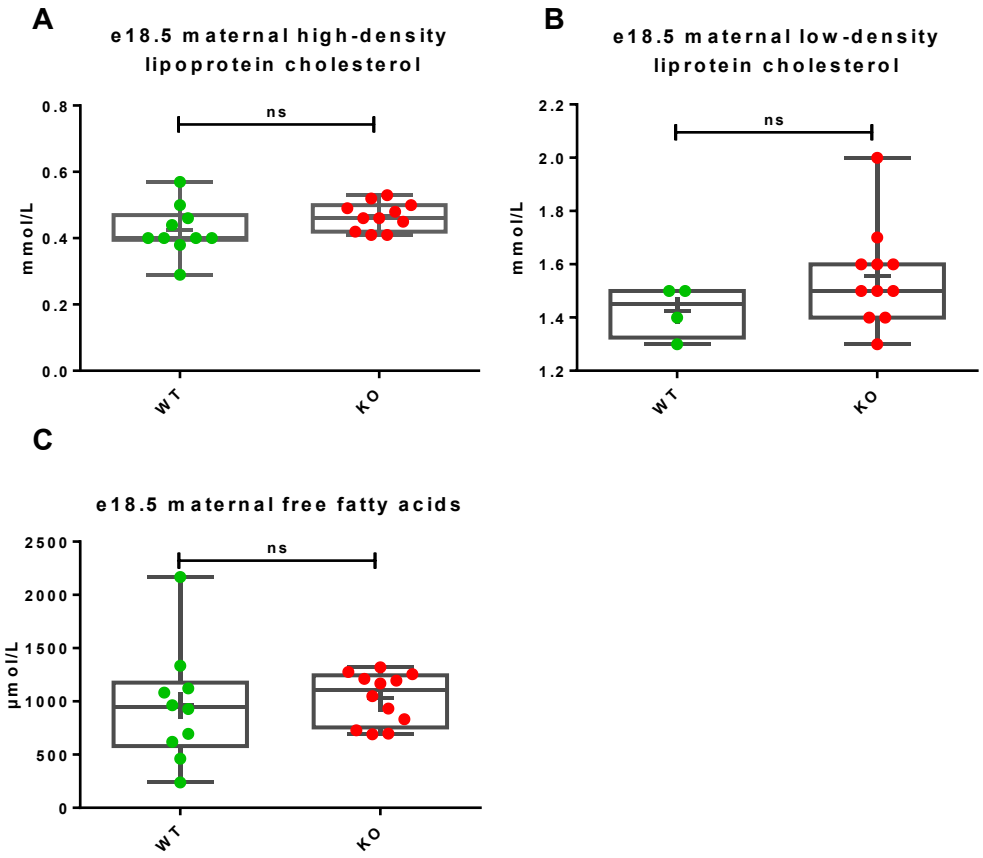

Figure 6.18.Maternal plasma levels of high-density and low density lipoprotein cholesterol and free fatty acid are comparable in *Pabp4*$^{-/-}$ and *Pabp4*$^{+/+}$ dams at e18.5.

Maternal blood plasma of *Pabp4*$^{+/+}$ (WT; green dots) and *Pabp4*$^{-/-}$ females (KO; red dots) collected at e18.5 analysed using Randox colourimetric assay to determine levels of (**A**) high-density lipoprotein (HDL) (WT n = 9; KO n = 12), (**B**) low-density lipoprotein (LDL) cholesterol (WT n = 10; KO n = 12) and a half micro test kit to determine (**C**) free fatty acids (FFA). Data are shown as shown as box and whisker plots with the median (long line) and mean (cross) indicated. Significance was analysed by student's T-test. ns p = ≥ 0.05.

Finally, plasma levels of maternal corticosterone were examined. Corticosterone has been shown to have an important role in regulating nutrient allocation between the mother and the feto-placental unit during periods of stress such as food restriction whereby it limits fetal

growth by reducing the amino acid supply and density of blood vessels in the placenta (Vaughan et al., 2012). Interestingly comparisons of plasma from *Pabp4*$^{+/+}$ and *Pabp4*$^{-/-}$ females, revealed that maternal corticosterone was significantly decreased in *Pabp4*$^{-/-}$ females (Figure 6.19 C) which has the potential to also be important in the phenotype and therefore this observation should be investigated further (see discussion).

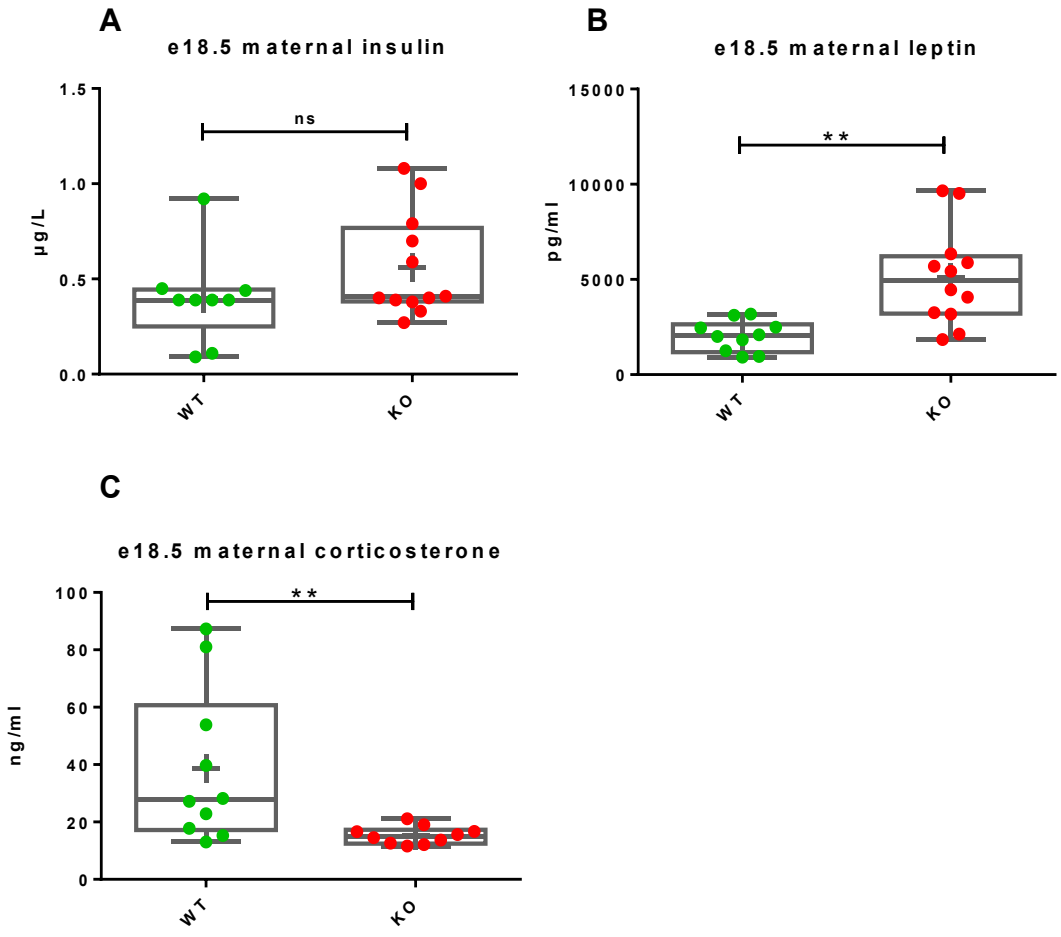

Figure 6.19. *Pabp4*$^{-/-}$ dams have normal plasma insulin levels, increased leptin levels and reduce corticosterone levels at e18.5.

Maternal blood plasma of *Pabp4*$^{+/+}$ (WT; green dots) and *Pabp4*$^{-/-}$ females (KO; red dots) collected at e18.5 analysed using electrochemical luminescence immunoassay to determine levels of (**A**) insulin (WT n = 9; KO n = 12), (**B**) leptin (WT n = 10; KO n = 12), and a competitive enzyme immunoassay (EIA) to determine (**C**) corticosterone (WT n = 10; KO n = 10). Data are shown as shown as box and whisker plots with the median (long line) and mean (cross) indicated. Significance was analysed by student's T-test. ns p = ≥ 0.05; ** p = ≤ 0.01.

Similarly to other systems, the haematological system also undergoes changes to adapt to pregnancy and to accommodate the fetoplacental unit. The levels of both white and red cells are critical in pregnancy and the spleen which becomes a site of red cell production was comparatively reduced in size during mid-pregnancy in *Pabp4*$^{-/-}$ females (Figure 6.12). As a first step towards determining if *Pabp4*$^{-/-}$ females have a maladapted haematological system, I examined their haematological state in non-pregnancy, as timing constraints did not allow for the necessary breeding cohorts to be set up for equivalent pregnancy based studies. To this end, we conducted a haematological investigation a of red blood cells, white blood cells and platelet in whole blood from non-pregnant *Pabp4*$^{-/-}$ and *Pabp4*$^{+/+}$females. This revealed that platelet and white blood cell count (the number of cells in a given volume of blood) were normal, with equivalent numbers of neutrophils, lymphocytes, monocytes and eosinophils (see Appendix Figure 8.5, Figure 8.6). Red blood cell (RBC) counts also showed no significant difference. Additional red blood cell characteristics were also examined. Importantly the haematocrit (HCT) which is the measure of volume of red blood cells as a percentage of whole blood was decreased. Whilst this is not due to a decrease in red cell number (1.21 A), or red blood cell distribution width (RDW) (1.21 F), the mean cell volume (MCV) (the average size of red blood cells) was decreased (1.21 D). Consistent with a reduced MCV, haemoglobin (Hb) (concentration measurement of total haemoglobin per volume of whole blood) was reduced (Figure 6.20C.) although mean cell haemoglobin (MCHC) (haemoglobin concentration divided by haematocrit) was not (Figure 6.20D.).

This data indicate that the red blood cells in non-pregnant *Pabp4*$^{-/-}$ mice are reduced in volume (microcytic) and contain less haemoglobin, hinting at a possible pre-existing condition, and warranting further investigation in pregnant mice (see discussion).

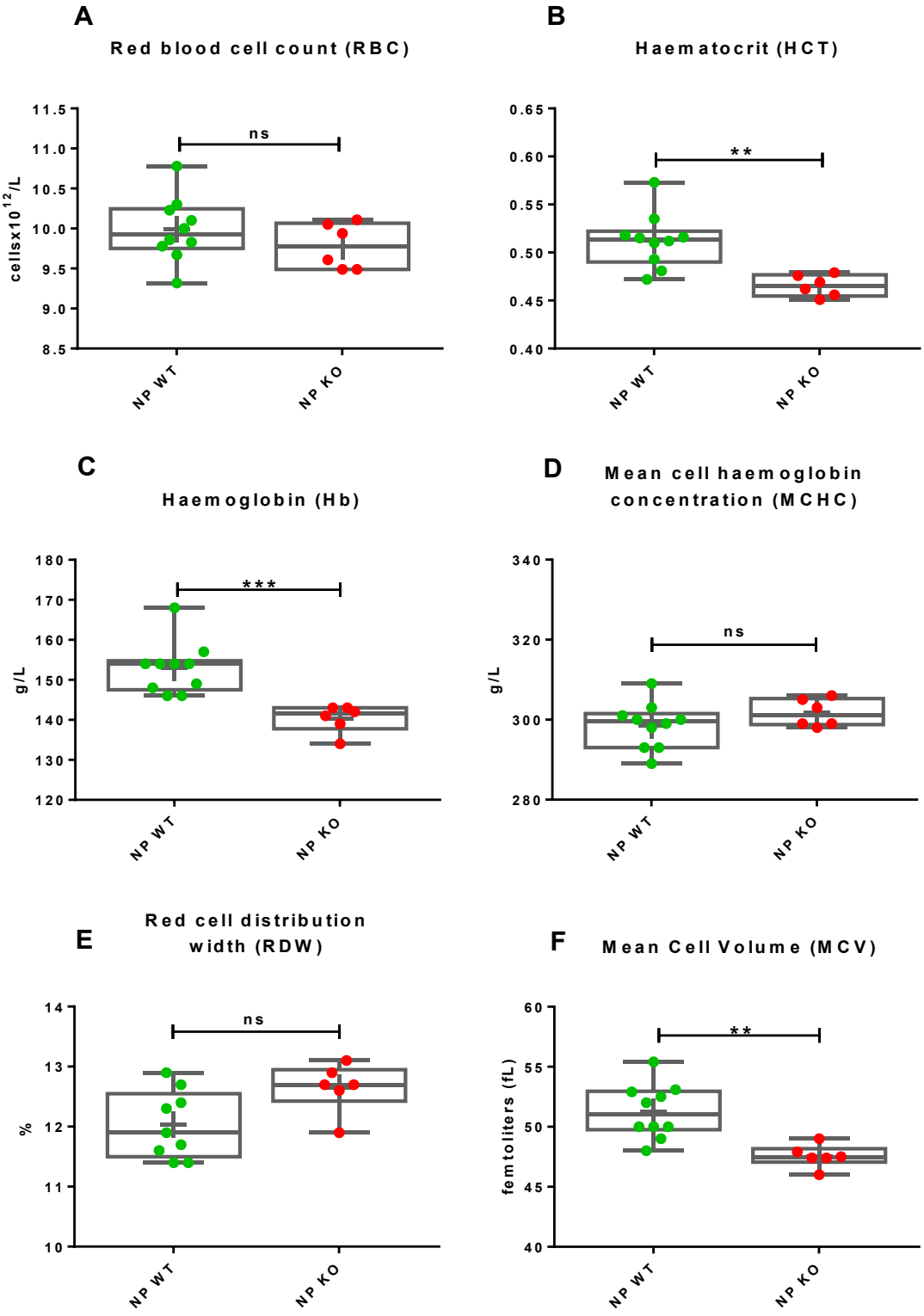

Figure 6.20.Red blood cell count and red blood cell indices analysis of non-pregnant *Pabp4*$^{+/+}$ and *Pabp4*$^{-/-}$ females.

Analysis of non-pregnant (NP) *Pabp4*$^{+/+}$ (WT; green dots; n = 10) and *Pabp4*$^{-/-}$ female blood (KO; red dots; n = 6) using an automated flow cytometer-based haematological analyser. (**A**) Red blood cell count and (**B**) haematocrit (HCT), (**C**) red blood cell haemoglobin (Hb), (**D**) mean cell haemoglobin concentration (MCHC),

(**E**) mean cell volume (MCV), (**F**) red cell distribution width (RDW). Data are shown as shown as box and whisker plots with the median (long line) and mean (cross) indicated. Significance was analysed by student's T-test. ns p = ≥0.05; ** p = ≤ 0.01; *** p = ≤ 0.001.

6.3 Discussion

The aim of this chapter was to shed light on the potential role of maternal physiology and adaptations to pregnancy in *Pabp4*$^{-/-}$ females. Whilst the genetics show that the primary defect is maternal in nature, they do not clarify whether the phenotype arises as a result of a pre-existing, but perhaps subtle, deficit in maternal physiology that becomes "functionally relevant" during pregnancy or one that is unique to the pregnant state. Furthermore, the placenta changes observed in Chapter 5 raise the possibility that rather than the maternal systems being unable to respond and adapt to the correct signals from the placenta, any mal-adaptation could arise from signalling from the placenta itself being compromised. In the latter case, the phenotype may arise from an early failure in materno-fetal communication where a deficit in one or more maternal cell type results in incorrect placentation, which in turn leads to maternal mal-adaptation. Whilst this is a complex problem, my data sheds some important light.

Firstly, by exploring the expression pattern of PABP4 (and PABP1), we expand upon published northern blot data ((Wilkie et al., 2005), to establish that both are expressed in a wide variety of tissues (i.e. kidney, liver, pancreas): in some cases showing highly similar (e.g. kidney) and others reciprocal expression patterns (e.g. pancreas). Therefore whilst the phenotypes are reproductive, the maternal defect may lie, or involve tissues, outside the reproductive tract. Confirming these patterns requires further work due to technical issues, a second PABP1 antibody (or PABP1$^{-/-}$ mouse tissue) to further control for its specificity and a more quantitative analysis of cell type specific changes in expression (e.g. immunofluorescence). Moreover markers are required to further inform which cells (e.g. in the red pulp of the spleen) are PABP expressing to relate these further to our other observations (e.g. genotype-dependent reduction in spleen; reduced haematocrit). Additionally, there are several limitations of the western blot data of which aimed to investigate whether there are any changes in the levels of PABP4 and/or PABP1 in maternal organs from non-pregnancy to pregnancy. Firstly, a negative control was not run alongside the samples such as a *Papb4*$^{-/-}$ sample to rule out any cross reaction, particularly with PABP1. Secondly, the signal in some cases varied substantially within a cohort of samples and therefore an n of 3 for each group is most likely insufficient to reveal any true differences in the levels of PABPs between non-pregnant and pregnant samples. Therefore an appropriate n number based on the variability of signal within a group should

have first been determined and subsequently used. Lastly, although the level of protein loaded per sample was the same, the levels of PABPs were not compared to that of the housekeeping gene used (GAPDH) which would have enabled a more quantitative interpretation of the results. Overall, these limitations of the western blot data hamper any interpretation of the results. However, in the future it would be worth repeating the experiment to accurately determine any changes in the levels of PABP4 with pregnancy as this may provide the basis of investigating specific organs in more detail as being implicated in the cause of the PABP4 phenotype. Western blots of the pancreas and kidney were not included in the thesis as they technically failed and need to be repeated in the future. It would also be of great interest to expand analysis to other organs such as the pituitary, adrenal gland and adipose tissue whose function may be relevant to changes uncovered in this chapter and the described pregnancy phenotypes.

Our analysis of PABP expression patterns, body weight and organ weights examined both pregnant and non-pregnant mice. Our data suggested that low pre-pregnancy weight was unlikely to be a cause of the phenotype, although weight gain was altered in pregnant mice. Similarly organ weight, both raw and normalised, argued against a pre-existing effect on their size in *Pabp4*$^{-/-}$ mice. Challenges posed in terms of the most appropriate method of normalisation precluded conclusions as to the changes in most organ sizes during pregnancy, since normalised and raw values lead to contradictory interpretations. However, spleen showed a pregnancy specific reduction in size compared to *Pabp4*$^{+/+}$ mice during gestation (e13.5-15.5), suggesting that this aspect of maternal adaptation has not proceeded normally. Detailed histological analysis of organs in which size (and/or functional, see below) genotype-dependent changes are present, combined with PABP expression patterns, may provide additional insight into their significance with respect to the observed phenotypes (e.g. in spleen does restricted expansion of the red pulp underlie the size difference?). Systematic histological analysis including use of appropriate markers and stains may also reveal genotype-dependent changes within these tissues that are not apparent at gross level (e.g. size). For instance several pregnancy specific diseases of the liver have been described (reviewed by (Hay, 2008), although they do not correlate well with our observations in *Pabp4*$^{-/-}$ mice.

In contrast to changes in body weight and organ size that were only observed during pregnancy, haematocrit was reduced in non-pregnant *Pabp4*$^{-/-}$ mice, suggestive of a pre-existing condition

that may contribute to the phenotype, as severe anaemia is associated with IUGR (Wollmann, 1998). In contrast WBC and platelet counted appeared normal, although substantial further work would be needed to rule out a functional deficiency in these cells, with immune cells in particular playing important roles in pregnancy. The reduced haematocrit in *Pabp4*$^{-/-}$ mice manifested as a significant reduction in haemoglobin and mean cell volume (MCV) (Figure 18.), which are features of microcytic anaemia (Massey, 1992), a condition often due to nutritional deficiencies or genetic mutations . This observation is lent weight by recent studies that identified PABP4 as a potential regulator of erythroid differentiation in cell lines, as its knock-down blunted the terminal stages of differentiation and haemoglobin levels (Kini et al., 2014). However, it is not yet clear whether abnormal erythropoiesis persists, is exacerbated or ameliorated during pregnancy. In non-pregnant adult mice, the bone marrow represents the primary site of erythropoiesis, emphasising a need to examine bone marrow and PABP4 expression therein. However, the red pulp of the spleen represents a second site of erythropoiesis during pregnancy with PABP4 being expressed in one, or more, cell types within this compartment. Thus it will be of interest to determine whether the reduced expansion of the spleen during pregnancy in *Pabp4*$^{-/-}$ mice correlates with decreased RBC volume in splenic erythropoiesis.

The work here also provides evidence for further work examining the metabolic changes that are necessary to meet the nutritional demands of the fetus. *Pabp4*$^{-/-}$ females show increased leptin, decreased corticosterone, decreased fetal blood glucose, and increased mRNA levels of glucose and amino acids transporter in the placenta. In contrast insulin, maternal blood glucose, cholesterol and FFA appeared within normal range, although further clarity with respect to cholesterol levels may be achieved with more animals and fasted glucose and insulin levels were not determined. Whilst a clear picture with respect to these metabolic changes is yet to emerge, these observations nonetheless inform on the potential origins of the phenotype.

For instance, expression of PABP4 in the exocrine rather than endocrine, insulin producing, cells of the pancreas is consistent with the normal maternal insulin and glucose levels in *Pabp4*$^{-/-}$ mice. The exocrine cells synthesize, store and secrete digestive enzymes which break down starch, protein and fat when secreted into the small intestine. Abnormal release of these hormones can lead to exocrine pancreatic insufficiency (EPI), characterised by an inability to properly digest food associated with growth failure, fat-soluble vitamin deficiencies decreased bone mineral density and kyphosis (Aris et al., 2005; Grey et al., 2008). Whilst a systemic

nutrient deficiency associated with poor nutrient uptake could explain poor fetal growth and upregulated placental transporters, *Pabp4*$^{-/-}$ females do not, for example, have low bodyweight prior to pregnancy; apparent concomitant up-regulation of PABP1 in these acinar exocrine cells, may therefore be able to partially or completely compensate for loss of *Pabp4*. As discussed earlier, other findings could also inform on the basis of the phenotype, for instance, studies of maternal hyperleptinemia (Yamashita et al., 2001) suggest that the observed increase in leptin in *Pabp4*$^{-/-}$ mice (Jansson et al., 2003) could contribute to the IUGR. Its contribution could be tested by the use of leptin agonists to reduce leptin levels in the *Pabp4*$^{-/-}$ mouse.

Maternal adaptations are driven by multiple secreted factors which derive from both the placenta (e.g. placental lactogens) and maternal organs (e.g. oestrogen, progesterone, corticosterone) and can often affect multiple target tissues altering their gene expression programs to adapt their structure (e.g. size) and/or function. In this regards it was interesting that whilst IGF-1 and insulin levels were normal, estradiol, progesterone, leptin and corticosterone were all changed, as discussed above. The results of such changes are likely to be complex, for instance, estradiol, has multiple adaptation roles meaning it is a candidate whose dysregulation could interplay with other changes observed here. For example, estradiol insufficiency caused by ovariectomy impairs central leptin sensitivity and increases circulating plasma leptin concentrations (Ainslie et al., 2001). Similarly, rising estradiol levels promote haematopoietic stem-cell division, frequency and erythropoiesis in the spleen during pregnancy (Nakada et al., 2014). Therefore it would be interesting to investigate whether normal leptin can be restored by exogenous estradiol or transplantation of wild-type ovaries (the source of estradiol), and whether erythropoiesis increases sub-optimally in pregnant *Pabp4*$^{-/-}$ dams.

In summary, whilst not an exhaustive study, this work provides evidence that aspects of maternal physiology beyond the sites of development of the materno-fetal units in the uterus, can influence their growth and survival. Future work (see chapter 7) will be aimed at adding to these snapshots to enable a clearer picture to emerge with the ultimate aim of identifying which, if any of these changes, are causative.

Chapter 7 – Final Discussion

The aim of this thesis was to establish the phenotypic consequences of the loss of PABP4 function in mammals, extending our previous knowledge of its function in non-mammalian vertebrates, and providing the first insight into the role of a non-germ cell specific PABP in mammals. In contrast to non-mammalian vertebrates, PABP4 was found not to be essential for embryogenesis in mice. Furthermore, the phenotype resulting from the loss of PABP4 differed from the phenotypes observed with loss of ePABP in *X. laevis* and mammals, as it was not required for oocyte development, despite being expressed small growing oocytes and granulosa cells (Chapter 3). Importantly though, it nonetheless impacted female fecundity as litter size was found to be reduced in late gestation and even more so by birth. Critically, this phenotype was dependent solely on the maternal genotype with paternal and fetal genotype having no impact (Chapter 3). Longitudinal analysis showed that implantation rates were not significantly altered but that fetal death was occurring primarily in late gestation (Chapter 3). In association with the maternally-dependent reduced litter size, fetuses of *Pabp4*$^{-/-}$ dams also presented with symmetrical IUGR which established prior to the most dramatic reduction in litter size; between e18.5 and birth (Chapter 4). However, the time-point at which IUGR becomes first apparent still needs to be determined, as the current dataset of the earliest time-point investigated (e13.5) is inconclusive. Together, these data provide evidence that *Pabp4*$^{-/-}$ dams offer an attractive, if not unique, opportunity for studying the maternal contribution to related pregnancy disorders that includes IUGR and stillbirth (Figure 7.1).

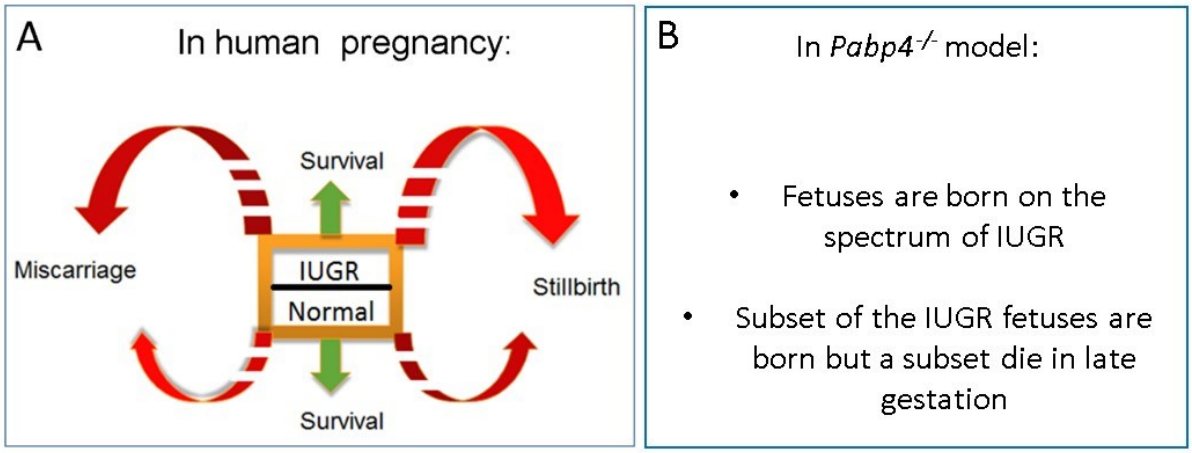

Figure 7.1 Similarities between human clinical settings and the *Pabp4*$^{-/-}$ pregnancy mouse model of IUGR and miscarriage/stillbirth.

In humans, not all pregnancies complicated by IUGR result in miscarriage or stillbirth and not all babies which are a 'normal' size survive with the underlying causes often unknown. Similarly in the Pabp4$^{-/-}$ mouse model of pregnancy, a range of growth restriction is present accompanied by late gestational lethality of a proportion of pups, with some more profoundly growth restricted pups born live, showing that the IUGR, does not *a priori* result in fetal death.

Despite the parallels between our model and human pregnancy disorders, it is often difficult to know how to relate IUGR datasets in mouse to that in human. In mouse, the genetic potential for growth can be relatively easily established, aiding the identification of IUGR. In humans SGA is defined as a birth weight below the 10th percentile for gestational age but does not distinguish between infants that are constitutionally small due to factors such as maternal weight or height, ethnicity or parity, and those that are small as a result of maternal, fetal/placental abnormalities and/or environmental factors. According to the World Health Organisation (WHO), birthweight below the 10th percentile of the recommended gender-specific birthweight for gestational age reference curves are considered as IUGR. Using the 10th percentile as a standard results in over diagnosis and therefore some have suggested using the 5th percentile to define IUGR infants (Bernstein, 1996).

In order to define IUGR observed in *Pabp4*$^{-/-}$ dams in a similar way to that used clinically in humans, we constructed frequency distribution curves, as described previously (Dilworth et al., 2011), of *Pabp4*$^{+/+}$ fetal weights at e18.5 from wild-type crosses and used these to calculated the 5th and 10th centiles as well as 25th and 75th centiles. These curves where then used to

determine which weights, specific to our wild-type population, represent IUGR versus AGA (Figure 7.2). 25% of *Pabp4*$^{+/-}$ fetuses from *Pabp4*$^{-/-}$ dams were found below the 10th percentile (<1035 mg) and 13.4% were below the 5th (<994.4 mg) in comparison to 25% of fetuses from *Pabp4*$^{-/-}$ dams were below the 10th percentile (<1035 mg) and 13.4% were below the 5th (<994.4 mg) in comparison to 5.2% and 1.97% from the WT cross, and 1.8% and 0.68% in the reciprocal cross.

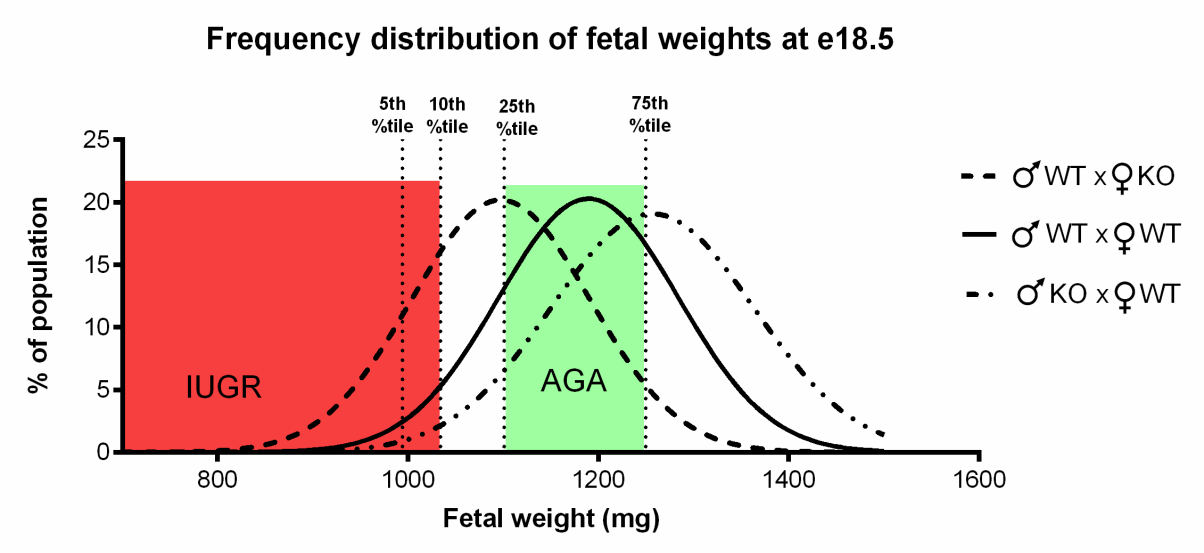

Figure 7.2 Frequency distribution curves for fetal weights from *Pabp4*$^{-/-}$ and *Pabp4*$^{+/+}$ dams at e18.5 shows that a higher percentage of fetuses from *Pabp4*$^{-/-}$ dams are growth restricted and small for their gestational age.

♂ WT x ♀ WT n =134; ♂ WT x ♀ KO n = 117; ♂ KO x ♀ WT n = 83. 5th percentile = 994.4 mg; 10th percentile = 1035 mg; 25th percentile = 1101.2 mg ; 75th percentile = 1249.7 mg. Intrauterine growth restriction, IUGR; Appropriate for gestational age, AGA; percentile, %tile.

This depiction of results, illustrate that fetal weights in litters from *Pabp4*$^{-/-}$ females show a relatively broad range when compared to other fetal genotype-dependent IUGR models such as the P0 mouse, which shows a smaller variation in size and weight reduction (Dilworth et al., 2011). Importantly it also illustrates not only that are litters in *Pabp4*$^{-/-}$ females smaller than in the WT cross, but also that they are smaller than those in the reciprocal cross, which share equivalent genetic background and heterozygosity for *Pabp4*, showing that those developing within a *Pabp4*$^{-/-}$ *in utero* environment have not reached their genetic growth potential and are growth restricted.

Whilst the interpretation that our mice have maternally derived mid-late gestational lethality accompanied by stillbirth is fully consistent with the data at hand, several pieces of additional evidence would further strengthen these conclusions. Firstly, it is difficult to definitively prove that mortality occurred before or during birth rather than immediately after. Cameras for filming birth proved ineffective at providing the required level of resolution to distinguish between dead and alive newborn fetuses. Secondly, a direct demonstration that Mendelian ratios are present at birth would strengthen the conclusion that increased loss of *Pabp4*$^{-/-}$ pups only occurs after birth, as, due to cannibalism of the carcasses, material is seldom available for genotyping of pups from inter-crosses that fail to survive. Thirdly, the use of embryo transfers in which *Pabp4*$^{+/+}$ embryos are transferred into *Pabp4*$^{-/-}$recipients and vice versa would further provide further insight into the maternal nature of the phenotype. The initial design was to use our existing mouse strain. However, the very low success rate of even *Pabp4*$^{+/+}$ embryo transfers into wild-type C57BL/6 recipients precluded this approach (M. Brook, pers. Comm.). Therefore, a hybrid *Pabp4*$^{+/+}$ CD1 strain has been created using the breeding strategy in Figure 7.3 to generate recipients that should enable good embryo transfer, as CD1 females are excellent recipients (Pomp et al., 1989). It is important to note that CD1 animals are an outbred stock and therefore genetically undefined and exhibit hybrid vigor including early fertility, large and frequent litters, low neonatal mortality and rapid growth and these characteristics as well as the genomic heterozygosity of these mice may impact the results obtained from the embryo transfer experiment and should be considered in interpretation. As discussed earlier, it will not be possible to assess effects on litter size using this approach, due to the inherent variability of embryo transfer rates, but measures of embryo weight, crown-rump length, placenta size and diameter at e18.5 will allow for investigation of the fetal/oocyte contribution to IUGR. This experiment is currently ongoing with the prediction that if the IUGR phenotype is related to the maternal ability to support pregnancy, but not fetal genotype, *Pabp4*$^{+/+}$ embryos should present with IUGR in *Pabp4*$^{-/-}$ dams (as seen with *Pabp4*$^{+/-}$ fetuses, Chapter 4) and *Pabp4*$^{-/-}$ fetuses in *Pabp4*$^{+/+}$ dams should present with normal weight and size. So far no differences were found between fetal or placental measurements when *Pabp4*$^{+/+}$ and *Pabp4*$^{-/-}$ embryos were transferred into *Pabp4*$^{+/+}$ dams, supporting this hypothesis (Figure 7.4).

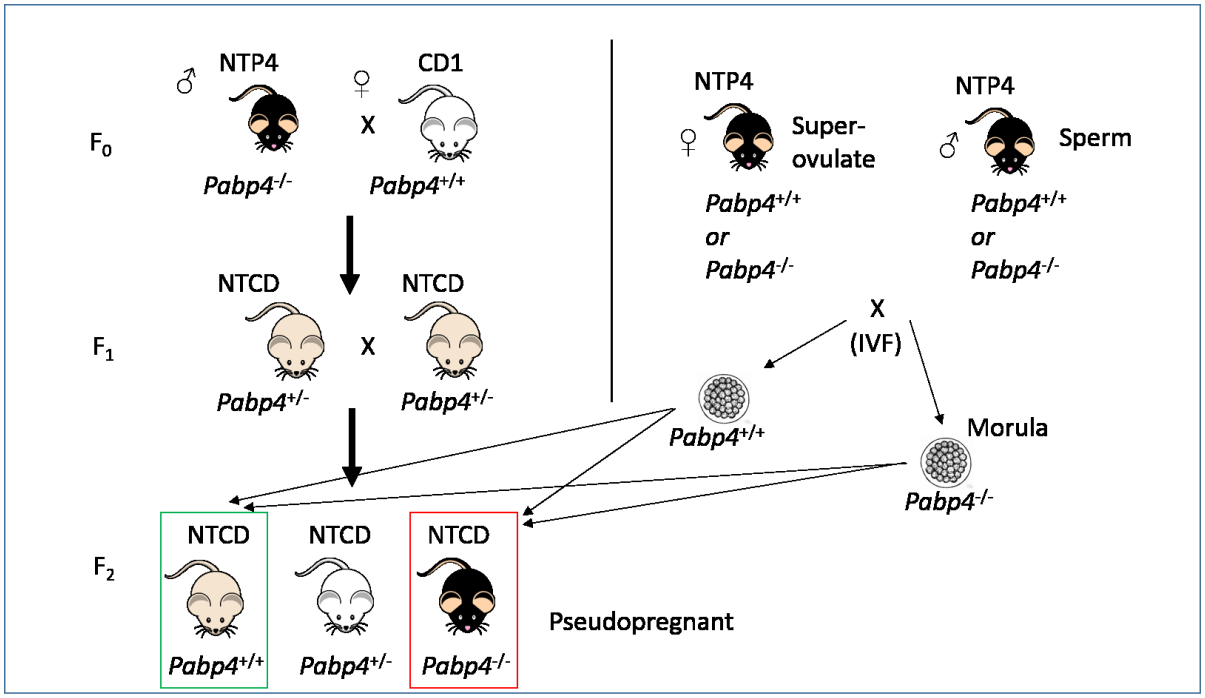

Figure 7.3 Strategy and design of embryo transfer experiment.

As C57BL/6 (NTP4) female mice are poor embryo recipients with a very low success rate of implantation, a hybrid strain created by crossing of NTP4 and CD1 mice, referred to as NTCD, was created as outlined above. *Pabp4*$^{+/+}$ and *Pabp4*$^{-/-}$ embryos at the morula stage are transferred into F_2 *Pabp4*$^{+/+}$ and *Pabp4*$^{-/-}$ NTCD females.

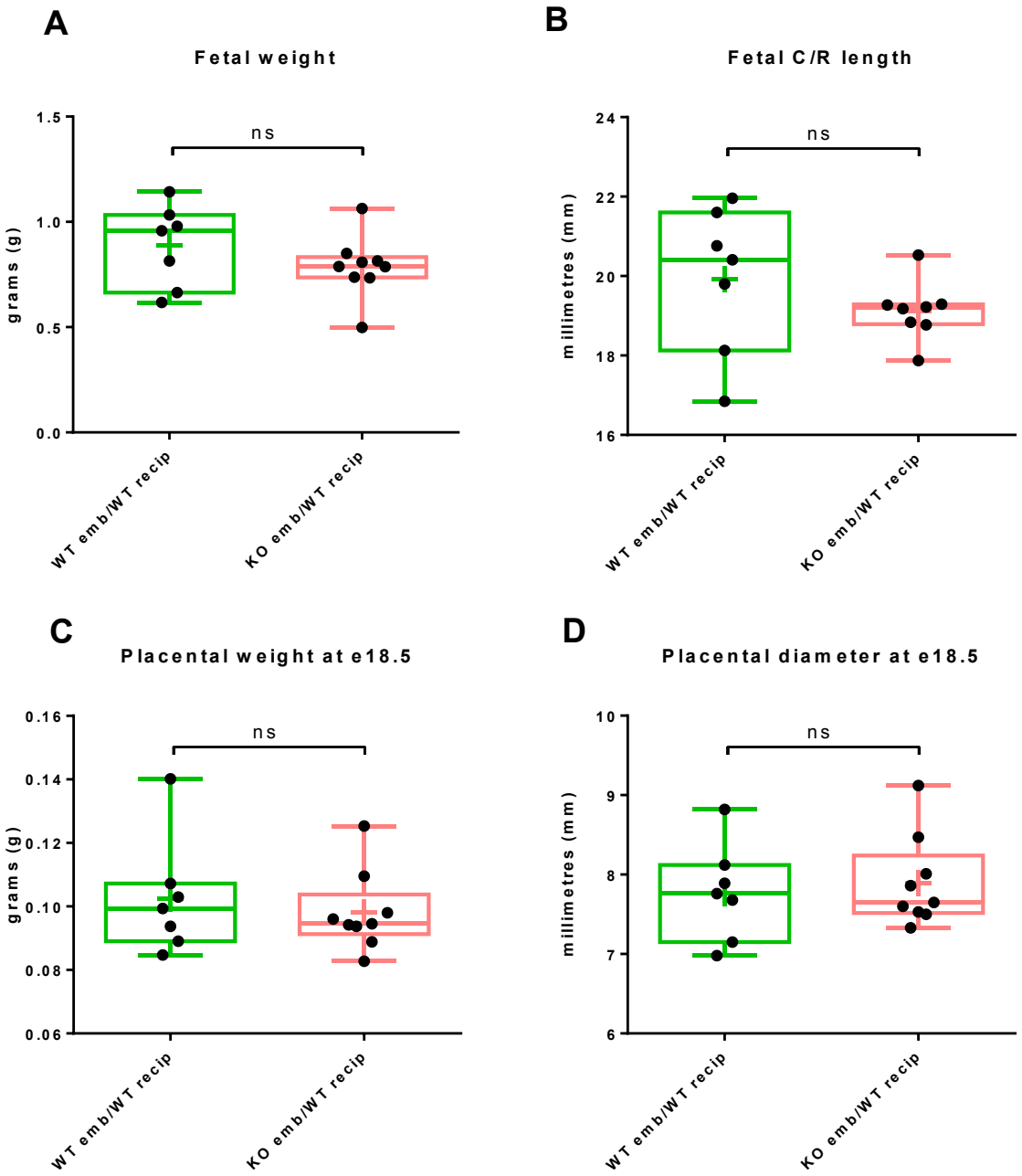

Figure 7.4 Weight and size of *Pabp4*$^{+/+}$ and *Pabp4*$^{-/-}$ fetuses and placentas at e18.5 which where transferred into *Pabp4*$^{+/+}$ NTCD females at the morula stage. (courtesy of Matt Brook)

Data are shown as box and whisker plots with median (long line) and mean (cross) indicated. Significance was analysed by Student's t-test. ns = > 0.05; * p = ≤ 0.05; ** p = ≤ 0.01; *** p = ≤ 0.001; **** p = ≤ 0.0001.

Insights into the potential underlying cause of the IUGR and mid-late gestational mortality have been gained from combined analysis of placentation/placenta as well as maternal physiology and adaptation to pregnancy in *Pabp4*$^{-/-}$ mice (Chapters 5 and 6). In mid-late gestation (e15.5 and e18.5) alterations in F:P ratios were detected which were solely due to the reduced fetal size with no contribution from changes in placental weight or diameter (Chapter 4). Volumetric analysis of the placenta did, however, reveal morphological changes in the relative volumes of the functional layers. In contrast to many IUGR models, the volume of the labyrinth was not altered but reciprocal changes in junctional zone and decidua basalis volumes were observed (Chapter 5). Interestingly, several lines of evidence pointed to a possible nutritional or metabolic component to the phenotype. For instance, reduced fetal glucose levels and potentially compensatory increases in levels of glucose and also amino acid transporter mRNAs (Chapter 5) were observed. An attractive hypothesis to explain these findings is that the smaller junctional zone compromises maternal adaptation and affects the circulating nutrient levels available for transfer. A smaller junctional zone could for example produce for example reduced levels of placental lactogen II which has lypolytic properties, promotes the expansion of pancreatic B cells and higher insulin levels which help shunt glucose to the fetus. Placental lactogens have also been shown to regulate maternal appetite via interaction with leptin and adipose tissue (Ben-Jonathan et al., 2006; Ladyman et al., 2010). Therefore it is plausible that a smaller junctional may negatively impact maternal metabolic adaptations to pregnancy and reduce the availability of both glucose and amino acids. However maternal blood glucose levels were not reduced. This raises the possibility that despite the absence of volumetric differences in the labyrinth, its function (e.g. nutrient transport) may be suboptimal leading to an attempt to compensate. Plasma analysis revealed that circulating levels of factors involved in driving maternal adaptation e.g. metabolism/nutrients were altered, namely leptin, corticosterone, estradiol and progesterone (Chapter 6). As these hormonal circuits do not operate in isolation but are often interconnected, the possible downstream effects of this are complex e.g. estradiol deficiency affects central leptin sensitivity and blood concentration (Ainslie et al., 2001). Finally, evidence of a pre-existing reduction in haematocrit (reduced red blood cell volume and haemoglobin) and reduced expansion of the spleen during pregnancy were obtained (Chapter 6), phenotypes that may be linked. Taken together these results provide many avenues for future research into the underlying causes of these pregnancy complications (Figure 7.5).

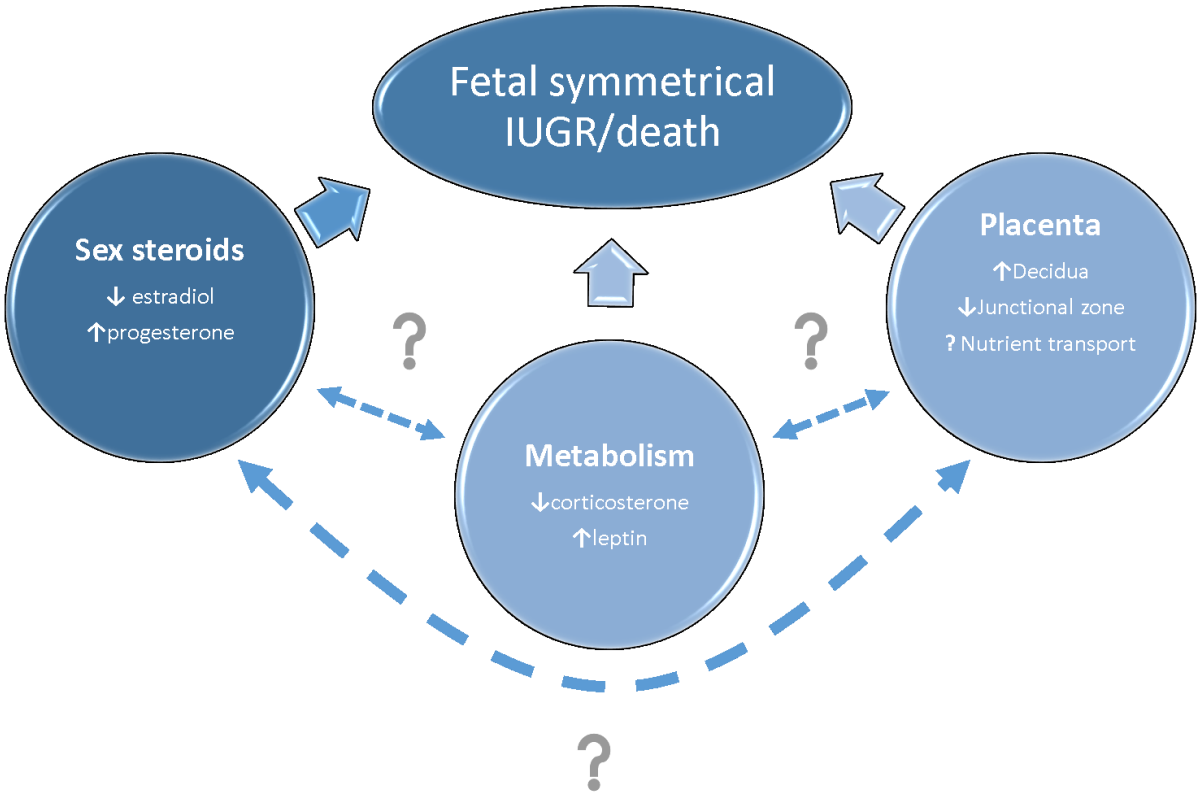

Figure 7.5 The underlying cause of the *Pabp4*$^{-/-}$ phenotype are currently unknown with interplay between different observations likely.

In interpreting how these data may result in the development of IUGR and/or stillbirth, it is important to bear in mind, as detailed in the discussion of chapter 6, the maternal genetics and the importance of the materno-fetal dialogue in placentation, and conversely the role of the placenta in adapting the maternal physiology. However, many pieces of the puzzle that could help to focus future research effort are missing. Notably, we need to know whether the morphological and functional placental changes detected thus far, are recapitulated in those from the paternal KO (reciprocal) cross, and what changes in cellular composition are present (e.g. investigation of cell specific markers). Further functional measures of the placenta at e18.5 are also required, for instance, to determine whether nutrient transport and/or paracrine/endocrine signalling are impacted, and whether glycogen stores are normal. Understanding nutrient transfer across the placenta can be gained by confirmation of current results at the protein level and similar studies of other transporters, but ultimately functional

transport assays should be used. These can examine passive/facilitated diffusion and active transport that are involved in nutrient supply/removal of metabolites (e.g. by infusing radioactive compounds such as 14C-methyl-*D*-glucose). Since our data do not point towards a defect in fetal vasculature and maternal blood spaces, high-resolution resin cast stereology to examine the architecture and to quantify interhaemal distance, the determinant of efficient materno-fetal gas exchange, do not appear a priority. Paracrine and endocrine signalling are associated with the decidua basalis and junctional zone and any perturbations due to changes in their relative volume can be detected by standard approaches such a qRT-PCR, ELISA, and radio-immune assays. Endocrine signalling to the corpus luteum of the ovary, for instance, is important for regulating estradiol (reduced in *Pabp4*$^{-/-}$ females) which in turns acts as a signal for many aspects of maternal adaptation (e.g. enlargement of spleen, which is blunted in *Pabp4*$^{-/-}$ females). To date we have no data implicating alterations in glycogen cells, but glycogen is used as a source for energy late in gestation and this involves movement of these cells from the junctional zone to the decidua basalis, and can be easily examining using glycogen assays (Lo et al., 1970).

Moreover we need to fill in many more "black boxes", for example, with respect to events at the maternal fetal interface prior to e18.5. Some snapshots are available at e5.5, e8.5 and e15.5 but events prior to e5.5 or between e5.5 and 8.5, when changes in implantation site shape are observed, and whether/how such changes lead to the morphological and functional changes observed at e18.5 is unknown. Whilst early events such as decidualisation and the control of trophoblast invasion are undoubtedly important questions and link to the maternality of the phenotype, arguably more direction may be gained by initially focusing on events between e8.5-e18.5, when differences may be more overt. Currently, we have no insight with respect to when, and where, PABP4 and PABP1 are expressed at the materno-fetal interface in this timeframe, which spans many important milestones in the development of the placenta (e.g. gains partial function at e10.5). Moreover, morphological and functional data for placentas from *Pabp4*$^{-/-}$ females at these milestones need to be obtained, applying information and approaches from studies at e18.5. This will help build a picture of the how and when changes observed at e18.5 may arise: the alterations in implantation site shape observed at e8.5 may be the first piece in this puzzle. Correlating the onset of morphological and functional placental changes in the initial onset of IUGR is important, and also will require the latter to be determined. This correlative information may provide insight into their likely involvement in the phenotypes e.g. changes arising after a phenotype is established are likely to be an effect (potentially compensatory) rather than a cause.

As the genetics point to a primary maternal defect and the placenta plays a major role in directing maternal adaptation, it is also important to examine maternal physiology outside of the immediate physical materno-fetal interface. To date, our data point to a pre-existing difference in red blood cells (microcytic), a change in the relative size of at least one organ (spleen) during pregnancy and differences in estradiol, progesterone, leptin and corticosterone at e18.5. Prior to pregnancy, red blood cells are normally synthesised in the bone marrow, which expresses PABP4 (Figure 1.15, 1.5 Work leading up to PhD project), with the red pulp of the spleen acting as a second site of erythropoiesis during pregnancy. Interestingly, the relative increase in spleen size during pregnancy is smaller in *Pabp4*$^{-/-}$females. Thus it is important to determine whether *Pabp4*$^{-/-}$ mice are also microcytic during pregnancy, whether the reduced weight of the spleen is due to a change in the red pulp and whether this is related to the reduced red cell volume. Support for a potential role of PABP4 in erythropoiesis comes from recent studies in cell lines (Kini et al., 2014). Dependent on outcome, the contribution of this pre-existing condition to the phenotype could be further investigated by taking advantage of the availability of a second *Pabp4* mouse containing the conditional ready allele (with both loxP sites intact and functional). For instance this could be bred to locally available VavCre mice (Georgiades et al., 2002b), removing Pabp4 from hematopoietic lineages (also some germ and endothelial cell expression). Normal pregnancy in these mice would suggest that the observed microcytic phenotype does not account for the phenotype. Since this would also target myeloid and lymphocyte lineages, this result would also provide additional information on the role, or lack thereof, of immune cell populations, which have key reproductive roles. Conversely, a recapitulation of the phenotype would imply a causative role, with more refined targeting with additional Cre lines allowing insight into the respective roles of different cell types. In contrast to data on RBCs, our results argue against low bodyweight prior to pregnancy as a pre-existing factor that contributes to the phenotype. However, weight gain is reduced during early pregnancy in *Pabp4*$^{-/-}$ mice, and levels of several hormones related to nutrients/metabolism and mRNA levels of placental nutrient transporters altered late in pregnancy. Thus the sensitivity of the phenotype to dietary manipulations may be informative with respect to whether further work into their nutritional status is warranted.

Currently, whilst intriguing, information on the hormonal status of *Pabp4*$^{-/-}$ mice is only available at e18.5, making it is unclear when these changes arise. In particular it would be informative to link this to the temporal analysis of placental endocrine function (e.g. placental lactogen, prolactin levels), placental morphology and IUGR onset. Whilst levels also need to be established in non-pregnant mice, their ability to maintain normal implantations rates, argue

that at least some of their levels were within a physiological range, prior to and during early pregnancy, which is compatible with ovulation and implantation. Determining the temporality of these events will shed light on whether these changes are downstream consequences of altered maternal adaptation (i.e. due to reduced hormone levels from the junctional zone) that nonetheless contribute to the phenotype due to their roles in maternal adaptation. For instance, in the redirecting maternal metabolism to meet nutritional needs. As discussed in chapter 6, modulation of these circulatory hormones to investigate their roles in phenotype development can be achieved by achieved without further genetic manipulation by exogenous supplementation, use of antagonists, and if warranted ovarian transplant (to restore estradiol and progesterone levels).

In addition to these "leads", many aspects of pregnant physiology in the *Pabp4*$^{-/-}$ mice have not yet been established, for instance, interpretable data on organ size was only achieved for spleen, and future analysis will include additional measures that can be utilised for normalisation e.g. tibia length, brain weight. Moreover, given the abundant evidence for changes in maternal adaptation, my data argue for a complete histopathological and body composition work up (e.g by TD-NMR time dependent-nuclear magnetic resonance) of pregnant *Pabp4*$^{-/-}$ mice to provide an overview of their health and maternal adaptation status. It is possible that the range of changes observed in the maternal environment may point towards a syndrome in which IUGR is one consequence and which may be caused by several different factors. There are currently no reports a syndrome in humans which matches our observations however anaemia is a known maternal factor associated with IUGR and high leptin levels have been reported in women with established IUGR (Savvidou et al., 2008).

In summary, we have only scratched the surface of understanding how *Pabp4* loss results in these phenotypes, but the above examples illustrate some of the important questions, avenues and tools that can be used to advance our knowledge. Whilst work in the shorter term should focus on gaining a complete picture of the pathophysiology of IUGR and stillbirth in these mice, a clear challenge is to utilise this information to track back to the primary defect. Clearly, in the long term, gaining a more cellular and molecular understanding of the phenotype will require identification of mis-regulated pathways and mRNAs (e.g. translational profiling combined with RNA-Seq), only then will we understand how and why this RNA-binding protein is necessary to support normal fetal growth and survival. Although it remains to be determined what the underlying cause of IUGR and late fetal death is, the likelihood of it being informative on human IUGR and stillbirth is likely because although differences between the two species exists in terms of pregnancy there are many similarities at the level of maternal

adaptation to pregnancy such as expansion of blood volume, increase in RBC number and insulin resistance as well as similarities at the level placental morphology and function such as production of placental lactogens by trophoblast cells which drive maternal adaptation. This model recapitulates many of the features associated with the spectrum of pregnancy disorders seen in humans, therefore the opportunities offered by it to understand specifically the maternal causes of IUGR and stillbirth argue strongly for pursing this challenging goal.

To date, little insight into the maternal genetic risk factors of IUGR and stillbirth (with the exception of genetic factors involving uterine natural killer cells and the remodelling of maternal vasculature) is available, meaning there is a lack of information on loci associated with these pregnancy complications. At present, it is too premature to look for *PABP4* mutations in women whom have had one, or more, growth restricted and or stillborn fetuses, and more information would be required to stratify patients for further study. However, at least in non-pregnant human endometrium, the expression patterns observed in mouse for PABP1 and PABP4 (Chapter 5) were broadly conserved, suggesting that it is present at the site at which the materno-fetal interface will subsequently develop. Moreover, translation of our findings is not dependent on the identification of patients containing PABP4 mutations, as study of the PABP4 mouse will reveal insight into maternal pathways which are important in pregnancy. Therefore, this work lays the foundation for disease causing mutations to be identified in these pathways, in addition to PABP4 itself.

Chapter 8 – Appendix

A

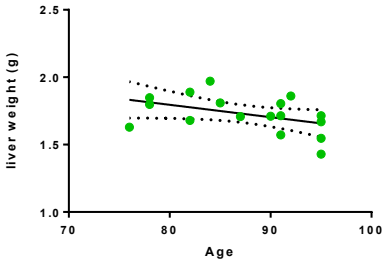

R square	0.1941
F	3.612
P value	0.0768
Deviation from zero?	Not Significant

B

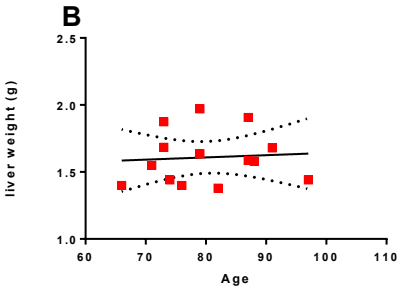

R square	0.005502
F	0.06639
P value	0.801
Deviation from zero?	Not Significant

C

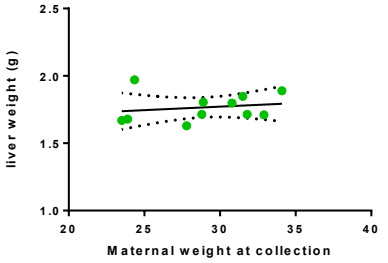

R square	0.03407
F	0.3174
P value	0.5869
Deviation from zero?	Not Significant

D

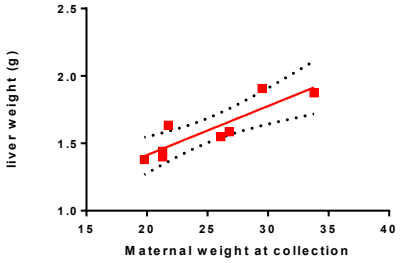

R square	0.7691
F	19.99
P value	0.0042
Deviation from zero?	Significant

E

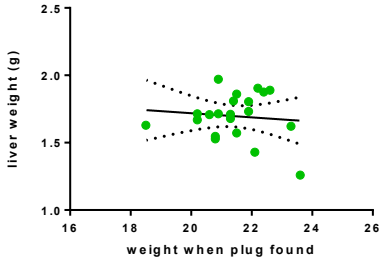

R square	0.01044
F	0.2004
P value	0.6595
Deviation from zero?	Not Significant

F

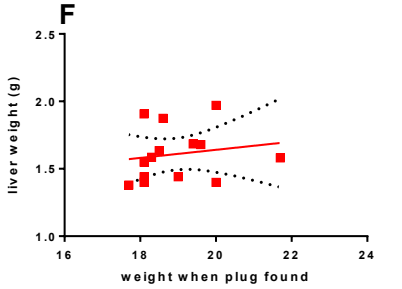

R square	0.02791
F	0.3446
P value	0.5681
Deviation from zero?	Not Significant

Figure 8.1 Liver weight at e15.5 of *Pabp4*$^{-/-}$ but not *Pabp4*$^{+/+}$ dams correlates with maternal weight at collection.

The weight of *Pabp4*$^{+/+}$ (*n* =11) and *Pabp4*$^{-/-}$ (*n* =8) liver collected at e15.5 plotted against (**A**, **B**) age, (**C**, **D**) maternal hysterectomised bodyweight at collection and (**E**, **F**) maternal bodyweight when plug was found. Data is presented on X/Y scatterplot with mean (full line) 5 and 95% percentiles (dotted lines) indicated. The relationship between X and Y was determined by calculating R square (R^2) and a P value was calculated from an F test to determine the probability that a randomly selected point would result in an R^2 value as high as the one observed.

A

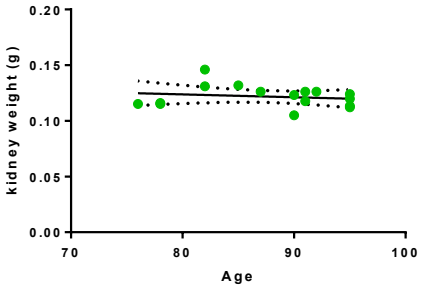

R square	0.03057
F	0.4414
P value	0.5172
Deviation from zero?	Not Significant

B

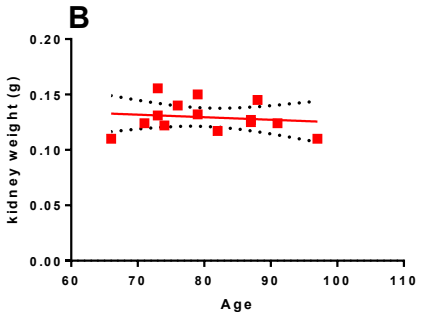

R square	0.02117
F	0.2595
P value	0.6197
Deviation from zero?	Not Significant

C

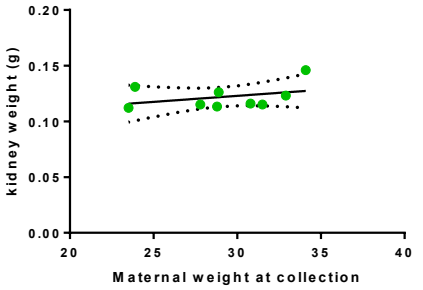

R square	0.1282
F	1.029
P value	0.3441
Deviation from zero?	Not Significant

D

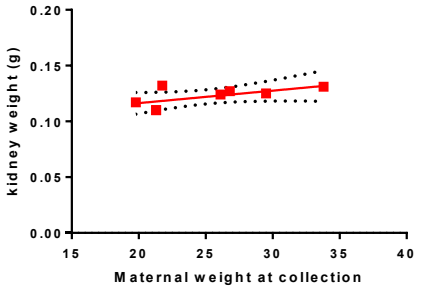

R square	0.3914
F	3.858
P value	0.0971
Deviation from zero?	Not Significant

E

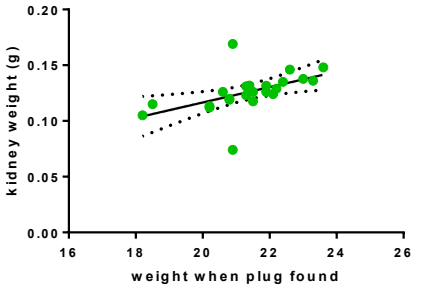

R square	0.2639
F	7.53
P value	0.0122
Deviation from zero?	Significant

F

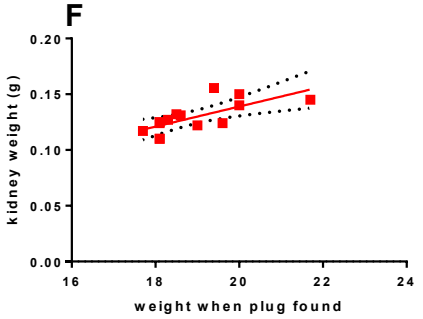

R square	0.5005
F	12.02
P value	0.0047
Deviation from zero?	Significant

Figure 8.2 Kidney weight at e15.5 of *Pabp4*$^{-/-}$ and *Pabp4*$^{+/+}$ dams correlates with weight when plug was found.

The weight of *Pabp4*$^{+/+}$ (*n* =11) and *Pabp4*$^{-/-}$ (*n* =8) kidney collected at e15.5 plotted against (**A**, **B**) age, (**C**, **D**) maternal hysterectomised bodyweight at collection and (**E**, **F**) maternal bodyweight when plug was found. Data is presented on X/Y scatterplot with mean (full line) 5 and 95% percentiles (dotted lines) indicated. The relationship between X and Y was determined by calculating R square (R^2) and a P value was calculated from an F test to determine the probability that a randomly selected point would result in an R^2 value as high as the one observed.

A

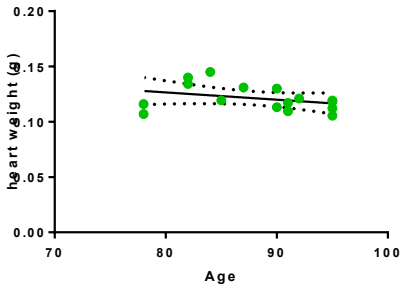

R square	0.1132
F	1.786
P value	0.2027
Deviation from zero?	Not Significant

B

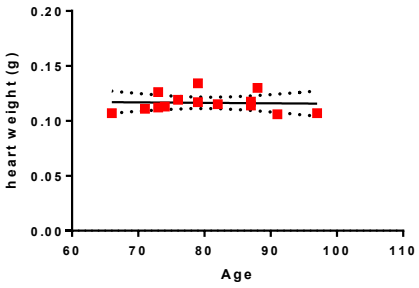

R square	0.001866
F	0.02244
P value	0.8834
Deviation from zero?	Not Significant

C

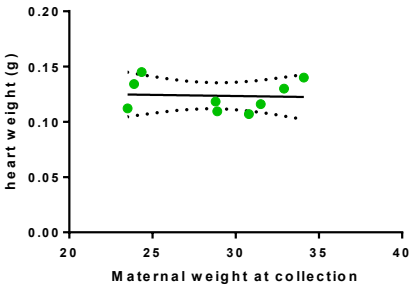

R square	0.003545
F	0.0249
P value	0.8791
Deviation from zero?	Not Significant

D

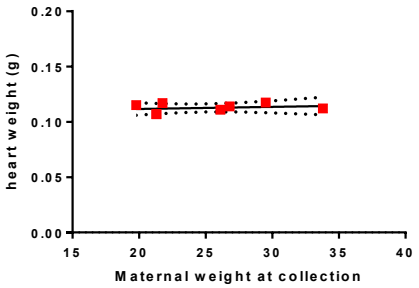

R square	0.05203
F	0.3293
P value	0.5869
Deviation from zero?	Not Significant

E

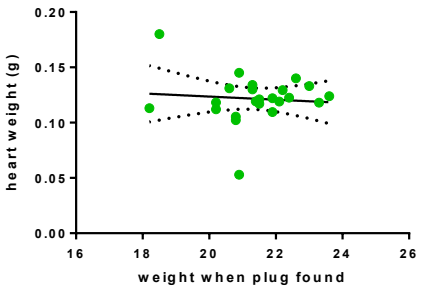

R square	0.007357
F	0.1557
P value	0.6972
Deviation from zero?	Not Significant

F

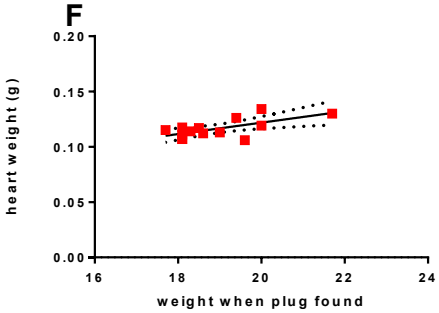

R square	0.4363
F	9.287
P value	0.0101
Deviation from zero?	Significant

Figure 8.3 Heart weight at e15.5 of *Pabp4*$^{-/-}$ but not *Pabp4*$^{+/+}$ dams correlates with weight when plug was found.

The weight of *Pabp4*$^{+/+}$ (*n* =11) and *Pabp4*$^{-/-}$ (*n* =8) heart collected at e15.5 plotted against (**A**, **B**) age, (**C**, **D**) maternal hysterectomised bodyweight at collection and (**E**, **F**) maternal bodyweight when plug was found. Data is presented on X/Y scatterplot with mean (full line) 5 and 95% percentiles (dotted lines) indicated. The relationship between X and Y was determined by calculating R square (R^2) and a P value was calculated from an F test to determine the probability that a randomly selected point would result in an R^2 value as high as the one observed.

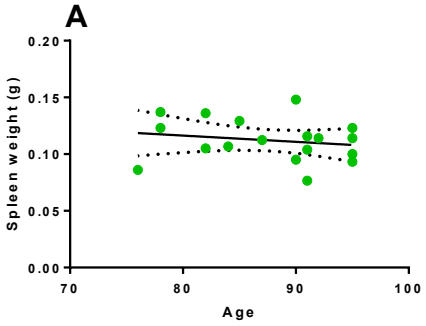

R square	0.03519
F	0.5836
P value	0.456
Deviation from zero?	Not Significant

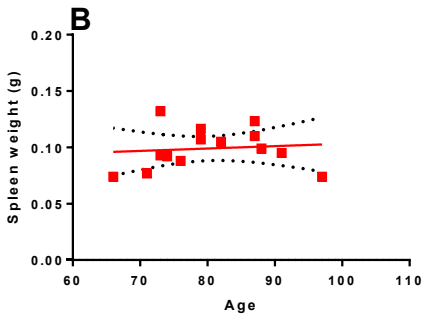

R square	0.01078
F	0.1308
P value	0.7239
Deviation from zero?	Not Significant

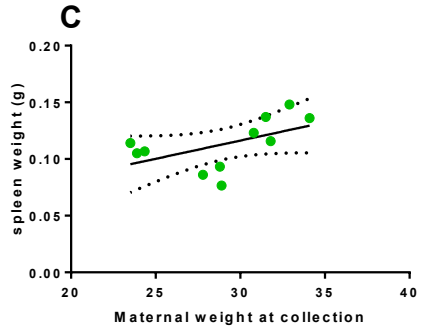

R square	0.2863
F	3.61
P value	0.0899
Deviation from zero?	Not Significant

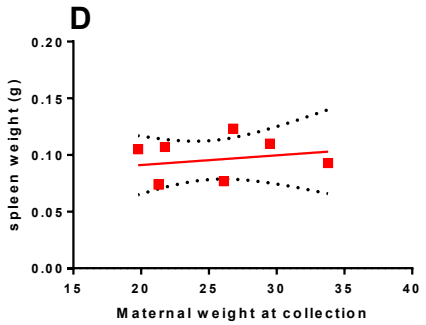

R square	0.04917
F	0.3103
P value	0.5977
Deviation from zero?	Not Significant

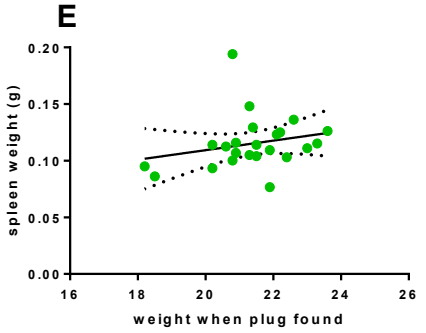

R square	0.05602
F	1.246
P value	0.2769
Deviation from zero?	Not Significant

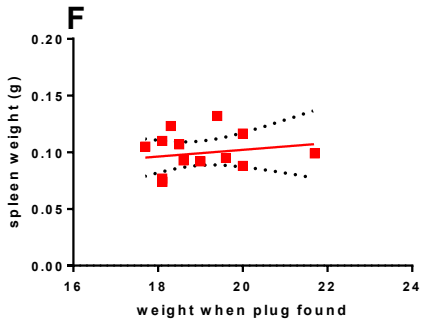

R square	0.03287
F	0.4079
P value	0.535
Deviation from zero?	Not Significant

Figure 8.4 Spleen weight at e15.5 of *Pabp4*$^{-/-}$ and *Pabp4*$^{+/+}$ dams do not correlate with age, maternal bodyweight or weight when plug found

The weight of *Pabp4*$^{+/+}$ (*n* =11) and *Pabp4*$^{-/-}$ (*n* =8) spleen collected at e15.5 plotted against (**A**, **B**) age, (**C**, **D**) maternal hysterectomised bodyweight at collection and (**E**, **F**) maternal bodyweight when plug was found. Data is presented on X/Y scatterplot with mean (full line) 5 and 95% percentiles (dotted lines) indicated. The relationship between X and Y was determined by calculating R square (R^2) and a P value was calculated from an F test to determine the probability that a randomly selected point would result in an R^2 value as high as the one observed.

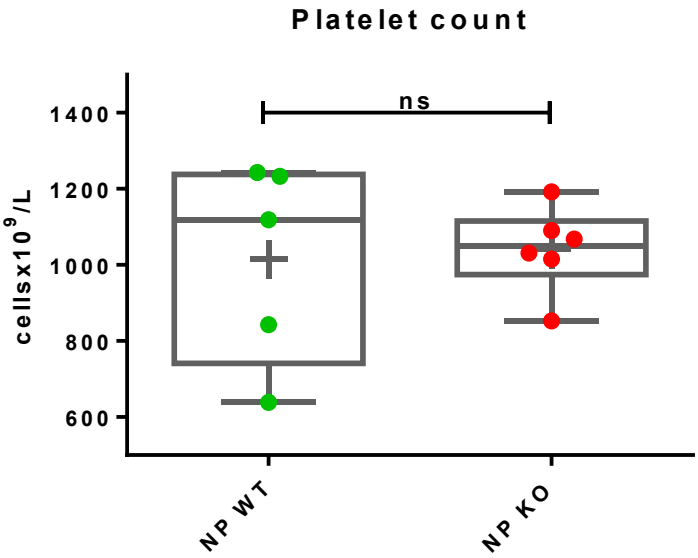

Figure 8.5 Platelet count is unaltered in *Pabp4*$^{-/-}$ non-pregnant females.

Platelet count using an automated flow cytometer-based haematological analyser of non-pregnant *Pabp4*$^{+/+}$ (green dots; n = 10) and *Pabp4*$^{-/-}$ females (red dots; n = 7). Data are shown as shown as box and whisker plots with the median (long line) and mean (cross) indicated. Significance was analysed by student's T-test. ns p = ≥0.05.

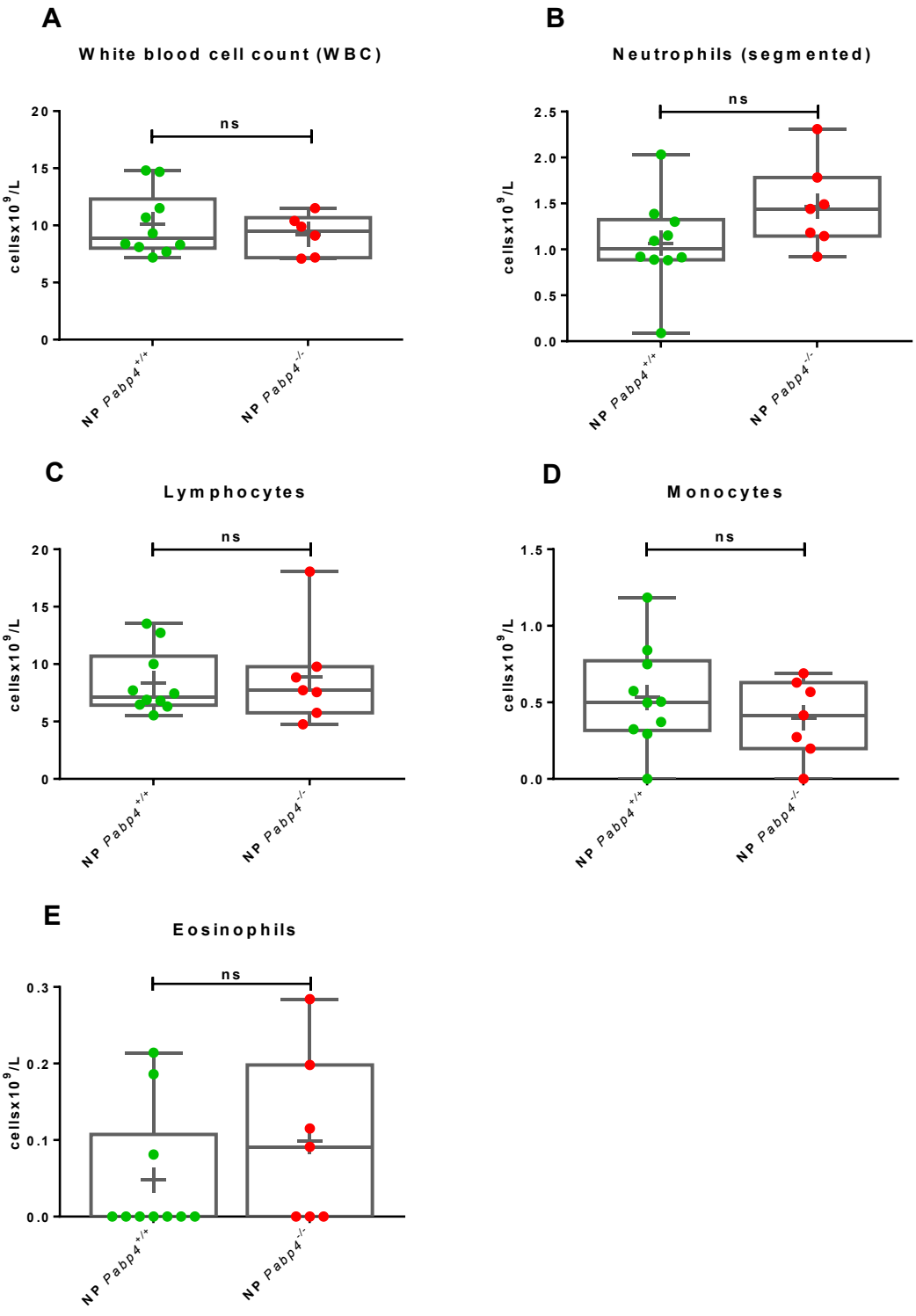

Figure 8.6 White blood cell count and differential white blood cell count of non-pregnant *Pabp4*$^{+/+}$ and *Pabp4*$^{-/-}$ females.

Analysis of non-pregnant *Pabp4*$^{+/+}$ (WT; green dots; n = 10) and *Pabp4*$^{-/-}$ female blood (KO; red dots; n = 7) using an automated flow cytometer-based haematological analyser. (**A**) White blood cell count and differential count analysis; (**B**) neutrophils (segmented), (**C**) lymphocytes, (**D**) monocytes, (**E**) eosinophils. Data are shown as shown as box and whisker plots with the median (long line) and mean (cross) indicated. Significance was analysed by student's T-test. ns p = ≥0.05.

Chapter 9 References

Abkowitz, J.L., Schaison, G., Boulad, F., Brown, D.L., Buchanan, G.R., Johnson, C.A., Murray, J.C., Sabo, K.M., 2002. Response of Diamond-Blackfan anemia to metoclopramide: evidence for a role for prolactin in erythropoiesis. Blood 100, 2687-2691.
Abrahams, V.M., Kim, Y.M., Straszewski, S.L., Romero, R., Mor, G., 2004. Macrophages and apoptotic cell clearance during pregnancy. American journal of reproductive immunology : AJRI : official journal of the American Society for the Immunology of Reproduction and the International Coordination Committee for Immunology of Reproduction 51, 275-282.
Abrahamsohn, P.A., Zorn, T.M., 1993. Implantation and decidualization in rodents. The Journal of experimental zoology 266, 603-628.
Adams, N.R., DeMayo, F.J., 2015. The Role of Steroid Hormone Receptors in the Establishment of Pregnancy in Rodents. Advances in anatomy, embryology, and cell biology 216, 27-49.
Adamson, J.W., 1996. Regulation of red blood cell production. The American journal of medicine 101, 4S-6S.
Adamson, S.L., Lu, Y., Whiteley, K.J., Holmyard, D., Hemberger, M., Pfarrer, C., Cross, J.C., 2002. Interactions between Trophoblast Cells and the Maternal and Fetal Circulation in the Mouse Placenta. Developmental Biology 250, 358-373.
Ainslie, D.A., Morris, M.J., Wittert, G., Turnbull, H., Proietto, J., Thorburn, A.W., 2001. Estrogen deficiency causes central leptin insensitivity and increased hypothalamic neuropeptide Y. International journal of obesity and related metabolic disorders : journal of the International Association for the Study of Obesity 25, 1680-1688.
Albrecht, E.D., Pepe, G.J., 1990. Placental steroid hormone biosynthesis in primate pregnancy. Endocrine reviews 11, 124-150.
Albrecht, M., Lengauer, T., 2004. Survey on the PABC recognition motif PAM2. Biochemical and biophysical research communications 316, 129-138.
Alexander, G.R., Himes, J.H., Kaufman, R.B., Mor, J., Kogan, M., 1996. A United States national reference for fetal growth. Obstetrics and gynecology 87, 163-168.
Allard, P., Yang, Q., Marzluff, W.F., Clarke, H.J., 2005. The stem-loop binding protein regulates translation of histone mRNA during mammalian oogenesis. Dev Biol 286, 195-206.
Aluvihare, V.R., Kallikourdis, M., Betz, A.G., 2004. Regulatory T cells mediate maternal tolerance to the fetus. Nature immunology 5, 266-271.
Alvarez, J.J., Montelongo, A., Iglesias, A., Lasuncion, M.A., Herrera, E., 1996. Longitudinal study on lipoprotein profile, high density lipoprotein subclass, and postheparin lipases during gestation in women. Journal of lipid research 37, 299-308.
Apponi, L.H., Leung, S.W., Williams, K.R., Valentini, S.R., Corbett, A.H., Pavlath, G.K., 2010. Loss of nuclear poly(A)-binding protein 1 causes defects in myogenesis and mRNA biogenesis. Human molecular genetics 19, 1058-1065.
Arck, P.C., Rucke, M., Rose, M., Szekeres-Bartho, J., Douglas, A.J., Pritsch, M., Blois, S.M., Pincus, M.K., Barenstrauch, N., Dudenhausen, J.W., Nakamura, K.,

Sheps, S., Klapp, B.F., 2008. Early risk factors for miscarriage: a prospective cohort study in pregnant women. Reproductive biomedicine online 17, 101-113.
Aris, R.M., Merkel, P.A., Bachrach, L.K., Borowitz, D.S., Boyle, M.P., Elkin, S.L., Guise, T.A., Hardin, D.S., Haworth, C.S., Holick, M.F., Joseph, P.M., O'Brien, K., Tullis, E., Watts, N.B., White, T.B., 2005. Guide to bone health and disease in cystic fibrosis. The Journal of clinical endocrinology and metabolism 90, 1888-1896.
Armistead, J., Triggs-Raine, B., 2014. Diverse diseases from a ubiquitous process: the ribosomopathy paradox. FEBS letters 588, 1491-1500.
Ashkar, A.A., Croy, B.A., 1999. Interferon-gamma contributes to the normalcy of murine pregnancy. Biology of reproduction 61, 493-502.
Ashkar, A.A., Croy, B.A., 2001. Functions of uterine natural killer cells are mediated by interferon gamma production during murine pregnancy. Seminars in immunology 13, 235-241.
Ashkar, A.A., Di Santo, J.P., Croy, B.A., 2000. Interferon gamma contributes to initiation of uterine vascular modification, decidual integrity, and uterine natural killer cell maturation during normal murine pregnancy. The Journal of experimental medicine 192, 259-270.
Atamer, Y., Kocyigit, Y., Yokus, B., Atamer, A., Erden, A.C., 2005. Lipid peroxidation, antioxidant defense, status of trace metals and leptin levels in preeclampsia. Eur J Obstet Gynecol Reprod Biol 119, 60-66.
Ategbo, J.M., Grissa, O., Yessoufou, A., Hichami, A., Dramane, K.L., Moutairou, K., Miled, A., Grissa, A., Jerbi, M., Tabka, Z., Khan, N.A., 2006. Modulation of adipokines and cytokines in gestational diabetes and macrosomia. The Journal of clinical endocrinology and metabolism 91, 4137-4143.
Athanassakis, I., Bleackley, R.C., Paetkau, V., Guilbert, L., Barr, P.J., Wegmann, T.G., 1987. The immunostimulatory effect of T cells and T cell lymphokines on murine fetally derived placental cells. Journal of immunology 138, 37-44.
Athanassakis, I., Vassiliadis, S., 2002. Interplay between T helper type 1 and type 2 cytokines and soluble major histocompatibility complex molecules: a paradigm in pregnancy. Immunology 107, 281-287.
Augustine, R.A., Ladyman, S.R., Grattan, D.R., 2008. From feeding one to feeding many: hormone-induced changes in bodyweight homeostasis during pregnancy. The Journal of physiology 586, 387-397.
Aydin, S., Guzel, S.P., Kumru, S., Aydin, S., Akin, O., Kavak, E., Sahin, I., Bozkurt, M., Halifeoglu, I., 2008. Serum leptin and ghrelin concentrations of maternal serum, arterial and venous cord blood in healthy and preeclamptic pregnant women. Journal of physiology and biochemistry 64, 51-59.
Backe, B., Nakling, J., 1993. Effectiveness of antenatal care: a population based study. British journal of obstetrics and gynaecology 100, 727-732.
Baker, J., Liu, J.P., Robertson, E.J., Efstratiadis, A., 1993. Role of insulin-like growth factors in embryonic and postnatal growth. Cell 75, 73-82.
Bany, B., . 2014. Pseudopregnant bead-induced mouse deciduoma model, in: Croy, B.Y., AT.; DeMayo, FJ.; Adamson, SL. (Ed.), The Guide to Investigation of Mouse Pregnancy. Academic Press (Elsevier), London, UK.
Barber, E.M., Pollard, J.W., 2003. The uterine NK cell population requires IL-15 but these cells are not required for pregnancy nor the resolution of a Listeria monocytogenes infection. Journal of immunology 171, 37-46.

Barzilai, N., Wang, J., Massilon, D., Vuguin, P., Hawkins, M., Rossetti, L., 1997. Leptin selectively decreases visceral adiposity and enhances insulin action. The Journal of clinical investigation 100, 3105-3110.
Baumann, M.U., Deborde, S., Illsley, N.P., 2002. Placental glucose transfer and fetal growth. Endocrine 19, 13-22.
Beagley, K.W., Gockel, C.M., 2003. Regulation of innate and adaptive immunity by the female sex hormones oestradiol and progesterone. FEMS immunology and medical microbiology 38, 13-22.
Belo, L., Caslake, M., Gaffney, D., Santos-Silva, A., Pereira-Leite, L., Quintanilha, A., Rebelo, I., 2002. Changes in LDL size and HDL concentration in normal and preeclamptic pregnancies. Atherosclerosis 162, 425-432.
Ben-Jonathan, N., Hugo, E.R., Brandebourg, T.D., LaPensee, C.R., 2006. Focus on prolactin as a metabolic hormone. Trends in endocrinology and metabolism: TEM 17, 110-116.
Bernard-Kargar, C., Ktorza, A., 2001. Endocrine pancreas plasticity under physiological and pathological conditions. Diabetes 50 Suppl 1, S30-35.
Bernstein, I.G., SG. , 1996. Intrauterine growth restriction, in: Gabbe, S.G.N., J.R.; Simpson, J.L.; Annas G.J. (Ed.), Obstetrics: normal and problem pregnancies, 3rd ed. hurchhill-Livingstone, New York, pp. 863–886.
Besse, F., Ephrussi, A., 2008. Translational control of localized mRNAs: restricting protein synthesis in space and time. Nat Rev Mol Cell Biol 9, 971-980.
Bevilacqua, E.L., AR.; Bandeira, CL.; Hoshida, M., 2014. Biology of the Ectoplacental Cone, in: Croy, B.Y., AT.; DeMayo, FJ.; Adamson, SL. (Ed.), The Guide to Investigation of Mouse Pregnancy. Academic Press (Elsevier), London, UK, pp. 113-124.
Bhat, M., Robichaud, N., Hulea, L., Sonenberg, N., Pelletier, J., Topisirovic, I., 2015. Targeting the translation machinery in cancer. Nature reviews. Drug discovery 14, 261-278.
Bilinski, P., Roopenian, D., Gossler, A., 1998. Maternal IL-11Ralpha function is required for normal decidua and fetoplacental development in mice. Genes & development 12, 2234-2243.
Bjorbaek, C., Kahn, B.B., 2004. Leptin signaling in the central nervous system and the periphery. Recent progress in hormone research 59, 305-331.
Blagden, S.P., Gatt, M.K., Archambault, V., Lada, K., Ichihara, K., Lilley, K.S., Inoue, Y.H., Glover, D.M., 2009. Drosophila Larp associates with poly(A)-binding protein and is required for male fertility and syncytial embryo development. Dev Biol 334, 186-197.
Blanco, P., Sargent, C.a., Boucher, C.a., Howell, G., Ross, M., Affara, N.a., 2001. A novel poly(A)-binding protein gene (PABPC5) maps to an X-specific subinterval in the Xq21.3/Yp11.2 homology block of the human sex chromosomes. Genomics 74, 1-11.
Boehlen, F., Hohlfeld, P., Extermann, P., Perneger, T.V., de Moerloose, P., 2000. Platelet count at term pregnancy: a reappraisal of the threshold. Obstetrics and gynecology 95, 29-33.
Bouillot, S., Rampon, C., Tillet, E., Huber, P., 2006. Tracing the glycogen cells with protocadherin 12 during mouse placenta development. Placenta 27, 882-888.
Boulenouar, S., Doisne, J.M., Sferruzzi-Perri, A., Gaynor, L.M., Kieckbusch, J., Balmas, E., Yung, H.W., Javadzadeh, S., Volmer, L., Hawkes, D.A., Phillips, K.,

Brady, H.J., Fowden, A.L., Burton, G.J., Moffett, A., Colucci, F., 2016. The Residual Innate Lymphoid Cells in NFIL3-Deficient Mice Support Suboptimal Maternal Adaptations to Pregnancy. Frontiers in immunology 7, 43.
Bouloumie, A., Drexler, H.C., Lafontan, M., Busse, R., 1998. Leptin, the product of Ob gene, promotes angiogenesis. Circulation research 83, 1059-1066.
Brannon, P.M., 2012. Vitamin D and adverse pregnancy outcomes: beyond bone health and growth. The Proceedings of the Nutrition Society 71, 205-212.
Brelje, T.C., Parsons, J.A., Sorenson, R.L., 1994. Regulation of islet beta-cell proliferation by prolactin in rat islets. Diabetes 43, 263-273.
Brelje, T.C., Scharp, D.W., Lacy, P.E., Ogren, L., Talamantes, F., Robertson, M., Friesen, H.G., Sorenson, R.L., 1993. Effect of homologous placental lactogens, prolactins, and growth hormones on islet B-cell division and insulin secretion in rat, mouse, and human islets: implication for placental lactogen regulation of islet function during pregnancy. Endocrinology 132, 879-887.
Brenner, W.E., Edelman, D.A., Hendricks, C.H., 1976. A standard of fetal growth for the United States of America. American journal of obstetrics and gynecology 126, 555-564.
Bronson, F.H., 1971. Rodent pheromones. Biology of reproduction 4, 344-357.
Bronson, F.H., Maruniak, J.A., 1975. Male-induced puberty in female mice: evidence for a synergistic action of social cues. Biology of reproduction 13, 94-98.
Brook, M., Gray, N.K., 2012. The role of mammalian poly(A)-binding proteins in co-ordinating mRNA turnover. Biochem Soc Trans 40, 856-864.
Brook, M., Smith, J.W.S., Gray, N.K., 2009. The DAZL and PABP families: RNA-binding proteins with interrelated roles in translational control in oocytes. Reproduction (Cambridge, England) 137, 595-617.
Brown, R.W., Diaz, R., Robson, A.C., Kotelevtsev, Y.V., Mullins, J.J., Kaufman, M.H., Seckl, J.R., 1996. The ontogeny of 11 beta-hydroxysteroid dehydrogenase type 2 and mineralocorticoid receptor gene expression reveal intricate control of glucocorticoid action in development. Endocrinology 137, 794-797.
Bryson, J.M., Phuyal, J.L., Swan, V., Caterson, I.D., 1999. Leptin has acute effects on glucose and lipid metabolism in both lean and gold thioglucose-obese mice. The American journal of physiology 277, E417-422.
Bulmer, J.N., Pace, D., Ritson, A., 1988. Immunoregulatory cells in human decidua: morphology, immunohistochemistry and function. Reproduction, nutrition, developpement 28, 1599-1613.
Bulmer, J.N., Williams, P.J., Lash, G.E., 2010. Immune cells in the placental bed. Int J Dev Biol 54, 281-294.
Burgess, H.M., Gray, N.K., 2010. mRNA-specific regulation of translation by poly(A)-binding proteins. Biochemical Society transactions 38, 1517-1522.
Burgess, H.M., Gray, N.K., 2012. Do not distribute . © 2012 Landes Bioscience . Do not distribute. 243-247.
Burgess, H.M., Richardson, W.a., Anderson, R.C., Salaun, C., Graham, S.V., Gray, N.K., 2011. Nuclear relocalisation of cytoplasmic poly(A)-binding proteins PABP1 and PABP4 in response to UV irradiation reveals mRNA-dependent export of metazoan PABPs. Journal of cell science 124, 3344-3355.
Burton, G.J., Fowden, A.L., 2012. Review: The placenta and developmental programming: balancing fetal nutrient demands with maternal resource allocation. Placenta 33 Suppl, S23-27.

Bustamante, J.J., Dai, G., Soares, M.J., 2008. Pregnancy and lactation modulate maternal splenic growth and development of the erythroid lineage in the rat and mouse. Reproduction, fertility, and development 20, 303-310.
Bustin, S.A., Benes, V., Garson, J.A., Hellemans, J., Huggett, J., Kubista, M., Mueller, R., Nolan, T., Pfaffl, M.W., Shipley, G.L., Vandesompele, J., Wittwer, C.T., 2009. The MIQE guidelines: minimum information for publication of quantitative real-time PCR experiments. Clinical chemistry 55, 611-622.
Butte, N.F., 2000. Carbohydrate and lipid metabolism in pregnancy: normal compared with gestational diabetes mellitus. The American journal of clinical nutrition 71, 1256S-1261S.
Cai, L.Q., Cao, Y.J., Duan, E.K., 2000. Effects of leukaemia inhibitory factor on embryo implantation in the mouse. Cytokine 12, 1676-1682.
Calado, A., Kutay, U., Kuhn, U., Wahle, E., Carmo-Fonseca, M., 2000. Deciphering the cellular pathway for transport of poly(A)-binding protein II. Rna 6, 245-256.
Campfield, L.A., Smith, F.J., Guisez, Y., Devos, R., Burn, P., 1995. Recombinant mouse OB protein: evidence for a peripheral signal linking adiposity and central neural networks. Science 269, 546-549.
Candeloro, L., Zorn, T.M., 2007. Granulated and non-granulated decidual prolactin-related protein-positive decidual cells in the pregnant mouse endometrium. American journal of reproductive immunology : AJRI : official journal of the American Society for the Immunology of Reproduction and the International Coordination Committee for Immunology of Reproduction 57, 122-132.
Cannizzo, E.S., Clement, C.C., Sahu, R., Follo, C., Santambrogio, L., 2011. Oxidative stress, inflamm-aging and immunosenescence. Journal of proteomics 74, 2313-2323.
Catalano, P.M., Hoegh, M., Minium, J., Huston-Presley, L., Bernard, S., Kalhan, S., Hauguel-De Mouzon, S., 2006. Adiponectin in human pregnancy: implications for regulation of glucose and lipid metabolism. Diabetologia 49, 1677-1685.
Catarino, C., Rebelo, I., Belo, L., Rocha-Pereira, P., Rocha, S., Castro, E.B., Patricio, B., Quintanilha, A., Santos-Silva, A., 2008. Fetal lipoprotein changes in pre-eclampsia. Acta obstetricia et gynecologica Scandinavica 87, 628-634.
Celton-Morizur, S., Merlen, G., Couton, D., Margall-Ducos, G., Desdouets, C., 2009. The insulin/Akt pathway controls a specific cell division program that leads to generation of binucleated tetraploid liver cells in rodents. The Journal of clinical investigation 119, 1880-1887.
Cha, J., Sun, X., Dey, S.K., 2012. Mechanisms of implantation: strategies for successful pregnancy. Nature medicine 18, 1754-1767.
Chaouat, G., Menu, E., Athanassakis, I., Wegmann, T.G., 1988. Maternal T cells regulate placental size and fetal survival. Regional immunology 1, 143-148.
Chazara, O., Xiong, S., Moffett, A., 2011. Maternal KIR and fetal HLA-C: a fine balance. Journal of leukocyte biology 90, 703-716.
Chen, Z., Li, Y., Krug, R.M., 1998. Chimeras containing influenza NS1 and HIV-1 Rev protein sequences: mechanism of their inhibition of nuclear export of Rev protein-RNA complexes. Virology 241, 234-250.
Chervoneva, I., Li, Y., Schulz, S., Croker, S., Wilson, C., Waldman, S.A., Hyslop, T., 2010. Selection of optimal reference genes for normalization in quantitative RT-PCR. BMC bioinformatics 11, 253.

Chiswick, M.L., 1985. Intrauterine growth retardation. British medical journal 291, 845-848.
Chung, E., Leinwand, L.A., 2014. Pregnancy as a cardiac stress model. Cardiovascular research 101, 561-570.
Chung, E., Yeung, F., Leinwand, L.A., 2012. Akt and MAPK signaling mediate pregnancy-induced cardiac adaptation. Journal of applied physiology 112, 1564-1575.
Ciosk, R., DePalma, M., Priess, J.R., 2004. ATX-2, the C. elegans ortholog of ataxin 2, functions in translational regulation in the germline. Development 131, 4831-4841.
Clapp, J.F., 3rd, Capeless, E., 1997. Cardiovascular function before, during, and after the first and subsequent pregnancies. The American journal of cardiology 80, 1469-1473.
Clausson, B., Gardosi, J., Francis, A., Cnattingius, S., 2001. Perinatal outcome in SGA births defined by customised versus population-based birthweight standards. BJOG : an international journal of obstetrics and gynaecology 108, 830-834.
Clouse, K.N., Ferguson, S.B., Schupbach, T., 2008. Squid, Cup, and PABP55B function together to regulate gurken translation in Drosophila. Dev Biol 313, 713-724.
Coan, P.M., Angiolini, E., Sandovici, I., Burton, G.J., Constancia, M., Fowden, A.L., 2008. Adaptations in placental nutrient transfer capacity to meet fetal growth demands depend on placental size in mice. The Journal of physiology 586, 4567-4576.
Coan, P.M., Conroy, N., Burton, G.J., Ferguson-Smith, A.C., 2006. Origin and characteristics of glycogen cells in the developing murine placenta. Developmental dynamics : an official publication of the American Association of Anatomists 235, 3280-3294.
Coan, P.M., Ferguson-Smith, A.C., Burton, G.J., 2004. Developmental dynamics of the definitive mouse placenta assessed by stereology. Biology of reproduction 70, 1806-1813.
Cohen-Tannoudji, M., Vandormael-Pournin, S., Drezen, J., Mercier, P., Babinet, C., Morello, D., 2000. lacZ sequences prevent regulated expression of housekeeping genes. Mechanisms of development 90, 29-39.
Collier, B., Gorgoni, B., Loveridge, C., Cooke, H.J., Gray, N.K., 2005. The DAZL family proteins are PABP-binding proteins that regulate translation in germ cells. EMBO J 24, 2656-2666.
Constancia, M., Angiolini, E., Sandovici, I., Smith, P., Smith, R., Kelsey, G., Dean, W., Ferguson-Smith, A., Sibley, C.P., Reik, W., Fowden, A., 2005. Adaptation of nutrient supply to fetal demand in the mouse involves interaction between the Igf2 gene and placental transporter systems. Proc Natl Acad Sci U S A 102, 19219-19224.
Constancia, M., Hemberger, M., Hughes, J., Dean, W., Ferguson-Smith, A., Fundele, R., Stewart, F., Kelsey, G., Fowden, A., Sibley, C., Reik, W., 2002. Placental-specific IGF-II is a major modulator of placental and fetal growth. Nature 417, 945-948.
Cordeau, M., Herblot, S., Charrier, E., Audibert, F., Cordeiro, P., Harnois, M., Duval, M., 2012. Defects in CD54 and CD86 up-regulation by plasmacytoid dendritic cells during pregnancy. Immunological investigations 41, 497-506.

Cosson, B., Couturier, A., Le Guellec, R., Moreau, J., Chabelskaya, S., Zhouravleva, G., Philippe, M., 2002. Characterization of the poly(A) binding proteins expressed during oogenesis and early development of Xenopus laevis. Biology of the cell / under the auspices of the European Cell Biology Organization 94, 217-231.
Coulon, A., Chow, C.C., Singer, R.H., Larson, D.R., 2013. Eukaryotic transcriptional dynamics: from single molecules to cell populations. Nat Rev Genet 14, 572-584.
Cox, B., Kotlyar, M., Evangelou, A.I., Ignatchenko, V., Ignatchenko, A., Whiteley, K., Jurisica, I., Adamson, S.L., Rossant, J., Kislinger, T., 2009. Comparative systems biology of human and mouse as a tool to guide the modeling of human placental pathology. Molecular systems biology 5, 279.
Cross, J.C., Hemberger, M., Lu, Y., Nozaki, T., Whiteley, K., Masutani, M., Adamson, S.L., 2002. Trophoblast functions, angiogenesis and remodeling of the maternal vasculature in the placenta. Molecular and cellular endocrinology 187, 207-212.
Cross, J.C., Nakano, H., Natale, D.R.C., Simmons, D.G., Watson, E.D., 2006. Branching morphogenesis during development of placental villi. Differentiation; research in biological diversity 74, 393-401.
Cross, J.C., Werb, Z., Fisher, S.J., 1994. Implantation and the placenta: key pieces of the development puzzle. Science 266, 1508-1518.
Croy, B.A., Ashkar, A.A., Foster, R.A., DiSanto, J.P., Magram, J., Carson, D., Gendler, S.J., Grusby, M.J., Wagner, N., Muller, W., Guimond, M.J., 1997. Histological studies of gene-ablated mice support important functional roles for natural killer cells in the uterus during pregnancy. Journal of reproductive immunology 35, 111-133.
Croy, B.A., Ashkar, A.A., Minhas, K., Greenwood, J.D., 2000. Can murine uterine natural killer cells give insights into the pathogenesis of preeclampsia? Journal of the Society for Gynecologic Investigation 7, 12-20.
Cui, C., Wani, M.A., Wight, D., Kopchick, J., Stambrook, P.J., 1994. Reporter genes in transgenic mice. Transgenic research 3, 182-194.
Dai, G., Bustamante, J.J., Zou, Y., Myronovych, A., Bao, Q., Kumar, S., Soares, M.J., 2011. Maternal hepatic growth response to pregnancy in the mouse. Experimental biology and medicine 236, 1322-1332.
Daikoku, T., Yoshie, M., Xie, H., Sun, X., Cha, J., Ellenson, L.H., Dey, S.K., 2013. Conditional deletion of Tsc1 in the female reproductive tract impedes normal oviductal and uterine function by enhancing mTORC1 signaling in mice. Molecular human reproduction 19, 463-472.
Dave-Sharma, S., Wilson, R.C., Harbison, M.D., Newfield, R., Azar, M.R., Krozowski, Z.S., Funder, J.W., Shackleton, C.H., Bradlow, H.L., Wei, J.Q., Hertecant, J., Moran, A., Neiberger, R.E., Balfe, J.W., Fattah, A., Daneman, D., Akkurt, H.I., De Santis, C., New, M.I., 1998. Examination of genotype and phenotype relationships in 14 patients with apparent mineralocorticoid excess. The Journal of clinical endocrinology and metabolism 83, 2244-2254.
De Benedetti, A., Graff, J.R., 2004. eIF-4E expression and its role in malignancies and metastases. Oncogene 23, 3189-3199.
de Jong, C.L., Gardosi, J., Dekker, G.A., Colenbrander, G.J., van Geijn, H.P., 1998. Application of a customised birthweight standard in the assessment of perinatal outcome in a high risk population. British journal of obstetrics and gynaecology 105, 531-535.

de Rijk, E.P., van Esch, E., Flik, G., 2002. Pregnancy dating in the rat: placental morphology and maternal blood parameters. Toxicologic pathology 30, 271-282.
DeChiara, T.M., Efstratiadis, A., Robertson, E.J., 1990. A growth-deficiency phenotype in heterozygous mice carrying an insulin-like growth factor II gene disrupted by targeting. Nature 345, 78-80.
Delepine, M., Nicolino, M., Barrett, T., Golamaully, M., Lathrop, G.M., Julier, C., 2000. EIF2AK3, encoding translation initiation factor 2-alpha kinase 3, is mutated in patients with Wolcott-Rallison syndrome. Nature genetics 25, 406-409.
Demicheva, E., Crispi, F., 2014. Long-term follow-up of intrauterine growth restriction: cardiovascular disorders. Fetal Diagn Ther 36, 143-153.
Derry, M.C., Yanagiya, A., Martineau, Y., Sonenberg, N., 2006. Regulation of poly(A)-binding protein through PABP-interacting proteins. Cold Spring Harbor symposia on quantitative biology 71, 537-543.
Dever, T.E., Green, R., 2012. The elongation, termination, and recycling phases of translation in eukaryotes. Cold Spring Harbor perspectives in biology 4, a013706.
Devlieger, R., Casteels, K., Van Assche, F.A., 2008. Reduced adaptation of the pancreatic B cells during pregnancy is the major causal factor for gestational diabetes: current knowledge and metabolic effects on the offspring. Acta obstetricia et gynecologica Scandinavica 87, 1266-1270.
Dey, S.K., 1996. Implantation, in: Adashi, E.Y.R., J.A.;Rosenwaks, Z. (Ed.), Reproductive Endocrinology, Surgery, and Technology. Lippincott-Raven, Philadelphia, pp. 421-434.
Diaz, P., Powell, T.L., Jansson, T., 2014. The role of placental nutrient sensing in maternal-fetal resource allocation. Biology of reproduction 91, 82.
Dilworth, M.R., Kusinski, L.C., Baker, B.C., Renshall, L.J., Greenwood, S.L., Sibley, C.P., Wareing, M., 2011. Defining fetal growth restriction in mice: A standardized and clinically relevant approach. Placenta 32, 914-916.
Doetschman, T., Azhar, M., 2012. Cardiac-specific inducible and conditional gene targeting in mice. Circulation research 110, 1498-1512.
Downe, S., Kingdon, C., Kennedy, R., Norwell, H., McLaughlin, M.J., Heazell, A.E., 2012. Post-mortem examination after stillbirth: views of UK-based practitioners. Eur J Obstet Gynecol Reprod Biol 162, 33-37.
Dugoff, L., Hobbins, J.C., Malone, F.D., Porter, T.F., Luthy, D., Comstock, C.H., Hankins, G., Berkowitz, R.L., Merkatz, I., Craigo, S.D., Timor-Tritsch, I.E., Carr, S.R., Wolfe, H.M., Vidaver, J., D'Alton, M.E., 2004. First-trimester maternal serum PAPP-A and free-beta subunit human chorionic gonadotropin concentrations and nuchal translucency are associated with obstetric complications: a population-based screening study (the FASTER Trial). American journal of obstetrics and gynecology 191, 1446-1451.
Dundar, O., Yoruk, P., Tutuncu, L., Erikci, A.A., Muhcu, M., Ergur, A.R., Atay, V., Mungen, E., 2008. Longitudinal study of platelet size changes in gestation and predictive power of elevated MPV in development of pre-eclampsia. Prenatal diagnosis 28, 1052-1056.
Duvekot, J.J., Cheriex, E.C., Pieters, F.A., Peeters, L.L., 1995. Severely impaired fetal growth is preceded by maternal hemodynamic maladaptation in very early pregnancy. Acta obstetricia et gynecologica Scandinavica 74, 693-697.
Eckmann, C.R., Rammelt, C., Wahle, E., 2011. Control of poly(A) tail length. Wiley interdisciplinary reviews. RNA 2, 348-361.

Eghbali, M., Deva, R., Alioua, A., Minosyan, T.Y., Ruan, H., Wang, Y., Toro, L., Stefani, E., 2005. Molecular and functional signature of heart hypertrophy during pregnancy. Circulation research 96, 1208-1216.
El Khattabi, I., Remacle, C., Reusens, B., 2006. The regulation of IGFs and IGFBPs by prolactin in primary culture of fetal rat hepatocytes is influenced by maternal malnutrition. American journal of physiology. Endocrinology and metabolism 291, E835-842.
Eliseeva, I.A., Lyabin, D.N., Ovchinnikov, L.P., 2013. Poly(A)-binding proteins: structure, domain organization, and activity regulation. Biochemistry. Biokhimiia 78, 1377-1391.
Erlebacher, A., 2013. Immunology of the maternal-fetal interface. Annual review of immunology 31, 387-411.
Ernst, S., Demirci, C., Valle, S., Velazquez-Garcia, S., Garcia-Ocana, A., 2011. Mechanisms in the adaptation of maternal beta-cells during pregnancy. Diabetes management 1, 239-248.
Erokhin, M., Vassetzky, Y., Georgiev, P., Chetverina, D., 2015. Eukaryotic enhancers: common features, regulation, and participation in diseases. Cellular and molecular life sciences : CMLS 72, 2361-2375.
Fasshauer, M., Paschke, R., 2003. Regulation of adipocytokines and insulin resistance. Diabetologia 46, 1594-1603.
Fatscher, T., Boehm, V., Gehring, N.H., 2015. Mechanism, factors, and physiological role of nonsense-mediated mRNA decay. Cellular and molecular life sciences : CMLS 72, 4523-4544.
Fausto, N., Campbell, J.S., 2003. The role of hepatocytes and oval cells in liver regeneration and repopulation. Mechanisms of development 120, 117-130.
Fay, R.A., Hughes, A.O., Farron, N.T., 1983. Platelets in pregnancy: hyperdestruction in pregnancy. Obstetrics and gynecology 61, 238-240.
Feral, C., Guellaen, G., Pawlak, A., 2001. Human testis expresses a specific poly(A)-binding protein. Nucleic acids research 29, 1872-1883.
Fielder, P.J., Talamantes, F., 1987. The lipolytic effects of mouse placental lactogen II, mouse prolactin, and mouse growth hormone on adipose tissue from virgin and pregnant mice. Endocrinology 121, 493-497.
Filant, J., Spencer, T.E., 2013. Endometrial glands are essential for blastocyst implantation and decidualization in the mouse uterus. Biology of reproduction 88, 93.
Finn, C.A., Hinchliffe, J.R., 1964. Reaction of the Mouse Uterus during Implantation and Deciduoma Formation as Demonstrated by Changes in the Distribution of Alkaline Phosphatase. Journal of reproduction and fertility 8, 331-338.
Flenady, V., Koopmans, L., Middleton, P., Froen, J.F., Smith, G.C., Gibbons, K., Coory, M., Gordon, A., Ellwood, D., McIntyre, H.D., Fretts, R., Ezzati, M., 2011. Major risk factors for stillbirth in high-income countries: a systematic review and meta-analysis. Lancet 377, 1331-1340.
Forbes, K., Westwood, M., Baker, P.N., Aplin, J.D., 2008. Insulin-like growth factor I and II regulate the life cycle of trophoblast in the developing human placenta. American journal of physiology. Cell physiology 294, C1313-1322.
Forss-Petter, S., Danielson, P.E., Catsicas, S., Battenberg, E., Price, J., Nerenberg, M., Sutcliffe, J.G., 1990. Transgenic mice expressing beta-galactosidase in mature neurons under neuron-specific enolase promoter control. Neuron 5, 187-197.

Fowler, J.H., Nash, D.J., 1968. Erythropoiesis in the spleen and bone marrow of the pregnant mouse. Dev Biol 18, 331-353.
Fowler, K.J., Hudson, D.F., Salamonsen, L.A., Edmondson, S.R., Earle, E., Sibson, M.C., Choo, K.H., 2000. Uterine dysfunction and genetic modifiers in centromere protein B-deficient mice. Genome research 10, 30-41.
Frederick, I.O., Williams, M.A., Sales, A.E., Martin, D.P., Killien, M., 2008. Pre-pregnancy body mass index, gestational weight gain, and other maternal characteristics in relation to infant birth weight. Maternal and child health journal 12, 557-567.
Freemark, M., 2006. Regulation of maternal metabolism by pituitary and placental hormones: roles in fetal development and metabolic programming. Hormone research 65 Suppl 3, 41-49.
Frias, A.E., Morgan, T.K., Evans, A.E., Rasanen, J., Oh, K.Y., Thornburg, K.L., Grove, K.L., 2011. Maternal high-fat diet disturbs uteroplacental hemodynamics and increases the frequency of stillbirth in a nonhuman primate model of excess nutrition. Endocrinology 152, 2456-2464.
Friend, K., Brook, M., Bezirci, F.B., Sheets, M.D., Gray, N.K., Seli, E., 2012. Embryonic poly(A)-binding protein (ePAB) phosphorylation is required for Xenopus oocyte maturation. Biochem J 445, 93-100.
Fukagawa, M., Hamada, Y., Nakanishi, S., Tanaka, M., 2006. The kidney and bone metabolism: Nephrologists' point of view. Journal of bone and mineral metabolism 24, 434-438.
Fuller, R., Barron, C., Mandala, M., Gokina, N., Osol, G., 2009. Predominance of local over systemic factors in uterine arterial remodeling during pregnancy. Reproductive sciences 16, 489-500.
Gainsford, T., Willson, T.A., Metcalf, D., Handman, E., McFarlane, C., Ng, A., Nicola, N.A., Alexander, W.S., Hilton, D.J., 1996. Leptin can induce proliferation, differentiation, and functional activation of hemopoietic cells. Proc Natl Acad Sci U S A 93, 14564-14568.
Gallie, D.R., 1991. The cap and poly(A) tail function synergistically to regulate mRNA translational efficiency. Genes & development 5, 2108-2116.
Gardosi, J., Kady, S.M., McGeown, P., Francis, A., Tonks, A., 2005. Classification of stillbirth by relevant condition at death (ReCoDe): population based cohort study. Bmj 331, 1113-1117.
Gardosi, J., Madurasinghe, V., Williams, M., Malik, A., 2013. Maternal and fetal risk factors for stillbirth : population. 108, 1-14.
Gardosi, J., Mongelli, M., Wilcox, M., Chang, A., 1995. An adjustable fetal weight standard. Ultrasound in obstetrics & gynecology : the official journal of the International Society of Ultrasound in Obstetrics and Gynecology 6, 168-174.
Gardosi, J., Mul, T., Mongelli, M., Fagan, D., 1998. Analysis of birthweight and gestational age in antepartum stillbirths. British journal of obstetrics and gynaecology 105, 524-530.
Gauster, M., Hiden, U., Blaschitz, A., Frank, S., Lang, U., Alvino, G., Cetin, I., Desoye, G., Wadsack, C., 2007. Dysregulation of placental endothelial lipase and lipoprotein lipase in intrauterine growth-restricted pregnancies. The Journal of clinical endocrinology and metabolism 92, 2256-2263.

Gavrilova, O., Barr, V., Marcus-Samuels, B., Reitman, M., 1997. Hyperleptinemia of pregnancy associated with the appearance of a circulating form of the leptin receptor. J Biol Chem 272, 30546-30551.
Georgiades, P., Ferguson-Smith, A.C., Burton, G.J., 2002a. Comparative developmental anatomy of the murine and human definitive placentae. Placenta 23, 3-19.
Georgiades, P., Ogilvy, S., Duval, H., Licence, D.R., Charnock-Jones, D.S., Smith, S.K., Print, C.G., 2002b. VavCre transgenic mice: a tool for mutagenesis in hematopoietic and endothelial lineages. Genesis 34, 251-256.
Ghildiyal, M., Zamore, P.D., 2009. Small silencing RNAs: an expanding universe. Nat Rev Genet 10, 94-108.
Gibson, J.M., Aplin, J.D., White, A., Westwood, M., 2001. Regulation of IGF bioavailability in pregnancy. Molecular human reproduction 7, 79-87.
Glaser, R., Kiecolt-Glaser, J.K., 2005. Stress-induced immune dysfunction: implications for health. Nature reviews. Immunology 5, 243-251.
Glasser, S.R., Julian, J., 1986. Intermediate filament protein as a marker of uterine stromal cell decidualization. Biology of reproduction 35, 463-474.
Golden-Mason, L., O'Farrelly, C., 2002. Having it all? Stem cells, haematopoiesis and lymphopoiesis in adult human liver. Immunology and cell biology 80, 45-51.
Goldstein, J., Sites, C.K., Toth, M.J., 2004. Progesterone stimulates cardiac muscle protein synthesis via receptor-dependent pathway. Fertility and sterility 82, 430-436.
Gordon, M., 2007. in: Gabbe, S.N.J.S.J. (Ed.), Obstretrics: Normal and Problem Pregnancies, 5th ed. Elsevier, Philadelphia, pp. 55-84.
Gorgoni, B., Gray, N.K., 2004. The roles of cytoplasmic poly(A)-binding proteins in regulating gene expression: a developmental perspective. Briefings in functional genomics & proteomics 3, 125-141.
Gorgoni, B., Richardson, W.a., Burgess, H.M., Anderson, R.C., Wilkie, G.S., Gautier, P., Martins, J.P.S., Brook, M., Sheets, M.D., Gray, N.K., 2011. Poly(A)-binding proteins are functionally distinct and have essential roles during vertebrate development. Proceedings of the National Academy of Sciences of the United States of America 108, 7844-7849.
Goring, D.R., Rossant, J., Clapoff, S., Breitman, M.L., Tsui, L.C., 1987. In situ detection of beta-galactosidase in lenses of transgenic mice with a gamma-crystallin/lacZ gene. Science 235, 456-458.
Goss, D.J., Kleiman, F.E., 2013. Poly(A) binding proteins: are they all created equal? Wiley interdisciplinary reviews. RNA 4, 167-179.
Graff, J.R., Konicek, B.W., Carter, J.H., Marcusson, E.G., 2008. Targeting the eukaryotic translation initiation factor 4E for cancer therapy. Cancer research 68, 631-634.
Gray, N.K., Coller, J.M., Dickson, K.S., Wickens, M., 2000. Multiple portions of poly(A)-binding protein stimulate translation in vivo. EMBO J 19, 4723-4733.
Gray, N.K., Hrabalkova, L., Scanlon, J.P., Smith, R.W., 2015. Poly(A)-binding proteins and mRNA localization: who rules the roost? Biochem Soc Trans 43, 1277-1284.
Green, M.W., BA. , 1991. Handbook on Genetically Standardized JAX Mice, Fourth edition ed, The Jackson Laboratory, Bar Harbor.

Grey, V., Atkinson, S., Drury, D., Casey, L., Ferland, G., Gundberg, C., Lands, L.C., 2008. Prevalence of low bone mass and deficiencies of vitamins D and K in pediatric patients with cystic fibrosis from 3 Canadian centers. Pediatrics 122, 1014-1020.
Gross, G.A., Solenberger, T., Philpott, T., Holcomb, W.L., Jr., Landt, M., 1998. Plasma leptin concentrations in newborns of diabetic and nondiabetic mothers. American journal of perinatology 15, 243-247.
Guenther, A.E., Conley, A.J., Van Orden, D.E., Farley, D.B., Ford, S.P., 1988. Structural and mechanical changes of uterine arteries during pregnancy in the pig. Journal of animal science 66, 3144-3152.
Guhaniyogi, J., Brewer, G., 2001. Regulation of mRNA stability in mammalian cells. Gene 265, 11-23.
Guimond, M., Wang, B., Croy, B.A., 1999. Immune competence involving the natural killer cell lineage promotes placental growth. Placenta 20, 441-450.
Guimond, M.J., Luross, J.A., Wang, B., Terhorst, C., Danial, S., Croy, B.A., 1997. Absence of natural killer cells during murine pregnancy is associated with reproductive compromise in TgE26 mice. Biology of reproduction 56, 169-179.
Gundersen, H.J., Osterby, R., 1981. Optimizing sampling efficiency of stereological studies in biology: or 'do more less well!'. Journal of microscopy 121, 65-73.
Gurdon, J.B., Bourillot, P.Y., 2001. Morphogen gradient interpretation. Nature 413, 797-803.
Guzeloglu-Kayisli, O., Lalioti, M.D., Aydiner, F., Sasson, I., Ilbay, O., Sakkas, D., Lowther, K.M., Mehlmann, L.M., Seli, E., 2012. Embryonic poly(A)-binding protein (EPAB) is required for oocyte maturation and female fertility in mice. The Biochemical journal 446, 47-58.
Gynecologists., C.o.P.B.G.A.C.o.O.a., 2001. Intrauterine growth restriction. Clinical management guidelines for obstetrician-gynecologists. Int. J. Gynaecol. Obstet., 85-96.
Hadlock, F.P., Harrist, R.B., Martinez-Poyer, J., 1991. In utero analysis of fetal growth: a sonographic weight standard. Radiology 181, 129-133.
Haig, D., 1993. Genetic conflicts in human pregnancy. The Quarterly review of biology 68, 495-532.
Handwerger, S., Freemark, M., 2000. The roles of placental growth hormone and placental lactogen in the regulation of human fetal growth and development. Journal of pediatric endocrinology & metabolism : JPEM 13, 343-356.
Hanna, J., Goldman-Wohl, D., Hamani, Y., Avraham, I., Greenfield, C., Natanson-Yaron, S., Prus, D., Cohen-Daniel, L., Arnon, T.I., Manaster, I., Gazit, R., Yutkin, V., Benharroch, D., Porgador, A., Keshet, E., Yagel, S., Mandelboim, O., 2006. Decidual NK cells regulate key developmental processes at the human fetal-maternal interface. Nature medicine 12, 1065-1074.
Hartmann, B.W., Wagenbichler, P., Soregi, G., 1997. Maternal and umbilical-cord serum leptin concentrations in normal, full-term pregnancies. The New England journal of medicine 337, 863.
Hartwig, I.R., Pincus, M.K., Diemert, A., Hecher, K., Arck, P.C., 2013. Sex-specific effect of first-trimester maternal progesterone on birthweight. Human reproduction 28, 77-86.
Haston, K.M., Tung, J.Y., Reijo Pera, R.A., 2009. Dazl functions in maintenance of pluripotency and genetic and epigenetic programs of differentiation in mouse primordial germ cells in vivo and in vitro. PloS one 4, e5654.

Hay, J.E., 2008. Liver disease in pregnancy. Hepatology 47, 1067-1076.
Hayward, C.E., Lean, S., Sibley, C.P., Jones, R.L., Wareing, M., Greenwood, S.L., Dilworth, M.R., 2016. Placental Adaptation: What Can We Learn from Birthweight:Placental Weight Ratio? Frontiers in physiology 7, 28.
He, Y., Smith, S.K., Day, K.A., Clark, D.E., Licence, D.R., Charnock-Jones, D.S., 1999. Alternative splicing of vascular endothelial growth factor (VEGF)-R1 (FLT-1) pre-mRNA is important for the regulation of VEGF activity. Molecular endocrinology 13, 537-545.
Heazell, A.E., Worton, S.A., Higgins, L.E., Ingram, E., Johnstone, E.D., Jones, R.L., Sibley, C.P., 2015. IFPA Gabor Than Award Lecture: Recognition of placental failure is key to saving babies' lives. Placenta 36 Suppl 1, S20-28.
Heikkinen, J., Mottonen, M., Komi, J., Alanen, A., Lassila, O., 2003. Phenotypic characterization of human decidual macrophages. Clinical and experimental immunology 131, 498-505.
Hemachandra, A.H., Klebanoff, M.A., Duggan, A.K., Hardy, J.B., Furth, S.L., 2006. The association between intrauterine growth restriction in the full-term infant and high blood pressure at age 7 years: results from the Collaborative Perinatal Project. International journal of epidemiology 35, 871-877.
Hendler, I., Blackwell, S.C., Mehta, S.H., Whitty, J.E., Russell, E., Sorokin, Y., Cotton, D.B., 2005. The levels of leptin, adiponectin, and resistin in normal weight, overweight, and obese pregnant women with and without preeclampsia. American journal of obstetrics and gynecology 193, 979-983.
Herrera, E., Lasuncion, M.A., Gomez-Coronado, D., Aranda, P., Lopez-Luna, P., Maier, I., 1988. Role of lipoprotein lipase activity on lipoprotein metabolism and the fate of circulating triglycerides in pregnancy. American journal of obstetrics and gynecology 158, 1575-1583.
Herrid, M., Palanisamy, S.K., Ciller, U.A., Fan, R., Moens, P., Smart, N.A., McFarlane, J.R., 2014. An updated view of leptin on implantation and pregnancy: a review. Physiological research / Academia Scientiarum Bohemoslovaca 63, 543-557.
Herse, F., Bai, Y., Staff, A.C., Yong-Meid, J., Dechend, R., Zhou, R., 2009. Circulating and uteroplacental adipocytokine concentrations in preeclampsia. Reproductive sciences 16, 584-590.
Hiby, S.E., Regan, L., Lo, W., Farrell, L., Carrington, M., Moffett, A., 2008. Association of maternal killer-cell immunoglobulin-like receptors and parental HLA-C genotypes with recurrent miscarriage. Human reproduction 23, 972-976.
Hladunewich, M., Karumanchi, S.A., Lafayette, R., 2007. Pathophysiology of the clinical manifestations of preeclampsia. Clinical journal of the American Society of Nephrology : CJASN 2, 543-549.
Hocine, S., Singer, R.H., Grunwald, D., 2010. RNA processing and export. Cold Spring Harbor perspectives in biology 2, a000752.
Hollams, E.M., Giles, K.M., Thomson, A.M., Leedman, P.J., 2002. MRNA stability and the control of gene expression: implications for human disease. Neurochemical research 27, 957-980.
Holmes, M.C., Abrahamsen, C.T., French, K.L., Paterson, J.M., Mullins, J.J., Seckl, J.R., 2006. The mother or the fetus? 11beta-hydroxysteroid dehydrogenase type 2 null mice provide evidence for direct fetal programming of behavior by endogenous glucocorticoids. The Journal of neuroscience : the official journal of the Society for Neuroscience 26, 3840-3844.

Holmes, R.P., Holly, J.M., Soothill, P.W., 1998. A prospective study of maternal serum insulin-like growth factor-I in pregnancies with appropriately grown or growth restricted fetuses. British journal of obstetrics and gynaecology 105, 1273-1278.
Holt, C.E., Schuman, E.M., 2013. The central dogma decentralized: new perspectives on RNA function and local translation in neurons. Neuron 80, 648-657.
Homko, C.J., Sivan, E., Reece, E.A., Boden, G., 1999. Fuel metabolism during pregnancy. Seminars in reproductive endocrinology 17, 119-125.
Hosoda, N., Funakoshi, Y., Hirasawa, M., Yamagishi, R., Asano, Y., Miyagawa, R., Ogami, K., Tsujimoto, M., Hoshino, S.-i., 2011. Anti-proliferative protein Tob negatively regulates CPEB3 target by recruiting Caf1 deadenylase. The EMBO journal 30, 1311-1323.
Houston, D.W., King, M.L., 2000. A critical role for Xdazl, a germ plasm-localized RNA, in the differentiation of primordial germ cells in Xenopus. Development 127, 447-456.
Hu, D., Cross, J.C., 2010. Development and function of trophoblast giant cells in the rodent placenta. The International Journal of Developmental Biology 54, 341-354.
Hua, X., Thompson, C.B., 2001. Quiescent T cells: actively maintaining inactivity. Nature immunology 2, 1097-1098.
Huet-Hudson, Y.M., Andrews, G.K., Dey, S.K., 1989. Cell type-specific localization of c-myc protein in the mouse uterus: modulation by steroid hormones and analysis of the periimplantation period. Endocrinology 125, 1683-1690.
Imada, S., Takagi, K., Kikuchi, A., Ishikawa, K., Tamaru, S., Horikoshi, T., Ogiso, Y., 2012. Birthweight placental weight ratio of appropriate-for-dates and light-for-dates infants in preterm delivery. The journal of obstetrics and gynaecology research 38, 122-129.
Imbasciati, E., Ponticelli, C., 1991. Pregnancy and renal disease: predictors for fetal and maternal outcome. American journal of nephrology 11, 353-362.
Islam, M.S., Morton, N.M., Hansson, A., Emilsson, V., 1997. Rat insulinoma-derived pancreatic beta-cells express a functional leptin receptor that mediates a proliferative response. Biochem Biophys Res Commun 238, 851-855.
Ivanov, P., Anderson, P., 2013. Post-transcriptional regulatory networks in immunity. Immunological reviews 253, 253-272.
Jackson, D., Volpert, O.V., Bouck, N., Linzer, D.I., 1994. Stimulation and inhibition of angiogenesis by placental proliferin and proliferin-related protein. Science 266, 1581-1584.
Jackson, R.J., Hellen, C.U., Pestova, T.V., 2010. The mechanism of eukaryotic translation initiation and principles of its regulation. Nat Rev Mol Cell Biol 11, 113-127.
Janas, M.M., Novina, C.D., 2012. Not lost in translation: stepwise regulation of microRNA targets. EMBO J 31, 2446-2447.
Jansson, N., Greenwood, S.L., Johansson, B.R., Powell, T.L., Jansson, T., 2003. Leptin stimulates the activity of the system A amino acid transporter in human placental villous fragments. The Journal of clinical endocrinology and metabolism 88, 1205-1211.
Jansson, N., Nilsfelt, A., Gellerstedt, M., Wennergren, M., Rossander-Hulthen, L., Powell, T.L., Jansson, T., 2008. Maternal hormones linking maternal body mass index and dietary intake to birth weight. The American journal of clinical nutrition 87, 1743-1749.

Jansson, N., Pettersson, J., Haafiz, A., Ericsson, A., Palmberg, I., Tranberg, M., Ganapathy, V., Powell, T.L., Jansson, T., 2006. Down-regulation of placental transport of amino acids precedes the development of intrauterine growth restriction in rats fed a low protein diet. The Journal of physiology 576, 935-946.
Jemiolo, B., Marchlewska-Koj, A., Buchalczyk, A., 1980. Acceleration of ovarian follicle maturation of female caused by male in Microtus agrestis and Clethrionomys glareolus. Folia biologica 28, 269-272.
Jepson, J.H., Lowenstein, L., 1964. Effect of Prolactin on Erythropoiesis in the Mouse. Blood 24, 726-738.
Jeyabalan, A., Conrad, K.P., 2007. Renal function during normal pregnancy and preeclampsia. Frontiers in bioscience : a journal and virtual library 12, 2425-2437.
Jin, L.P., Chen, Q.Y., Zhang, T., Guo, P.F., Li, D.J., 2009. The CD4+CD25 bright regulatory T cells and CTLA-4 expression in peripheral and decidual lymphocytes are down-regulated in human miscarriage. Clinical immunology 133, 402-410.
Johansson, E.D., 1969. Plasma levels of progesterone in pregnancy measured by a rapid competitive protein binding technique. Acta endocrinologica 61, 607-617.
Kahvejian, A., Roy, G., Sonenberg, N., 2001. The mRNA closed-loop model: the function of PABP and PABP-interacting proteins in mRNA translation. Cold Spring Harbor symposia on quantitative biology 66, 293-300.
Kahvejian, A., Svitkin, Y.V., Sukarieh, R., M'Boutchou, M.N., Sonenberg, N., 2005. Mammalian poly(A)-binding protein is a eukaryotic translation initiation factor, which acts via multiple mechanisms. Genes & development 19, 104-113.
Kamal-Eldin, A., Appelqvist, L.A., 1996. The chemistry and antioxidant properties of tocopherols and tocotrienols. Lipids 31, 671-701.
Kamohara, S., Burcelin, R., Halaas, J.L., Friedman, J.M., Charron, M.J., 1997. Acute stimulation of glucose metabolism in mice by leptin treatment. Nature 389, 374-377.
Kanat-Pektas, M., Yesildager, U., Tuncer, N., Arioz, D.T., Nadirgil-Koken, G., Yilmazer, M., 2014. Could mean platelet volume in late first trimester of pregnancy predict intrauterine growth restriction and pre-eclampsia? The journal of obstetrics and gynaecology research 40, 1840-1845.
Karimi, K., Arck, P.C., 2010. Natural Killer cells: keepers of pregnancy in the turnstile of the environment. Brain, behavior, and immunity 24, 339-347.
Karkkainen, H., Saarelainen, H., Valtonen, P., Laitinen, T., Raitakari, O.T., Juonala, M., Kahonen, M., Hutri-Kahonen, N., Heinonen, S., Laitinen, T., 2014. Carotid artery elasticity decreases during pregnancy - the Cardiovascular Risk in Young Finns study. BMC pregnancy and childbirth 14, 98.
Karumanchi, S.A., Maynard, S.E., Stillman, I.E., Epstein, F.H., Sukhatme, V.P., 2005. Preeclampsia: a renal perspective. Kidney international 67, 2101-2113.
Kashiwabara, S., Tsuruta, S., Okada, K., Saegusa, A., Miyagaki, Y., Baba, T., 2016. Functional compensation for the loss of testis-specific poly(A)-binding protein, PABPC2, during mouse spermatogenesis. The Journal of reproduction and development 62, 305-310.
Kautzky-Willer, A., Pacini, G., Tura, A., Bieglmayer, C., Schneider, B., Ludvik, B., Prager, R., Waldhausl, W., 2001. Increased plasma leptin in gestational diabetes. Diabetologia 44, 164-172.
Kedersha, N., Ivanov, P., Anderson, P., 2013. Stress granules and cell signaling: more than just a passing phase? Trends in biochemical sciences 38, 494-506.

Keller-Wood, M., Feng, X., Wood, C.E., Richards, E., Anthony, R.V., Dahl, G.E., Tao, S., 2014. Elevated maternal cortisol leads to relative maternal hyperglycemia and increased stillbirth in ovine pregnancy. American journal of physiology. Regulatory, integrative and comparative physiology 307, R405-413.
Kershaw, E.E., Flier, J.S., 2004. Adipose tissue as an endocrine organ. The Journal of clinical endocrinology and metabolism 89, 2548-2556.
Kersten, S., 2001. Mechanisms of nutritional and hormonal regulation of lipogenesis. EMBO reports 2, 282-286.
Khosravi, S., Tam, K.J., Ardekani, G.S., Martinka, M., McElwee, K.J., Ong, C.J., 2015. eIF4E is an adverse prognostic marker of melanoma patient survival by increasing melanoma cell invasion. The Journal of investigative dermatology 135, 1358-1367.
Kieckbusch, J., Balmas, E., Hawkes, D.A., Colucci, F., 2015. Disrupted PI3K p110delta Signaling Dysregulates Maternal Immune Cells and Increases Fetal Mortality In Mice. Cell reports 13, 2817-2828.
Kieckbusch, J., Gaynor, L.M., Moffett, A., Colucci, F., 2014. MHC-dependent inhibition of uterine NK cells impedes fetal growth and decidual vascular remodelling. Nature communications 5, 3359.
Kimura, M., Ishida, K., Kashiwabara, S., Baba, T., 2009. Characterization of two cytoplasmic poly(A)-binding proteins, PABPC1 and PABPC2, in mouse spermatogenic cells. Biology of reproduction 80, 545-554.
Kini, H.K., Kong, J., Liebhaber, S.A., 2014. Cytoplasmic poly(A) binding protein C4 serves a critical role in erythroid differentiation. Mol Cell Biol 34, 1300-1309.
Kitajima, M., Oka, S., Yasuhi, I., Fukuda, M., Rii, Y., Ishimaru, T., 2001. Maternal serum triglyceride at 24--32 weeks' gestation and newborn weight in nondiabetic women with positive diabetic screens. Obstetrics and gynecology 97, 776-780.
Klarsfeld, A., Bessereau, J.L., Salmon, A.M., Triller, A., Babinet, C., Changeux, J.P., 1991. An acetylcholine receptor alpha-subunit promoter conferring preferential synaptic expression in muscle of transgenic mice. EMBO J 10, 625-632.
Kleene, K.C., Wang, M.Y., Cutler, M., Hall, C., Shih, D., 1994. Developmental expression of poly(A) binding protein mRNAs during spermatogenesis in the mouse. Molecular reproduction and development 39, 355-364.
Ko, S., Kawasaki, I., Shim, Y.H., 2013. PAB-1, a Caenorhabditis elegans poly(A)-binding protein, regulates mRNA metabolism in germline by interacting with CGH-1 and CAR-1. PloS one 8, e84798.
Ko, S., Park, J.H., Lee, A.R., Kim, E., Jiyoung, K., Kawasaki, I., Shim, Y.H., 2010. Two mutations in pab-1 encoding poly(A)-binding protein show similar defects in germline stem cell proliferation but different longevity in C. elegans. Molecules and cells 30, 167-172.
Koopman, L.A., Kopcow, H.D., Rybalov, B., Boyson, J.E., Orange, J.S., Schatz, F., Masch, R., Lockwood, C.J., Schachter, A.D., Park, P.J., Strominger, J.L., 2003. Human decidual natural killer cells are a unique NK cell subset with immunomodulatory potential. The Journal of experimental medicine 198, 1201-1212.
Kotelevtsev, Y., Brown, R.W., Fleming, S., Kenyon, C., Edwards, C.R., Seckl, J.R., Mullins, J.J., 1999. Hypertension in mice lacking 11beta-hydroxysteroid dehydrogenase type 2. The Journal of clinical investigation 103, 683-689.
Kozak, M., 1999. Initiation of translation in prokaryotes and eukaryotes. Gene 234, 187-208.

Kozera, B., Rapacz, M., 2013. Reference genes in real-time PCR. Journal of applied genetics 54, 391-406.
Kozlov, G., Trempe, J.F., Khaleghpour, K., Kahvejian, a., Ekiel, I., Gehring, K., 2001. Structure and function of the C-terminal PABC domain of human poly(A)-binding protein. Proceedings of the National Academy of Sciences of the United States of America 98, 4409-4413.
Kraus FT, S.L., Tocker JT, 2004. Anatomy, structure and function., in: Kraus FT, S.L., Tocker JT (Ed.), Placental Pathology. , Washington, DC: AFIP, pp. 1–22.
Kugler, J.M., Lasko, P., 2009. Localization, anchoring and translational control of oskar, gurken, bicoid and nanos mRNA during Drosophila oogenesis. Fly 3, 15-28.
Kühn, U., Pieler, T., 1996. Xenopus poly(A) binding protein: functional domains in RNA binding and protein-protein interaction. Journal of molecular biology 256, 20-30.
Kühn, U., Wahle, E., 2004. Structure and function of poly(A) binding proteins. Biochimica et biophysica acta 1678, 67-84.
Kuhnert, M., Strohmeier, R., Stegmuller, M., Halberstadt, E., 1998. Changes in lymphocyte subsets during normal pregnancy. Eur J Obstet Gynecol Reprod Biol 76, 147-151.
Kulandavelu, S., Whiteley, K.J., Qu, D., Mu, J., Bainbridge, S.A., Adamson, S.L., 2012. Endothelial nitric oxide synthase deficiency reduces uterine blood flow, spiral artery elongation, and placental oxygenation in pregnant mice. Hypertension 60, 231-238.
Kusinski, L.C., Stanley, J.L., Dilworth, M.R., Hirt, C.J., Andersson, I.J., Renshall, L.J., Baker, B.C., Baker, P.N., Sibley, C.P., Wareing, M., Glazier, J.D., 2012. eNOS knockout mouse as a model of fetal growth restriction with an impaired uterine artery function and placental transport phenotype. American journal of physiology. Regulatory, integrative and comparative physiology 303, R86-93.
La Rocca, C., Carbone, F., Longobardi, S., Matarese, G., 2014. The immunology of pregnancy: regulatory T cells control maternal immune tolerance toward the fetus. Immunology letters 162, 41-48.
Ladyman, S.R., Augustine, R.A., Grattan, D.R., 2010. Hormone interactions regulating energy balance during pregnancy. Journal of neuroendocrinology 22, 805-817.
Lager, S., Powell, T.L., 2012. Regulation of nutrient transport across the placenta. Journal of pregnancy 2012, 179827.
Lall, S., Piano, F., Davis, R.E., 2005. Caenorhabditis elegans decapping proteins: localization and functional analysis of Dcp1, Dcp2, and DcpS during embryogenesis. Molecular biology of the cell 16, 5880-5890.
Lamont, K., Scott, N.W., Jones, G.T., Bhattacharya, S., 2015. Risk of recurrent stillbirth: systematic review and meta-analysis. Bmj 350, h3080.
Lanier, L.L., 2008. Up on the tightrope: natural killer cell activation and inhibition. Nature immunology 9, 495-502.
Lazaris-Karatzas, A., Montine, K.S., Sonenberg, N., 1990. Malignant transformation by a eukaryotic initiation factor subunit that binds to mRNA 5' cap. Nature 345, 544-547.
Lee, K.Y., Jeong, J.W., Wang, J., Ma, L., Martin, J.F., Tsai, S.Y., Lydon, J.P., DeMayo, F.J., 2007. Bmp2 is critical for the murine uterine decidual response. Mol Cell Biol 27, 5468-5478.

Lees, C., Parra, M., Missfelder-Lobos, H., Morgans, A., Fletcher, O., Nicolaides, K.H., 2001. Individualized risk assessment for adverse pregnancy outcome by uterine artery Doppler at 23 weeks. Obstetrics and gynecology 98, 369-373.
Lepercq, J., Cauzac, M., Lahlou, N., Timsit, J., Girard, J., Auwerx, J., Hauguel-de Mouzon, S., 1998. Overexpression of placental leptin in diabetic pregnancy: a critical role for insulin. Diabetes 47, 847-850.
Levitz, M., Young, B.K., 1977. Estrogens in pregnancy. Vitamins and hormones 35, 109-147.
Lihn, A.S., Pedersen, S.B., Richelsen, B., 2005. Adiponectin: action, regulation and association to insulin sensitivity. Obesity reviews : an official journal of the International Association for the Study of Obesity 6, 13-21.
Lin, Y., Page, D.C., 2005. Dazl deficiency leads to embryonic arrest of germ cell development in XY C57BL/6 mice. Dev Biol 288, 309-316.
Lindberg, B.S., Johansson, E.D., Nilsson, B.A., 1974. Plasma levels of nonconjugated oestrone, oestradiol-17beta and oestriol during uncomplicated pregnancy. Acta obstetricia et gynecologica Scandinavica. Supplement 32, 21-36.
Lipshitz, H.D., 2009. Follow the mRNA: a new model for Bicoid gradient formation. Nat Rev Mol Cell Biol 10, 509-512.
Liu, J.P., Baker, J., Perkins, A.S., Robertson, E.J., Efstratiadis, A., 1993. Mice carrying null mutations of the genes encoding insulin-like growth factor I (Igf-1) and type 1 IGF receptor (Igf1r). Cell 75, 59-72.
Liu, L.X., Arany, Z., 2014. Maternal cardiac metabolism in pregnancy. Cardiovascular research 101, 545-553.
Lo, S., Russell, J.C., Taylor, A.W., 1970. Determination of glycogen in small tissue samples. J Appl Physiol 28, 234-236.
Longo, L.D., 1983. Maternal blood volume and cardiac output during pregnancy: a hypothesis of endocrinologic control. The American journal of physiology 245, R720-729.
Lopez-Luna, P., Maier, I., Herrera, E., 1991. Carcass and tissue fat content in the pregnant rat. Biology of the neonate 60, 29-38.
Louton, T., Domarus, H., Hartmann, P., 1988. The position effect in mice on day 19. Teratology 38, 67-74.
Lowe, L.P., Metzger, B.E., Lowe, W.L., Jr., Dyer, A.R., McDade, T.W., McIntyre, H.D., Group, H.S.C.R., 2010. Inflammatory mediators and glucose in pregnancy: results from a subset of the Hyperglycemia and Adverse Pregnancy Outcome (HAPO) Study. The Journal of clinical endocrinology and metabolism 95, 5427-5434.
Lu, C., Makala, L., Wu, D., Cai, Y., 2016. Targeting translation: eIF4E as an emerging anticancer drug target. Expert reviews in molecular medicine 18, e2.
Lu, D., Yang, X., Wu, Y., Wang, H., Huang, H., Dong, M., 2006. Serum adiponectin, leptin and soluble leptin receptor in pre-eclampsia. International journal of gynaecology and obstetrics: the official organ of the International Federation of Gynaecology and Obstetrics 95, 121-126.
Lyall, F., Robson, S.C., Bulmer, J.N., 2013. Spiral artery remodeling and trophoblast invasion in preeclampsia and fetal growth restriction: relationship to clinical outcome. Hypertension 62, 1046-1054.

Macdonald, E.M., Koval, J.J., Natale, R., Regnault, T., Campbell, M.K., 2014. Population-based placental weight ratio distributions. International journal of pediatrics 2014, 291846.
Maciejowski, J., Ahn, J.H., Cipriani, P.G., Killian, D.J., Chaudhary, A.L., Lee, J.I., Voutev, R., Johnsen, R.C., Baillie, D.L., Gunsalus, K.C., Fitch, D.H., Hubbard, E.J., 2005. Autosomal genes of autosomal/X-linked duplicated gene pairs and germ-line proliferation in Caenorhabditis elegans. Genetics 169, 1997-2011.
Magarinos, M.P., Sanchez-Margalet, V., Kotler, M., Calvo, J.C., Varone, C.L., 2007. Leptin promotes cell proliferation and survival of trophoblastic cells. Biology of reproduction 76, 203-210.
Magness, R.R., Parker, C.R., Jr., Rosenfeld, C.R., 1993. Systemic and uterine responses to chronic infusion of estradiol-17 beta. The American journal of physiology 265, E690-698.
Makarova, E.N., Chepeleva, E.V., Panchenko, P.E., Bazhan, N.M., 2013. Influence of abnormally high leptin levels during pregnancy on metabolic phenotypes in progeny mice. American journal of physiology. Regulatory, integrative and comparative physiology 305, R1268-1280.
Malandro, M.S., Beveridge, M.J., Kilberg, M.S., Novak, D.A., 1996. Effect of low-protein diet-induced intrauterine growth retardation on rat placental amino acid transport. The American journal of physiology 271, C295-303.
Malassine, A., Frendo, J.L., Evain-Brion, D., 2003. A comparison of placental development and endocrine functions between the human and mouse model. Human reproduction update 9, 531-539.
Malik, N.M., Carter, N.D., Murray, J.F., Scaramuzzi, R.J., Wilson, C.A., Stock, M.J., 2001. Leptin requirement for conception, implantation, and gestation in the mouse. Endocrinology 142, 5198-5202.
Malik, N.M., Carter, N.D., Wilson, C.A., Scaramuzzi, R.J., Stock, M.J., Murray, J.F., 2005. Leptin expression in the fetus and placenta during mouse pregnancy. Placenta 26, 47-52.
Maltepe, E., Bakardjiev, A.I., Fisher, S.J., 2010. Review series The placenta : transcriptional , epigenetic , and physiological integration during development. 120.
Mandala, M., Osol, G., 2012. Physiological remodelling of the maternal uterine circulation during pregnancy. Basic & clinical pharmacology & toxicology 110, 12-18.
Mangus, D.A., Evans, M.C., Jacobson, A., 2003. Poly(A)-binding proteins: multifunctional scaffolds for the post-transcriptional control of gene expression. Genome biology 4, 223.
Marchini, G., Fried, G., Ostlund, E., Hagenas, L., 1998. Plasma leptin in infants: relations to birth weight and weight loss. Pediatrics 101, 429-432.
Massey, A.C., 1992. Microcytic anemia. Differential diagnosis and management of iron deficiency anemia. The Medical clinics of North America 76, 549-566.
Masuzaki, H., Ogawa, Y., Sagawa, N., Hosoda, K., Matsumoto, T., Mise, H., Nishimura, H., Yoshimasa, Y., Tanaka, I., Mori, T., Nakao, K., 1997. Nonadipose tissue production of leptin: leptin as a novel placenta-derived hormone in humans. Nature medicine 3, 1029-1033.
Mathews, F., Youngman, L., Neil, A., 2004. Maternal circulating nutrient concentrations in pregnancy: implications for birth and placental weights of term infants. The American journal of clinical nutrition 79, 103-110.

Mattsson, R., Mattsson, A., Lindahl-Kiessling, K., 1984. Anemia causes erythropoiesis and increased antibody synthesis in the spleen of the pregnant mouse. Developmental and comparative immunology 8, 169-178.
Maulik, D., Mundy, D., Heitmann, E., Maulik, D., 2010. Evidence-based approach to umbilical artery Doppler fetal surveillance in high-risk pregnancies: an update. Clinical obstetrics and gynecology 53, 869-878.
McGrew, L.L., Dworkin-Rastl, E., Dworkin, M.B., Richter, J.D., 1989. Poly(A) elongation during Xenopus oocyte maturation is required for translational recruitment and is mediated by a short sequence element. Genes & development 3, 803-815.
McTernan, C.L., Draper, N., Nicholson, H., Chalder, S.M., Driver, P., Hewison, M., Kilby, M.D., Stewart, P.M., 2001. Reduced placental 11beta-hydroxysteroid dehydrogenase type 2 mRNA levels in human pregnancies complicated by intrauterine growth restriction: an analysis of possible mechanisms. The Journal of clinical endocrinology and metabolism 86, 4979-4983.
Mebius, R.E., Kraal, G., 2005. Structure and function of the spleen. Nature reviews. Immunology 5, 606-616.
Meikar, O., Vagin, V.V., Chalmel, F., Sostar, K., Lardenois, A., Hammell, M., Jin, Y., Da Ros, M., Wasik, K.A., Toppari, J., Hannon, G.J., Kotaja, N., 2014. An atlas of chromatoid body components. Rna 20, 483-495.
Melo, E.O., Dhalia, R., Martins de Sa, C., Standart, N., de Melo Neto, O.P., 2003. Identification of a C-terminal poly(A)-binding protein (PABP)-PABP interaction domain: role in cooperative binding to poly (A) and efficient cap distal translational repression. The Journal of biological chemistry 278, 46357-46368.
Merrick, W., 2003. Initiation of protein biosynthesis in eukaryotes. Biochemistry and Molecular Biology Education 31, 378-385.
Milona, A., Owen, B.M., van Mil, S., Dormann, D., Mataki, C., Boudjelal, M., Cairns, W., Schoonjans, K., Milligan, S., Parker, M., White, R., Williamson, C., 2010. The normal mechanisms of pregnancy-induced liver growth are not maintained in mice lacking the bile acid sensor Fxr. American journal of physiology. Gastrointestinal and liver physiology 298, G151-158.
Mizuno, M., Aoki, K., Kimbara, T., 1994. Functions of macrophages in human decidual tissue in early pregnancy. American journal of reproductive immunology : AJRI : official journal of the American Society for the Immunology of Reproduction and the International Coordination Committee for Immunology of Reproduction 31, 180-188.
Moffett, A., Colucci, F., 2014. Uterine NK cells: active regulators at the maternal-fetal interface. The Journal of clinical investigation 124, 1872-1879.
Moffett, A., Hiby, S.E., Sharkey, A.M., 2015. The role of the maternal immune system in the regulation of human birthweight. Philosophical transactions of the Royal Society of London. Series B, Biological sciences 370, 20140071.
Moffett, A., Loke, C., 2006. Immunology of placentation in eutherian mammals. Nature reviews. Immunology 6, 584-594.
Molteni, R.A., Stys, S.J., Battaglia, F.C., 1978. Relationship of fetal and placental weight in human beings: fetal/placental weight ratios at various gestational ages and birth weight distributions. The Journal of reproductive medicine 21, 327-334.
Moncada, S., Palmer, R.M., Higgs, E.A., 1991. Nitric oxide: physiology, pathophysiology, and pharmacology. Pharmacological reviews 43, 109-142.

Montelongo, A., Lasuncion, M.A., Pallardo, L.F., Herrera, E., 1992. Longitudinal study of plasma lipoproteins and hormones during pregnancy in normal and diabetic women. Diabetes 41, 1651-1659.
Moore, M.J., Proudfoot, N.J., 2009. Pre-mRNA processing reaches back to transcription and ahead to translation. Cell 136, 688-700.
Mor, G., Abrahams, V.M., 2003. Potential role of macrophages as immunoregulators of pregnancy. Reproductive biology and endocrinology : RB&E 1, 119.
Mu, J., Adamson, S.L., 2006. Developmental changes in hemodynamics of uterine artery, utero- and umbilicoplacental, and vitelline circulations in mouse throughout gestation. American journal of physiology. Heart and circulatory physiology 291, H1421-1428.
Muller-McNicoll, M., Neugebauer, K.M., 2013. How cells get the message: dynamic assembly and function of mRNA-protein complexes. Nat Rev Genet 14, 275-287.
Muresan, D., Rotar, I.C., Stamatian, F., 2016. The usefulness of fetal Doppler evaluation in early versus late onset intrauterine growth restriction. Review of the literature. Medical ultrasonography 18, 103-109.
Murphy, S.P., Fast, L.D., Hanna, N.N., Sharma, S., 2005. Uterine NK cells mediate inflammation-induced fetal demise in IL-10-null mice. Journal of immunology 175, 4084-4090.
Musa, J., Orth, M.F., Dallmayer, M., Baldauf, M., Pardo, C., Rotblat, B., Kirchner, T., Leprivier, G., Grunewald, T.G., 2016. Eukaryotic initiation factor 4E-binding protein 1 (4E-BP1): a master regulator of mRNA translation involved in tumorigenesis. Oncogene.
Naccasha, N., Gervasi, M.T., Chaiworapongsa, T., Berman, S., Yoon, B.H., Maymon, E., Romero, R., 2001. Phenotypic and metabolic characteristics of monocytes and granulocytes in normal pregnancy and maternal infection. American journal of obstetrics and gynecology 185, 1118-1123.
Nagaishi, V.S., Cardinali, L.I., Zampieri, T.T., Furigo, I.C., Metzger, M., Donato, J., Jr., 2014. Possible crosstalk between leptin and prolactin during pregnancy. Neuroscience 259, 71-83.
Nakada, D., Oguro, H., Levi, B.P., Ryan, N., Kitano, A., Saitoh, Y., Takeichi, M., Wendt, G.R., Morrison, S.J., 2014. Oestrogen increases haematopoietic stem-cell self-renewal in females and during pregnancy. Nature 505, 555-558.
Nakatsukasa, H., Masuyama, H., Takamoto, N., Hiramatsu, Y., 2008. Circulating leptin and angiogenic factors in preeclampsia patients. Endocrine journal 55, 565-573.
Nardozza, L.M., Araujo Junior, E., Barbosa, M.M., Caetano, A.C., Lee, D.J., Moron, A.F., 2012. Fetal growth restriction: current knowledge to the general Obs/Gyn. Archives of gynecology and obstetrics 286, 1-13.
Naruse, K., Yamasaki, M., Umekage, H., Sado, T., Sakamoto, Y., Morikawa, H., 2005. Peripheral blood concentrations of adiponectin, an adipocyte-specific plasma protein, in normal pregnancy and preeclampsia. Journal of reproductive immunology 65, 65-75.
Newbern, D., Freemark, M., 2011. Placental hormones and the control of maternal metabolism and fetal growth. Current opinion in endocrinology, diabetes, and obesity 18, 409-416.

Nolan, C.J., Riley, S.F., Sheedy, M.T., Walstab, J.E., Beischer, N.A., 1995. Maternal serum triglyceride, glucose tolerance, and neonatal birth weight ratio in pregnancy. Diabetes care 18, 1550-1556.
Ogren, L., Talamantes, F., 1988. Prolactins of pregnancy and their cellular source. International review of cytology 112, 1-65.
Okereke, N.C., Uvena-Celebrezze, J., Hutson-Presley, L., Amini, S.B., Catalano, P.M., 2002. The effect of gender and gestational diabetes mellitus on cord leptin concentration. American journal of obstetrics and gynecology 187, 798-803.
Okochi, K., Suzuki, T., Inoue, J.-i., Matsuda, S., Yamamoto, T., 2005. Interaction of anti-proliferative protein Tob with poly(A)-binding protein and inducible poly(A)-binding protein: implication of Tob in translational control. Genes to cells : devoted to molecular & cellular mechanisms 10, 151-163.
Orphanides, G., Reinberg, D., 2002. A unified theory of gene expression. Cell 108, 439-451.
Osol, G., Mandala, M., 2009. Maternal uterine vascular remodeling during pregnancy. Physiology 24, 58-71.
Ouyang, Y.Q., Li, S.J., Zhang, Q., Xiang, W.P., Shen, H.L., Chen, H.P., Chen, H., Chen, H.Z., 2009. Plasma sFlt-1-to-PlGF ratio is correlated with inflammatory but not with oxidative stress in Chinese preeclamptic women. Archives of gynecology and obstetrics 280, 91-97.
Ozkan, S., Erel, C.T., Madazli, R., Aydinli, K., 2005. Serum leptin levels in hypertensive disorder of pregnancy. Eur J Obstet Gynecol Reprod Biol 120, 158-163.
Ozturk, S., Guzeloglu-Kayisli, O., Demir, N., Sozen, B., Ilbay, O., Lalioti, M.D., Seli, E., 2012. Epab and Pabpc1 are differentially expressed during male germ cell development. Reproductive sciences 19, 911-922.
Ozturk, S., Guzeloglu-Kayisli, O., Lowther, K.M., Lalioti, M.D., Sakkas, D., Seli, E., 2014. Epab is dispensable for mouse spermatogenesis and male fertility. Molecular reproduction and development 81, 390.
Paiva, P., Menkhorst, E., Salamonsen, L., Dimitriadis, E., 2009. Leukemia inhibitory factor and interleukin-11: critical regulators in the establishment of pregnancy. Cytokine & growth factor reviews 20, 319-328.
Palmer, S.K., Zamudio, S., Coffin, C., Parker, S., Stamm, E., Moore, L.G., 1992. Quantitative estimation of human uterine artery blood flow and pelvic blood flow redistribution in pregnancy. Obstetrics and gynecology 80, 1000-1006.
Pardi, G., Marconi, A.M., Cetin, I., 2002. Placental-fetal interrelationship in IUGR fetuses--a review. Placenta 23 Suppl A, S136-141.
Parham, P., Moffett, A., 2013. Variable NK cell receptors and their MHC class I ligands in immunity, reproduction and human evolution. Nature reviews. Immunology 13, 133-144.
Parsons, J.A., Brelje, T.C., Sorenson, R.L., 1992. Adaptation of islets of Langerhans to pregnancy: increased islet cell proliferation and insulin secretion correlates with the onset of placental lactogen secretion. Endocrinology 130, 1459-1466.
Pausch, H., Flisikowski, K., Jung, S., Emmerling, R., Edel, C., Gotz, K.U., Fries, R., 2011. Genome-wide association study identifies two major loci affecting calving ease and growth-related traits in cattle. Genetics 187, 289-297.
Peixeiro, I., Silva, A.L., Romao, L., 2011. Control of human beta-globin mRNA stability and its impact on beta-thalassemia phenotype. Haematologica 96, 905-913.

Pepe, G.J., Albrecht, E.D., 1995. Actions of placental and fetal adrenal steroid hormones in primate pregnancy. Endocrine reviews 16, 608-648.
Perez-Perez, A., Gambino, Y., Maymo, J., Goberna, R., Fabiani, F., Varone, C., Sanchez-Margalet, V., 2010. MAPK and PI3K activities are required for leptin stimulation of protein synthesis in human trophoblastic cells. Biochem Biophys Res Commun 396, 956-960.
Pestova, T.V.L.J.H.C., 2007. The Mechanism of Translation Initiation in Eukaryotes, in: Mathews, M.S., N.; Hershey, JWB (Ed.), Translational Control in Biology and Medicine. Cold Spring Harbor Laboratory Press, New York, pp. 87-128.
Petersen, B.E., Goff, J.P., Greenberger, J.S., Michalopoulos, G.K., 1998. Hepatic oval cells express the hematopoietic stem cell marker Thy-1 in the rat. Hepatology 27, 433-445.
Pijnenborg, R., Bland, J.M., Robertson, W.B., Brosens, I., 1983. Uteroplacental arterial changes related to interstitial trophoblast migration in early human pregnancy. Placenta 4, 397-413.
Plaks, V., Rinkenberger, J., Dai, J., Flannery, M., Sund, M., Kanasaki, K., Ni, W., Kalluri, R., Werb, Z., 2013. Matrix metalloproteinase-9 deficiency phenocopies features of preeclampsia and intrauterine growth restriction. Proc Natl Acad Sci U S A 110, 11109-11114.
Pollock, K.E., Stevens, D., Pennington, K.A., Thaisrivongs, R., Kaiser, J., Ellersieck, M.R., Miller, D.K., Schulz, L.C., 2015. Hyperleptinemia During Pregnancy Decreases Adult Weight of Offspring and Is Associated With Increased Offspring Locomotor Activity in Mice. Endocrinology 156, 3777-3790.
Pomp, D., Cowley, D.E., Eisen, E.J., Atchley, W.R., Hawkins-Brown, D., 1989. Donor and recipient genotype and heterosis effects on survival and prenatal growth of transferred mouse embryos. Journal of reproduction and fertility 86, 493-500.
Prasad, C.K., Mahadevan, M., MacNicol, M.C., MacNicol, A.M., 2008. Mos 3' UTR regulatory differences underlie species-specific temporal patterns of Mos mRNA cytoplasmic polyadenylation and translational recruitment during oocyte maturation. Molecular reproduction and development 75, 1258-1268.
Qiao, L., Yoo, H.S., Madon, A., Kinney, B., Hay, W.W., Jr., Shao, J., 2012. Adiponectin enhances mouse fetal fat deposition. Diabetes 61, 3199-3207.
Qiu, Q., Basak, A., Mbikay, M., Tsang, B.K., Gruslin, A., 2005. Role of pro-IGF-II processing by proprotein convertase 4 in human placental development. Proc Natl Acad Sci U S A 102, 11047-11052.
Qiu, Y., Krug, R.M., 1994. The influenza virus NS1 protein is a poly(A)-binding protein that inhibits nuclear export of mRNAs containing poly(A). Journal of virology 68, 2425-2432.
Qu, D.A., SL., 2014. Method to locate the uterine artery in mice for micro-ultrasound doppler blood velocity examination, in: Croy, B.Y., AT.; DeMayo, FJ.; Adamson, SL. (Ed.), The Guide to Investigation of Mouse Pregnancy. Academic Press (Elsevier), London, UK.
Ramos, P., Herrera, E., 1995. Reversion of insulin resistance in the rat during late pregnancy by 72-h glucose infusion. The American journal of physiology 269, E858-863.
Ranson, J.H., Roses, D.F., Fink, S.D., 1973. Early respiratory insufficiency in acute pancreatitis. Annals of surgery 178, 75-79.

Rawn, S.M., Cross, J.C., 2008. The evolution, regulation, and function of placenta-specific genes. Annual review of cell and developmental biology 24, 159-181.
Reijo, R., Lee, T.Y., Salo, P., Alagappan, R., Brown, L.G., Rosenberg, M., Rozen, S., Jaffe, T., Straus, D., Hovatta, O., et al., 1995. Diverse spermatogenic defects in humans caused by Y chromosome deletions encompassing a novel RNA-binding protein gene. Nature genetics 10, 383-393.
Resnik, R., 2007. One size does not fit all. American journal of obstetrics and gynecology 197, 221-222.
Richter, J.D., Bassell, G.J., Klann, E., 2015. Dysregulation and restoration of translational homeostasis in fragile X syndrome. Nature reviews. Neuroscience 16, 595-605.
Rinker-Schaeffer, C.W., Graff, J.R., De Benedetti, A., Zimmer, S.G., Rhoads, R.E., 1993. Decreasing the level of translation initiation factor 4E with antisense RNA causes reversal of ras-mediated transformation and tumorigenesis of cloned rat embryo fibroblasts. International journal of cancer. Journal international du cancer 55, 841-847.
Risnes, K.R., Romundstad, P.R., Nilsen, T.I., Eskild, A., Vatten, L.J., 2009. Placental weight relative to birth weight and long-term cardiovascular mortality: findings from a cohort of 31,307 men and women. American journal of epidemiology 170, 622-631.
Robertson, S.A., Guerin, L.R., Moldenhauer, L.M., Hayball, J.D., 2009. Activating T regulatory cells for tolerance in early pregnancy - the contribution of seminal fluid. Journal of reproductive immunology 83, 109-116.
Roetto, A., Bosio, S., Gramaglia, E., Barilaro, M.R., Zecchina, G., Camaschella, C., 2002. Pathogenesis of hyperferritinemia cataract syndrome. Blood cells, molecules & diseases 29, 532-535.
Rossant, J., Cross, J.C., 2001. Placental development: lessons from mouse mutants. Nature reviews. Genetics 2, 538-548.
Roux, P.P., Topisirovic, I., 2012. Regulation of mRNA translation by signaling pathways. Cold Spring Harbor perspectives in biology 4.
Rozanowska, M., Cantrell, A., Edge, R., Land, E.J., Sarna, T., Truscott, T.G., 2005. Pulse radiolysis study of the interaction of retinoids with peroxyl radicals. Free radical biology & medicine 39, 1399-1405.
Ruggero, D., Montanaro, L., Ma, L., Xu, W., Londei, P., Cordon-Cardo, C., Pandolfi, P.P., 2004. The translation factor eIF-4E promotes tumor formation and cooperates with c-Myc in lymphomagenesis. Nature medicine 10, 484-486.
Ruggiu, M., Speed, R., Taggart, M., McKay, S.J., Kilanowski, F., Saunders, P., Dorin, J., Cooke, H.J., 1997. The mouse Dazla gene encodes a cytoplasmic protein essential for gametogenesis. Nature 389, 73-77.
Sachs, A.B., Davis, R.W., Kornberg, R.D., 1987. A single domain of yeast poly(A)-binding protein is necessary and sufficient for RNA binding and cell viability. Mol Cell Biol 7, 3268-3276.
Sagawa, N., Yura, S., Itoh, H., Kakui, K., Takemura, M., Nuamah, M.A., Ogawa, Y., Masuzaki, H., Nakao, K., Fujii, S., 2002a. Possible role of placental leptin in pregnancy: a review. Endocrine 19, 65-71.
Sagawa, N., Yura, S., Itoh, H., Mise, H., Kakui, K., Korita, D., Takemura, M., Nuamah, M.A., Ogawa, Y., Masuzaki, H., Nakao, K., Fujii, S., 2002b. Role of leptin in pregnancy--a review. Placenta 23 Suppl A, S80-86.

Saito, S., Tsukaguchi, N., Hasegawa, T., Michimata, T., Tsuda, H., Narita, N., 1999. Distribution of Th1, Th2, and Th0 and the Th1/Th2 cell ratios in human peripheral and endometrial T cells. American journal of reproductive immunology : AJRI : official journal of the American Society for the Immunology of Reproduction and the International Coordination Committee for Immunology of Reproduction 42, 240-245.
Sakaguchi, S., 2004. Naturally arising CD4+ regulatory t cells for immunologic self-tolerance and negative control of immune responses. Annual review of immunology 22, 531-562.
Sakaguchi, S., 2005. Naturally arising Foxp3-expressing CD25+CD4+ regulatory T cells in immunological tolerance to self and non-self. Nature immunology 6, 345-352.
Salam, R.A., Das, J.K., Bhutta, Z.A., 2014. Impact of intrauterine growth restriction on long-term health. Current opinion in clinical nutrition and metabolic care 17, 249-254.
Salas, S.P., Altermatt, F., Campos, M., Giacaman, A., Rosso, P., 1995. Effects of long-term nitric oxide synthesis inhibition on plasma volume expansion and fetal growth in the pregnant rat. Hypertension 26, 1019-1023.
Savvidou, M.D., Sotiriadis, A., Kaihura, C., Nicolaides, K.H., Sattar, N., 2008. Circulating levels of adiponectin and leptin at 23-25 weeks of pregnancy in women with impaired placentation and in those with established fetal growth restriction. Clinical science 115, 219-224.
Schaefer-Graf, U.M., Graf, K., Kulbacka, I., Kjos, S.L., Dudenhausen, J., Vetter, K., Herrera, E., 2008. Maternal lipids as strong determinants of fetal environment and growth in pregnancies with gestational diabetes mellitus. Diabetes care 31, 1858-1863.
Schulz, L.C., Widmaier, E.P., 2004. The effect of leptin on mouse trophoblast cell invasion. Biology of reproduction 71, 1963-1967.
Schulz, L.C., Widmaier, E.P., Qiu, J., Roberts, R.M., 2009. Effect of leptin on mouse trophoblast giant cells. Biology of reproduction 80, 415-424.
Schwanhäusser, B., Busse, D., Li, N., Dittmar, G., Schuchhardt, J., Wolf, J., Chen, W., Selbach, M., 2011. Global quantification of mammalian gene expression control. Nature 473, 337-342.
Scott, D.E., 1972. Anemia in pregnancy. Obstetrics and gynecology annual 1, 219-244.
Seli, E., Lalioti, M.D., Flaherty, S.M., Sakkas, D., Terzi, N., Steitz, J.a., 2005. An embryonic poly(A)-binding protein (ePAB) is expressed in mouse oocytes and early preimplantation embryos. Proceedings of the National Academy of Sciences of the United States of America 102, 367-372.
Serdar, Z., Gur, E., Colakoethullary, M., Develioethlu, O., Sarandol, E., 2003. Lipid and protein oxidation and antioxidant function in women with mild and severe preeclampsia. Archives of gynecology and obstetrics 268, 19-25.
Sferruzzi-Perri, A.N., Owens, J.A., Pringle, K.G., Robinson, J.S., Roberts, C.T., 2006. Maternal insulin-like growth factors-I and -II act via different pathways to promote fetal growth. Endocrinology 147, 3344-3355.
Sharma, A., Satyam, A., Sharma, J.B., 2007. Leptin, IL-10 and inflammatory markers (TNF-alpha, IL-6 and IL-8) in pre-eclamptic, normotensive pregnant and healthy non-pregnant women. American journal of reproductive immunology : AJRI

: official journal of the American Society for the Immunology of Reproduction and the International Coordination Committee for Immunology of Reproduction 58, 21-30.
Shi, Q.J., Lei, Z.M., Rao, C.V., Lin, J., 1993. Novel role of human chorionic gonadotropin in differentiation of human cytotrophoblasts. Endocrinology 132, 1387-1395.
Shima, T., Sasaki, Y., Itoh, M., Nakashima, A., Ishii, N., Sugamura, K., Saito, S., 2010. Regulatory T cells are necessary for implantation and maintenance of early pregnancy but not late pregnancy in allogeneic mice. Journal of reproductive immunology 85, 121-129.
Shin, S., Jang, J.Y., Roh, E.Y., Yoon, J.H., Kim, J.S., Han, K.S., Kim, S., Yun, Y., Choi, Y.S., Choi, J.D., Kim, S.H., Kim, S.J., Song, E.Y., 2009. Differences in circulating dendritic cell subtypes in pregnant women, cord blood and healthy adult women. Journal of Korean medical science 24, 853-859.
Siegel, I., Gleicher, N., 1981. Changes in peripheral mononuclear cells in pregnancy. American journal of reproductive immunology : AJRI : official journal of the American Society for the Immunology of Reproduction and the International Coordination Committee for Immunology of Reproduction 1, 154-155.
Silver, L., 1995. Mouse Genetics Concepts and Applications. Oxford University Press, New York.
Simmer, F., Moorman, C., van der Linden, A.M., Kuijk, E., van den Berghe, P.V., Kamath, R.S., Fraser, A.G., Ahringer, J., Plasterk, R.H., 2003. Genome-wide RNAi of C. elegans using the hypersensitive rrf-3 strain reveals novel gene functions. PLoS biology 1, E12.
Simmons, D.G., Fortier, A.L., Cross, J.C., 2007. Diverse subtypes and developmental origins of trophoblast giant cells in the mouse placenta. Developmental biology 304, 567-578.
Simmons, D.G., Rawn, S., Davies, A., Hughes, M., Cross, J.C., 2008. Spatial and temporal expression of the 23 murine Prolactin/Placental Lactogen-related genes is not associated with their position in the locus. BMC genomics 9, 352.
Simon, C., Frances, A., Piquette, G.N., el Danasouri, I., Zurawski, G., Dang, W., Polan, M.L., 1994. Embryonic implantation in mice is blocked by interleukin-1 receptor antagonist. Endocrinology 134, 521-528.
Simon, C., Valbuena, D., Krussel, J., Bernal, A., Murphy, C.R., Shaw, T., Pellicer, A., Polan, M.L., 1998. Interleukin-1 receptor antagonist prevents embryonic implantation by a direct effect on the endometrial epithelium. Fertility and sterility 70, 896-906.
Sims, R.J., 3rd, Belotserkovskaya, R., Reinberg, D., 2004. Elongation by RNA polymerase II: the short and long of it. Genes & development 18, 2437-2468.
Singh, N., Morlock, H., Hanes, S.D., 2011. The Bin3 RNA methyltransferase is required for repression of caudal translation in the Drosophila embryo. Dev Biol 352, 104-115.
Sivan, E., Mazaki-Tovi, S., Pariente, C., Efraty, Y., Schiff, E., Hemi, R., Kanety, H., 2003. Adiponectin in human cord blood: relation to fetal birth weight and gender. The Journal of clinical endocrinology and metabolism 88, 5656-5660.
Skjaerven, R., Wilcox, A.J., Oyen, N., Magnus, P., 1997. Mothers' birth weight and survival of their offspring: population based study. Bmj 314, 1376-1380.

Skjaerven, R., Wilcox, A.J., Russell, D., 1988. Birthweight and perinatal mortality of second births conditional on weight of the first. International journal of epidemiology 17, 830-838.
Sladic, R.T., Lagnado, C.A., Bagley, C.J., Goodall, G.J., 2004. Human PABP binds AU-rich RNA via RNA-binding domains 3 and 4. European journal of biochemistry / FEBS 271, 450-457.
Small, H.Y., Morgan, H., Beattie, E., Griffin, S., Indahl, M., Delles, C., Graham, D., 2016. Abnormal uterine artery remodelling in the stroke prone spontaneously hypertensive rat. Placenta 37, 34-44.
Smith, G.C., Fretts, R.C., 2007. Stillbirth. Lancet 370, 1715-1725.
Smith, G.C., Stenhouse, E.J., Crossley, J.A., Aitken, D.A., Cameron, A.D., Connor, J.M., 2002. Early pregnancy levels of pregnancy-associated plasma protein a and the risk of intrauterine growth restriction, premature birth, preeclampsia, and stillbirth. The Journal of clinical endocrinology and metabolism 87, 1762-1767.
Smith, R.W., Blee, T.K., Gray, N.K., 2014. Poly(A)-binding proteins are required for diverse biological processes in metazoans. Biochem Soc Trans 42, 1229-1237.
Song, H., Lim, H., Paria, B.C., Matsumoto, H., Swift, L.L., Morrow, J., Bonventre, J.V., Dey, S.K., 2002. Cytosolic phospholipase A2alpha is crucial [correction of A2alpha deficiency is crucial] for 'on-time' embryo implantation that directs subsequent development. Development 129, 2879-2889.
Sorenson, R.L., Brelje, T.C., 1997. Adaptation of islets of Langerhans to pregnancy: beta-cell growth, enhanced insulin secretion and the role of lactogenic hormones. Hormone and metabolic research = Hormon- und Stoffwechselforschung = Hormones et metabolisme 29, 301-307.
Sorge, R.E., Martin, L.J., Isbester, K.A., Sotocinal, S.G., Rosen, S., Tuttle, A.H., Wieskopf, J.S., Acland, E.L., Dokova, A., Kadoura, B., Leger, P., Mapplebeck, J.C., McPhail, M., Delaney, A., Wigerblad, G., Schumann, A.P., Quinn, T., Frasnelli, J., Svensson, C.I., Sternberg, W.F., Mogil, J.S., 2014. Olfactory exposure to males, including men, causes stress and related analgesia in rodents. Nature methods 11, 629-632.
Spriggs, K.A., Bushell, M., Willis, A.E., 2010. Translational regulation of gene expression during conditions of cell stress. Molecular cell 40, 228-237.
Stanley, K., 2012. Enjoying healthy eating: dairy foods. Diabetes self-management 29, 21-24.
Stephansson, O., Dickman, P.W., Johansson, A., Cnattingius, S., 2000. Maternal hemoglobin concentration during pregnancy and risk of stillbirth. Jama 284, 2611-2617.
Stewart, C.L., Kaspar, P., Brunet, L.J., Bhatt, H., Gadi, I., Kontgen, F., Abbondanzo, S.J., 1992. Blastocyst implantation depends on maternal expression of leukaemia inhibitory factor. Nature 359, 76-79.
Strauss, J.F., 3rd, Martinez, F., Kiriakidou, M., 1996. Placental steroid hormone synthesis: unique features and unanswered questions. Biology of reproduction 54, 303-311.
Stumpo, D.J., Byrd, N.A., Phillips, R.S., Ghosh, S., Maronpot, R.R., Castranio, T., Meyers, E.N., Mishina, Y., Blackshear, P.J., 2004. Chorioallantoic fusion defects and embryonic lethality resulting from disruption of Zfp36L1, a gene encoding a CCCH tandem zinc finger protein of the Tristetraprolin family. Mol Cell Biol 24, 6445-6455.

Svitkin, Y.V., Sonenberg, N., 2004. An efficient system for cap- and poly(A)-dependent translation in vitro. Methods in molecular biology 257, 155-170.
Sykes, L., MacIntyre, D.A., Yap, X.J., Teoh, T.G., Bennett, P.R., 2012. The Th1:th2 dichotomy of pregnancy and preterm labour. Mediators of inflammation 2012, 967629.
Talamantes, F., Ogren, L., Markoff, E., Woodard, S., Madrid, J., 1980. Phylogenetic distribution, regulation of secretion, and prolactin-like effects of placental lactogens. Federation proceedings 39, 2582-2587.
Tanaka, M., Natori, M., Ishimoto, H., Miyazaki, T., Kobayashi, T., Nozawa, S., 1994. Experimental growth retardation produced by transient period of uteroplacental ischemia in pregnant Sprague-Dawley rats. American journal of obstetrics and gynecology 171, 1231-1234.
Tanaka, Y., Park, J.H., Tanwar, P.S., Kaneko-Tarui, T., Mittal, S., Lee, H.J., Teixeira, J.M., 2012. Deletion of tuberous sclerosis 1 in somatic cells of the murine reproductive tract causes female infertility. Endocrinology 153, 404-416.
Tesser, R.B., Scherholz, P.L.A., do Nascimento, L., Katz, S.G., 2010. Trophoblast glycogen cells differentiate early in the mouse ectoplacental cone: putative role during placentation. Histochemistry and cell biology 134, 83-92.
Thiele, K., Kessler, T., Arck, P., Erhardt, A., Tiegs, G., 2013. Acetaminophen and pregnancy: short- and long-term consequences for mother and child. Journal of reproductive immunology 97, 128-139.
Tiralongo, G.M., Lo Presti, D., Pisani, I., Gagliardi, G., Scala, R.L., Novelli, G.P., Vasapollo, B., Andreoli, A., Valensise, H., 2015. Assessment of total vascular resistance and total body water in normotensive women during the first trimester of pregnancy. A key for the prevention of preeclampsia. Pregnancy hypertension 5, 193-197.
Todros, T., Sciarrone, A., Piccoli, E., Guiot, C., Kaufmann, P., Kingdom, J., 1999. Umbilical Doppler waveforms and placental villous angiogenesis in pregnancies complicated by fetal growth restriction. Obstetrics and gynecology 93, 499-503.
Tomsin, K., Mesens, T., Molenberghs, G., Peeters, L., Gyselaers, W., 2012. Time interval between maternal electrocardiogram and venous Doppler waves in normal pregnancy and preeclampsia: a pilot study. Ultraschall in der Medizin 33, E119-125.
Tsuchiya, T., Shimizu, H., Horie, T., Mori, M., 1999. Expression of leptin receptor in lung: leptin as a growth factor. European journal of pharmacology 365, 273-279.
Tulchinsky, D., Hobel, C.J., Yeager, E., Marshall, J.R., 1972. Plasma estrone, estradiol, estriol, progesterone, and 17-hydroxyprogesterone in human pregnancy. I. Normal pregnancy. American journal of obstetrics and gynecology 112, 1095-1100.
Umar, S., Nadadur, R., Iorga, A., Amjedi, M., Matori, H., Eghbali, M., 2012. Cardiac structural and hemodynamic changes associated with physiological heart hypertrophy of pregnancy are reversed postpartum. Journal of applied physiology 113, 1253-1259.
Vaisse, C., Halaas, J.L., Horvath, C.M., Darnell, J.E., Jr., Stoffel, M., Friedman, J.M., 1996. Leptin activation of Stat3 in the hypothalamus of wild-type and ob/ob mice but not db/db mice. Nature genetics 14, 95-97.
van der Heijden, O.W., Essers, Y.P., Spaanderman, M.E., De Mey, J.G., van Eys, G.J., Peeters, L.L., 2005. Uterine artery remodeling in pseudopregnancy is comparable to that in early pregnancy. Biology of reproduction 73, 1289-1293.

van Eickels, M., Grohe, C., Cleutjens, J.P., Janssen, B.J., Wellens, H.J., Doevendans, P.A., 2001. 17beta-estradiol attenuates the development of pressure-overload hypertrophy. Circulation 104, 1419-1423.
Van Kerkhove, M.D., Vandemaele, K.A., Shinde, V., Jaramillo-Gutierrez, G., Koukounari, A., Donnelly, C.A., Carlino, L.O., Owen, R., Paterson, B., Pelletier, L., Vachon, J., Gonzalez, C., Hongjie, Y., Zijian, F., Chuang, S.K., Au, A., Buda, S., Krause, G., Haas, W., Bonmarin, I., Taniguichi, K., Nakajima, K., Shobayashi, T., Takayama, Y., Sunagawa, T., Heraud, J.M., Orelle, A., Palacios, E., van der Sande, M.A., Wielders, C.C., Hunt, D., Cutter, J., Lee, V.J., Thomas, J., Santa-Olalla, P., Sierra-Moros, M.J., Hanshaoworakul, W., Ungchusak, K., Pebody, R., Jain, S., Mounts, A.W., Infection, W.H.O.W.G.f.R.F.f.S.H.N.p., 2011. Risk factors for severe outcomes following 2009 influenza A (H1N1) infection: a global pooled analysis. PLoS medicine 8, e1001053.
Vandesompele, J., De Preter, K., Pattyn, F., Poppe, B., Van Roy, N., De Paepe, A., Speleman, F., 2002. Accurate normalization of real-time quantitative RT-PCR data by geometric averaging of multiple internal control genes. Genome biology 3, RESEARCH0034.
Var, A., Kuscu, N.K., Koyuncu, F., Uyanik, B.S., Onur, E., Yildirim, Y., Oruc, S., 2003. Atherogenic profile in preeclampsia. Archives of gynecology and obstetrics 268, 45-47.
Vassalli, J.D., Huarte, J., Belin, D., Gubler, P., Vassalli, A., O'Connell, M.L., Parton, L.A., Rickles, R.J., Strickland, S., 1989. Regulated polyadenylation controls mRNA translation during meiotic maturation of mouse oocytes. Genes & development 3, 2163-2171.
Vaughan, O.R., Sferruzzi-Perri, A.N., Fowden, A.L., 2012. Maternal corticosterone regulates nutrient allocation to fetal growth in mice. The Journal of physiology 590, 5529-5540.
Vazquez-Pianzola, P., Urlaub, H., Suter, B., 2011. Pabp binds to the osk 3'UTR and specifically contributes to osk mRNA stability and oocyte accumulation. Dev Biol 357, 404-418.
Veenstra van Nieuwenhoven, A.L., Bouman, A., Moes, H., Heineman, M.J., de Leij, L.F., Santema, J., Faas, M.M., 2002. Cytokine production in natural killer cells and lymphocytes in pregnant women compared with women in the follicular phase of the ovarian cycle. Fertility and sterility 77, 1032-1037.
Verrey, F., 2003. System L: heteromeric exchangers of large, neutral amino acids involved in directional transport. Pflugers Archiv : European journal of physiology 445, 529-533.
Visontai, Z., Lenard, Z., Studinger, P., Rigo, J., Jr., Kollai, M., 2002. Impaired baroreflex function during pregnancy is associated with stiffening of the carotid artery. Ultrasound in obstetrics & gynecology : the official journal of the International Society of Ultrasound in Obstetrics and Gynecology 20, 364-369.
Vodstrcil, L.A., Tare, M., Novak, J., Dragomir, N., Ramirez, R.J., Wlodek, M.E., Conrad, K.P., Parry, L.J., 2012. Relaxin mediates uterine artery compliance during pregnancy and increases uterine blood flow. FASEB journal : official publication of the Federation of American Societies for Experimental Biology 26, 4035-4044.
Voeltz, G.K., Ongkasuwan, J., Standart, N., Steitz, J.A., 2001. A novel embryonic poly (A) binding protein , ePAB , regulates mRNA deadenylation in Xenopus egg extracts. 774-788.

Wallace, J.M., Bourke, D.A., Aitken, R.P., Leitch, N., Hay, W.W., Jr., 2002. Blood flows and nutrient uptakes in growth-restricted pregnancies induced by overnourishing adolescent sheep. American journal of physiology. Regulatory, integrative and comparative physiology 282, R1027-1036.
Waller, D.K., Lustig, L.S., Smith, A.H., Hook, E.B., 1993. Alpha-fetoprotein: a biomarker for pregnancy outcome. Epidemiology 4, 471-476.
Watson, E.D., Cross, J.C., 2005. Development of structures and transport functions in the mouse placenta. Physiology (Bethesda, Md.) 20, 180-193.
Wells, S.E., Hillner, P.E., Vale, R.D., Sachs, A.B., 1998. Circularization of mRNA by eukaryotic translation initiation factors. Molecular cell 2, 135-140.
Welniak, L.A., Richards, S.M., Murphy, W.J., 2001. Effects of prolactin on hematopoiesis. Lupus 10, 700-705.
Welsh, A.O., Enders, A.C., 1985. Light and electron microscopic examination of the mature decidual cells of the rat with emphasis on the antimesometrial decidua and its degeneration. The American journal of anatomy 172, 1-29.
Weyer, C., Funahashi, T., Tanaka, S., Hotta, K., Matsuzawa, Y., Pratley, R.E., Tataranni, P.A., 2001. Hypoadiponectinemia in obesity and type 2 diabetes: close association with insulin resistance and hyperinsulinemia. The Journal of clinical endocrinology and metabolism 86, 1930-1935.
Wigglesworth, J.S., 1974. Fetal growth retardation. Animal model: uterine vessel ligation in the pregnant rat. The American journal of pathology 77, 347-350.
Wilkie, G.S., Gautier, P., Lawson, D., Gray, N.K., 2005. Embryonic Poly (A) - Binding Protein Stimulates Translation in Germ Cells. 25, 2060-2071.
Wilson, M.E., Ford, S.P., 2001. Comparative aspects of placental efficiency. Reproduction 58, 223-232.
Wing, K., Sakaguchi, S., 2010. Regulatory T cells exert checks and balances on self tolerance and autoimmunity. Nature immunology 11, 7-13.
Winger, E.E., Reed, J.L., 2011. Low circulating CD4(+) CD25(+) Foxp3(+) T regulatory cell levels predict miscarriage risk in newly pregnant women with a history of failure. American journal of reproductive immunology : AJRI : official journal of the American Society for the Immunology of Reproduction and the International Coordination Committee for Immunology of Reproduction 66, 320-328.
Wollmann, H.A., 1998. Intrauterine growth restriction: definition and etiology. Hormone research 49 Suppl 2, 1-6.
Xue, L., Cai, J.Y., Ma, J., Huang, Z., Guo, M.X., Fu, L.Z., Shi, Y.B., Li, W.X., 2013. Global expression profiling reveals genetic programs underlying the developmental divergence between mouse and human embryogenesis. BMC genomics 14, 568.
Yamada, A., 2014. Unique features of endometrial dynamics during pregnancy, in: Croy, B.Y., AT.; DeMayo, FJ.; Adamson, SL. (Ed.), The Guide to Investigation of Mouse Pregnancy. Academic Press (Elsevier), London, UK.
Yamamoto, Y., Moore, R., Hess, H.A., Guo, G.L., Gonzalez, F.J., Korach, K.S., Maronpot, R.R., Negishi, M., 2006. Estrogen receptor alpha mediates 17alpha-ethynylestradiol causing hepatotoxicity. J Biol Chem 281, 16625-16631.
Yamashita, H., Shao, J., Ishizuka, T., Klepcyk, P.J., Muhlenkamp, P., Qiao, L., Hoggard, N., Friedman, J.E., 2001. Leptin administration prevents spontaneous gestational diabetes in heterozygous Lepr(db/+) mice: effects on placental leptin and fetal growth. Endocrinology 142, 2888-2897.

Yamauchi, Y., Riel, J.M., Ruthig, V.A., Ortega, E.A., Mitchell, M.J., Ward, M.A., 2016. Two genes substitute for the mouse Y chromosome for spermatogenesis and reproduction. Science 351, 514-516.
Yanagiya, A., Svitkin, Y.V., Shibata, S., Mikami, S., Imataka, H., Sonenberg, N., 2009. Requirement of RNA binding of mammalian eukaryotic translation initiation factor 4GI (eIF4GI) for efficient interaction of eIF4E with the mRNA cap. Mol Cell Biol 29, 1661-1669.
Yang, H., Duckett, C.S., Lindsten, T., 1995. iPABP, an inducible poly(A)-binding protein detected in activated human T cells. Molecular and cellular biology 15, 6770-6776.
Yang, M., Lei, Z.M., Rao Ch, V., 2003. The central role of human chorionic gonadotropin in the formation of human placental syncytium. Endocrinology 144, 1108-1120.
Ye, X., Hama, K., Contos, J.J., Anliker, B., Inoue, A., Skinner, M.K., Suzuki, H., Amano, T., Kennedy, G., Arai, H., Aoki, J., Chun, J., 2005. LPA3-mediated lysophosphatidic acid signalling in embryo implantation and spacing. Nature 435, 104-108.
Yung, H.W., Calabrese, S., Hynx, D., Hemmings, B.A., Cetin, I., Charnock-Jones, D.S., Burton, G.J., 2008. Evidence of placental translation inhibition and endoplasmic reticulum stress in the etiology of human intrauterine growth restriction. The American journal of pathology 173, 451-462.
Zenclussen, A.C., Gerlof, K., Zenclussen, M.L., Sollwedel, A., Bertoja, A.Z., Ritter, T., Kotsch, K., Leber, J., Volk, H.D., 2005. Abnormal T-cell reactivity against paternal antigens in spontaneous abortion: adoptive transfer of pregnancy-induced CD4+CD25+ T regulatory cells prevents fetal rejection in a murine abortion model. The American journal of pathology 166, 811-822.
Zhang, J., Croy, B.A., 2009. Using ultrasonography to define fetal-maternal relationships: moving from humans to mice. Comparative medicine 59, 527-533.
Zhang, J., Mikolajczyk, R., Grewal, J., Neta, G., Klebanoff, M., 2011. Prenatal application of the individualized fetal growth reference. American journal of epidemiology 173, 539-543.
Zhang, Y., Kaufman, S., 2000. Effect of nitric oxide synthase inhibition on cardiovascular and hormonal regulation during pregnancy in the rat. Canadian journal of physiology and pharmacology 78, 423-427.
Zhiqin, F.V.J., 1992. Male Chemosignals Increase Litter Size in House Mice, in: Doty, R.M.-S., D. (Ed.), Chemical Signals in Vertebrates IV. Plenum Press, New York.
Zhou, B., Lum, H.E., Lin, J., Linzer, D.I., 2002. Two placental hormones are agonists in stimulating megakaryocyte growth and differentiation. Endocrinology 143, 4281-4286.